

Membrane Enhanced Peptide Synthesis (MEPS) – Process Development and Application

By

Wenqian Chen
(CID 00476737)

Academic supervisor (Imperial College London, UK):
Prof. Andrew G. Livingston

Industrial supervisor (Lonza AG, Switzerland):
Dr. Michele Cristau and Dr. Juergen Riegler

A Dissertation Submitted to Imperial College London for the Degree of Doctor of
Philosophy

Department of Chemical Engineering
Imperial College London
South Kensington
London SW7 2AZ

March 2015

Abstract

Peptides are polymers of amino acids and are better drug candidates than traditional small-molecule compounds due to high specificity and potency. Conventional synthesis methods include Solid Phase Peptide Synthesis (SPPS) and Liquid Phase Peptide Synthesis (LPPS), which have different technical limitations. Significant improvements can be made by a new technology, Membrane Enhanced Peptide Synthesis (MEPS), which integrates nanofiltration into LPPS for the purification of intermediate products. The research work described in this thesis is an outcome of the MemTide consortium (Imperial College London, Institute for Research in Biomedicine (Barcelona) (IRB) and University of Turku) and three companies (Evonik Membrane Extraction Technology (MET) Ltd, Janssen Pharmaceutica and Lonza AG), whose task was to investigate membrane enhanced synthesis for both peptides and oligonucleotides.

This research project demonstrates that MEPS is ready for industrial application in terms of technical feasibility and economic performance relative to SPPS and LPPS. The MEPS of two peptides (Fmoc-Arg-Ala-Asp-Ala-NH₂ (fully deprotected Fmoc-RADA-NH₂) and Pyr-Ser(Bzl)-Ala-Phe-Asp-Leu-NH₂ (partially deprotected Pyr-SAFDL-NH₂)) is presented in the form of case studies. In the first case study, MEPS of fully deprotected Fmoc-RADA-NH₂ was attempted four times. The first three attempts encountered the problem of incomplete coupling after the post-de-Fmoc diafiltration, which was solved by the extended diafiltration (14 wash volumes). At a scale of 10.01 mmol (those in the proof of concept studies were 0.9 and 1.8 mmol), the fourth attempt at MEPS was successful with a purity of 98.5 % and an overall yield of 78.6 % before cleavage and global deprotection. This shows that the integration of nanofiltration into LPPS was technically feasible for obtaining high purity and decent yield of the anchored peptide that were comparable to those of SPPS (85.3 % and 78.3 % respectively before cleavage and global deprotection).

In the second case study, a similar research approach was adopted for the partially deprotected Pyr-SAFDL-NH₂ and the same problem of incomplete coupling occurred even with increased wash volumes. The cause was found to be residual piperidine in the system after the post-de-Fmoc diafiltration. The solution was to add a base (diisopropylethylamine (DIEA), which was also a reagent in each coupling) into the system during diafiltration to assist the removal of piperidine. At a scale of 33.65 mmol and an anchor concentration of 10.4 weight % in the starting solution, the third attempt at MEPS was successful with a purity of 88.1 % and an overall yield of 71.2 % before cleavage and global deprotection (98.6 % and 72.6 % respectively for SPPS; 100.0 % and 72.4 % respectively for LPPS (by precipitation)). Furthermore, MEPS outperformed SPPS and LPPS (by precipitation) in terms of material cost (8.7 – 13.0 % lower), process time (33.3 – 91.7 % shorter), volumetric efficiency (15.4 – 15.9 % higher) and E-factor (29.3 – 68.8 % lower). The results proved that this novel process is indeed an attractive alternative to SPPS and LPPS (by precipitation) and is ready for industrial application.

Encouraged by the positive results from the two case studies, attempts were made to further improve the performance of MEPS before cleavage and global deprotection by reducing the significant yield loss during diafiltration. Peptide synthesis was performed on two alternative anchors (amine-functionalised silica nanoparticles and a branched compound with poly(ethylene glycol) (PEG) arms (PyPEG)), but each had technical limitations during the coupling of amino acids. On the other hand, promising results were obtained from the modelling of MEPS in a two-stage membrane cascade system, as the second membrane served to recover the anchored peptide that permeated through the first one during diafiltration. As a result, the overall yield would increase from 71.2 to 93.8 %, making the new process even more attractive in terms of material cost (23.6 – 33.5 % lower than the single-stage MEPS and SPPS).

Table of Content

Abstract

Acknowledgement

Declaration of Originality

Copyright Declaration

Conferences

List of Figures

List of Tables

Abbreviations

Nomenclature

Page

Chapter One – Introduction

| | |
|--|-----------|
| 1.1 - Peptides and Their Applications | 1 |
| 1.2 - Chemical Synthesis and Membrane Enhanced Peptide Synthesis (MEPS) ... | 5 |
| 1.3 - Research Strategy | 10 |
| 1.3.1 - Background | 10 |
| 1.3.2 - Aim and Objectives | 11 |
| 1.3.2.1 - Overall Aim | 11 |
| 1.3.2.2 - Specific Objectives | 11 |
| 1.3.3 - Research Strategy | 11 |

Chapter Two – Literature Review

| | |
|---|----|
| 2.1- Peptide Chemistry | 13 |
| 2.1.1- Overview | 13 |
| 2.1.2- From Amino Acids to Peptide | 13 |
| 2.1.3- Peptide Synthesis | 15 |
| 2.1.4- Protection of the N-terminus and Side Chain of an Amino Acid | 28 |
| 2.1.5- Activation of an Amino Acid and Formation of a Peptide Bond | 32 |
| 2.1.6- Side Reactions | 34 |
| 2.1.6.1 - During Activation | 34 |
| 2.1.6.2 - During De-Fmoc | 37 |
| 2.1.6.3 - During Cleavage and Global Deprotection of Peptide | 39 |
| 2.2- OSN and MEPS | 40 |
| 2.2.1- Overview | 40 |
| 2.2.2- Organic Solvent Nanofiltration (OSN) | 41 |
| 2.2.3- Membrane Enhanced Peptide Synthesis (MEPS) | 42 |
| 2.2.4- Major Components of MEPS | 42 |
| 2.2.5- OSN Membrane | 42 |
| 2.2.6- Material and Fabrication Method | 43 |
| 2.2.7- Characterisation of Membrane | 46 |
| 2.2.8- Membrane Configuration | 48 |

| | |
|---|-----------|
| 2.2.9 - Polymeric Membrane vs Ceramic Membrane for MEPS | 50 |
| 2.2.10 - Nanofiltration System | 51 |
| 2.2.11 - Purification through Diafiltration | 53 |
| 2.2.12 - Soluble Anchors for Liquid Phase Synthesis | 56 |
| 2.2.13 - First Study of MEPS | 58 |
| 2.2.13.1 - Critical Issues and Corresponding Solutions | 59 |
| 2.2.13.2 - Membrane | 59 |
| 2.2.13.3 - Soluble Anchor | 60 |
| 2.2.13.4 - Peptide Chemistry | 60 |
| 2.2.13.5 - MEPS of Model Peptides | 61 |
| 2.2.13.6 - Improvements | 64 |
| 2.2.13.7 - Suggestions | 64 |
| 2.2.13.8 - Major Aspects of MEPS | 65 |

Chapter Three –

Case Study One: Synthesis of Fully Deprotected Fmoc-RADA-NH₂

| | |
|--|----|
| 3.1- Introduction | 66 |
| 3.2- Experimental | 69 |
| 3.2.1- Materials | 69 |
| 3.2.2- Apparatus | 71 |
| 3.2.2.1 - Cross-flow OSN System | 71 |
| 3.2.2.2 - Analytical Equipment | 73 |
| 3.2.3- Analytical Methods | 73 |
| 3.2.3.1 - HPLC Methods | 73 |
| 3.2.3.2 - Chloranil Test | 75 |
| 3.2.3.3 - Ninhydrin Test | 75 |
| 3.2.4- General Procedures | 76 |
| 3.2.4.1 - Synthesis of DDBA | 78 |
| 3.2.4.2 - Anchor Screening | 80 |
| 3.2.4.3 - LPPS of Fully Protected Fmoc-RADA-DDBA by Precipitation | 82 |
| 3.2.4.4 - Synthesis of H₂N-Rink-DDBA | 85 |
| 3.2.4.5 - SPPS of Fully Deprotected Fmoc-RADA-NH₂ | 87 |
| 3.2.4.6 - Small-scale Coupling Tests for Fully Protected Fmoc-RADA- Rink-DDBA in Liquid Phase by Precipitation | 89 |

| | |
|---|------------|
| 3.2.4.7 - MEPS of Fully Deprotected Fmoc-RADA-NH₂ on H₂N-Rink-DDBA | 92 |
| 3.3- Results and Discussion | 96 |
| 3.3.1 - Synthesis of DDBA | 96 |
| 3.3.2 - Analysis of DDBA and Related Compounds | 102 |
| 3.3.3 - Anchor Screening | 103 |
| 3.3.4 - SPPS of Fully Deprotected Fmoc-RADA-NH₂ | 113 |
| 3.3.5 - LPPS of Fully Protected Fmoc-RADA-DDBA by Precipitation | 116 |
| 3.3.6 - Synthesis of H₂N-Rink-DDBA | 122 |
| 3.3.7 - Small-scale Coupling Tests for Fully Protected Fmoc-RADA-Rink-DDBA in Liquid Phase by Precipitation | 125 |
| 3.3.8 - MEPS of Fully Deprotected Fmoc-RADA-NH₂ on H₂N-Rink-DDBA | 126 |
| 3.3.8.1 - Screening of Membrane with DDBA | 126 |
| 3.3.8.2 - MEPS | 127 |
| 3.3.8.2.1 - MEPS (First Attempt) | 128 |
| 3.3.8.2.2 - MEPS (Second Attempt) | 131 |
| 3.3.8.2.3 - MEPS (Third Attempt) | 135 |
| 3.3.8.2.4 - MEPS (Fourth Attempt) | 142 |
| 3.3.9 - Comparison between MEPS and SPPS | 149 |
| 3.4- Conclusions | 159 |

Chapter Four –

Case Study Two: MEPS of Partially Deprotected Pyr-SAFDL-NH₂

| | |
|---|-----|
| 4.1- Introduction | 161 |
| 4.2- Experimental | 163 |
| 4.2.1 - Analytical Methods | 163 |
| 4.2.2 - General Procedures | 164 |
| 4.2.2.1 - SPPS of Partially Deprotected Pyr-SAFDL-NH₂ | 164 |
| 4.2.2.2 - LPPS of Partially Deprotected Pyr-SAFDL-NH₂ on H₂N-Rink-DDBA by Precipitation | 166 |
| 4.2.2.3 - MEPS of Partially Deprotected Pyr-SAFDL-NH₂ on H₂N-Rink-DDBA ... | 171 |
| 4.3- Results and Discussion | 174 |
| 4.3.1 - SPPS of Partially Deprotected Pyr-SAFDL-NH₂ | 174 |
| 4.3.2 - LPPS of Partially Deprotected Pyr-SAFDL-NH₂ on H₂N-Rink-DDBA by Precipitation | 181 |
| 4.3.3 - MEPS of Partially Deprotected Pyr-SAFDL-NH₂ on H₂N-Rink-DDBA | 185 |
| 4.3.3.1 - MEPS (First Attempt) | 186 |
| 4.3.3.2 - Side Reaction Induced by Piperidine and Tests of Mitigation Method | 191 |
| 4.3.3.3 - Replacement of Piperidine with Diethylamine (DEA) for De-Fmoc ... | 198 |
| 4.3.3.4 - MEPS (Second Attempt) | 200 |

| | |
|--|------------|
| 4.3.3.5 - MEPS (Third Attempt) | 204 |
| 4.3.3.6 - Stability of Fmoc-Rink Linker in TFA Solution | 207 |
| 4.3.3.7 - Small-scale Tests for Cleavage and Global Deprotection of Fully Protected Pyr-SAFDL-Rink | 208 |
| 4.3.3.8 - Cleavage and Global Deprotection for Fully Protected Pyr-SAFDL-Rink-DDBA | 210 |
| 4.3.4 - Comparison between MEPS, SPPS and LPPS | 213 |
| 4.4- Conclusions | 218 |

Chapter Five –

Alternative Anchors and OSN System for Better Performance

| | |
|--|-----|
| 5.1 - Introduction | 220 |
| 5.2 - Experimental | 224 |
| 5.2.1 - Materials | 224 |
| 5.2.2 - Apparatus | 224 |
| 5.2.3 - Analytical Methods | 224 |
| 5.2.4 - General Procedures | 225 |
| 5.2.4.1 - Quantification of Free Amine Groups on Silica Nanoparticles | 225 |
| 5.2.4.2 - Loading of Fmoc-Rink Linker and Amino Acid on Silica Nanoparticles... | 225 |
| 5.2.4.3 - Diafiltration of PyPEG | 226 |
| 5.2.4.4 - Loading of Fmoc-Rink Linker on PyPEG | 226 |
| 5.2.4.5 - MEPS of Fully Deprotected Fmoc-RADA-NH₂ on Fmoc-Rink-PyPEG ... | 226 |
| 5.2.4.6 - Modelling of MEPS in a Two-stage Membrane Cascade | 228 |
| 5.2.4.6.1 - Summary of Experimental Data | 229 |
| 5.2.4.6.2 - Proposed Model for the Single-Stage Membrane System | 232 |
| 5.2.4.6.3 - General Equations for Mass Balance | 232 |
| 5.2.4.6.4 - Rates of Generation and Consumption | 233 |
| 5.2.4.6.5 - Scheduling | 235 |

| | |
|--|-----|
| 5.3- Results and Discussion | 236 |
| 5.3.1.1 - Silica Nanoparticles | 236 |
| 5.3.1.2 - Loading of Free Amine Group on Silica Nanoparticles | 236 |
| 5.3.1.3 - Loading of Fmoc-Rink Linker on Silica Nanoparticles | 237 |
| 5.3.1.4 - Capping of Free Amine Groups | 237 |
| 5.3.1.5 - Chemical Modification of Silica Nanoparticles | 238 |
| 5.3.2- MEPS of Fully Deprotected Fmoc-RADA-NH₂ on Rink-PyPEG | 239 |
| 5.3.2.1 - Synthesis and Purification of PyPEG | 239 |
| 5.3.2.2 - Loading of Fmoc-Rink Linker on PyPEG | 242 |
| 5.3.2.3 - MEPS of Fully Deprotected Fmoc-RADA-NH₂ on Rink-PyPEG | 246 |
| 5.3.3- Modelling of Membrane Cascade for MEPS | 249 |
| 5.3.3.1 - Validation of MEPS in Single-stage System | 249 |
| 5.3.3.2 - MEPS in Two-stage Membrane Cascade System | 253 |
| 5.4- Conclusions | 260 |

Chapter Six – Conclusions and Suggestions for Future Work

| | |
|---|-----|
| 6.1- Overall Conclusions | 263 |
| 6.2- Summary of Findings | 263 |
| 6.3- Updates on the Major Aspects of MEPS | 267 |
| 6.4- Recommendations for Future Work | 271 |

References

Appendix

Acknowledgement

I have been extremely grateful that I could be part of the MemTide consortium and was given the opportunity to conduct interesting research that received funding from the European Community's Seventh Framework Programme (FP7/2007-2013) under grant agreement number 238291.

For their generous guidance and support throughout my PhD, I would like to express my sincere gratitude to my academic supervisor, Prof. Andrew G. Livingston, and my industrial supervisors, Dr. Michele Cristau and Dr. Juergen Riegler.

In addition, I would like to thank all the research partners in the MemTide consortium as well as all my colleagues in Imperial College London and Lonza AG for their generous help.

Declaration of Originality

This thesis describes the research work of the author in Lonza AG (Visp, Switzerland) and Imperial College London (Department of Chemical Engineering, London, United Kingdom) between November 2010 and December 2014 under the supervision of Prof. Andrew G. Livingston, Dr. Michele Cristau and Dr. Juergen Riegler. All the material that is not the original work of the author is properly acknowledged. None of the material in this thesis has been submitted for a degree at any other university.

Copyright Declaration

The copyright of this thesis rests with the author and is made available under a Creative Commons Attribution Non-Commercial No Derivatives licence. Researchers are free to copy, distribute or transmit the thesis on the condition that they attribute it, that they do not use it for commercial purposes and that they do not alter, transform or build upon it. For any reuse or redistribution, researchers must make clear to others the licence terms of this work.

Conferences

Chen, W.Q., Cristau, M., Giraud, M., & Livingston, A.G. (2nd – 7th September 2012)
Novel liquid phase peptide synthesis (LPPS) technology: Elongation using Organic Solvent Nanofiltration (OSN). Poster presentation, 32nd European Peptide Symposium, Athens, Greece.

Chen, W.Q., Cristau, M., Giraud, M., & Livingston, A.G. (23rd – 27th September 2012)
Novel liquid phase peptide synthesis (LPPS) technology: Elongation using Organic Solvent Nanofiltration (OSN). Poster presentation, Euromembrane 2012, London, UK.

Chen, W.Q., Cristau, M., Riegler, J., & Livingston, A.G. (12th – 14th March 2013) Novel Peptide Synthesis Technology: Integration of OSN into Liquid Phase Peptide Synthesis (LPPS). Oral presentation, 4th International Conference on Organic Solvent Nanofiltration, Aachen, Germany.

Chen, W.Q., Cristau, M., Riegler, J., & Livingston, A.G. (12th – 14th March 2013) Novel Peptide Synthesis Technology: Integration of OSN into Liquid Phase Peptide Synthesis (LPPS). Poster presentation, 9th European Congress of Chemical Engineering, Hague, Netherlands

List of Figures

| | Page |
|---|-------------|
| Figure 1.1. (a) Number of newly launched small-molecule drugs from 1998 to 2008. (b) Number of peptide drugs entering clinical study from 1940's to 2008. | 1 |
| Figure 1.2. Sequence of human insulin. | 4 |
| Figure 1.3. Peptide synthesis methods. | 5 |
| Figure 1.4. Conventional chemical synthesis methods. | 6 |
| Figure 1.5. Membrane Enhanced Peptide Synthesis (MEPS): (a) the overall concept; (b) removal of impurities during diafiltration. | 9 |
| Figure 1.6. Peptide synthesis cluster in the MemTide consortium | 10 |
| Figure 2.1. General structure of an amino acid. | 14 |
| Figure 2.2. General structure of a pentapeptide. | 14 |
| Figure 2.3. Typical procedure for stepwise SPPS. | 18 |
| Figure 2.4. (a) Hybrid SPPS-LPPS. (b) Convergent SPPS. | 21 |
| Figure 2.5. Typical procedure for fragment synthesis in solution phase peptide synthesis. | 24 |
| Figure 2.6. Target peptide synthesised on (a) Fmoc-Rink amide resin and (b) H ₂ N-Rink-DBBA. ... | 25 |
| Figure 2.7. A procedure for liquid phase peptide synthesis on anchor. | 27 |
| Figure 2.8. Protection of the N-terminus and side chain of an amino acid. | 28 |
| Figure 2.9. Elongation of a peptide. | 28 |
| Figure 2.10. Amino acids used in this project. | 29 |

| | |
|---|----|
| Figure 2.11. De-Fmoc mechanism by piperidine and reaction between piperidine and dibenzofulvene. | 30 |
| Figure 2.12. Peptide bond formation. | 32 |
| Figure 2.13. Aminolysis via activation of amino acid by DIC and HOBt. | 33 |
| Figure 2.14. Aminolysis via activation of amino acid by HBTU. | 33 |
| Figure 2.15. Racemisation of activated amino acid via direct abstraction of the α -proton. | 34 |
| Figure 2.16. Racemisation of activated amino acid via reversible β -elimination. | 34 |
| Figure 2.17. Racemisation of activated peptide fragment via azlactone. | 35 |
| Figure 2.18. Formation of amino acid anhydride. | 35 |
| Figure 2.19. Formation of unreactive N-acylurea. | 36 |
| Figure 2.20. Formation of guanidine. | 36 |
| Figure 2.21. Formation of DKP. | 37 |
| Figure 2.22. Formation of aspartimide in the presence of piperidine. | 38 |
| Figure 2.23. Decomposition of Rink amide linker during cleavage and global deprotection of peptide. | 39 |
| Figure 2.24. 1,3-dimethoxybenzene (DMB) ... | 39 |
| Figure 2.25. (a) General structure of OSN membrane. (b) Permeation of solute B and solvent through an OSN membrane. | 43 |
| Figure 2.26. Fabrication of polymeric membrane via casting on support and phase inversion. ... | 44 |
| Figure 2.27. SEM image of the cross-section of a typical polymeric membrane. | 44 |

| | |
|---|----|
| Figure 2.28. Fabrication of ceramic membrane by sol-gel method. | 45 |
| Figure 2.29. SEM image of the cross-section of a typical ceramic membrane. | 45 |
| Figure 2.30. A typical rejection curve for a membrane. | 47 |
| Figure 2.31. Compounds used for determining the rejection curve of a membrane: (a) PEG; (b) PS..... | 47 |
| Figure 2.32. The structure of a typical spiral module. | 49 |
| Figure 2.33. Typical ceramic multi-channel tubes. | 49 |
| Figure 2.34. Flow direction of feed/retentate in typical (a) dead-end cell and (b) cross-flow cell. | 51 |
| Figure 2.35. Simplified schematics of typical (a) single-stage system and (b) membrane cascade system. | 52 |
| Figure 2.36. Simplified schematic of a single-stage system for constant volume diafiltration. | 53 |
| Figure 2.37. Concentration of component i at time t over initial concentration during constant volume diafiltration.. | 54 |
| Figure 2.38. Tetrabenzo[a,c,g,i]fluorine (Tbf). | 57 |
| Figure 2.39. Original schematic representation of MEPS | 58 |
| Figure 3.1. Fmoc-Arg-Ala-Asp-Ala-NH ₂ (fully deprotected Fmoc-RADA-NH ₂) | 66 |
| Figure 3.2. 2,4-didocosyloxybenzalcohol (DDBA). | 67 |
| Figure 3.3. Cross-flow OSN system in (a) diafiltration mode and (b) full recycle mode | 72 |
| Figure 3.4. HPLC result for a dried product that contains four components | 76 |
| Figure 3.5. Synthesis of DDBA. | 78 |
| Figure 3.6. Synthesis of fully protected Fmoc-RADA-DDBA. | 82 |

| | |
|---|-----|
| Figure 3.7. Synthesis of H ₂ N-Rink-DDBA. | 85 |
| Figure 3.8. SPPS of fully deprotected Fmoc-RADA-NH ₂ | 87 |
| Figure 3.9. Coupling steps in the synthesis of fully protected Fmoc-RADA-Rink-DDBA. | 90 |
| Figure 3.10. Synthesis of fully deprotected Fmoc-RADA- NH ₂ | 94 |
| Figure 3.11. LC/MS result of 2,4-didocosyloxybenzaldehyde (dried product of Reaction 1 in Table 3.1). | 97 |
| Figure 3.12. NMR result of 2,4-didocosyloxybenzaldehyde (dried product of Reaction 1 in Table 3.1). | 98 |
| Figure 3.13. LC/MS result of DDBA (dried product of Reaction 10 in Table 3.2). | 100 |
| Figure 3.14. NMR result of DDBA (dried product of Reaction 10 in Table 3.2). | 101 |
| Figure 3.15. Rejection of anchor vs molecular weight for (a) Inopor 450 and (b) Inopor 750. | 111 |
| Figure 3.16. LC/MS result of the dried fully deprotected Fmoc-RADA-NH ₂ | 115 |
| Figure 3.17. HPLC results for the de-Fmoc of Fmoc-Asp(OtBu)-Ala-DDBA: (a) 1 hour of de-Fmoc; (b) 2 hours of de-Fmoc; (c) 3 hours of de-Fmoc; (d) overnight de-Fmoc. | 119 |
| Figure 3.18. LC/MS result for the 3-hour de-Fmoc of Fmoc-Asp(OtBu)-Ala-DDBA (Table 3.12) ... | 120 |
| Figure 3.19. DKP formation. | 121 |
| Figure 3.20. LC/MS result for the loading of Fmoc-Rink linker unto DDBA | 123 |
| Figure 3.21. LC/MS result for the de-Fmoc of Fmoc-Rink-DDBA... .. | 124 |
| Figure 3.22. Incomplete third coupling with Fmoc-Ala-OH: (a) 2.5 hours of coupling; (b) overnight coupling after the addition of second portion of DIC; (c) 30 minutes after the addition of HBTU/DIEA; (d) overnight after the addition of second portion of HBTU/DIEA. | 129 |

| | |
|--|-----|
| Figure 3.23. Incomplete fourth coupling with Fmoc-Arg(Pbf)-OH. | 130 |
| Figure 3.24. Second coupling with Fmoc-Asp(OtBu)-OH: (a) 3 hours of coupling; (b) 3 hours after the addition of second portion of Fmoc-Asp(OtBu)-OH and HBTU. | 131 |
| Figure 3.25. Third coupling with Fmoc-Ala-OH: (a) 3 hours of coupling; (b) 2 hours after the addition of second portion of Fmoc-Ala-OH/HBTU/DIEA; (c) 3 hours after the first diafiltration (5 wash volumes) and addition of third portion of Fmoc-Ala-OH/HBTU/DIEA; (d) 30 minutes after the second diafiltration (10 wash volumes) and addition of fourth portion of Fmoc-Ala-OH/HBTU/DIEA; (e) 30 minutes after the addition of fifth portion of Fmoc-Ala-OH/HBTU/DIEA; (f) 30 minutes after the addition of sixth portion of Fmoc-Ala-OH/HBTU/DIEA. | 133 |
| Figure 3.26. Fourth coupling with Fmoc-Arg(Pbf)-OH: (a) 1 hours of coupling; (b) 1 hour after the addition of second portion of Fmoc-Arg(Pbf)-OH/HBTU/DIEA; (c) 30 minutes after the addition of third portion of Fmoc-Arg(Pbf)-OH/HBTU/DIEA.... | 134 |
| Figure 3.27. Second coupling with Fmoc-Asp(OtBu)-OH: (a) 30 minutes of coupling; (b) 30 minutes after the diafiltration and addition of second portion of Fmoc-Asp(OtBu)-OH and HBTU. | 135 |
| Figure 3.28. Third coupling with Fmoc-Ala-OH: (a) 30 minutes of coupling; (b) 30 minutes after the first diafiltration (2 wash volumes) and addition of second portion of Fmoc-Ala-OH/HBTU/DIEA; (c) 30 minutes after the second diafiltration (2 wash volumes) and addition of third portion of Fmoc-Ala-OH/HBTU/DIEA. | 137 |
| Figure 3.29. Fourth coupling with Fmoc-Arg(Pbf)-OH (30 minutes of reaction). | 138 |
| Figure 3.30. LC/MS result for dried Fmoc-Arg(Pbf)-Aal-Asp(OtBu)-Ala-Rink-DDBA (3 rd attempt) ... | 139 |
| Figure 3.31. Decomposition of Rink linker during global deprotection. | 140 |
| Figure 3.32. HPLC of product after cleavage and global deprotection (peak identities based on TOF/MS result). (b) is the zoom-in image of (a). | 140 |

| | |
|--|-----|
| Figure 3.33. LC/MS result for globally deprotected product (3 rd attempt) | 141 |
| Figure 3.34. Coupling of amino acids (30 minutes of reaction): | |
| (a) First coupling with Fmoc-Ala-OH; | |
| (b) second coupling with Fmoc-Asp(OtBu)-OH; | |
| (c) Third coupling with Fmoc-Ala-OH; | |
| (d) Fourth coupling with Fmoc-Arg(Pbf)-OH. | 143 |
| Figure 3.35. LC/MS result for dried Fmoc-Arg(Pbf)-Aal-Asp(OtBu)-Ala-Rink-DDBA (4 th attempt) ... | 144 |
| Figure 3.36. HPLC of product of cleavage and global deprotection (peak identities based on TOF/MS result). | 146 |
| Figure 3.37. LC/MS result for globally deprotected product (4 th attempt) | 148 |
| Figure 3.38. Performance of MEPS relative to SPPS: | |
| (a) before cleavage and global deprotection; | |
| (b) after cleavage and global deprotection... .. | 152 |
| Figure 3.39. Material cost breakdown for SPPS and MEPS. | 154 |
| Figure 3.40. Performance of MEPS: | |
| (a) with improvement 1 before cleavage and global deprotection; | |
| (b) with improvement 1 after cleavage and global deprotection; | |
| (c) with improvement 2 after cleavage and global deprotection | 158 |
| Figure 4.1. Pyr-Ser(Bzl)-Ala-Phe-Asp-Leu-NH ₂ (partially deprotected Pyr-SAFDL-NH ₂) | 161 |
| Figure 4.2. SPPS of partially deprotected Pyr-SAFDL-NH ₂ on Fmoc-Rink resin. | 164 |
| Figure 4.3. LPPS of partially deprotected Pyr-SAFDL-NH ₂ on H ₂ N-Rink-DDBA. | 168 |
| Figure 4.4. HPLC results of cleaved and global deprotected products of SPPS: | |
| (a) 1 st attempt (1.50 eq amino acid for coupling); | |
| (b) 2 nd attempt (1.05 eq amino acid for coupling). | 175 |
| Figure 4.5. LC/MS result of the partially deprotected product (1 st attempt) | 177 |
| Figure 4.6. LC/MS result of the partially deprotected product (2 nd attempt) | 179 |

| | |
|--|-----|
| Figure 4.7. Partially deprotected Pyr-SAFDL-Rink-fragment. | 180 |
| Figure 4.8. HPLC result of global deprotected product. | 182 |
| Figure 4.9. LC/MS result of the partially deprotected product ... | 184 |
| Figure 4.10. Coupling with Fmoc-Asp(OtBu)-OH: | |
| (a) 1 hour of reaction; | |
| (b) 30 minutes after the diafiltration and addition of reagents. | 186 |
| Figure 4.11. Coupling with Fmoc-Phe-OH (30 minutes of reaction). | 187 |
| Figure 4.12. Coupling with Fmoc-Ala-OH (30 minutes of reaction). | 188 |
| Figure 4.13. Coupling with Fmoc-Ser(Bzl)-OH: | |
| (a) 30 minutes of reaction; | |
| (b) 30 minutes after the diafiltration and addition of reagents. | 190 |
| Figure 4.14. Formation of Fmoc-X-piperidine. | 191 |
| Figure 4.15. Formation of guanidine. | 194 |
| Figure 4.16. Compounds tested for the mitigation of piperidine-induced side reaction (Test 2 to 4 in Table 4.5). | 197 |
| Figure 4.17. Deprotection of Fmoc-Leu-Rink-DDBA by DEA. | 199 |
| Figure 4.18. Small-scale coupling test during diafiltration: | |
| (a) After 10 wash volumes; | |
| (b) after 12 wash volumes; | |
| (c) after 14 wash volumes; | |
| (d) after 16 wash volumes with 1.2 eq coupling reagents; | |
| (e) after 16 wash volumes with 1.5 eq coupling reagents. | 201 |
| Figure 4.19. Coupling with Fmoc-Phe-OH: | |
| (a) 30 minutes of reaction; | |
| (b) recoupling after diafiltration. | 202 |

| | |
|---|-----|
| Figure 4.20. Synthesis of fully protected Pyr-SAFDL-Rink-DDBA: | |
| (a) coupling with Fmoc-Leu-OH; | |
| (b) coupling with Fmoc-Asp(OtBu)-OH; | |
| (c) coupling with Fmoc-Phe-OH; | |
| (d) coupling with Fmoc-Ala-OH; | |
| (e) coupling with Fmoc-Ser(Bzl)-OH; | |
| (f) coupling with Pyr-OH. | 205 |
| Figure 4.21. LC/MS result of the dried fully protected Pyr-SAFDL-Rink-DDBA ... | 206 |
| Figure 4.22. HPLC result of the global deprotection product. | 210 |
| Figure 4.23. LC/MS result of the partially deprotected Pyr-SAFDL-NH ₂ ... | 212 |
| Figure 4.24. Performance of MEPS relative to SPPS (1 & 2) and LPPS: | |
| (a) before cleavage and global deprotection; | |
| (b) after cleavage and global deprotection... | 215 |
| Figure 4.25. Cost breakdown for the four processes. | 216 |
| Figure 5.1. PyPEG. | 221 |
| Figure 5.2. Two-stage membrane cascade ... | 222 |
| Figure 5.3. Schematic of the model for the single-stage membrane system. | 232 |
| Figure 5.4. (a) adipic acid and (b) hexamethylenediamine.... | 238 |
| Figure 5.5. HPLC result of crude PyPEG. | 239 |
| Figure 5.6. Synthesis of PyPEG. | 239 |
| Figure 5.7. NMR result of PyPEG. | 241 |
| Figure 5.8. Ratio of peak integration area in NMR for retentate samples during diafiltration. ... | 241 |
| Figure 5.9. HPLC results of: (a) PyPEG and (b) loading of Fmoc-Rink linker overnight. ... | 242 |
| Figure 5.10. HPLC result of Fmoc-Rink-PyPEG before diafiltration. | 244 |

| | |
|---|-----|
| Figure 5.11. HPLC results for: | |
| (a) Fmoc-A-Rink-PyPEG, | |
| (b) Fmoc-DA-Rink-PyPEG, | |
| (c) Fmoc-ADA-Rink-PyPEG and | |
| (d) Fmoc-RADA-Rink-PyPEG after post-coupling diafiltration | |
| (10 wash volumes for (a)-(c); 6 wash volumes for (d)). | 247 |
| Figure 5.12. MEPS of fully protected Pyr-SAFDL-Rink-DDBA | 249 |
| Figure 5.13. The concentrations of the relevant components in: | |
| (a) the entire first cycle of operation; | |
| (b) in the coupling and diafiltration; | |
| (c) in the de-Fmoc and diafiltration | 251 |
| Figure 5.14. Schematic of the modified single-stage membrane system. | 253 |
| Figure 5.15. Schematic of the two-stage membrane cascade system. | 254 |
| Figure 5.16. The concentrations of the relevant components in: | |
| (a) the entire first cycle of operation and coupling of Fmoc-Asp(OtBu)-OH; | |
| (b) in the coupling, diafiltration and de-Fmoc; | |
| (c) & (d) in the de-Fmoc, diafiltration and coupling | 257 |
| Figure 5.17. Performance of MEPS (Two-stage) in comparison to SPPS and MEPS (Single-stage). | 259 |

List of Tables

| | Page |
|--|-------------|
| Table 1.1. Advantages and disadvantages of peptide drugs vs traditional small-molecule drugs. | 3 |
| Table 1.2. Comparison of the chemical synthesis methods. | 7 |
| Table 2.1. Suitability of various candidates for C- or N-terminal residue. | 19 |
| Table 2.2. Summary of results for H-Tyr-Ala-Tyr-Ala-Tyr-OH. | 62 |
| Table 2.3. Summary of results for Thymopentin(TP-5). | 63 |
| Table 3.1. Summary of results for the synthesis of 2,4-didocosyloxybenzaldehyde. | 96 |
| Table 3.2. Summary of results for the reduction of 2,4-didocosyloxybenzaldehyde. | 99 |
| Table 3.3. Compounds to be removed by diafiltration during peptide synthesis. | 104 |
| Table 3.4. Compounds for rejection tests. | 109 |
| Table 3.5. Rejection data of Fmoc-Ala-OH and soluble anchors. | 111 |
| Table 3.6. Summary of results for SPPS. | 113 |
| Table 3.7. Experimental data of the de-Fmoc. | 113 |
| Table 3.8. Experimental data of the couplings. | 114 |
| Table 3.9. Loading of Fmoc-Ala-OH under different conditions. | 117 |
| Table 3.10. De-Fmoc of Fmoc-Ala-DDBA under different conditions. | 117 |
| Table 3.11. Coupling of Fmoc-Asp(OtBu)-OH under different conditions. | 118 |
| Table 3.12. De-Fmoc of Fmoc-Asp(OtBu)-Ala-DDBA under different conditions. | 118 |

| | |
|---|-----|
| Table 3.13. Summary of results for the synthesis of Fmoc-Rink-DDBA. | 122 |
| Table 3.14. Summary of results for the synthesis of H ₂ N-Rink-DDBA. | 122 |
| Table 3.15. Small-scale coupling tests at 1.0 weight% of deprotected peptide-anchor. | 125 |
| Table 3.16. Rejection tests of DDBA by ceramic membranes. | 126 |
| Table 3.17. Summary of results for the fourth attempt at MEPS. | 142 |
| Table 3.18. Experimental data of the de-Fmoc. | 142 |
| Table 3.19. Experimental data of the couplings. | 143 |
| Table 3.20. Performance of SPPS and MEPS. | 151 |
| Table 3.21. Performance of MEPS with improvements. | 157 |
| Table 4.1. Summary of results for SPPS. | 174 |
| Table 4.2. Summary of results for LPPS by precipitation. | 181 |
| Table 4.3. Summary of results for MEPS. | 185 |
| Table 4.4. Summary of results for the small-scale tests. | 192 |
| Table 4.5. Summary of results for the tests of mitigation method. | 195 |
| Table 4.6. Effect of diethylamine on activated Fmoc-Phe-OH. | 199 |
| Table 4.7. Stability tests of Fmoc-Rink linker in TFA solution. | 207 |
| Table 4.8. Cleavage tests of fully protected Pyr-SAFDL-Rink from DDBA. | 208 |
| Table 4.9. Performance of SPPS, LPPS and MEPS. | 214 |
| Table 5.1. Summary of OSN system parameters. | 229 |

| | |
|--|-----|
| Table 5.2. Rejection of anchored peptide. | 229 |
| Table 5.3. Summary of reaction conditions and results. | 230 |
| Table 5.4. Operation schedule of MEPS in the model. | 235 |
| Table 5.5. Addition of reagents for the loading of Fmoc-Rink linker over seven days | 243 |
| Table 5.6. Solvent swap during diafiltration and its effect on the removal of Fmoc-Rink linker. | 244 |
| Table 5.7. Solvent swap during diafiltration and its effect on the removal of Fmoc-Arg(Pbf)-OH. | 248 |
| Table 5.8. Performance of SPPS, MEPS (single-stage) and MEPS (Two-stage). | 259 |

Abbreviations

Chemicals

| Solvents | |
|-------------------------------------|--|
| Abbreviation | Full term |
| ACN | Acetonitrile |
| DCM | Dichloromethane |
| DMF | Dimethylformamide |
| NMP | N-Methyl-2-pyrrolidone |
| THF | Tetrahydrofuran |
| Peptide synthesis reagents | |
| Abbreviation | Full term |
| DIC | N,N'-diisopropylcarbodiimide |
| DIEA | Diisopropylethylamine |
| DMAP | 4-Dimethylaminopyridine |
| DMB | 1,3-dimethoxybenzene |
| EDT | 1,2-ethanedithiol |
| HBTU | O-(Benzotriazol-1-yl)-N,N,N',N'-tetramethyluronium Hexafluorophosphate |
| HF | Hydrogen Fluoride |
| HOBt | Hydroxybenzotriazole |
| TBTU | O-(Benzotriazol-1-yl)-N,N,N',N'-tetramethyluronium Tetrafluoroborate |
| TFA | Trifluoroacetic Acid |
| TIS | Triisopropylsilane |
| Amino acids | |
| Abbreviation | Full term |
| AA | Amino Acid |
| A | Alanine |
| D | Aspartic Acid |
| F | Phenylalanine |
| L | Leucine |
| R | Arginine |
| S | Serine |
| Amino acid protecting groups | |
| Abbreviation | Full term |
| Bn/Bzl | Benzyl |
| Boc | Tert-butyloxycarbonyl |
| Fmoc | 9-Fluorenylmethoxycarbonyl |
| Pbf | 2,2,4,6,7-pentamethyldihydrobenzofuran-5-sulfonyl |
| tBu | Tert-butyl |
| Z | Benzyloxycarbonyl |
| Anchor-related compounds | |
| Abbreviation | Full term |
| DDBA | 2,4-didocosyloxybenzalcohol |
| NCPS | Non-cross-linked Poly(styrene) |
| PEG | Poly(ethylene glycol) |
| PS | Polystyrene |
| Tbf | Tetrabenzo[a,c,g,i]fluorine |

| Others | |
|---------------------|------------------|
| Abbreviation | Full term |
| DBF | Dibenzofulvene |
| DKP | Diketopiperazine |
| TP-5 | Thymopentin |

Peptide synthesis

| Abbreviation | Full term |
|---------------------|-------------------------------------|
| LPPS | Liquid Phase Peptide Synthesis |
| MEPS | Membrane Enhanced Peptide Synthesis |
| SPPS | Solid Phase Peptide Synthesis |

Membrane Process

| Abbreviation | Full term |
|---------------------|----------------------------------|
| MF | Microfiltration |
| MW | Molecular Weight |
| MWCO | Molecular Weight Cut-Off |
| NF | Nanofiltration |
| OSN | Organic Solvent Nanofiltration |
| PANI | Polyaniline |
| PE | Polyethylene |
| PES | Polyethersulfone |
| PI | Polyimide |
| PP | Polypropylene |
| RO | Reverse Osmosis |
| SRNF | Solvent Resistant Nanofiltration |
| UF | Ultrafiltration |

Analytical Techniques

| Abbreviation | Full term |
|---------------------|--|
| AFM | Atomic Force Microscopy |
| FTIR-ATR | Fourier Transform Infrared- Attenuated Total Reflectance |
| HPLC | High-Performance Liquid Chromatography |
| LC/MS | Liquid Chromatography/Mass Spectroscopy |
| MS | Mass Spectroscopy |
| NMR | Nuclear Magnetic Resonance |
| SEM | Scanning Electron Microscopy |
| TEM | Transmission Electron Microscopy |
| UV | Ultraviolet |
| XPS | X-ray Photoelectron Spectroscopy |

Others

| Abbreviation | Full term |
|---------------------|-----------------------------------|
| CAS | Chemical Abstract Service |
| DNA | Deoxyribonucleic Acid |
| FDA | Food and Drug Administration (US) |
| GMP | Good Manufacturing Practice |
| LD ₅₀ | Lethal Dose, 50% |

Nomenclature

| | |
|------------------------------------|--|
| C_{initial} | Initial concentration of a particular compound ($kmol \cdot m^{-3}$) |
| C_{final} | Final concentration of a particular compound ($kmol \cdot m^{-3}$) |
| [AA] | Concentration of amino acid ($kmol \cdot m^{-3}$) |
| [Compound] | Concentration of compound in the reactor ($kmol \cdot m^{-3}$) |
| [Compound]_{in} | Concentration of compound in the stream that goes into the reactor ($kmol \cdot m^{-3}$) |
| [P_{deprotected}] | Concentration of deprotected anchored peptide ($kmol \cdot m^{-3}$) |
| [P_{protected}] | Concentration of protected anchored peptide ($kmol \cdot m^{-3}$) |
| [piperidine] | Concentration of piperidine ($kmol \cdot m^{-3}$) |
| F_{in} | Volumetric flow rate into the reactor ($m^3 \cdot s^{-1}$) |
| F_{out} | Volumetric flow rate out of the reactor ($m^3 \cdot s^{-1}$) |
| k_{coupling} | Rate constant for coupling ($kmol \cdot m^{-3} \cdot s^{-1}$) |
| k_{deFmoc} | Rate constant for deFmoc ($kmol \cdot m^{-3} \cdot s^{-1}$) |
| Mass_{nanoparticle} | Mass of amine-functionalised silica nanoparticles (g) |
| R_{generation} | Rate of generation ($kmol \cdot m^{-3} \cdot s^{-1}$) |
| R_{consumption} | Rate of consumption ($kmol \cdot m^{-3} \cdot s^{-1}$) |
| R_{ej} | Rejection (<i>dimensionless</i>) |
| t | Reaction time (s) |
| u | Axial flow rate in the pipe ($m \cdot s^{-1}$) |
| V | Volume of reactor (m^3) |
| V_{HCL_Standard} | Volume of hydrochloric acid stand (mL) |
| V_{NaOH_Standard} | Volume of sodium hydroxide stand (mL) |
| V_{NaOH_test} | Volume of hydrochloric acid used in the test (mL) |
| W | Wash volume (<i>dimensionless</i>) |
| x | Displacement from the pipe inlet (m) |

Chapter One - Introduction

1.1. Peptides and Their Applications

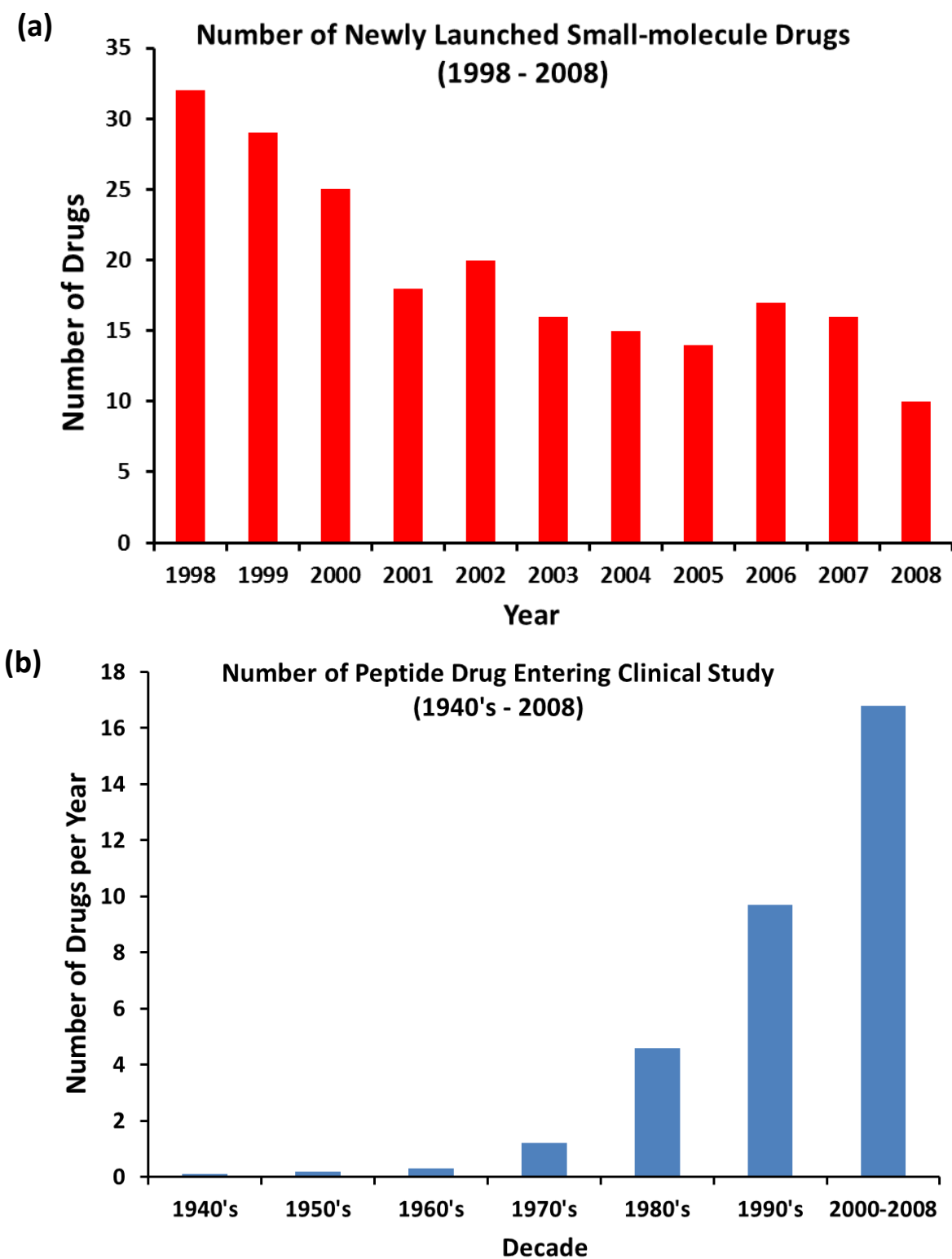


Figure 1.1. (a) Number of newly launched small-molecule drugs from 1998 to 2008 (Trusheim, Aitken & Berndt, 2010). (b) Number of peptide drugs entering clinical study from 1940's to 2008 (Peptide Therapeutics Foundation, 2010).

Peptides and proteins are polymers of amino acids, which are joined by the amide bond. The former is loosely defined as a polymer of less than 50 amino acids in order to differentiate it from the latter (Craik et al., 2013). This group of compounds often serve to control, direct and/or coordinate inter- and intracellular communications and cellular functions in living systems (Korhonen & Pihlanto, 2006; Danquah & Agyei, 2012). Many bioactive peptides, which are defined as specific protein fragments that have positive biological effects on the human body, have been subjected to extensive studies over the past decades (McLay, Pan & Kastin, 2001; Yu et al., 2004). The findings of such studies have enabled the application of bioactive peptides in agriculture (Keymanesh & Soltani, 2009), food packaging (Espitia et al., 2012) and medicine (Kelley, 1996; Korhonen & Pihlanto, 2006; Tauzin, 2008; Leader, Baca & Golan, 2008; Lax, 2010; Thayer, 2011; Silva & Machado, 2012; Danquah & Agyei, 2012; Phylogica, 2012; Craik et al., 2013).

Historically, small molecules have dominated the drug development in the 20th century, especially those with molecular weight (MW) below 500 Dalton due to their oral bioavailability. However, it has become extremely difficult to identify potential drug candidates from the small-molecule pool after decades of intense research and development, resulting in a steady decline in the number of new small-molecule drugs as shown in Figure 1.1 (a).

At the same time, the synthesis, purification and analysis technologies for bioactive peptides have become mature enough to show that peptides are indeed better than the traditional small-molecule compound in a number of ways (Table 1.1). For instance, bioactive peptides can bind specifically to their *in vivo* targets and hence cause fewer off-target side-effects in patients than their small-molecule counterparts.

Table 1.1. Advantages and disadvantages of peptide drugs compared to traditional small-molecule drugs (Craik et al., 2013).

| Advantage | Disadvantage |
|---|---|
| High selectivity High potency Broad range of targets Potentially lower toxicity Low accumulation in tissues High chemical and biological diversity Discoverable at peptide and/or nucleic acid levels | Poor metabolic stability Poor membrane permeability Poor oral bioavailability High production cost Rapid clearance Poor solubility in some cases |

Therefore, bioactive peptides have attracted immense interest in the pharmaceutical industry, which can be illustrated by the consistent increase in the number of peptide drugs entering clinical studies over the past three decades (Figure 1.1 (b)). In the 1970s, only 1.2 peptide drug entered clinical study per year, but the number increased significantly to 4.6 in the 1980s, 9.7 in 1990s and subsequently 16.8 between 2000 and 2008 (Peptide Therapeutics Foundation, 2010). This growth is expected to continue as the pharmaceutical community invests more resources into this field of research. In 2010, there were already 360 peptide drugs in different stages of clinical studies (57 approved, 91 in phase I, 99 in phase II, 113 in phase III and pre-registration) (Peptide Therapeutics Foundation, 2010). In the same year, 60 peptide drugs had combined sales near US\$13 billion worldwide and the market for peptide drugs was expected to grow in the foreseeable future (Phylogica, 2012).

One famous example of a bioactive peptide is insulin, the pancreatic hormone that regulates the blood sugar level in animals. Diabetes patients suffer from a deficiency of insulin, a condition that can lead to death if left untreated.

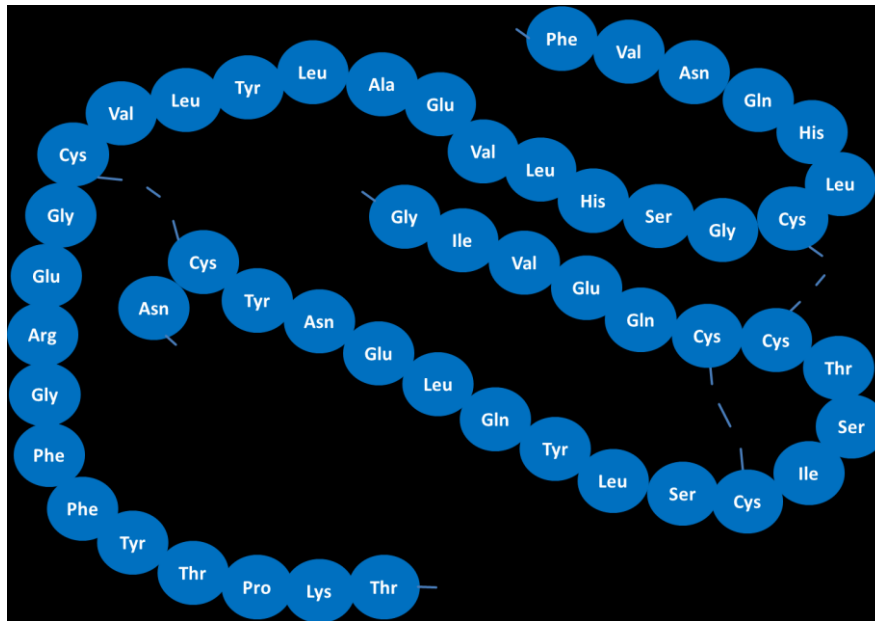


Figure 1.2. Sequence of human insulin.

First isolated from the pancreatic extracts of dogs in 1921-1922, insulin was produced at commercial scale from cattle or pig pancreases for the following decades until the 1980s when recombinant DNA technology enabled the large-scale production of human insulin (Figure 1.2) by inserting its gene into the *Escherichia coli* bacterial cell. Subsequent developments in the production technology have gradually phased out the use of bovine and porcine insulin, which can induce rejection in some patients (Sneader, 2001).

1.2. Chemical Synthesis and Membrane Enhanced Peptide Synthesis (MEPS)

During the development of a peptide drug, the required quantity and delivery time affect the choice of synthesis methods. In general, three methods are available: chemical synthesis, enzymatic synthesis and DNA recombinant synthesis (Figure 1.3). Chemical synthesis has significantly shorter process development time, but higher cost of goods compared to the other two methods which are normally developed for long-term large-scale production. In this research, peptides were synthesised via the chemical route that is discussed in depth below.

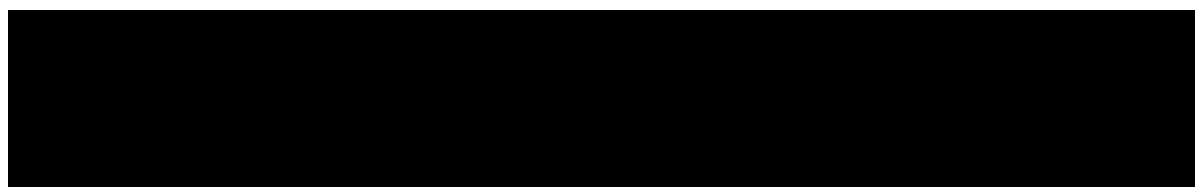


Figure 1.3. Peptide synthesis methods.

Conventional chemical synthesis consists of Solid Phase Peptide Synthesis (SPPS) and Liquid Phase Peptide Synthesis (LPPS) (Figure 1.4). The former is mainly used for step-by-step synthesis of peptides of moderate length (10- to 20-mer; anything longer is still possible on a case-by-case basis). The target peptide is grown on insoluble polymer resins, which are functionalised with linkers. The elongation of peptide is achieved by cycles of N-terminus deprotection of the peptide fragment, isolation (washing and microfiltration), coupling and isolation (washing and microfiltration). Long peptides (20- to 50- mer) are usually split into fragments that are synthesised stepwise by SPPS, followed by the condensation of fragments, which can be performed either in liquid phase (as in LPPS) or on a resin-bound peptide fragment (as in Convergent SPPS). On the other hand, LPPS can be used for the synthesis of short peptides (usually less than 10 amino acids) and fragment condensations (as mentioned above). It comprises similar cycles of N-terminus deprotection, isolation, coupling and isolation, but the isolation step involves time-consuming extraction,

precipitation, microfiltration and drying. Detailed explanation of SPPS and LPPS can be found in Section 2.1.3.

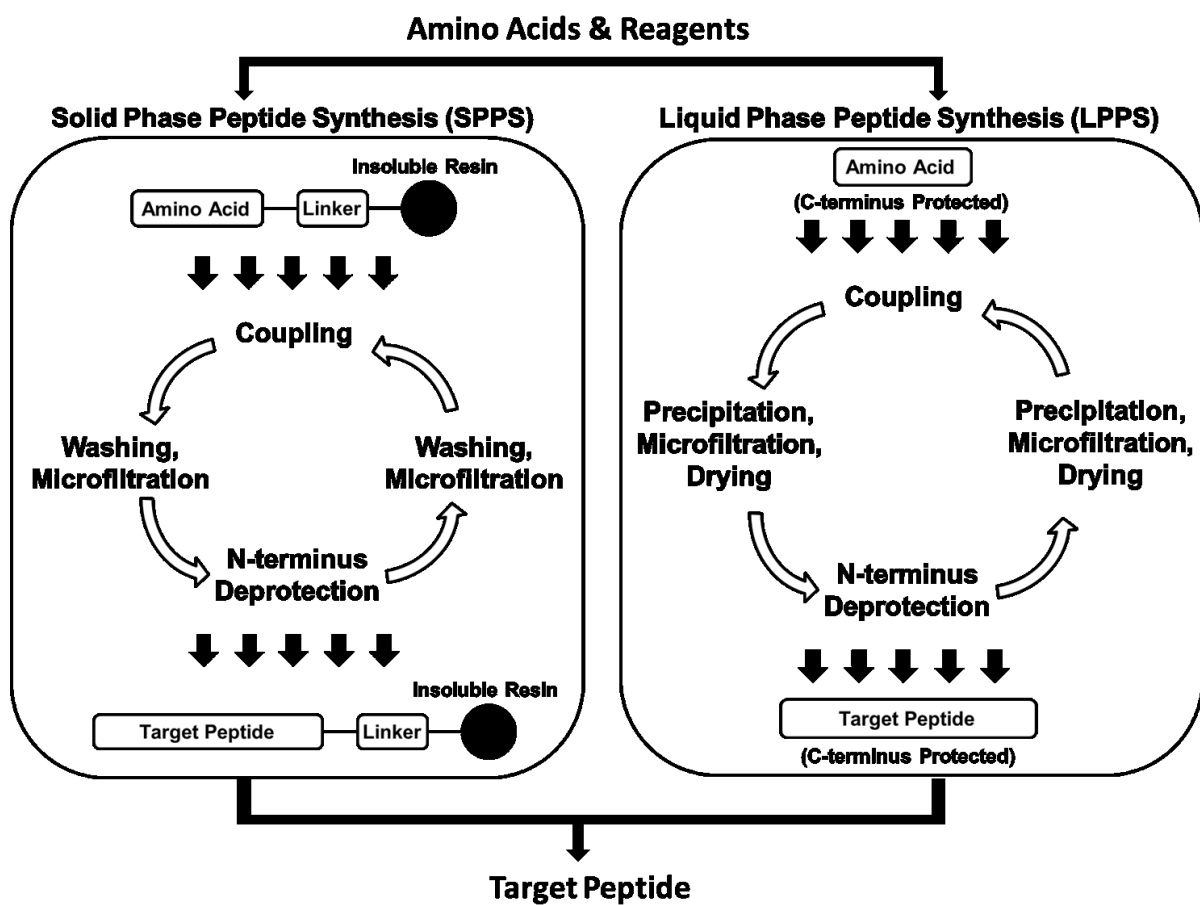


Figure 1.4. Conventional chemical synthesis methods.

As summarised in Table 1.2, SPPS is advantageous in terms of process development time and cycle time as the isolation of the resin-bound intermediate product by microfiltration is simple and quick. LPPS has lower cost of goods as couplings can be achieved with close-to-equivalent quantities of amino acids and coupling reagents. Out of the two methods, only SPPS is automatable, as LPPS is laborious due to the isolation steps. On the other hand, LPPS normally has less complicated impurity profiles than SPPS, making purification of the target peptide easier (Werbitzky, 2004; Bourgin, 2005).

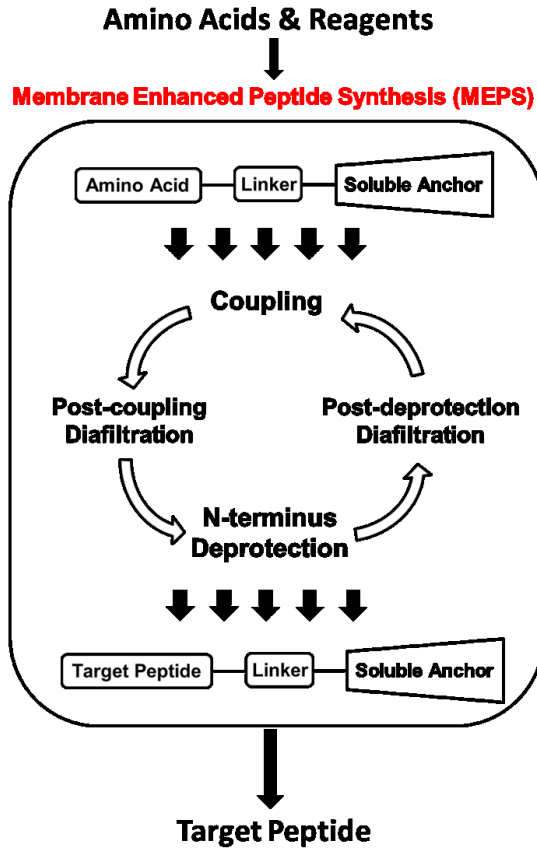
Table 1.2. Comparison of the chemical synthesis methods (Werbitzky, 2004; Bourgin, 2005).

| | SPPS | LPPS | MEPS* |
|---------------------------------|---|--|---|
| Process Development Time | Short | Long | Short |
| Cycle Time | | | |
| Cost of Goods | High | Low | Low |
| Length of Peptide | 10-50 mer or < 10 mer (for fragment condensations with LPPS or Convergent SPPS) | < 10 mer | < 50 mer |
| Scale per Batch | Grams to kilograms | Grams to tons | Grams to tons |
| Advantages | <ul style="list-style-type: none"> • Short process development time and cycle time • Scalable and automatable | <ul style="list-style-type: none"> • Method of choice for short peptides • Less expensive raw materials with BOC, Cbz strategy • Normally simple impurity profile • Scalable | <ul style="list-style-type: none"> • Scalable and automatable • Often simple impurity profile • Lower cost of goods compared to SPPS • Shorter process development time and cycle time compared to LPPS |
| Disadvantages | <ul style="list-style-type: none"> • Expensive raw materials • Often complicated impurity profile | <ul style="list-style-type: none"> • Limitation in the length of peptide • Laborious • Long process development time and cycle time | <ul style="list-style-type: none"> • Higher solvent cost due to large volumes of solvent for diafiltrations • Loss of intermediate products through diafiltrations |

*Note: prospects of the new process.

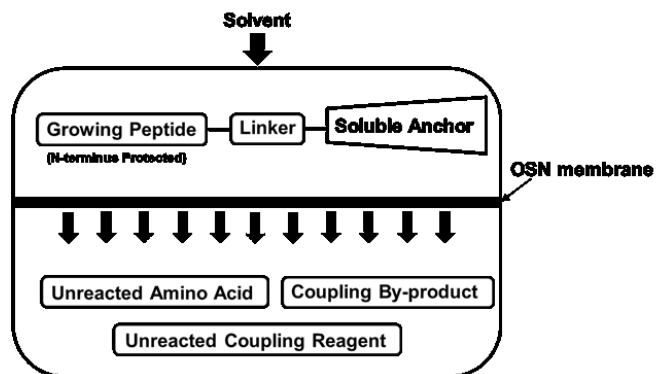
In this thesis, the new technology to be explored in depth is Membrane Enhanced Peptide Synthesis (MEPS) (Figure 1.5) (So, 2009; So et al., 2010b). The innovation lies in the utilisation of a functionalised soluble anchor for peptide synthesis, which allows the anchored intermediate products to be retained by OSN membranes during diafiltration. Compared with the isolation steps in LPPS (extraction/precipitation/microfiltration/drying), the diafiltration step in MEPS not only is automatable, but also has significantly shorter process time by simply using a system with high membrane area/volume ratio. As shown in Table 1.2, MEPS is expected to have lower cost of goods compared to SPPS, but shorter process development time and cycle time compared to conventional LPPS. Furthermore, it is expected to be suitable for both short and long peptides, scalable from grams to tons and automatable. Similar to LPPS, it should have less complicated impurity profile than SPPS. The foreseeable shortcomings are higher solvent cost and higher E-factor due to the large amount of solvent used for diafiltration after each reaction step and the loss of anchored peptide through membrane during diafiltration. Detailed explanation of MEPS can be found in the Section 2.2.13.

(a)



(b)

Post-coupling Diafiltration



Post-deprotection Diafiltration

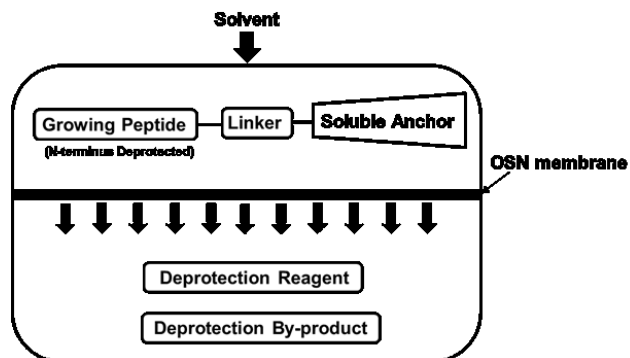


Figure 1.5. Membrane Enhanced Peptide Synthesis (MEPS): (a) the overall concept; (b) removal of impurities during diafiltration.

1.3. Research Strategy

1.3.1. Background

The research project was part of the MemTide (“Membrane Enhanced Tide Synthesis”) consortium, which consisted of three universities (Imperial College London (UK), Institut de Recerca Biomèdica (IRB) (Spain) and University of Turku (Finland)) and three companies (Evonik Membrane Extraction Technology (MET) Ltd (UK), Janssen Pharmaceutica (Belgium) and Lonza AG (Switzerland)).

Four highly specialised research partners collaborated closely in the peptide synthesis cluster for the further development of MEPS. Lonza AG is a global leader in peptide manufacturing, where the author was based at and worked on the process development by combining the different elements that were provided by the corresponding partners (Figure 1.6). Evonik MET Ltd is a specialist of OSN membrane, whereas Professor Andrew Livingston’s research group from Imperial College London is an expert of OSN system and Professor Fernando Albericio’s research group from IRB has extensive knowledge about peptide chemistry and soluble anchor for peptide synthesis.

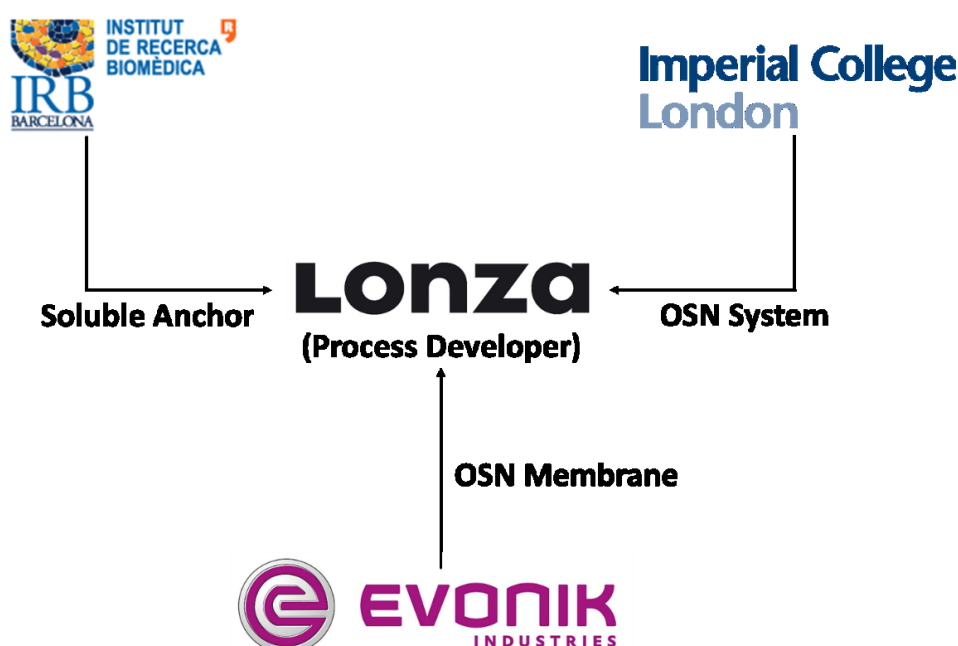


Figure 1.6. Peptide synthesis cluster in the MemTide consortium.

1.3.2. Aim and Objectives

1.3.2.1. Overall Aim

This research project aimed to scale up the recently developed MEPS from a few grams of peptide in the proof of concept study to tens of grams of peptide, laying the foundation for its adoption for industrial application.

1.3.2.2. Specific Objectives

1. Obtain an in-depth understanding of the technology by assessing critically:
 - the peptide chemistry on soluble anchor;
 - the separation performance of anchored peptide from impurities by the nanofiltration membrane;
 - the performance of MEPS compared to existing peptide synthesis technologies (i.e. SPPS and LPPS);
 - the alternatives (e.g. different kinds of anchors) that can be adopted by MEPS to improve its performance.
2. Improve the process in terms of various performance metrics (yield, purity, material cost and process time etc) and make it a competitive alternative to SPPS.

1.3.3. Research Strategy

The proof of concept for MEPS was established by Dr. Sheung So (So, 2009; So et al., 2010a; So et al., 2010b). Various aspects of the process including the choice of membrane and soluble anchor were modified during the scale-up of MEPS in this study in order to demonstrate the technical viability

and cost competitiveness of MEPS in comparison to SPPS, which has been the most commonly used method for peptide synthesis in industry over the past three decades.

In terms of technical viability, experiments were designed to show that MEPS could achieve high yield and purity of product. The critical issues that affected the performance of MEPS were identified and investigated in order to offer mitigations. For cost competitiveness, the total material costs for SPPS and MEPS were compared and the technical parameters that could provide significant improvement for the cost of MEPS were identified so that they could be investigated in the future.

The MEPS of a tetrapeptide and a hexapeptide were presented in the form of case studies. The first case study (Chapter Three) served to integrate the components provided by different research partners in the MemTide consortium (Figure 1.6) for the MEPS of the model peptide. Based on the lessons learned from this case study, the MEPS of the second model peptide (Chapter Four) was performed with refinements to further improve its overall performance relative to SPPS, which represents the state of the art for peptide synthesis technology.

After the two case studies of MEPS, several alternatives were explored both experimentally and computationally (Chapter Five) for the further improvement of the novel process, in order to make it an attractive alternative to the existing peptide synthesis method.

Chapter Two – Literature Review

2.1. Peptide Chemistry

2.1.1. Overview

Since the pioneering works of Vigneaud and Merrifield for LPPS (Vigneaud et al., 1953) and SPPS (Merrifield, 1963), peptide chemistry has gradually evolved into a mature field of research. This section presents the general principles of peptide synthesis and the detailed explanation of the relevant chemistry that was applied in this research project. Readers should refer to many reviews and books available for a broader coverage of the topic (Lloyd-Williams, Albericio, & Giralt, 1997; Albericio, 2000; Benoiton, 2005; Bodanszky, 1985; Fields & Noble, 1990; Okada, 2001; Montalbetti & Falque, 2005; Jung, Wiehn, & Braese, 2007; Isidro-Llobet, Alvarez, & Albericio, 2009).

2.1.2. From Amino Acids to Peptide

Amino acids are the building blocks of peptides and proteins, comprising 21 natural and hundreds of unnatural ones. Figure 2.1 shows the general structure of an amino acid that consists of an amino group, a carboxyl group and a side-chain (R). The classification of amino acid is based on the properties of the side-chain. For example, alanine (Ala) with a methyl side-chain is nonpolar, whereas aspartic acid (Asp) with a methyl carboxylic acid side-chain belongs to the opposite category. By convention, the sequence of a peptide is written in the N- to C-terminus direction (H-AA₁-AA₂-...-AA_n-OH), but the synthesis proceeds in the opposite direction (Figure 2.2).

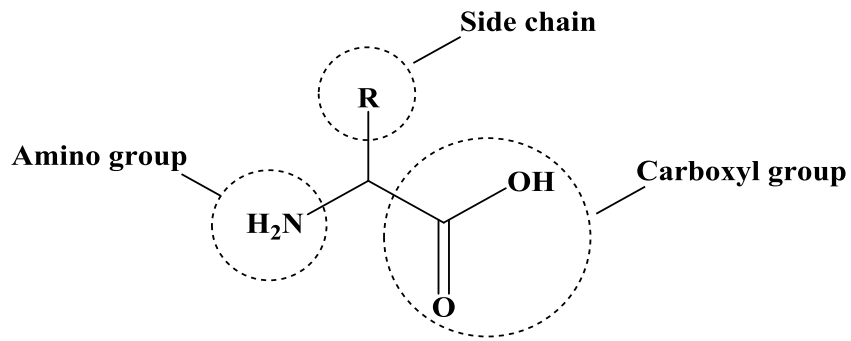


Figure 2.1. General structure of an amino acid.

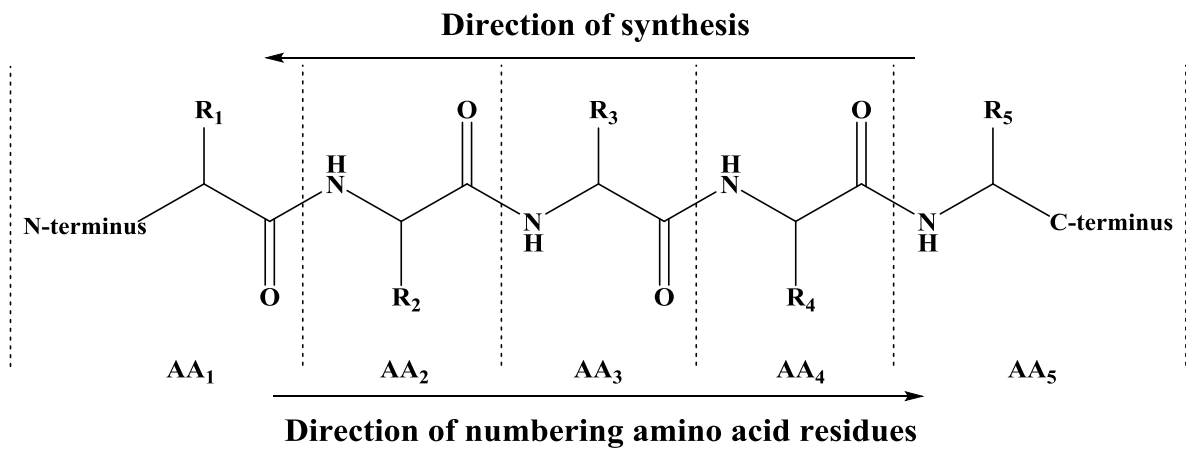


Figure 2.2. General structure of a pentamer (i.e. five-amino-acid peptide).

2.1.3. Peptide Synthesis

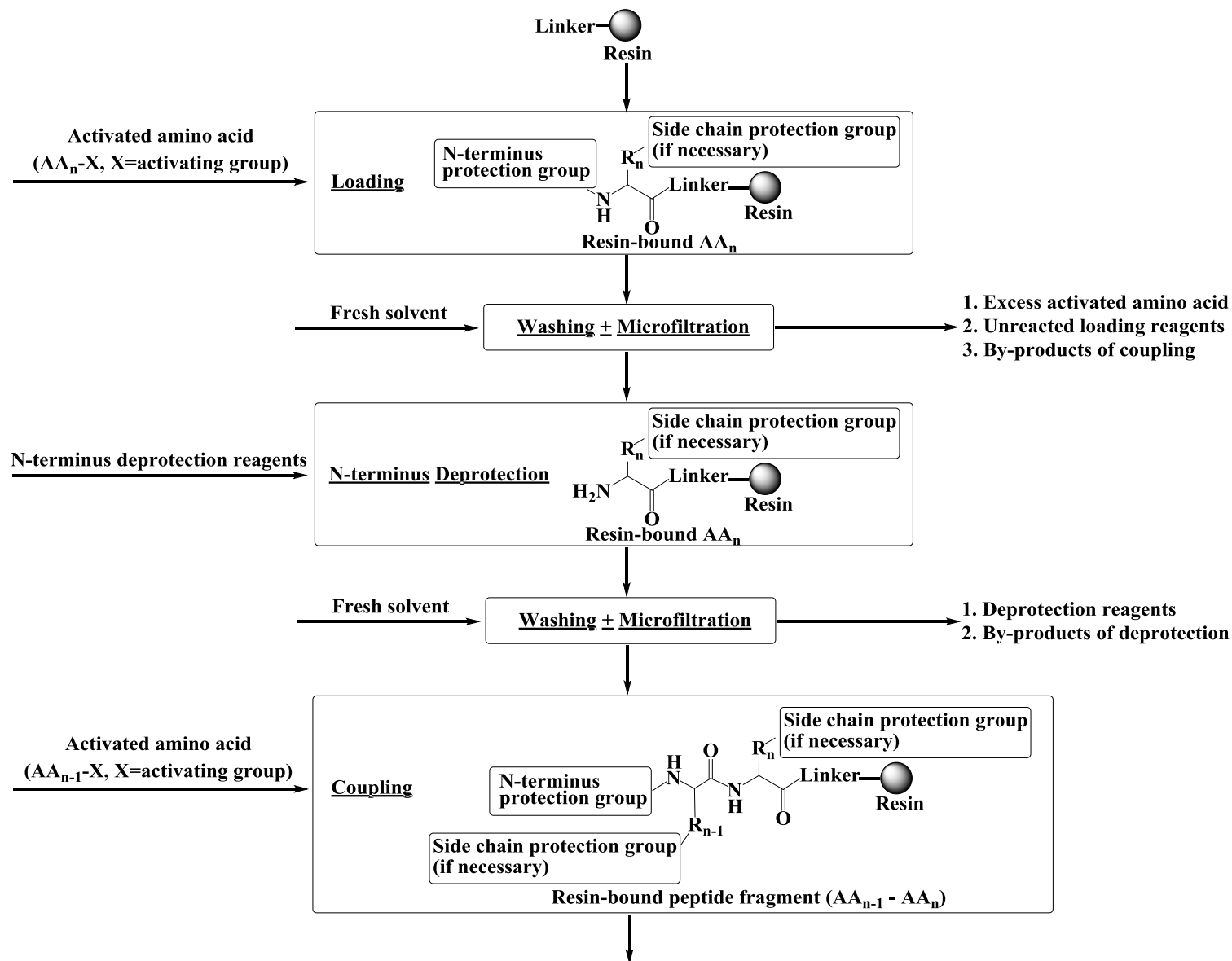
Peptide synthesis can be classified into Solid Phase Peptide Synthesis (SPPS) or Liquid Phase Peptide Synthesis (LPPS). The last amino acid in the sequence (AA_n in Figure 2.2) is the starting point of synthesis. To ensure the peptide elongation goes in the C- to N-terminus direction, this amino acid has protection for its C-terminus that determines the isolation method of subsequent intermediate products and the state, in which peptide synthesis proceeds.

In SPPS (Figure 2.3), the last amino acid is attached to the resin via a linker, which influences the cleavage of peptide from the resin after the completion of peptide elongation (Jung, Wiehn, & Braese, 2007; Martin & Albericio, 2008). Throughout the synthesis, the resin remains insoluble, allowing the bound peptide to be isolated by simple microfiltration.

The resin comprises micro-meter-size beads that are made of polymeric material which have multiple linkers embedded in their polymeric matrix (Sarin, Kent, & Merrifield, 1980; Sherrington, 1998; Czarnik, 1998; Garcia Martin & Albericio, 2008). The resin beads swell in the presence of solvent, allowing the activated amino acids and other reagents to diffuse through the polymeric matrix to reach the active sites. As the peptide increases in length, the interaction between the peptide and polymeric matrix has a large influence on the solvation of peptide and consequently the difficulty of further elongation. Therefore, the choice of resin (type of polymer and extent of linker loading ($\text{mmol} \cdot \text{g}^{-1}$ resin)) is an important consideration for SPPS.

Generally, the resin is allowed to swell in solvent before being used for the loading of amino acid (Figure 2.3), after which the excess reagents and by-products of loading are removed through a microfilter that retains the resin-bound amino acid. Washing of the resin-bound compound is repeated with fresh solvent before its N-terminus deprotection and a few more cycles of washing for the removal of deprotection reagents. The next amino acid is then activated and coupled to the free

amino group of the resin-bound compound. Cycles of N-terminus deprotection of peptide fragment and coupling with new amino acid are then repeated for the elongation of peptide, after which the peptide is globally deprotected (and cleaved from the resin simultaneously), isolated and finally dried (note: it is also possible to cleave the peptide from the resin in the fully protected form before global deprotection) (Kent, 1988; Fields & Noble, 1990; Amblard et al., 2006; Coin, Beyermann, & Bienert, 2007; Perez Espitia et al., 2012).



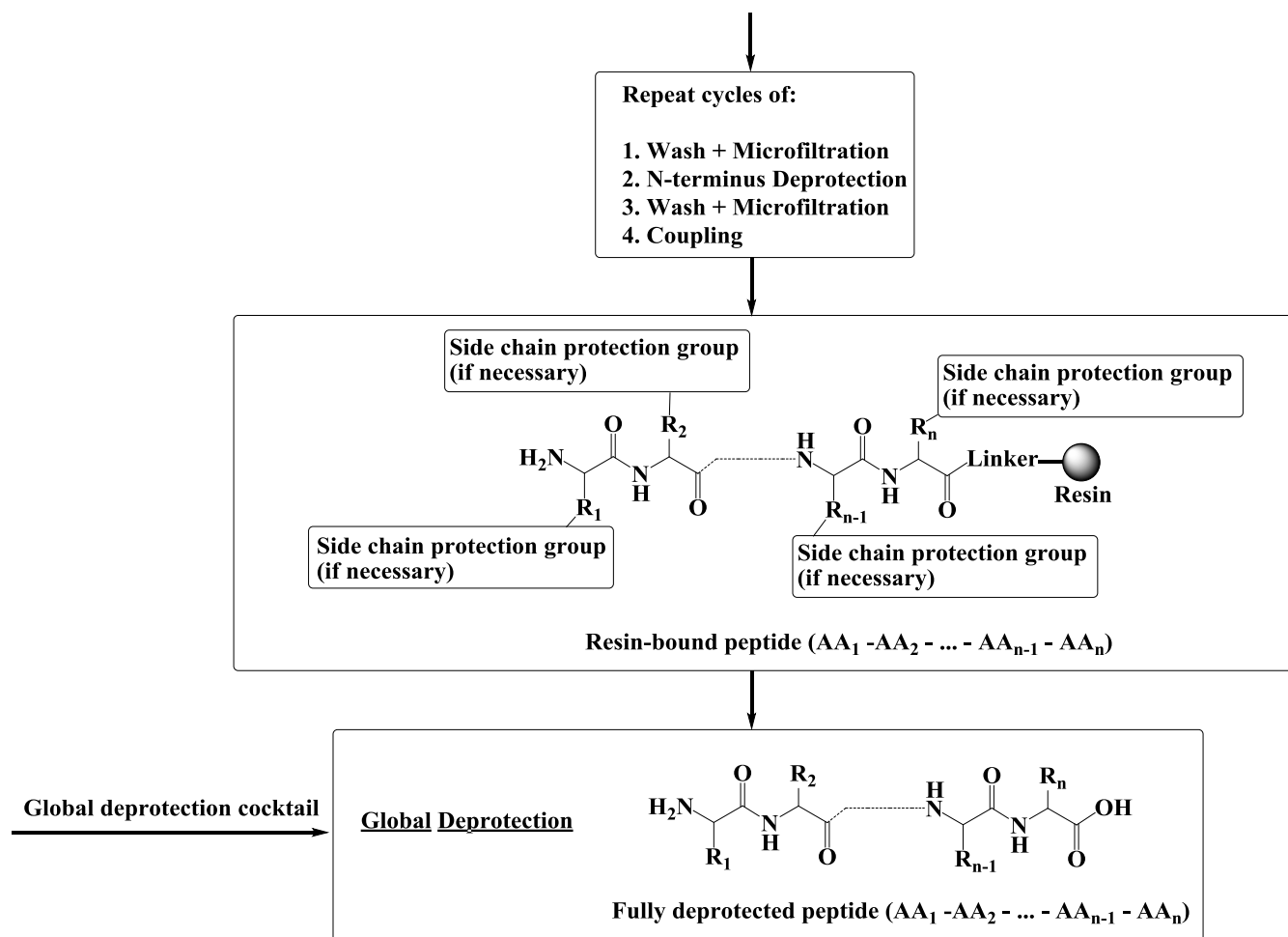


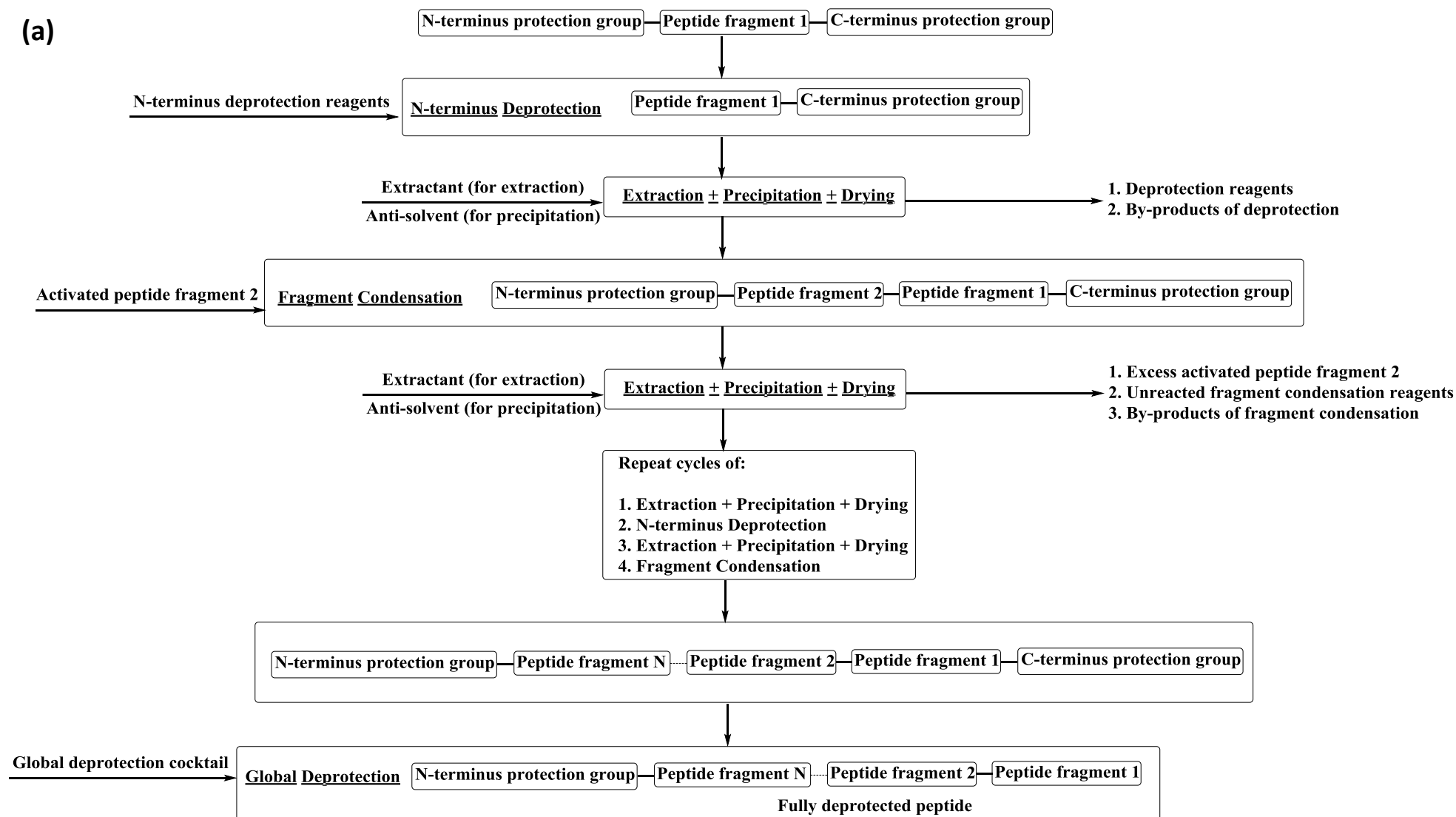
Figure 2.3. Typical procedure for stepwise SPPS (note: it is also possible to cleave the peptide from the resin in the fully protected form before global deprotection).

Stepwise SPPS up to 50 amino acid residues is possible (Barany & Merrifield, 1979), but long peptides (20- to 50-mer) are usually synthesised through fragment synthesis and condensation by a hybrid of SPPS and LPPS, and sometimes by Convergent SPPS. The long sequence is first split into several fragments for concurrent stepwise syntheses by SPPS. The fragment condensations can then be carried out with the similar coupling and N-terminus deprotection chemistry by LPPS (Figure 2.4 (a)) or on solid support (Figure 2.4 (b)). (Note: fragment condensation can also be achieved by orthogonal peptide ligation, which was not employed in this study and is hence not covered in the following section. Interested readers can refer to several reviews on this topic (Tam, Yu, & Miao, 1999; Tam, Xu, & Eom, 2001; Malins, Mitchell, & Payne, 2014).) These approaches minimise the cumulative loss of yield in the stepwise synthesis (Kelley, 1996), allow more robust quality control of the intermediate products, and significantly shorten the overall process time. To ensure fast coupling and avoid side reactions, the choice of fragments must be considered carefully. In general, the N-terminus should not have amino acids that are prone to racemisation. In addition, an amino acid with a sterically hindered structure should not be the C- or N-terminus of a fragment in order to avoid prolonged fragment condensation during which racemisation can occur (Sakakibara, 1999). Table 2.1 shows the suitable candidates for C- or N-terminal residue.

Table 2.1. Suitability of various candidates for C- or N-terminal residue (Sakakibara, 1999).

| For C-terminal Residue | | |
|--|------------------------------------|---|
| Suitable | Acceptable | Not Suitable |
| Ala, Asn, Gln, Glu(OcHx), Gly, Hyp(Bzl), Leu, Pro | Asp(OcHx), Lys(ClZ), Met, Ser(Bzl) | Arg(Tos), Cys(Acm), His(Bom), Ile, Phe, Thr(Bzl), Trp(Hoc), Tyr(BrZ), Tyr(Pen), Val |
| For N-terminal Residue | | |
| Suitable | Acceptable | Not Suitable |
| Ala, Asn, Asp, Arg, Gln, Glu, Gly, His, Leu, Lys, Met, Phe, Ser, Thr, Trp, Tyr | Ile, Val | Hyp, Pro |

(a)



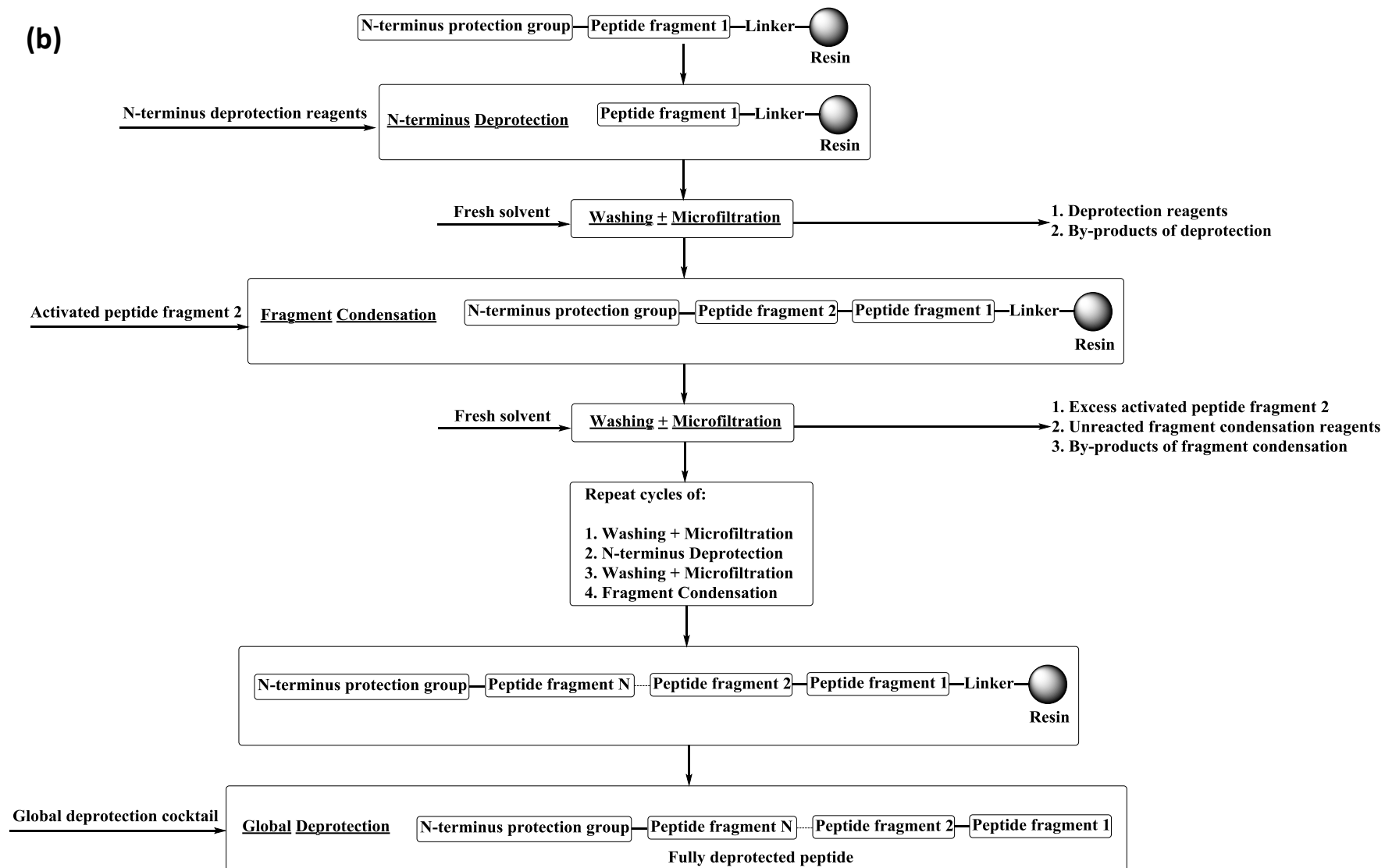
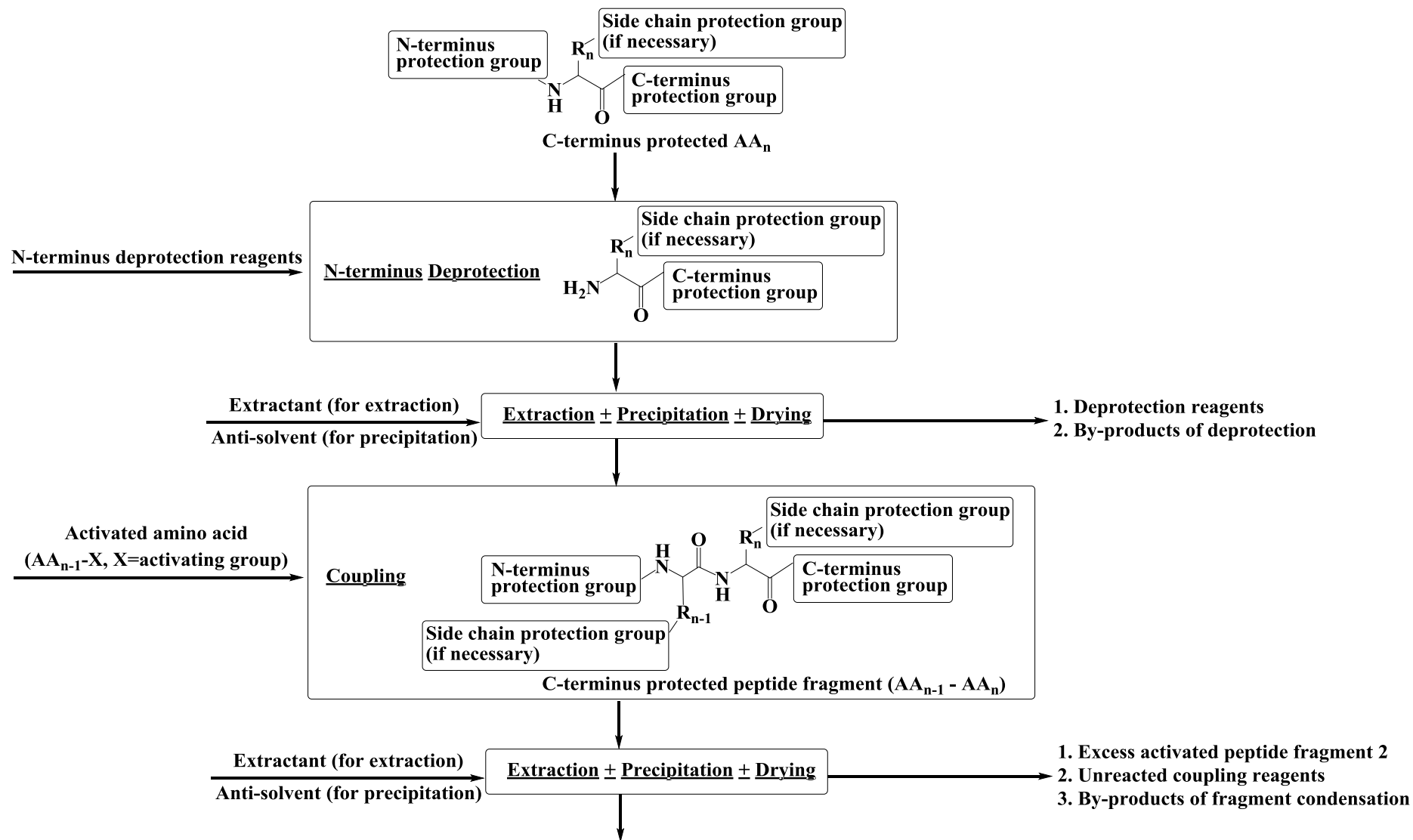


Figure 2.4. (a) SPPS-LPPS hybrid. (b) Convergent SPPS. (Note: it is also possible to cleave the peptide from the C-terminus protection group or from the linker-resin in the fully protected form before global deprotection)

Peptide synthesis in liquid phase is conventionally referred to as “Solution Phase Peptide Synthesis” or “Liquid Phase Peptide Synthesis” in literature. Both methods use similar chemistry for peptide elongation as in SPPS, but differ in terms of the C-terminus protection of the polymer. The former utilises small protecting groups such as benzoyl (Obzl), while the later utilises bulky soluble anchors such as polymers.

Stepwise Solution Phase Peptide Synthesis is limited to short peptides, as long ones usually have solubility problems in common organic solvents (Okada, 2001; Kuroda et al., 2001; Carpino et al., 2003; Meneses, Nicoll, & Trembleau, 2009; Peterson et al., 2010; Reddy et al., 2012). As a result, long peptides are usually split into fragments that have less than ten amino acid residues for stepwise syntheses (Sakakibara, 1999), and the choice of C- and N-terminal residues follows the similar rule as mentioned earlier (Table 2.1). After another amino acid is coupled to the C-terminus protected amino acid, the intermediate product can be isolated by extraction (the intermediate product remains in the organic phase, while excess reagents and by-products are removed by acidic or basic aqueous solution), precipitation, microfiltration and drying. The peptide fragment then undergoes N-terminus deprotection and another isolation cycle. Peptide elongation is achieved by repeating cycles of coupling, isolation, N-terminus deprotection and isolation as shown in Figure 2.5 (a). A similar procedure is employed for fragment condensation as discussed previously (Figure 2.5 (b)).



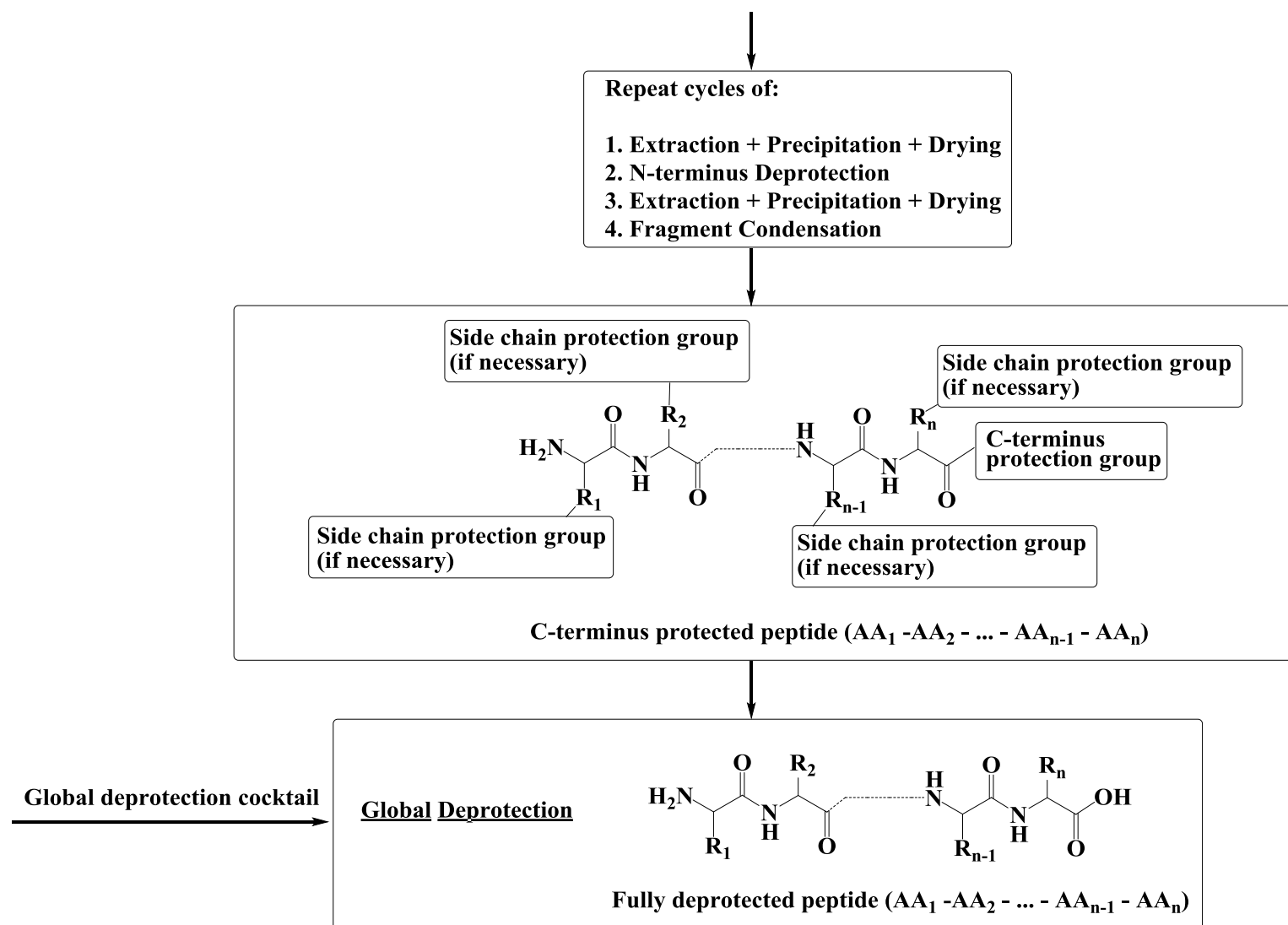


Figure 2.5. Typical procedure for fragment synthesis in solution phase peptide synthesis. (Note: it is also possible to cleave the peptide from the C-terminus protection group in the fully protected form before global deprotection)

On the other hand, stepwise Liquid Phase Peptide Synthesis can synthesise long peptide on a soluble anchor (an example is shown in Figure 2.6 (b)), which improves the solubility of long peptides in organic solvents and facilitates the isolation of intermediate products (Figure 2.7). For example, peptides can be grown on soluble poly(ethylene glycol) (PEG) and then precipitated by an anti-solvent (Mutter, Hagenmaier, & Bayer, 1971; Bayer & Mutter, 1972; Pillai et al., 1980) or grown on a phase tag that improves the efficiency of extraction (Yoshida & Itami, 2002). In MEPS, the anchored peptide is retained by the OSN membrane during diafiltration, in which excess reagents and by-products permeate through the membrane. Since the extent of anchor retention determines the overall yield of peptide synthesis, the choice of anchor is of paramount importance in such a process.

In this research project, two peptides were synthesised via stepwise elongations by both solid-phase and liquid-phase routes, which utilised Fmoc-Rink amide resin and H₂N-Rink-DDBA for C-terminus protection respectively (Figure 2.6).

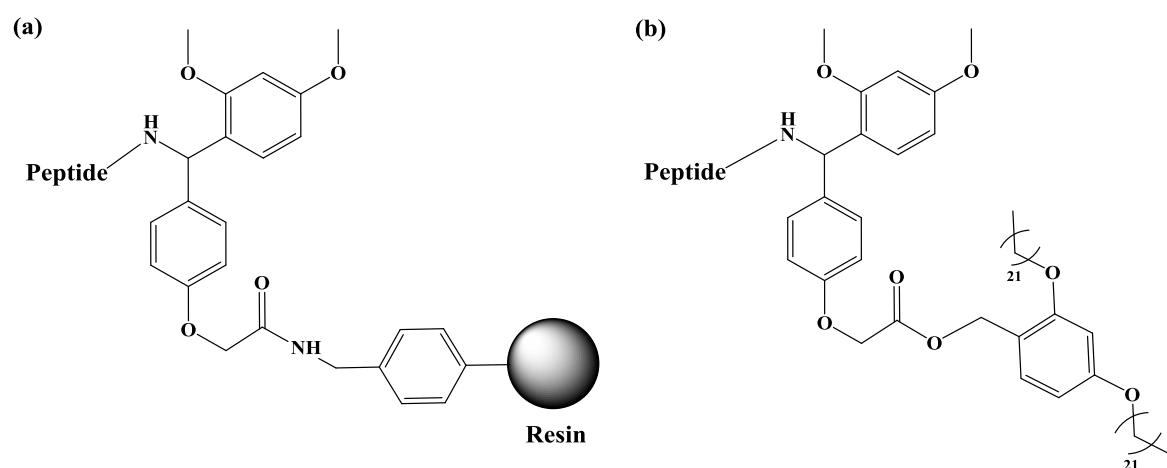
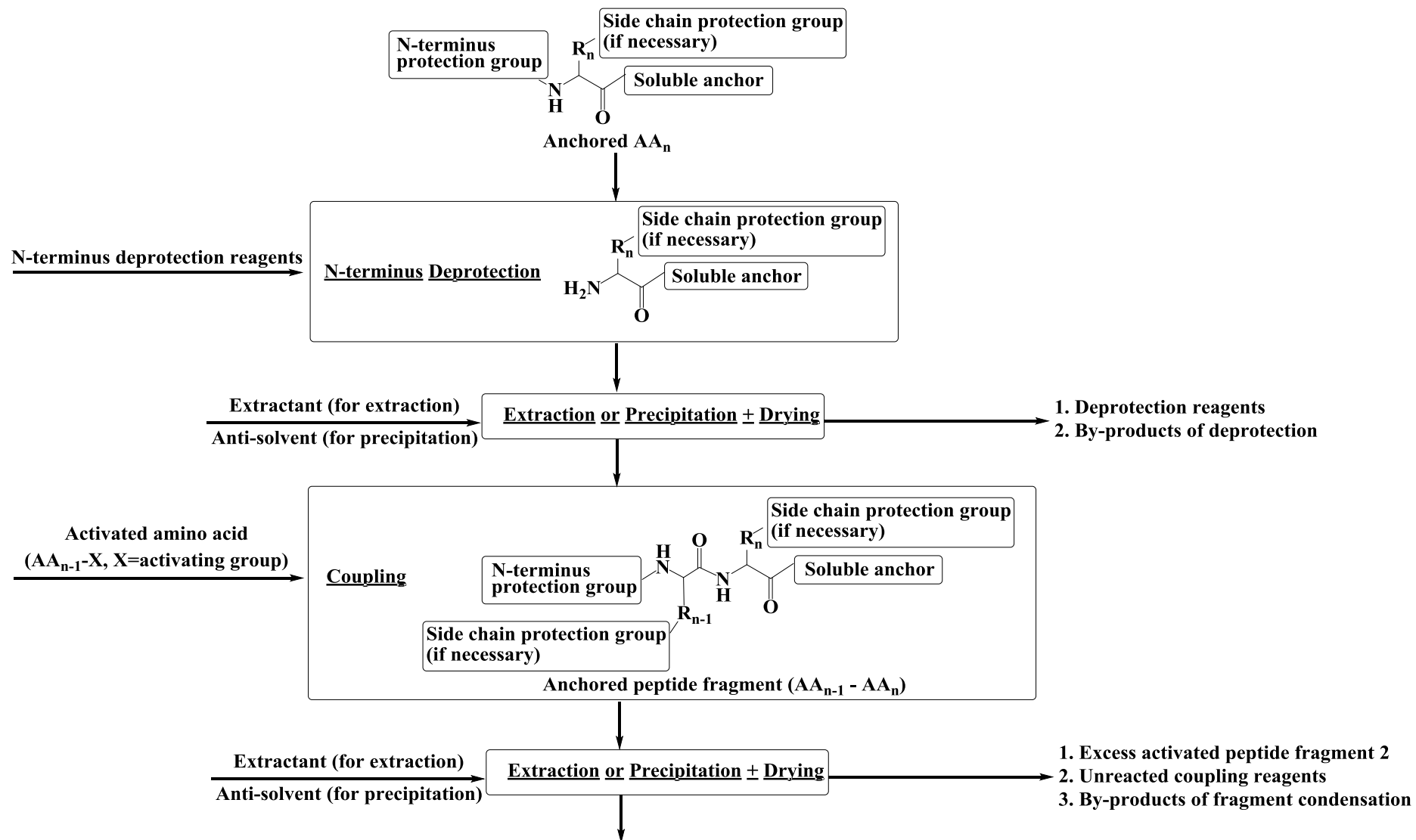


Figure 2.6. Target peptide synthesised on (a) Fmoc-Rink amide resin and (b) H₂N-Rink-DDBA.



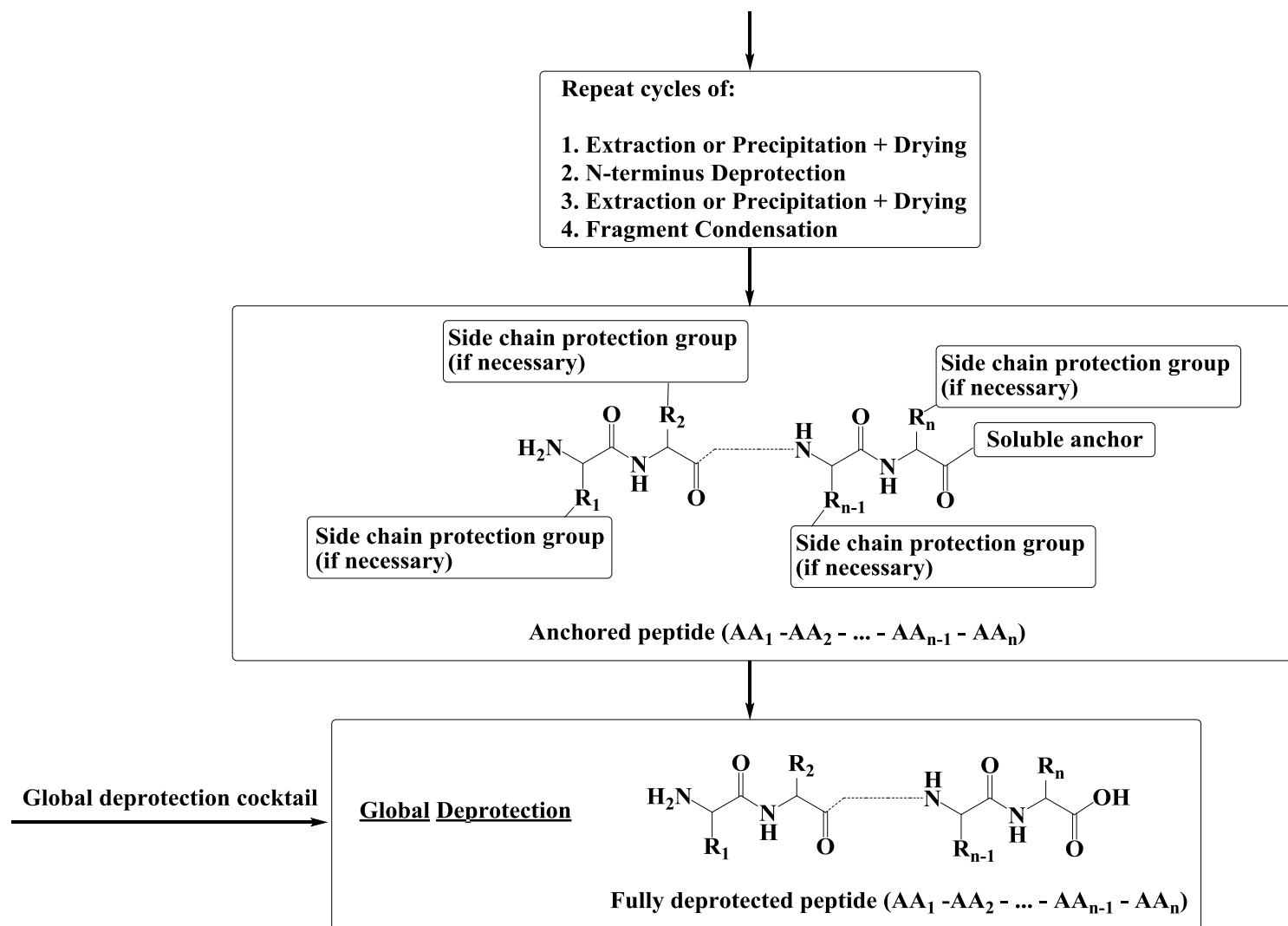


Figure 2.7. A procedure for liquid phase peptide synthesis on anchor. (Note: it is possible to cleave the peptide from the anchor in the fully protected form before global deprotection. Also, a linker can be attached to the anchor before the amino acid (AA_n) is attached.)

2.1.4. Protection of the N-terminus and Side Chain of an Amino Acid

In order to incorporate an amino acid to a growing peptide fragment, the N-terminus and side chain of the amino acid must be protected (except for nonpolar side chains), allowing the activation of the carboxyl group of the amino acid, which facilitates the regio-selective peptide bond formation with the N-terminus of the peptide fragment (Figure 2.8). The N-terminus of the new peptide fragment is then deprotected, rendering it available for the coupling with the next amino acid. Throughout the peptide elongation process, the side chains of amino acid residues must remain protected to avoid side-reactions at these sites (Figure 2.9). In other words, the N-terminus has temporary protection groups, whereas the side chains have permanent ones that are only removed during the final global deprotection step.

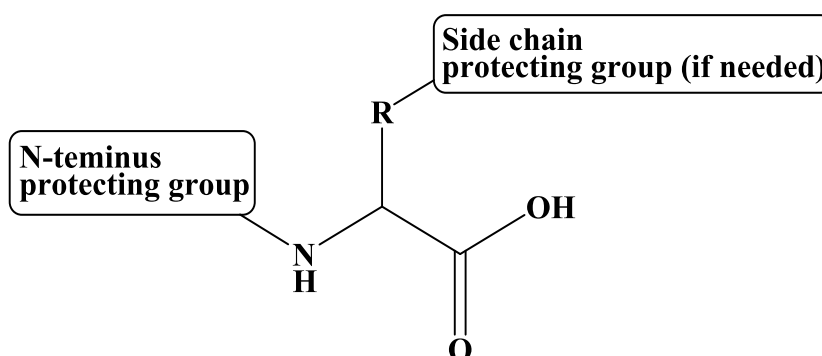


Figure 2.8. Protection of the N-terminus and side chain of an amino acid.

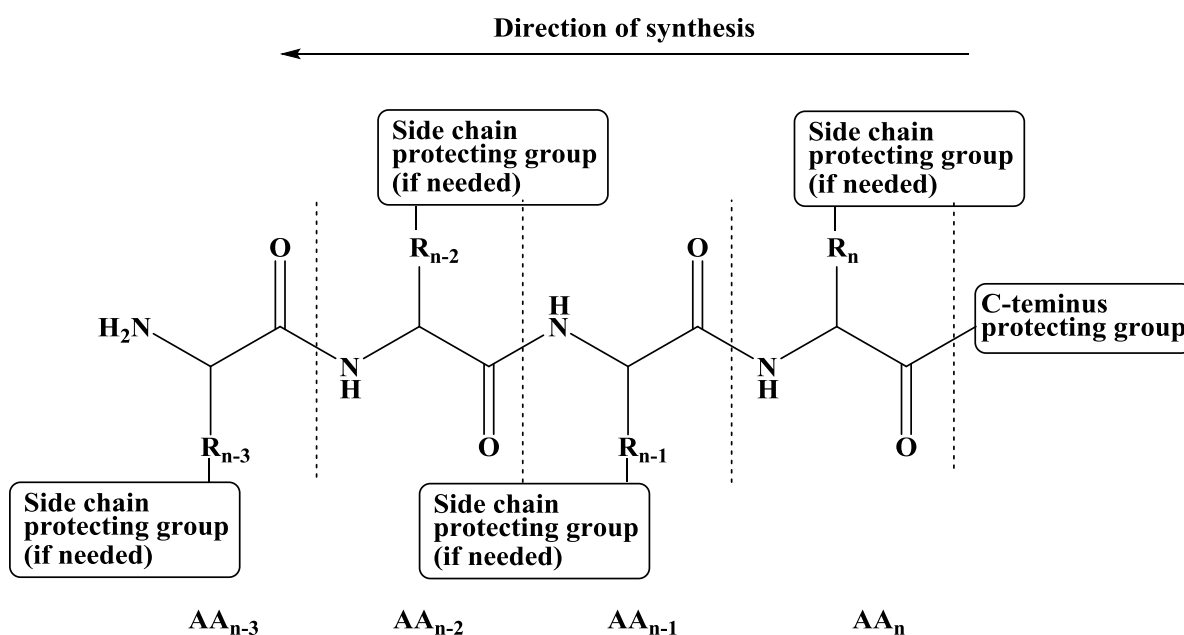


Figure 2.9. Elongation of a peptide.

In general, both temporary and permanent protecting groups should be stable over a broad range of reaction conditions and be easily removed when necessary. A large number of such protecting groups have been developed for different synthesis methods (SPPS or LPPS) and peptide sequences (Isidro-Llobet, Alvarez, & Albericio, 2009).

For this research project, the target peptides consisted of seven amino acids, among which six were Fmoc-protected and the remaining one (H-Pyr-OH) had no temporary protecting group. Four amino acids (H-Pyr-OH, Fmoc-Ala-OH, Fmoc-Leu-OH and Fmoc-Phe-OH) have nonpolar side-chains, whereas the other three (Fmoc-Arg(Pbf)-OH, Fmoc-Asp(OtBu)-OH and Fmoc-Ser(Bzl)-OH) have side chains that required protection (Figure 2.10).

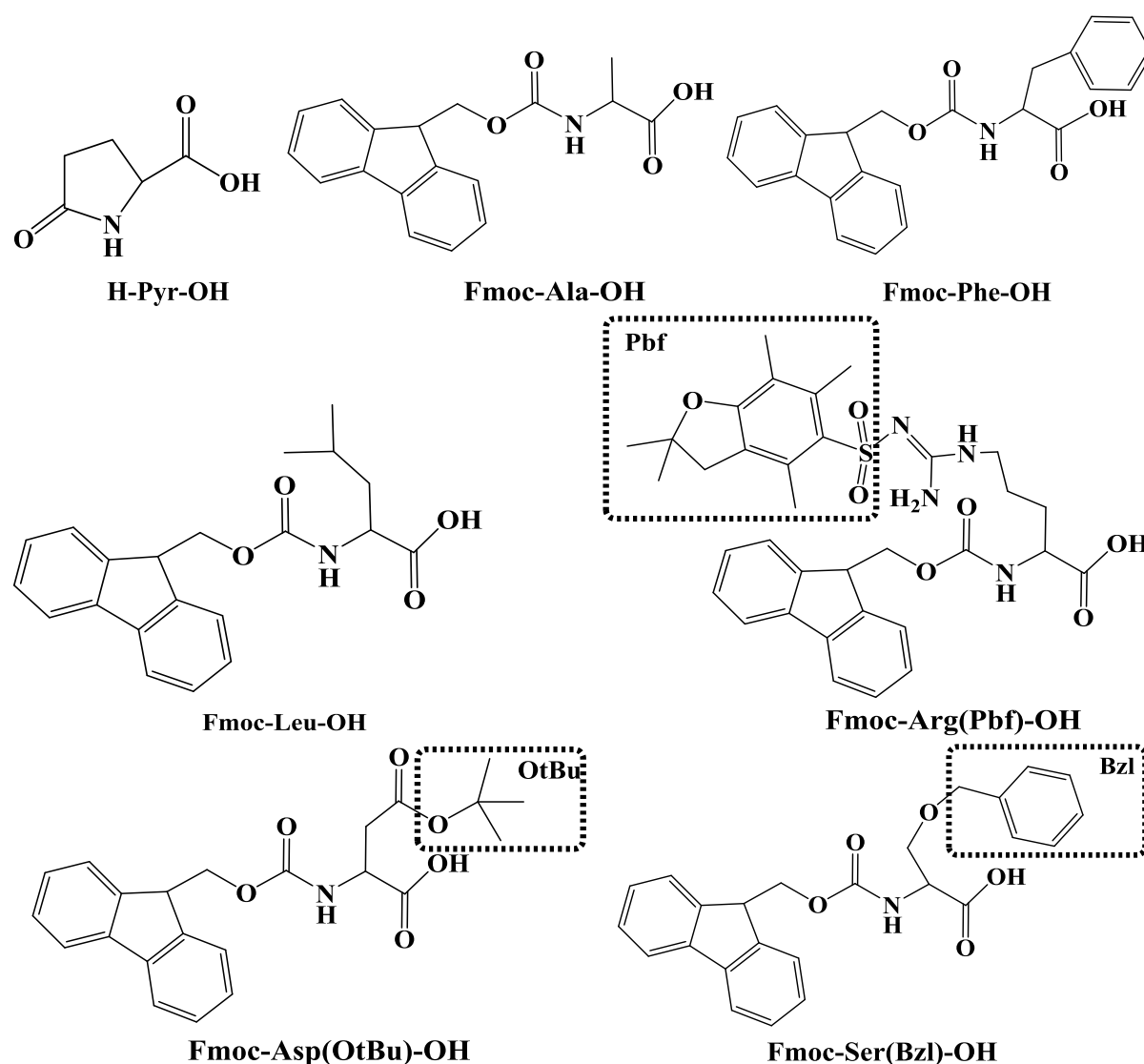


Figure 2.10. Amino acids used in this project.

The mechanism of Fmoc removal or de-Fmoc by a secondary base (usually piperidine) is illustrated in Figure 2.11. Piperidine attacks the fluorenyl proton, producing the dibenzocyclopentadienyl anion that subsequently undergoes β -elimination to yield the deprotected amino acid/peptide, carbon dioxide and dibenzofulvene (DBF) (Carpino & Han, 1970; Carpino & Han, 1972). Subsequently, piperidine scavenges the DBF and suppresses its reaction with the deprotected peptide fragment (Sheppeck, Kar, & Hong, 2000; Gude, Ryf, & White, 2002). Hydroxybenzotriazole (HOBt) is often added into the de-Fmoc solution in order to minimise side-reactions during de-Fmoc (details found in Section 2.1.6.2).

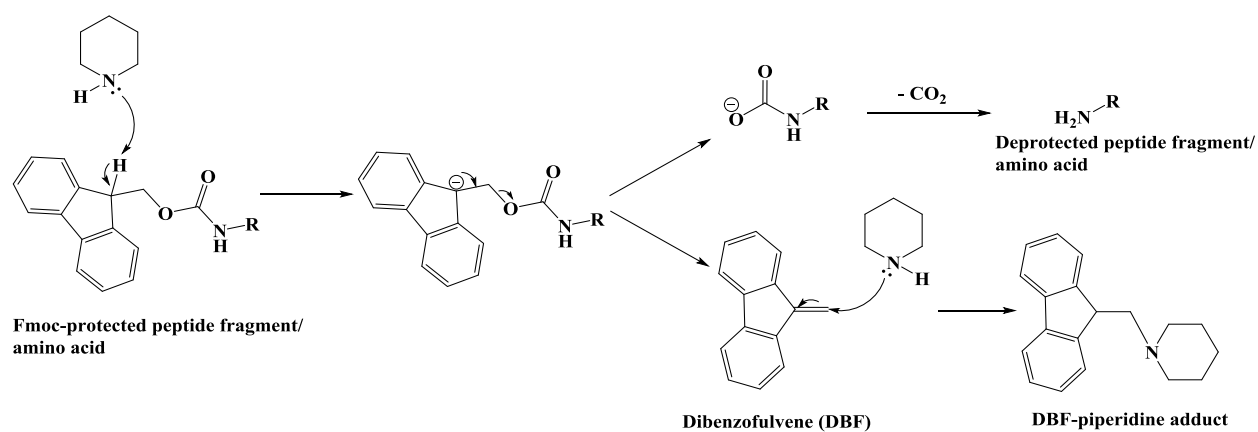


Figure 2.11. De-Fmoc mechanism by piperidine and reaction between piperidine and dibenzofulvene (DBF).

The removal of side chain protecting groups by TFA must be performed in the presence of scavengers as the carbocations of protecting groups can undergo side reactions with certain amino acid residues such as cysteine (Cys), tryptophan (Trp) and tyrosine (Tyr) (Fields & Noble, 1990; Stathopoulos, Papas, & Tsikaris, 2006). Commonly used scavengers include anisole, 1,2-ethanedithiol (EDT), thioanisole, triisopropylsilane (TIS) and water. One distinct problem associated with the sulphur-containing scavengers (EDT and thioanisole) is their odorous nature, which can be overcome by their replacement with TIS (Pearson et al., 1989). By varying the composition of these scavengers in a TFA solution, a number of cleavage cocktails (Reagent B, Reagent H, Reagent K, Reagent L, Reagent M, Reagent R etc.) have been developed (Sole & Barany, 1992; Huang & Rabenstein, 1999; King, Fields, & Fields, 1990; Bonner et al., 2001; Grandas et al., 1986; Albericio et al., 1990; Angell et

al., 2002). In particular, Reagent R (90% TFA, 5% thioanisole, 3% EDT, 2% anisole) is commonly used for the cleavage and global deprotection for arginine-containing peptides, whereas a mixture of TFA/H₂O/TIS (95:2.5:2.5, v/v/v) can be used for other peptides that have no sensitive amino acids such as Cys, Trp, Tyr and Met (Stathopoulos, Papas, & Tsikaris, 2006).

In this research project, the side chain deprotection of Arg(Pbf) and Asp(OtBu) required scavengers to capture the Pbf and tBu carbocations (Ser(Bzl) was not deprotected). Water and EDT have been reported as being effective for quenching tBu cation and tBu trifluoroacetate (Lundt et al., 1978; Nutt et al., 1988), whereas anisole has been identified as an effective scavenger of the Pbf carbocation (Albericio et al., 1990; Angell et al., 2002).

2.1.5. Activation of an Amino Acid and Formation of a Peptide Bond

Under room temperature and pressure, carboxylic acids and amines undergo the conventional acid-base reaction to yield a salt, instead of forming an amide. The C-terminus of amino acid must be activated to enable the amide bond formation (Figure 2.12). A large number of activators have been developed (Montalbetti 2005), but only N,N'-diisopropylcarbodiimide (DIC) and O-(1Hbenzotriazol-1-yl)-N,N,N',N'-tetramethyluronium hexafluorophosphate (HBTU) are discussed in depth here because of their relevance in this research project.

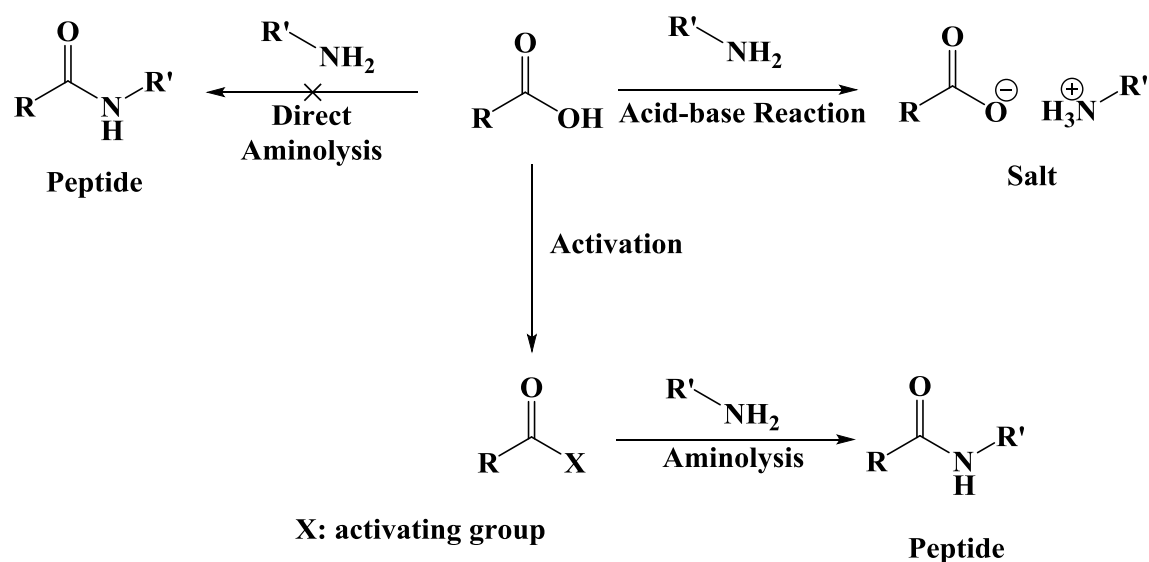


Figure 2.12. Peptide bond formation.

DIC reacts with the C-terminal of an amino acid to form the o-acylisourea mixed anhydride in order to enable the nucleophilic attack of the carbon centre by the amino group of the growing peptide fragment (Figure 2.13) (Sheehan & Hess, 1955; Smith, Moffatt & Khorana, 1958; DeTar & Silverstein, 1966; Merrifield, Gisin, & Bach, 1977). The driving force for peptide bond formation is the formation of urea by-product. The side reaction can occur (more details in the later part of this chapter (Section 2.1.6.1)), but can be prevented by the addition of HOBT, which forms the 7-azabenzotriazol-1-yl ester with the amino acid during activation.

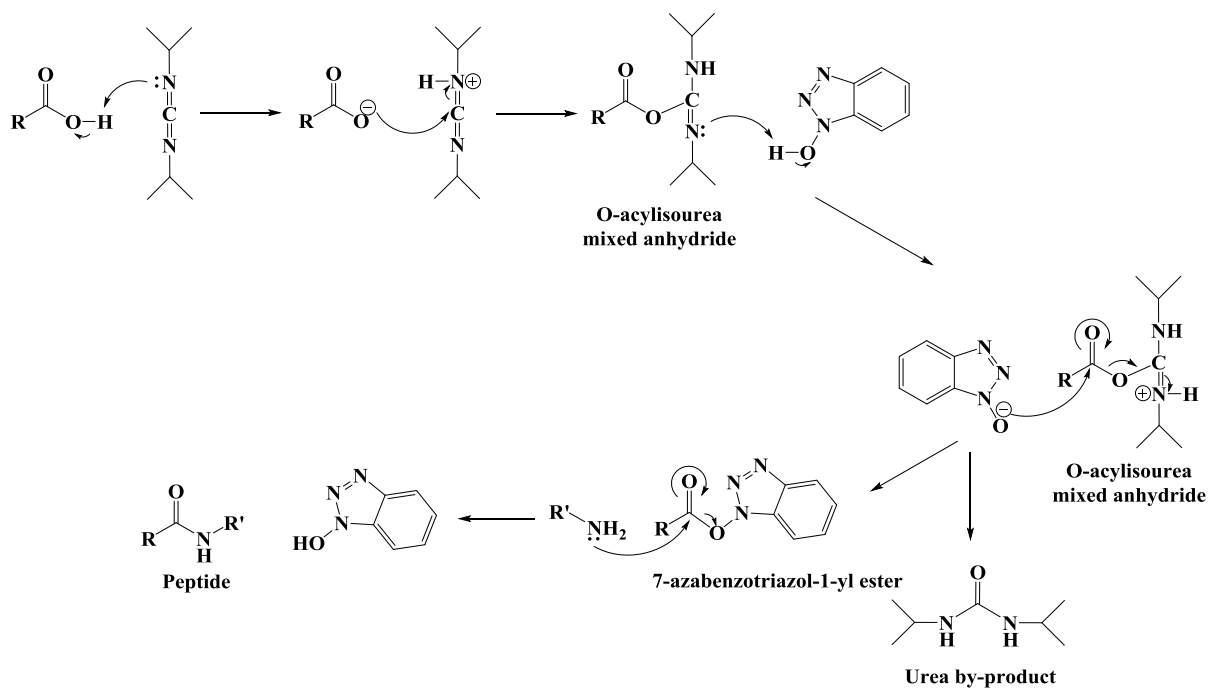


Figure 2.13. Aminolysis via activation of amino acid by DIC and HOBt.

The activation of amino acid by HBTU requires basic conditions to deprotonate the C-terminus of the amino acid, which then reacts with HBTU to yield the 7-azabenzotriazol-1-yl ester for the formation of peptide bond (Figure 2.14) (Knorr et al., 1989; Abdelmoty et al., 1994; Speicher, Klaus, & Eicher, 1998; Albericio et al., 1998).

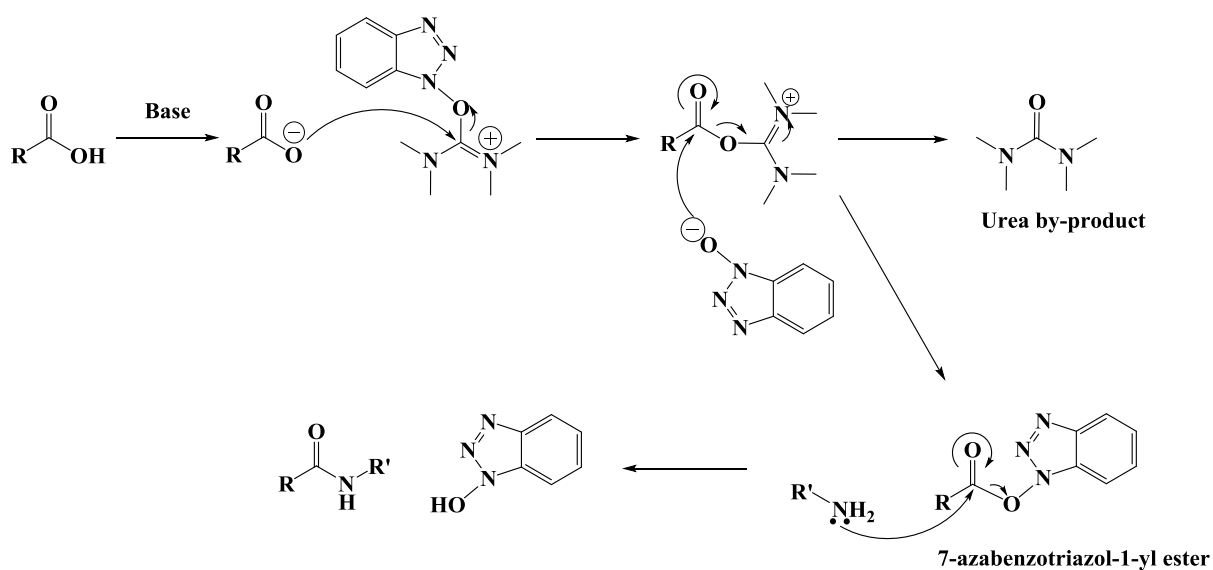


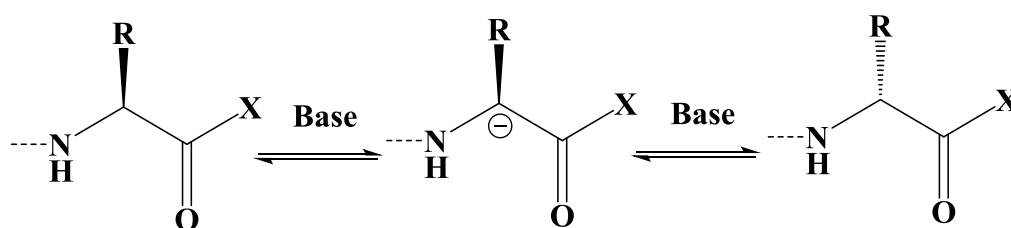
Figure 2.14. Aminolysis via activation of amino acid by HBTU.

2.1.6. Side Reactions

Various side reactions can occur during peptide synthesis. This section explores their mechanisms and the corresponding mitigation methods.

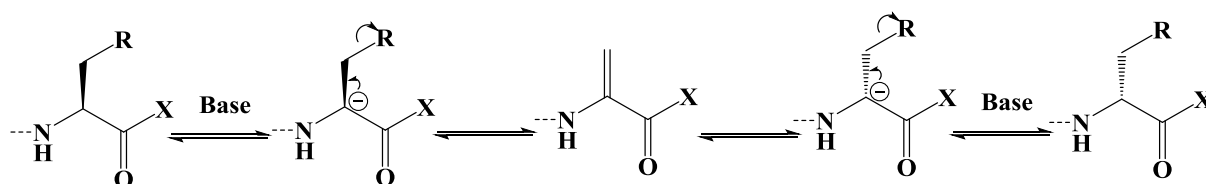
2.1.6.1. During Activation

During the activation of amino acid in basic condition, racemisation can occur via direct abstraction of the α -proton and reversible β -elimination (Figure 2.15 and Figure 2.16) (Okada, 2001). This side reaction is mainly suppressed by limiting the exposure of amino acid to a tertiary base (Kemp et al., 1970) and by using additives such as HOBT and TBTU (Jablonski, Shpritzer, & Powers, 2002). In fragment condensation, racemisation of the activated fragment can occur via the formation of azlactone (Figure 2.17) (Goodman & Levine, 1964; Goodman & McGahren, 1965; Benoiton & Chen, 1981).



X: Activating group

Figure 2.15. Racemisation of activated amino acid via direct abstraction of the α -proton.



X: Activating group

Figure 2.16. Racemisation of activated amino acid via reversible β -elimination.

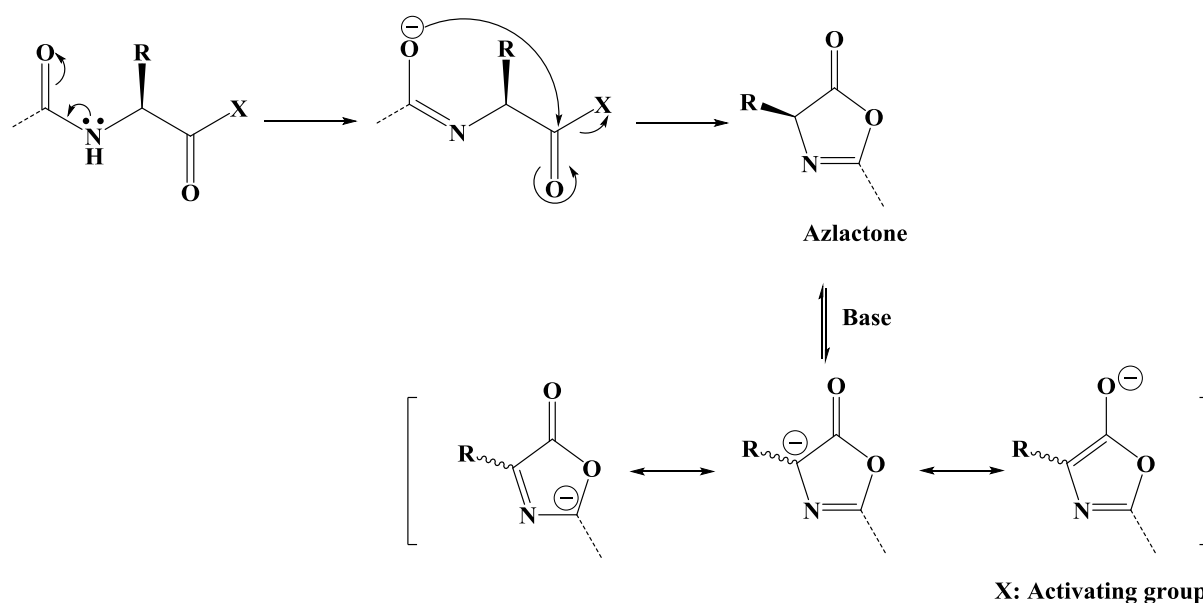


Figure 2.17. Racemisation of activated peptide fragment via azlactone.

When the amino acid is activated by DIC, the *o*-acylisourea mixed anhydride can react with another unactivated amino acid to form an anhydride, which subsequently reacts with the amino group of the growing peptide fragment to form a peptide bond (Figure 2.18). Despite the slow reaction rate, the *o*-acylisourea mixed anhydride can also undergo rearrangement to form the unreactive *N*-acylurea (Figure 2.19). To minimise this side reaction, HOBt is added into the system to transform the *o*-acylisourea mixed anhydride into the 7-azabenzotriazol-1-yl ester, which is then consumed during the formation of peptide bond (Figure 2.18) (Montalbetti & Falque, 2005; Windridge & Jorgensen, 1971).

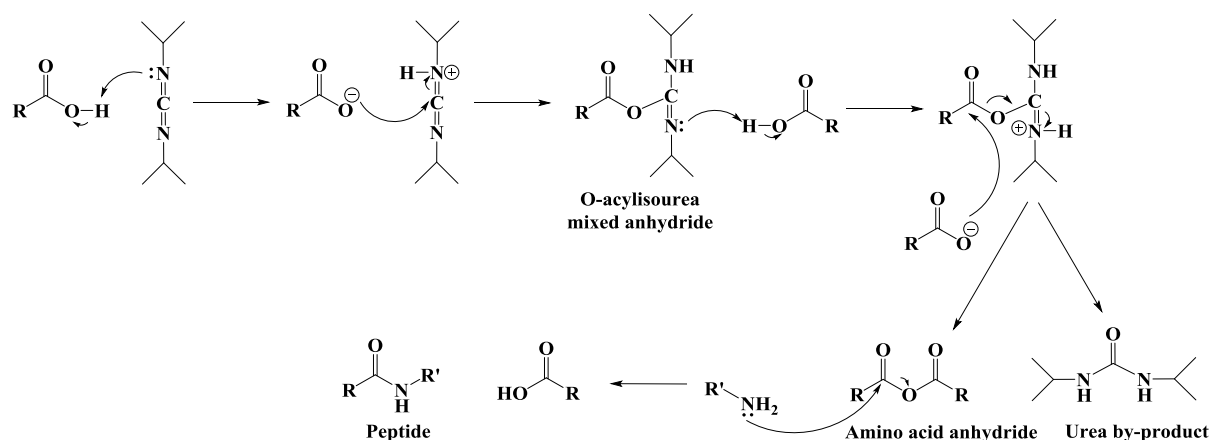


Figure 2.18. Formation of amino acid anhydride.

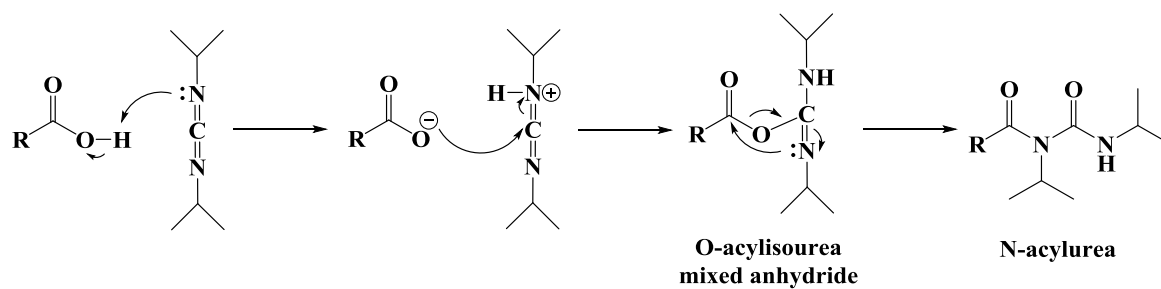


Figure 2.19. Formation of unreactive N-acylurea.

For the activation of amino acid by HBTU, the amino group of the growing peptide fragment can react with HBTU to form guanidine, preventing the formation of a peptide bond (Figure 2.20). To minimise this side reaction, HBTU should not be used in large excess and the amino acid should be activated with HBTU in the presence of HOBT before reacting with the growing peptide fragment (Montalbetti & Falque, 2005; Abdelmoty et al., 1994).

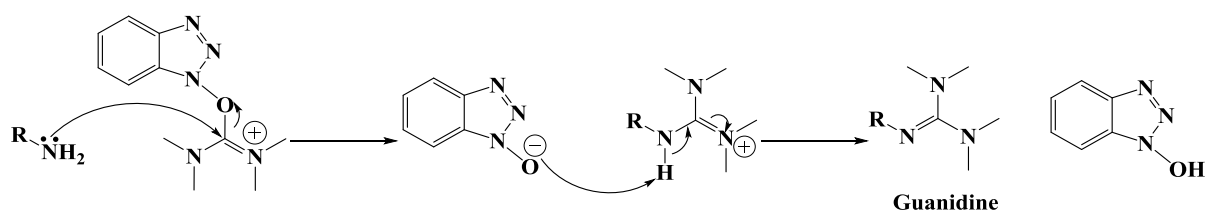


Figure 2.20. Formation of guanidine.

2.1.6.2. During De-Fmoc

Another common side reaction during peptide synthesis is the intramolecular aminolysis of dipeptide fragment with the formation of a cyclic dipeptide (diketopiperazine or DKP) (Fischer, 2003). This side reaction can be acid- (Gisin & Merrifield, 1972) or base-catalysed (Rothe & Mazánek, 1974) and the cyclic side-product can undergo hydrolysis to yield dipeptide fragments, one of which has the reverse sequence (Steinberg & Bada, 1983; Gaines & Bada, 1988). For peptide synthesis with Fmoc-protected amino acids, DKP formation can occur during the de-Fmoc of dipeptide fragment and in the following isolation cycle (washing and microfiltration in SPPS; precipitation, microfiltration and washing in LPPS; diafiltration in MEPS). Therefore, the duration of de-Fmoc should be kept to the minimum by using a high concentration of piperidine (Fischer, 2003). In this research, DKP formation was observed in the peptide synthesis on a particular soluble anchor (Figure 2.21) and was overcome by attaching a linker with a sterically hindered structure to the soluble anchor (more details in the later Section 3.3.7).

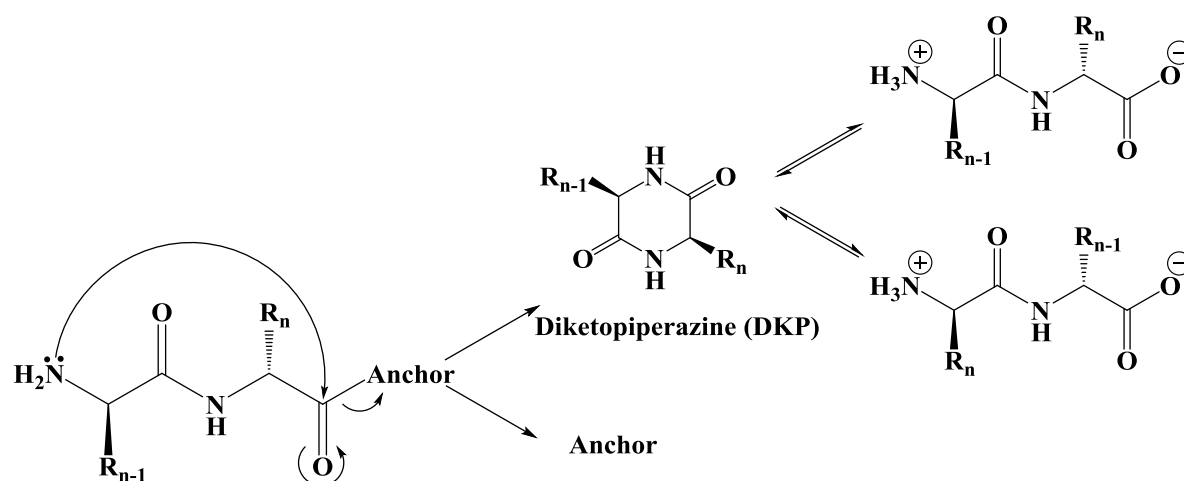


Figure 2.21. Formation of DKP.

Certain peptide sequences such as Asp-Tyr, Asp-Trp and Asp-His have been found to be prone to the formation of aspartimide (Mergler et al., 2003b; Michels et al., 2012), which can be acid- or base-catalysed (Yang et al., 1994). The mechanism of aspartimide formation in the presence of piperidine is shown in Figure 2.22. The aspartimide further reacts with piperidine to form piperidides. The extent of this side reaction can be reduced by several methods: 1) using bulky protecting groups for the side chain of aspartic acid residue (Quibell et al., 1994; Offer, Quibell, & Johnson, 1996; Mergler et al., 2003a; Mergler & Dick, 2005); 2) replacing piperidine with a milder base (Wade et al., 2000); 3) employing microwave heating (Nissen et al., 2010); 4) using additives during the piperidine-induced de-Fmoc (Wade et al., 2000; Michels et al., 2012). In this research project, HOBt was added into the reaction solution during de-Fmoc of peptide fragments in order to suppress this side reaction.

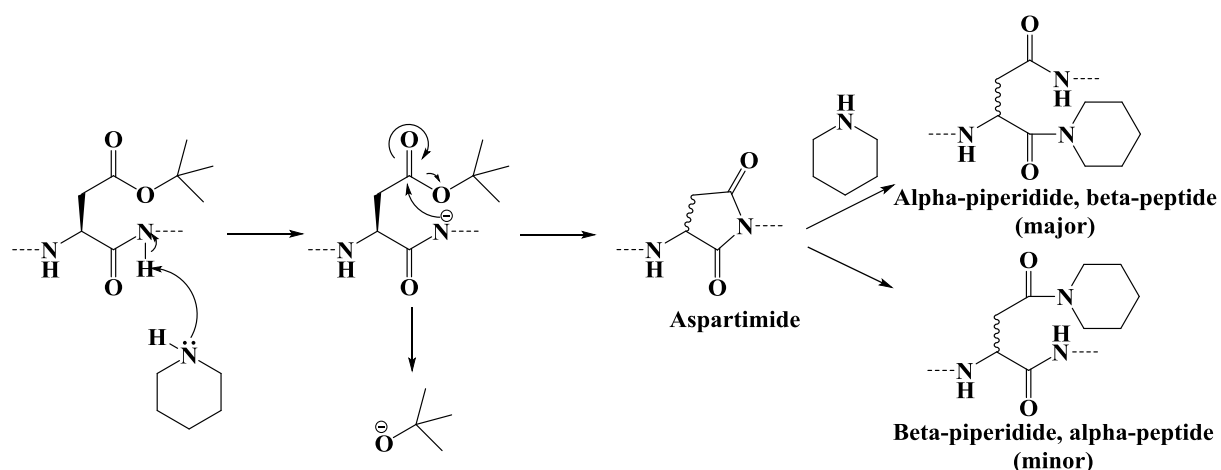


Figure 2.22. Formation of aspartimide in the presence of piperidine.

2.1.6.3. During Cleavage and Global Deprotection of Peptide

In this research project, the Rink linker was attached to the soluble anchor for peptide synthesis. The decomposition of the Rink linker occurred in highly concentrated TFA solution during the global deprotection of peptide and a fragment of the linker remained attached to the target peptide, forming a major impurity (Figure 2.23). 1,3-dimethoxybenzene (DMB) (Figure 2.24) has been reported as an effective suppresser for the decomposition of the Rink linker in TFA solution (Stathopoulos, Papas, & Tsikaris, 2006) as it “represents the parent molecule of the resulting carbocation if the linker decomposition occurs at position 2”. The use of DMB for suppressing Rink decomposition in the concentrated TFA solution was tested in this project (more details can be found in Section 4.3.3.7).

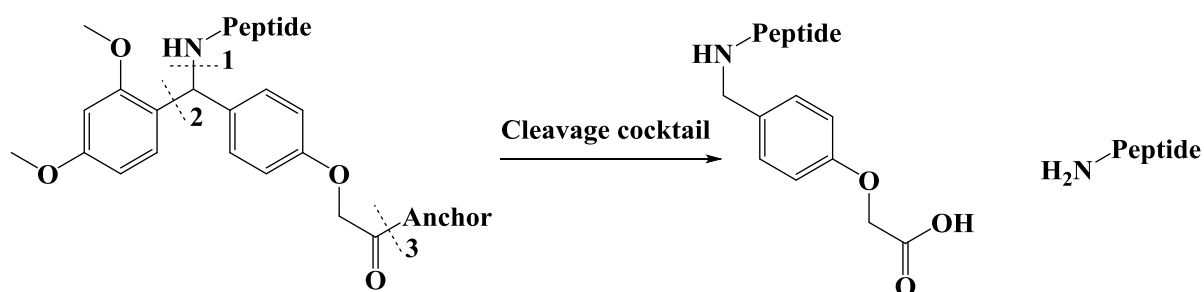


Figure 2.23. Decomposition of Rink amide linker during cleavage and global deprotection of peptide.

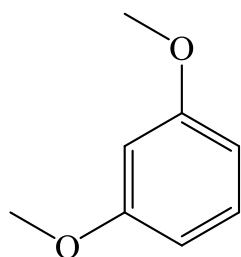


Figure 2.24. 1,3-dimethoxybenzene (DMB).

2.2. OSN and MEPS

2.2.1. Overview

Traditionally, most of the research on nanofiltration and other filtration processes is related to water purification, but since the 1990's, academia and industry have been increasingly interested in nanofiltration for the purification of compounds in organic-solvent systems (Yang, Livingston & Freitas dos Santos, 2001; Gibbins et al., 2002; Bhanushali & Bhattacharyya, 2003). Organic Solvent Nanofiltration (OSN) is therefore still a relatively young technology compared to other separation technologies such as distillation and crystallisation. However, a growing number of literature has been published with regard to different aspects of OSN (e.g. membrane development, system development, applications of OSN and modelling of mass transport). This section is dedicated to the literature which is relevant to the application of OSN for peptide synthesis, which is the focus of this research project. Interested readers should refer to reviews and books available for a wider coverage of OSN (Vandezande, Gevers & Vankelecom, 2008; Van der Bruggen, Mänttari & Nyström, 2008; Schäfer, Fane & Waite, 2005; Nunes & Peinemann, 2006; Li, 2007; Anim-Mensah, 2012; Baker, 2012; Marchetti, Jimenez Solomon, Szekely & Livingston, 2014; Szekely, Jimenez-Solomon, Marchetti, Kim & Livingston, 2014).

2.2.2. Organic Solvent Nanofiltration (OSN)

Filtration is a separation process that involves the mass transfer of molecules across a physical barrier (a membrane). Given specific membrane properties and filtration conditions, different molecules have different rates of mass transfer across the membrane, resulting in their separation from one another.

Filtration processes include microfiltration (MF), ultrafiltration (UF), nanofiltration (NF) and reverse osmosis (RO), which are classified according to the size of molecule that can permeate through the membrane. According to the 1996 IUPAC-nomenclature, molecules with diameter of 2 - 100 nm can permeate through UF membranes and their counterparts that are less than 2 nm can permeate through NF membranes, whereas RO membranes only allow solvents to pass through (Koros, Ma & Shimidzu, 1996).

Organic Solvent Nanofiltration (OSN) or Solvent Resistant Nanofiltration (SRNF) refers to a nanofiltration process that is designed for the purification of compounds that are dissolved in organic solvents. Whereas traditional separation methods such as distillation rely on the manipulation of temperature, OSN can be performed isothermally or at a specific temperature that is suitable for ensuring the stability of target compounds, since the driving force for separation is cross-membrane pressure difference. This makes OSN ideal for the purification of pharmaceutical compounds that are susceptible to degradation and side reactions at an elevated temperature (Vandezande, Gevers & Vankelecom, 2008).

2.2.3. Membrane Enhanced Peptide Synthesis (MEPS)

The past two decades have witnessed the adoption of OSN for various applications such as food processing (Raman, Cheryan & Rajagopalan, 1996; Darnoko & Cheryan, 2006; de Morais Coutinho et al., 2009; Sereewatthanawut et al., 2011) and the recovery of solvent (White, 2006; Chapman, Oliveira, Livingston & Li, 2008), catalyst (Scarpello et al., 2002; Mertens et al., 2005; Chavan et al., 2005; Wong et al., 2006; de Jesús & Flores, 2008; Cano-Odena et al., 2010) and pharmaceutical compounds (Geens, De Witte & Van der Bruggen, 2007; Pink et al., 2008; Sereewatthanawut et al., 2010; Marchetti, 2013). Membrane Enhanced Peptide Synthesis (MEPS) is a novel application of OSN that was first developed by Dr. Sheung So under the supervision of Professor Andrew Livingston in 2005-2009 (So, 2009; So et al., 2010a; So et al., 2010b).

2.2.4. Major Components of MEPS

The development of MEPS mainly involves the integration of three components (OSN membranes, nanofiltration systems and soluble anchors) that have been developed separately. This section provides a general understanding of these important components and serves as the foundation for the discussion of experimental results in this thesis.

2.2.5. OSN Membrane

Since the separation performance of an OSN membrane is closely related to the intrinsic properties and configuration of the membrane, a brief explanation is given on these aspects before a comparison between polymeric and ceramic membranes is made in the context of MEPS.

2.2.6. Material and Fabrication Method

In general, an OSN membrane consists of an active layer on top of a porous support (Figure 2.25 (a)). During OSN, the active layer is in contact with a pressurised solution, whose properties such as viscosity and concentration control the permeation of solutes and solvents (Figure 2.25 (b)). Increasing the thickness of the active layer improves the quality assurance of membrane performance by lowering the probability of defects and improving the stability of the active layer under high pressure, but reduces the permeance of the membrane. By incorporating the active layer on a porous material that provides mechanical support, the thickness of the active layer can be reduced significantly to give a higher permeance, which will result in shorter process time for the OSN.

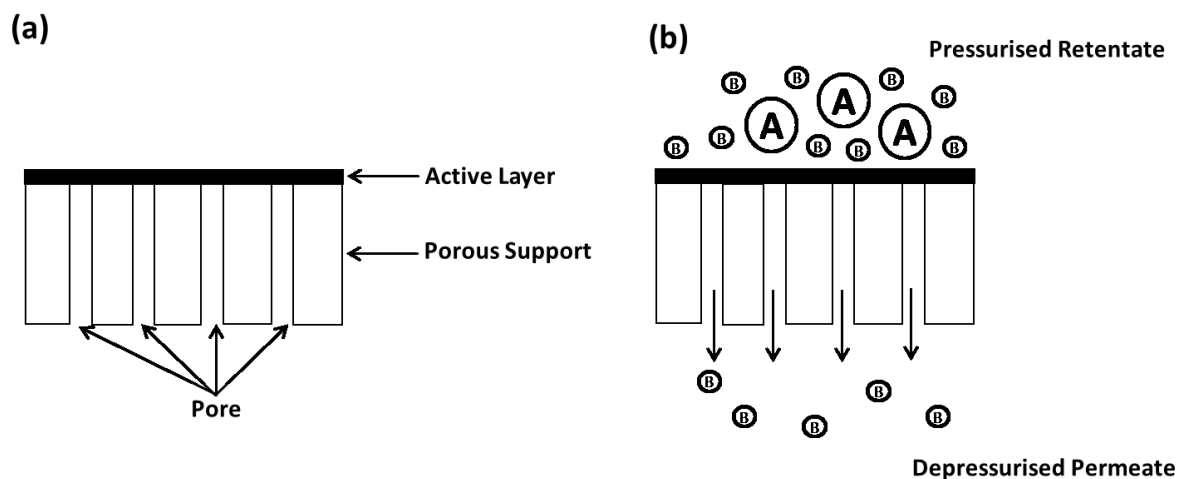


Figure 2.25. (a) General structure of OSN membrane. (b) Permeation of solute B and solvent through an OSN membrane (note: solute A and B are dissolved in solvent, but solute A is retained by the membrane due to its larger size).

Based on the fabrication materials, OSN membranes can be categorised into polymeric and ceramic membranes. The fabrication of polymeric membranes normally begins with the preparation of a polymer solution (Figure 2.26, Step 1), which is then cast on a porous support (Figure 2.26, Step 2). The wet membrane then undergoes phase inversion, during which the solvent is removed and the polymer solidifies on the support (Figure 2.26, Step 3). Finally, the membrane is subject to post treatments such as annealing and cross-linking, which improves the performance and stability of the

membrane. Many polymers can be used to prepare the active layer, including polyimide (PI) (Vankelecom, Merckx, Luts, & Uytterhoeven, 1995; Gevers et al., 2006; See-Toh, Ferreira, & Livingston, 2007; Jiang, 2007; See Toh, Lim, & Livingston, 2007; Vanherck, Vandezande, Aldea, & Vankelecom, 2008; Vandezande, Gevers, Jacobs, & Vankelecom, 2009; Soroko, Bhole, & Livingston, 2011; Dobrak-Van Berlo, Vankelecom, & Van der Bruggen, 2011), polyaniline (PANI) (Patel, 2007; Chapman et al., 2008; Wong, 2008; Loh et al., 2009; Sairam et al., 2009) and polyethersulfone (PES) (Sotto et al., 2011) etc. For the porous support, polypropylene (PP) and polyethylene (PE) are popular choices among others (See Toh, Lim, & Livingston, 2007).

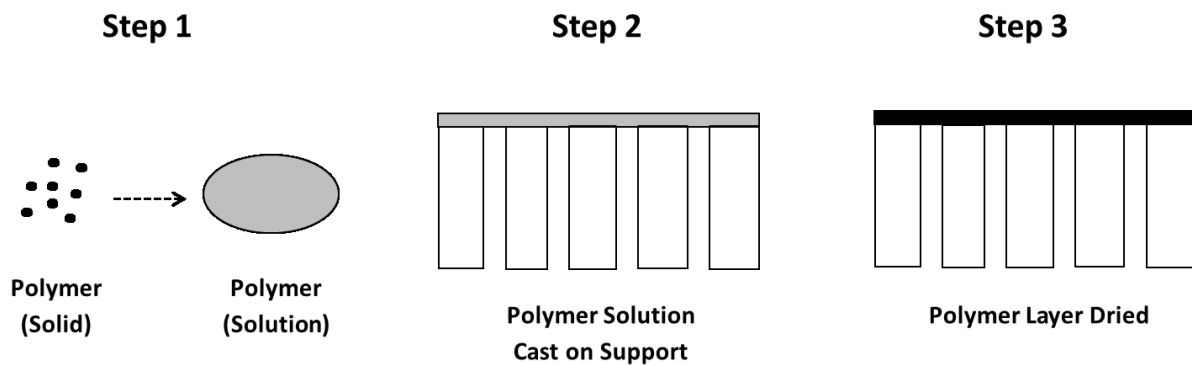


Figure 2.26. Fabrication of polymeric membrane via casting on support and phase inversion.

The structure of the membrane can be analysed by Scanning Electron Microscope (SEM). The SEM images of membrane available in literature normally exclude the support layer, as researchers are more interested in the separation layer. As shown in Figure 2.27, the separation layer typically consists of the top separation layer and microvoids.

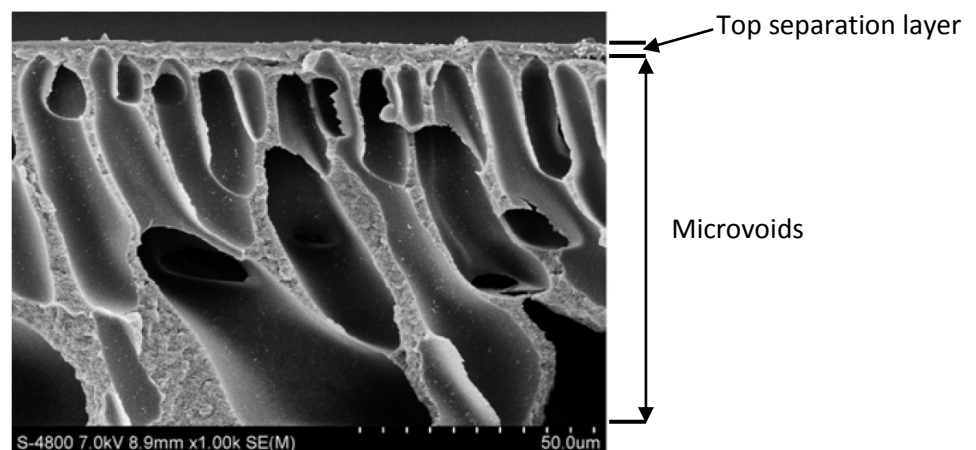


Figure 2.27. SEM image of the cross-section of a typical polymeric membrane (Xu, Feng, Chen, & Gao, 2012).

On the other hand, ceramic membranes for OSN are normally prepared by the sol-gel method (Figure 2.28), in which the sol is a suspension of nanoclusters which are formed via hydrolysis and condensation of the corresponding alkoxide. The sol is coated on a ceramic support and then dried to form the gel. Finally, the membrane is subject to thermal treatment at a much higher temperature in order to sinter the gel layer (Li, 2007). As shown in Figure 2.29, the ceramic membrane consists of three layers: the top separation layer, the intermediate layer and the support layer (bottom).

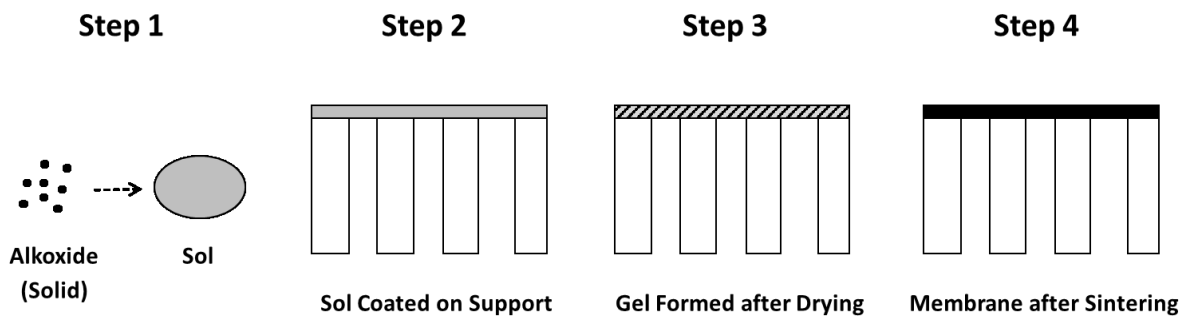


Figure 2.28. Fabrication of ceramic membrane by sol-gel method.

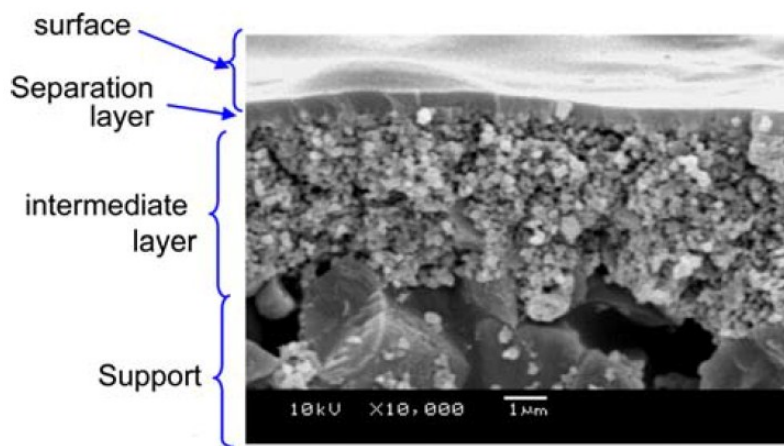


Figure 2.29. SEM image of the cross-section of a typical ceramic membrane (Tsuru, 2008).

2.2.7. Characterisation of Membrane

Various techniques can be employed to analyse the intrinsic (physical and chemical) properties and rejection performance of OSN membrane. The chemical property of the active layer of membrane can be analysed by spectroscopies (Boussu et al., 2007; So, 2009), whereas the physical structure of the membrane can be characterised by various microscopies and the measurement of adsorption isotherm (Maes, Zhu & Vansant, 1995; Zhu & Vansant, 1995; Vercauteren et al., 1998).

The separation performance of an OSN membrane can be expressed in terms of permeance (the flux of solvent/solution through the membrane normalised by the cross-membrane pressure difference. Unit: $L \cdot m^{-2} \cdot h^{-1} \cdot bar^{-1}$) and Molecular Weight Cut-Off (MWCO) (unit: $g \cdot mol^{-1}$). The former reflects the permeable nature of the membrane and is related to the process time for a particular OSN operation (e.g. high permeance results in short filtration time), while the latter is related to the selective separation between the target compound from impurities.

To determine the MWCO of a particular membrane, OSN is performed with a solution that contains a series of compounds, which have similar chemical structures, but increasing molecular weights. Ideally, the rejection curve of these compounds should start with a low value (e.g. < 30 %) and then increase to almost 100 % as the molecular weight of compound increases (Figure 2.30). MWCO is defined as the molecular weight of the compound that has 90% rejection and can be easily determined from the rejection curve.

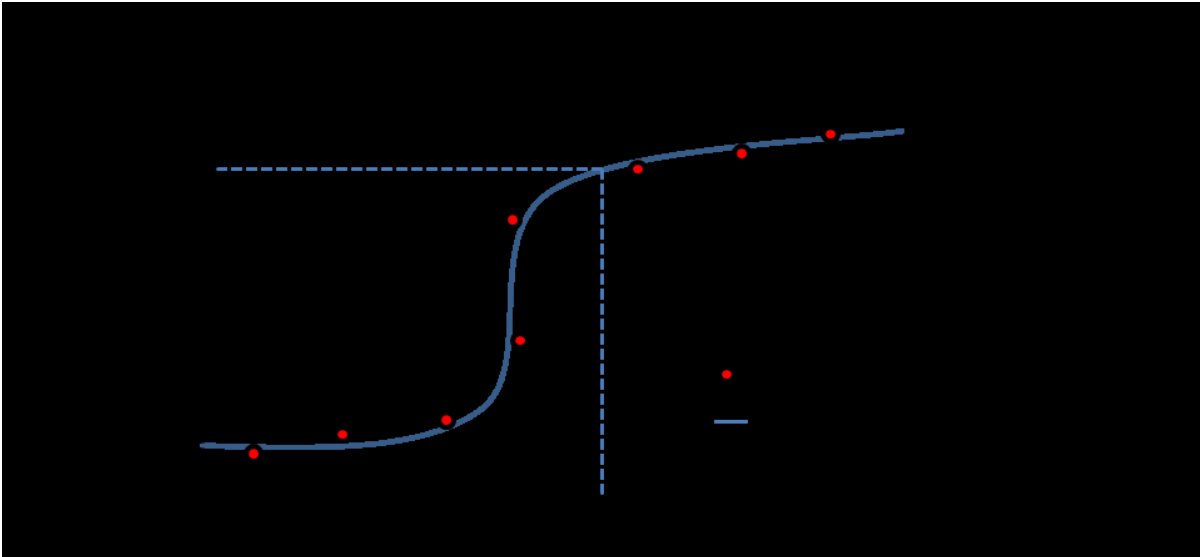
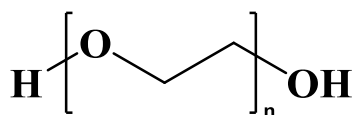


Figure 2.30. A typical rejection curve for a membrane (definition of rejection is given in Section 2.2.11).

PEG, polystyrene (PS) (Figure 2.31) and several other compounds have been used for obtaining the rejection curves of membranes (Yang, Livingston & Freitas dos Santos, 2001; Tsuru, Sudoh, Yoshioka & Asaeda, 2001; Gibbins et al., 2002; Bhanushali, Kloos & Bhattacharyya, 2002; White, 2002; Stafie, Stamatialis & Wessling, 2004; Tarleton, Robinson, Millington & Nijmeijer, 2005; Kwiatkowski & Cheryan, 2005; Geens et al., 2005; See Toh et al., 2007), but no agreement has been reached in either academia or industry regarding a standard test for the separation performance characterisation.

(a)



(b)

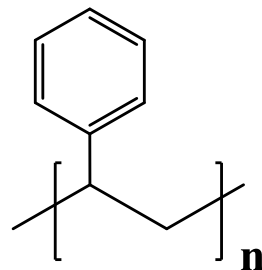


Figure 2.31. Compounds used for determining the rejection curve of a membrane: (a) PEG; (b) PS.

2.2.8. Membrane Configuration

Besides the intrinsic properties of the membrane itself, the configuration of membrane (flat sheet vs spiral module or monolith) is also an important factor for the overall separation performance of the OSN process.

Flat sheets are available for both ceramic and polymeric membranes and are useful for screening in order to identify the suitable candidate for a particular OSN process (Vandezande et al., 2005; Silva, Han & Livingston, 2005; Vandezande, Gevers, Vankelecom & Jacobs, 2006). However, flat sheet membrane cannot provide sufficient membrane area within a reasonable cell-volume. To overcome this problem, polymeric membranes can be rolled into a spiral module (Figure 2.32). Ceramic membranes on the other hand are generally formed on porous organic supports which are usually monoliths. These are then scaled up to multi-channel tube (Figure 2.33). In terms of commercial availability, spiral modules of polymeric OSN membranes are not as accessible as the multi-channel ceramic membrane, mainly because much of the research and development is still in progress (in contrast, spiral module of RO or UF membrane is easy to obtain from commercial suppliers) (Silva, Peeva & Livingston, 2010; Sairam et al., 2010).

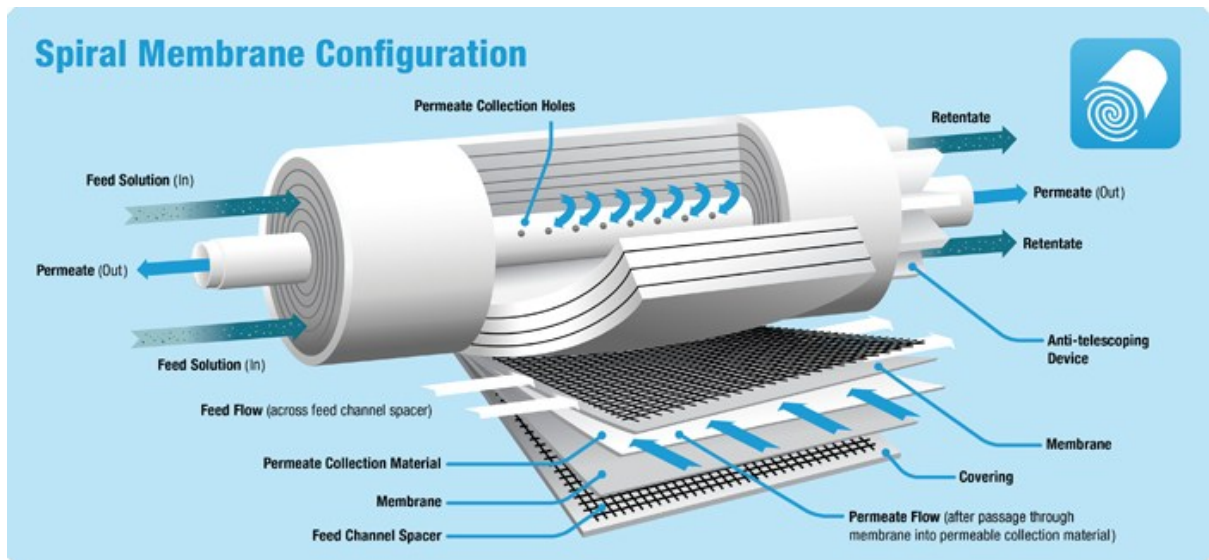


Figure 2.32. The structure of a typical spiral module.*

*www.kochmembrane.com/Learning-Center/Configurations/What-are-Spiral-Membranes.aspx

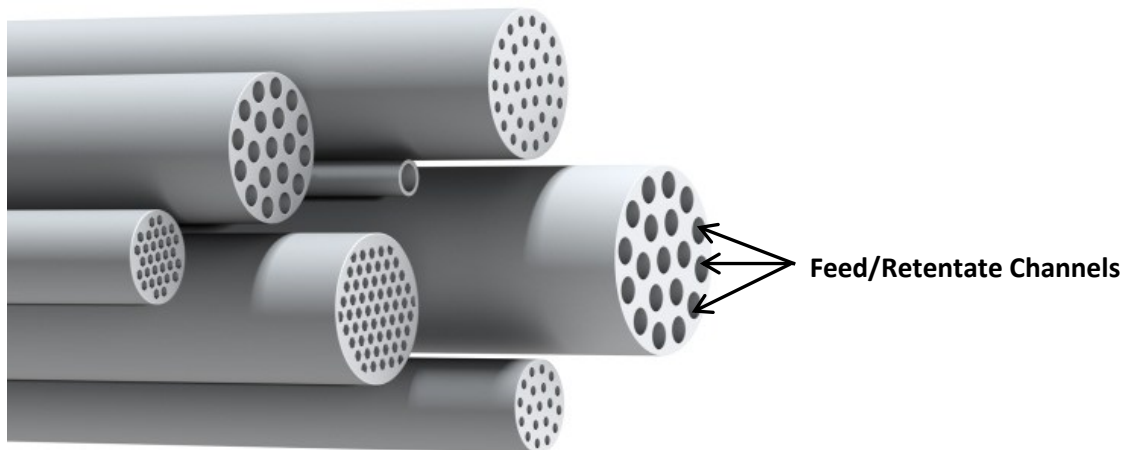


Figure 2.33. Typical ceramic multi-channel tubes.**

**<http://www.filtsep.com/view/21508/ceramic-membranes-high-filtration-area-packing-densities-improve-membrane-performance/>

2.2.9. Polymeric Membrane vs Ceramic Membrane for MEPS

As mentioned in the discussion of Dr. So's work (So, 2009; So et al., 2010a; So et al., 2010b), OSN membranes must possess chemical stability and exhibit reliable separation performance under MEPS conditions. In this respect, ceramic membranes are generally more stable than their polymeric counterparts in organic solvent and strong acids/bases. Furthermore, their separation performance over time is not affected by compaction, which can be a problem for their polymeric counterparts over a prolonged operation under high pressure (Silva, Han & Livingston, 2005). In addition, commercial ceramic membranes are available in the form of multi-channel tubes, which have significantly larger membrane areas than commercial flat sheet polymeric membranes (flat sheet membrane is more accessible than spiral module for OSN polymeric membrane). As a result, the use of ceramic membranes can lead to shorter filtration times than the polymeric ones.

2.2.10. Nanofiltration System

In terms of system configuration, flow direction of feed/retentate with respect to membrane surface is an important factor to be considered, since the separation performance of membranes could vary with different flow directions, probably due to concentration polarisation (Tansel et al., 2006; Patterson et al., 2008).

Early studies on OSN utilised dead-end cells (Figure 2.34 (a)) to determine the rejection curve of membranes, in which the test solution permeated directly through the flat sheet membrane under pressure (Yang, Livingston & Freitas dos Santos, 2001; Gibbins et al., 2002). Cross-flow cells (Figure 2.34 (b)), in which the feed/retentate flows tangentially across the membrane surface, have gradually replaced the dead-end cells for rejection testing of membranes, as the flow direction in cross-flow cells is similar to that for spiral modules or multi-channel tubes that are used for large scale OSN processes. Therefore, the experimental results obtained with a cross-flow cell are usually more useful for scaling up the process compared to the ones obtained with a dead-end cell.

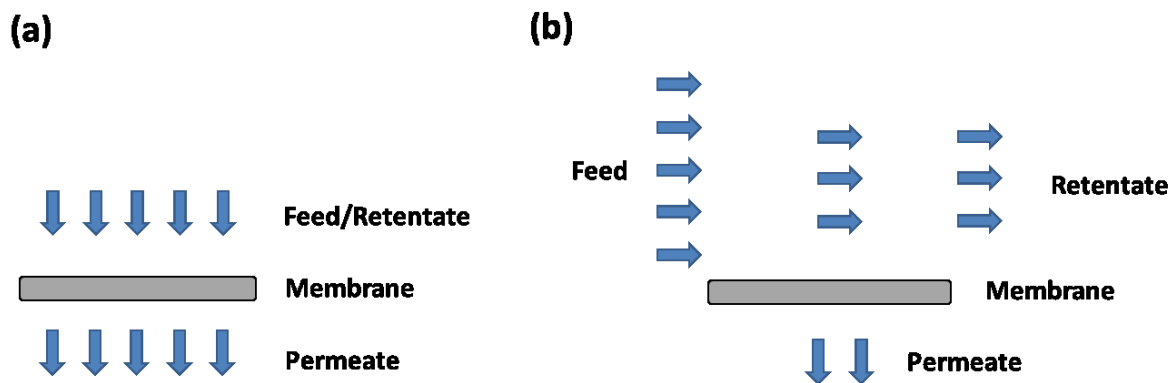


Figure 2.34. Flow direction of feed/retentate in typical (a) dead-end cell and (b) cross-flow cell.

Up to the present time, most OSN studies have been conducted using single-stage systems (Figure 2.35 (a)), in which the feed permeates through the membrane without further purification of the permeate. Such a system is easy to operate, but inefficient in separating molecules with similar rejection values (e.g. separating compound A from B which have rejection values of 90% and 80% respectively). This problem can be overcome by using a membrane cascade system (Figure 2.35 (b)), in which multiple membrane stages are in place to separate the target compound from impurities and recycle any target compound that permeates through the membranes back to the system (Siew, Livingston, Ates & Merschaert, 2013; Kim, Freitas da Silva, Valtcheva & Livingston, 2013).

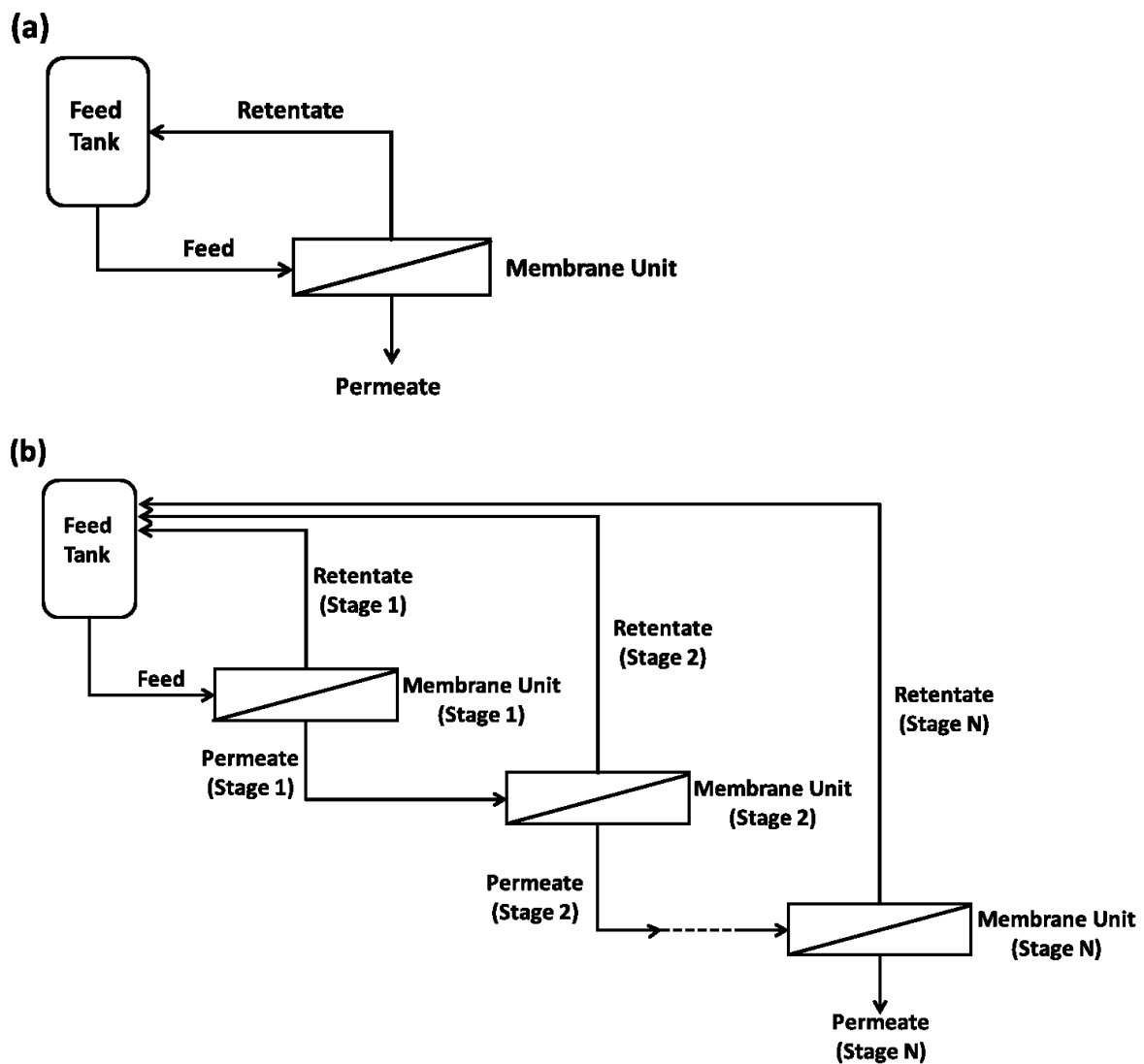


Figure 2.35. Simplified schematics of typical (a) single-stage system and (b) membrane cascade system.

2.2.11. Purification through Diafiltration

The purpose of the membrane unit in MEPS is to purify the target component from other impurities through constant volume diafiltration, in which the mixture of target component and impurities is filtered through the membrane under pressure and fresh solvent is added continuously into the feed tank in order to keep the mixture volume constant in the system as shown in Figure 2.36

$$(F_{\text{fresh_solvent}} = F_{\text{permeate}}).$$

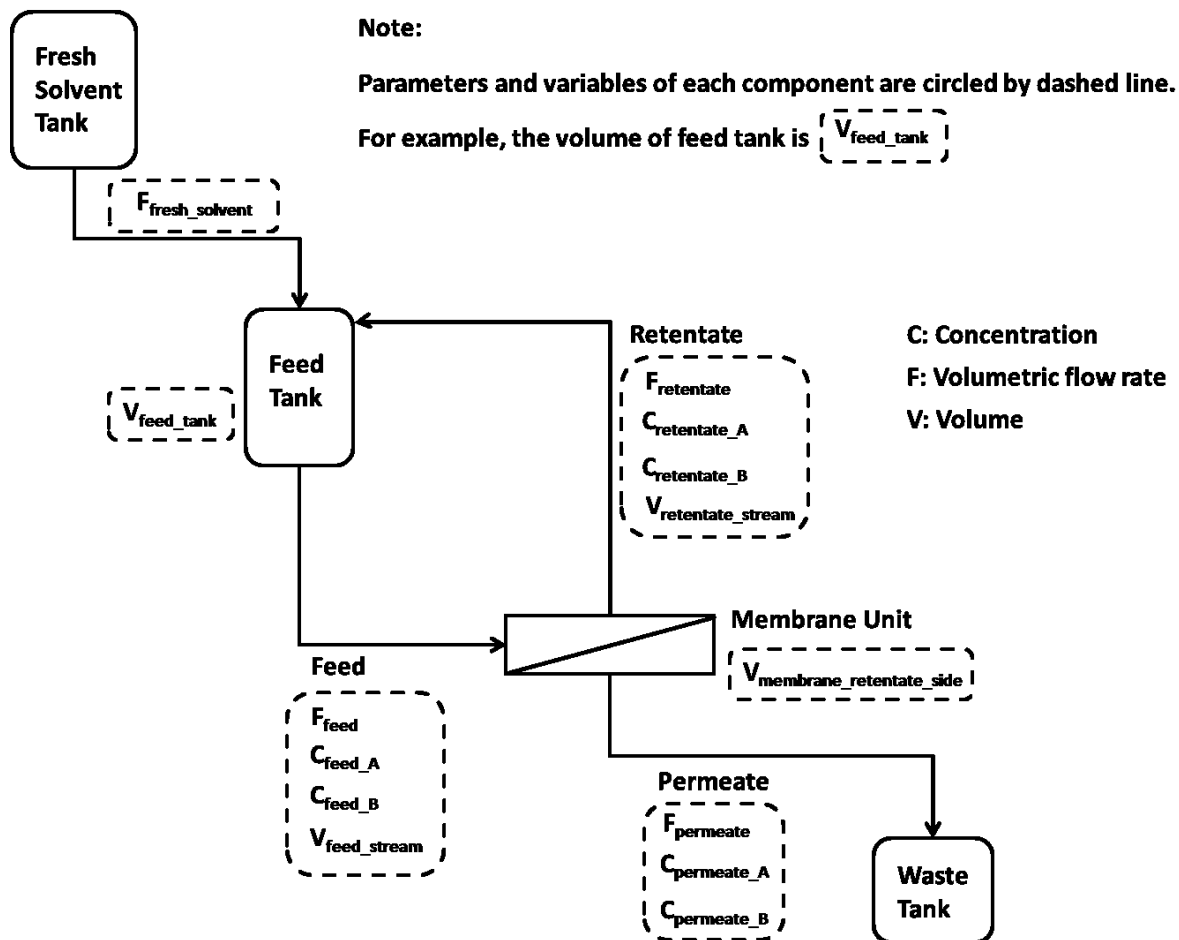


Figure 2.36. Simplified schematic of a single-stage system for constant volume diafiltration (solute A and B dissolved in a solvent).

In constant volume diafiltration, the concentration of a particular component (i) in the system (i.e. the feed concentration into the membrane) decreases exponentially with respect to the wash volume or diavolume (Equation 2.1), which is defined as the ratio between the cumulative volume of permeate and the system volume (in this thesis, the term “wash volume” is used). For example, 10

wash volumes is equivalent to 5 L for a system volume of 500 mL. Detailed calculation of the mass balance during constant volume diafiltration can be found in the appendix (Section A1).

$$\frac{C_{feed_i(t)}}{C_{feed_i(initial)}} = \exp(-W \times (1 - R_i)) \quad \text{Equation 2.1}$$

$$R_i = \left(1 - \frac{C_{permeate_i(t)}}{C_{retentate_i(t)}} \right) \quad \text{Equation 2.2}$$

where $C_{feed_i(t)}$ is the feed concentration of component i at time t , $C_{feed_i(initial)}$ is the initial feed concentration of component i (i.e. $t = 0$), W is the wash volume, R_i is the rejection of component i by the membrane (assumed to be constant with respect to time), $C_{retentate_i(t)}$ and $C_{permeate_i(t)}$ are the retentate and permeate concentration of component i at time t .

Equation 2.1 also shows that the concentration of component i decreases with $(1 - R_i)$, where R_i is the rejection of that component. In other words, a higher rejection will lead to a smaller decrease in concentration over the same wash volumes. As shown in Figure 2.37, if a component has 10% rejection (i.e. $R=0.1$), its concentration can be reduced to a negligible level with 6 wash volumes. If the component has a rejection of 90%, its concentration will be reduced to 54.9% of the initial value with the same wash volumes.

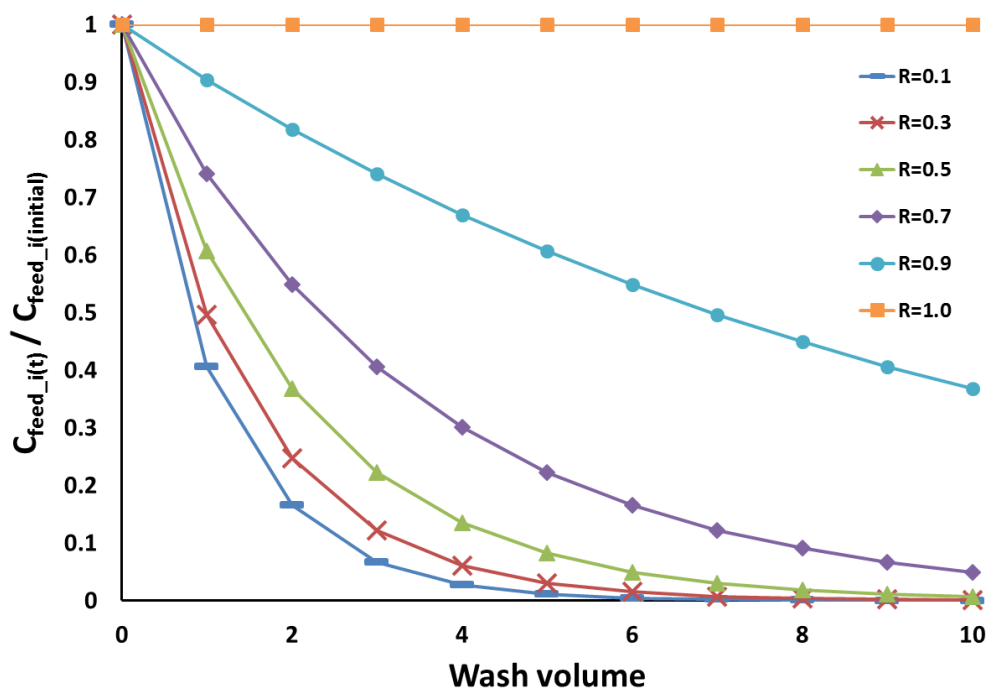


Figure 2.37. Concentration of component i at time (t) over initial concentration during constant volume diafiltration.

This means if compound A is to be separated from compound B by constant volume diafiltration as shown in Figure 2.37, the rejection of compound A must be significantly higher than its counterpart or vice versa. In MEPS, the peptide is grown on a soluble anchor that has close to 100% rejection, which allows the anchored peptide to be separated from various reagents during post-reaction diafiltrations as these reagents have significantly lower rejections.

2.2.12. Soluble Anchors for Liquid Phase Synthesis

Many soluble anchors have been developed for LPPS and other liquid phase reactions, in which the anchored product can be isolated by extraction or precipitation. These compounds are either bulky polymers (Dickerson, Reed & Janda, 2002; Bergbreiter, 2002; Lu & Toy, 2009) or small phase tags (Yoshida & Itami, 2002), some of which are potential candidates for MEPS, where the retention of anchor is directly related to the overall yield of peptide.

Among the large number of linear polymeric anchors available, PEG (Figure 2.31 (a)) is the most popular choice for LPPS because of its excellent solubility in polar aprotic solvents such as DMF and NMP that are commonly used for peptide synthesis, and its poor solubility in nonpolar solvents such as hexane and diethyl ether which can be used to precipitate the PEG-bound peptide (Fischer & Zheleva, 2002). Another popular soluble polymeric anchor is non-cross-linked PS (Figure 2.31 (b)) due to its high loading ($>1.5 \text{ mmol} \cdot \text{g}^{-1}$ polymer), solubility in ethyl acetate and DCM and insolubility in water and methanol. The last two characteristics allow the purification of anchored peptide by simple extraction and precipitation (Chen, Yang, Zhang & Chen, 2006).

On the other hand, a phase tag is attached to a compound in order to facilitate the purification of the compound by extraction or precipitation. For example, a phase tag can be designed to carry charges for the recovery by ionic liquid (Yoshida & Itami, 2002). Phase tags are generally much smaller than polymeric anchors, but can have sterically hindered structures that are likely to be retained by OSN membrane, making them the potential candidates for MEPS. An example is tetrabenzo[a,c,g,i]fluorine (Tbf) (Figure 2.38), which has a multiple-ring structure and hence a relatively large diameter in comparison with the typical pore size of OSN membrane (1-2 nm) (Ramage, Swenson & Shaw, 1998).

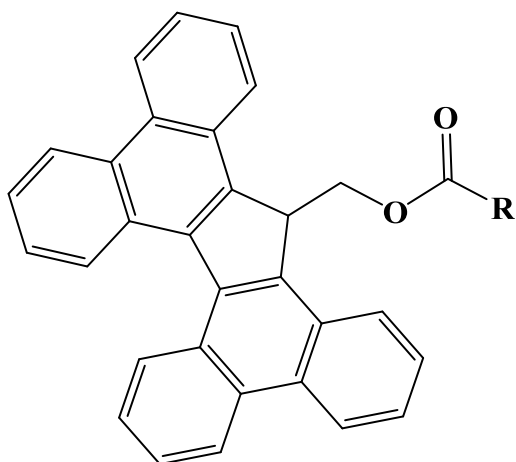


Figure 2.38. Tetrabenzo[a,c,g,i]fluorine (Tbf).

In this project, several anchors that are related to polymeric anchors or phase tags were screened for MEPS. Detailed information of these compounds is presented in the following chapters (Section 3.2.4.2 and Section 5.1).

2.2.13. First Study of MEPS

In Dr. So's work on MEPS (Figure 2.39), the anchor (PEG-linker) first reacts with the activated Fmoc-protected amino acid and then diafiltration is performed to remove the excess activated amino acid and the by-product of coupling. The deprotection reagent is then added into the system to remove the Fmoc group, after which another diafiltration is performed to remove the deprotection reagent and the by-product of deprotection. Further peptide elongation is achieved by cycles of coupling, diafiltration, deprotection and diafiltration. Finally, the peptide is cleaved from the anchor, globally deprotected and purified by preparative HPLC.

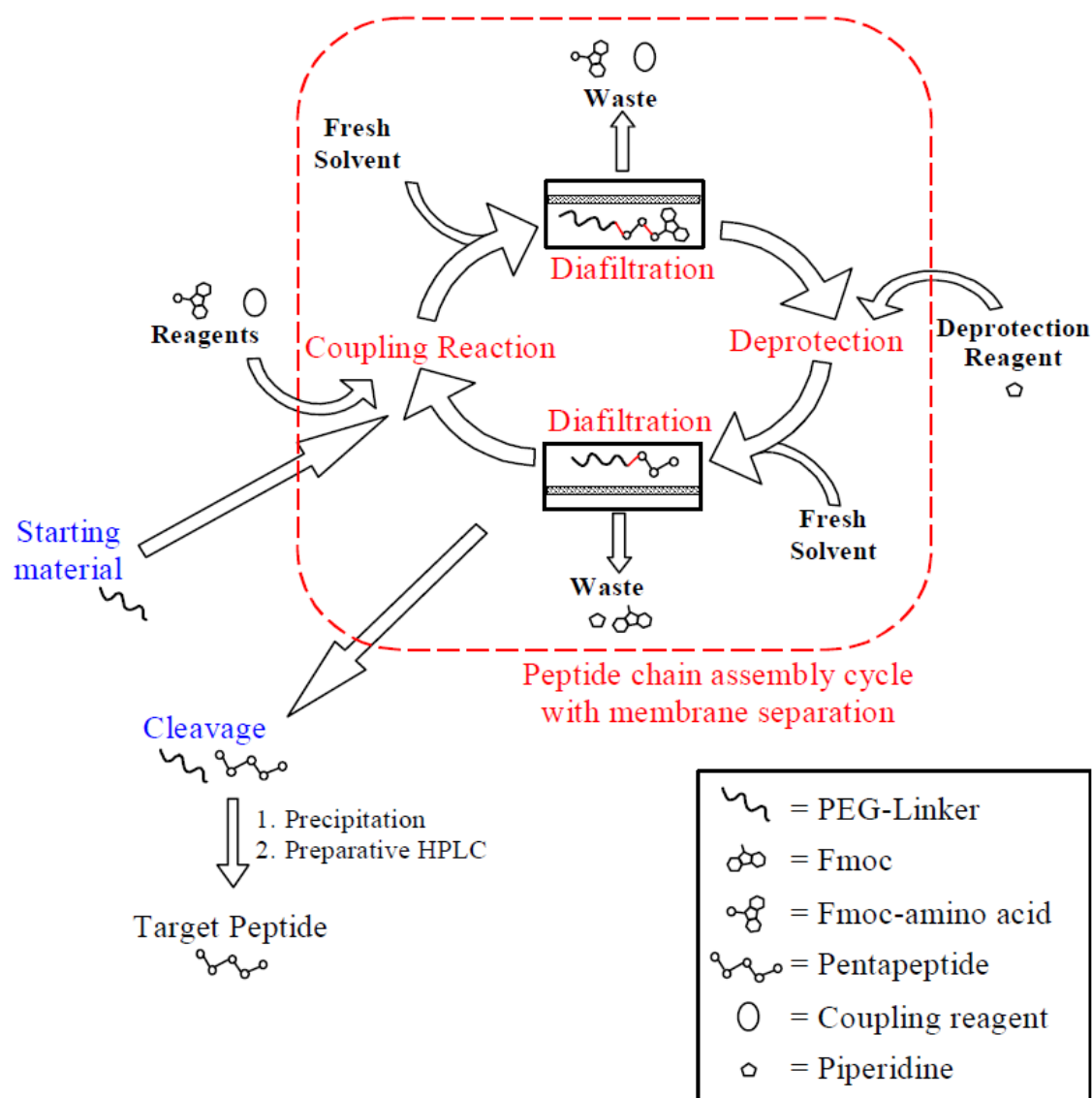


Figure 2.39. Original schematic representation of MEPS (So, 2009; So et al., 2010a; So et al., 2010b).

Since the current research project has benefitted tremendously from the innovative works of Dr. So, it is worthwhile to present a summary of his findings in order to answer the following questions:

- 1) What are the critical issues and corresponding solutions in the development of MEPS?
- 2) How does MEPS compare with conventional peptide synthesis methods like SPPS?
- 3) What improvements can be made?

2.2.13.1. Critical Issues and Corresponding Solutions

Critical issues in the development of MEPS are generally related to three aspects, namely membrane, soluble anchor and peptide chemistry.

2.2.13.2. Membrane

The first criterion for membrane is stability in organic solvents commonly used for peptide synthesis (e.g. DMF and NMP) and 20% piperidine/DMF solution (for de-Fmoc of peptide fragment). The strong dissolution power of DMF and NMP excluded most of the polymeric membranes available at that time for this process (e.g. the StarMemTM membranes from W.R.Grace (USA)). Only three membranes were found to possess the required stability: a composite membrane (MPTM-50 from Koch Membrane System Ltd (USA)), a ceramic membrane (Inopor 2000 (MWCO: 2000 g · mol⁻¹; material: ZrO₂/Al₂O₃; pore size: 3 nm) from Inopor GmbH (Germany)) and a cross-linked polyimide membrane made by Dr. So himself (note: it was later found out that the polyimide membrane still suffered degradation after four couplings in MEPS, due to prolonged exposure to DMF and 20% piperidine/DMF).

The next criterion for a suitable membrane is low rejection of amino acids, coupling and de-Fmoc reagents, but high rejection of anchored peptide. Only two of the candidates met this criterion: the Inopor 2000 membrane and the cross-linked polyimide membrane.

The last criterion for membrane is performance reproducibility. Although the cross-linked polyimide membrane was a promising candidate, new membranes produced under the same conditions did not give the same performance as the one used for the initial MEPS test. On the other hand, being a commercially available membrane, the performance of Inopor 2000 had better reproducibility due to quality control in the manufacturing process.

Considering all three criteria, Inopor 2000 membrane was chosen by Dr. So to synthesise two model peptides (H-Tyr-Ala-Tyr-Ala-Tyr-OH and H-Arg-Lys-Asp-Val-Tyr-OH) via MEPS.

2.2.13.3. Soluble Anchor

As for the membrane, the soluble anchor should be stable under the synthesis conditions (especially in 20% piperidine/DMF). In addition, it should have good retention by the membrane (ideally close to 100%), so that the loss of anchored peptide during post-coupling and post-de-Fmoc diafiltration is minimised.

In many earlier studies of Solution Phase Peptide Synthesis, PEG was used as a soluble anchor to allow the precipitation of anchored peptide for purification purposes, implying that PEG is stable in the peptide synthesis condition. Therefore, a bulky linear PEG (MW=5000 g · mol⁻¹) was used for MEPS and its retention by the Inopor 2000 membrane was found to be 99%.

2.2.13.4. Peptide Chemistry

As the Fmoc-chemistry for peptide synthesis has been optimised in the past few decades, the elongation of peptide is relatively straightforward. However, the cleavage and global deprotection chemistry, where the anchored peptide is subject to concentrated tetrafluoroacetic acid (TFA) solution for breaking the peptide-linker bond and for the removal of side-chain protecting groups of amino acids, has to be optimised in order to improve the overall yield of the process. In Dr. So's work, the un-optimised cleavage and global deprotection resulted in significant loss of overall yields (H-Tyr-Ala-Tyr-Ala-Tyr-OH: from 97% to 55%; H-Arg-Lys-Asp-Val-Tyr-OH: from 98% to 82%).

2.2.13.5. MEPS of Model Peptides

Two penta-peptides were synthesised by both MEPS and SPPS: the first one was an arbitrary sequence (H-Tyr-Ala-Tyr-Ala-Tyr-OH) and the other was Thymopentin (TP-5, H-Arg-Lys-Asp-Val-Tyr-OH), which is a derivative of the human hormone Thymopoietin. For both synthesis methods, PyBOP (2 eq)/HOBt (2 eq)/DIEA (1 eq) was used for the activation of amino acids (2 eq each) for coupling and 20% piperidine/DMF solution was used for the de-Fmoc of anchored peptide fragment. The results of these syntheses are summarised in Table 2.2 and Table 2.3.

Results showed that MEPS achieved high purity and overall yield of the target peptides before cleavage and global deprotection (purity of 100% and overall yield of 81% for H-Tyr-Ala-Tyr-Ala-Tyr-OH; purity of 94% and overall yield of 92% for TP-5). Significant loss of yield was observed due to un-optimised cleavage and global deprotection (from 81% to 55% for H-Tyr-Ala-Tyr-Ala-Tyr-OH; from 92% to 82% for TP-5). According to Dr. So, the products of MEPS had higher purity than those of SPPS for both cases.

Table 2.2. Summary of results for H-Tyr-Ala-Tyr-Ala-Tyr-OH.

| | | |
|---|--|--|
| Peptide | H-Tyr-Ala-Tyr-Ala-Tyr-OH | |
| Synthesis Method | SPPS | MEPS |
| Scale (mmol) | 0.1* | 1.8 |
| Membrane | --- | Inopor 2000 |
| Soluble Anchor | --- | Methoxy-amino-PEG (MeO-PEG-NH ₂ , MW= 5000 g · mol ⁻¹) |
| Linker | --- | HMPA |
| Resin | Wang (Loading=1 mmol · g ⁻¹) | --- |
| Solvent | DMF | |
| Amino Acids | Fmoc-protected Amino Acids (2 eq) | |
| Coupling Reagents | PyBOP (2 eq), HOBT (2 eq), DIEA (1 eq) | |
| deFmoc Reagents | 20% Piperidine/DMF | |
| System Volume (mL) | --- | 54** |
| Volumes of Solvent for Diafiltration after each Coupling (mL) | --- | 54x10 |
| Volumes of Solvent for Washing of Resin after each Coupling (mL) | (Bed volume x 2) x 5 | --- |
| Volumes of Solvent for Diafiltration after each De-Fmoc (mL) | --- | 54x12 |
| Volumes of Solvent for Washing of Resin after each De-Fmoc (mL) | (Bed volume x 2) x 6 | --- |
| Purity before Cleavage and Global Deprotection (%)*** | --- | 100% |
| Overall Yield before Cleavage and Global Deprotection (%)*** | --- | 81% |
| Overall Yield after Cleavage and Global Deprotection (%) | --- | 55% |

*Back-calculated based on 0.1 g resin used and loading of resin (So, 2009, 8.4--Protocol of SPPS).

**Back-calculated based on 10 wash volumes for the coupling step and the volume of used solvents (So, 2010b, Table 3).

***Purity of peptide analysed by small cleavage and global deprotection test.

Table 2.3. Summary of results for Thymopentin (TP-5).

| | | |
|---|--|--|
| Peptide | H-Arg-Lys-Asp-Val-Tyr-OH (TP-5) | |
| Synthesis Method | SPPS | MEPS |
| Scale (mmol) | 0.1* | 0.9 |
| Membrane | --- | Inopor 2000 |
| Soluble Anchor | --- | Methoxy-amino-PEG (MeO-PEG-NH ₂ , MW= 5000 g · mol ⁻¹) |
| Linker | --- | HMPA |
| Resin | Wang (Loading=1 mmol · g ⁻¹) | --- |
| Solvent | DMF | |
| Amino Acids | Fmoc-protected Amino Acids (2 eq) | |
| Coupling Reagents | PyBOP (2 eq), HOBt (2 eq), DIEA (1 eq) | |
| deFmoc Reagents | 20% Piperidine/DMF | |
| System Volume (mL) | --- | 54** |
| Volumes of Solvent for Diafiltration after each Coupling (mL) | --- | 54x10 |
| Volumes of Solvent for Washing of Resin after each Coupling (mL) | (Bed volume x 2) x 5 | --- |
| Volumes of Solvent for Diafiltration after each De-Fmoc (mL) | --- | 54x12 |
| Volumes of Solvent for Washing of Resin after each De-Fmoc (mL) | (Bed volume x 2) x 6 | --- |
| Purity before Cleavage and Global Deprotection (%)*** | 77% | 94% |
| Overall Yield before Cleavage and Global Deprotection (%)*** | --- | 92% |
| Overall Yield after Cleavage and Global Deprotection (%) | --- | 82% |

*Back-calculated based on 0.1 g resin used and loading of resin (So, 2009, 8.4--Protocol of SPPS).

**Back-calculated based on 10 wash volumes for the coupling step and the volume of used solvents (So, 2010b, Table 3).

***Purity of peptide analysed by small cleavage and global deprotection test.

2.2.13.6. Improvements

Attempts were made to improve two aspects of MEPS: the performance of the cross-linked polyimide membrane and the development of a degradable polymeric anchor. Although a cross-linked polyimide membrane with better stability, selectivity and reproducibility was not achieved, fabrication parameters that had major influences on the performance of membranes were identified, paving the way for future works in this direction. On the other hand, the poly(ethylene glycol) (PEG) anchor was precipitated together with the target peptides after global deprotection, making it an impurity that requires removal. Hence, a significant amount of effort was invested in the search for a polymeric anchor that would degrade in the global deprotection solution (a concentrated TFA solution with scavengers). Poly(lactic acid) (PLA) was found to be a promising candidate that could be completely hydrolysed by 70% TFA solution in three to four hours and was stable in 20% piperidine/DMF. However, MEPS of H-Tyr-Ala-Tyr-Ala-Tyr-OH on PLA showed that couplings had diminishing yields, presumably due to the aggregation of peptide fragments with PLA.

2.2.13.7. Suggestions

Suggestions were made with regard to anchor, OSN system and membrane. Firstly, instead of linear polymeric compounds, dendritic polymers were proposed as soluble anchors, since their branched structures would logically result in higher membrane rejection. For the degradable anchor, two new candidates were recommended for future studies. Secondly, an automated OSN system was proposed to reduce the time and human labour requirement of MEPS. Lastly, two alkene diamines were recommended for the cross-linking of polyimide for the improvement of membrane performance.

2.2.13.8. Major Aspects of MEPS

Based on the work of Dr. So (as summarised above) and the general knowledge about OSN, the following statements can be made with regard to the major aspects of MEPS, which are examined closely in the following chapters based on the experimental and computational data obtained by the author.

1. With regard to the choice of membrane:
 - Ceramic multi-tube membrane has better stability and higher membrane area/volume ratio than polymeric OSN flat sheet membrane (note: spiral module of polymeric OSN membrane is still difficult to obtain).
2. For soluble anchor:
 - A branched structure is expected to have higher rejection than a linear structure with the same molecular weight.
 - The rejection of anchor is expected to increase proportionally with its molecular size, which is reflected by the molecular weight.
3. In terms of peptide synthesis:
 - 2 eq amino acid and coupling reagents are required for each coupling.
 - 20% piperidine solution is required for each de-Fmoc.
 - Cleavage and global deprotection is expected to result in significant yield loss.
4. Concerning the OSN system and operation procedure:
 - Single-stage system is sufficient for retaining the anchored peptide (i.e. no significant yield loss is expected) if the anchor rejection is higher than 99%.
 - The removal of excess amino acid after each coupling is critical for preventing the formation of error sequence during the subsequent de-Fmoc and couplings.

Chapter Three –

Case Study One: MEPS of Fully Deprotected Fmoc-RADA-NH₂

3.1. Introduction

RADA₁₆-I (i.e. Ac-(RADA)₄-NH₂) is a synthetic peptide designed to mimic a segment of the yeast Zuotin protein (Ye et al., 2008). Its ability to self-assemble into a well-defined nanofiber scaffold (Yokoi, Kinoshita, & Zhang, 2005) makes it a promising candidate for three-dimensional cell culture and regenerative medicine (Cormier et al., 2013). A fragment of this peptide, Fmoc-Arg-Ala-Asp-Ala-NH₂ (fully deprotected Fmoc-RADA-NH₂) (Figure 3.1), was chosen for the initial investigation of MEPS, in which the excess reagents and by-products can be removed rapidly through the membrane after each reaction, while the anchored peptide fragments are retained by the OSN membrane. More explanation of the MEPS concept can be found in the previous chapter (Section 2.2.13).

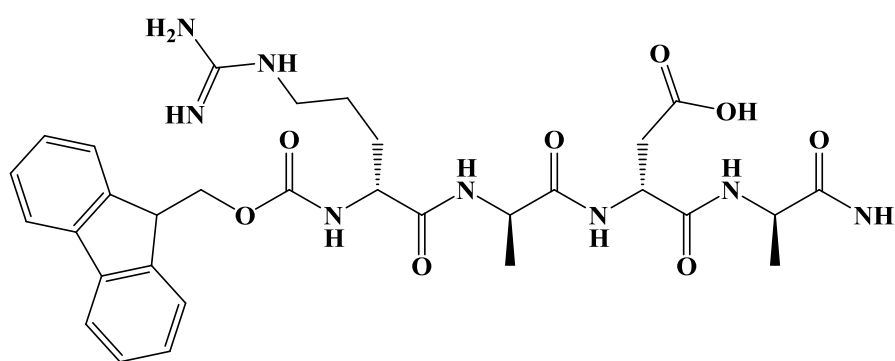


Figure 3.1. Fmoc-Arg-Ala-Asp-Ala-NH₂ (fully deprotected Fmoc-RADA-NH₂) (MW = 653 g · mol⁻¹).

This chapter details the research work by the author on the various aspects of MEPS (anchor, membrane, choice of peptide chemistry, diafiltration), which was aimed to scale up and improve the novel process over the original design (detailed summary in previous chapter (Section 2.2.13.5)).

Industry-standard peptide chemistry was applied for the easy adoption of MEPS in the near future.

The choice of OSN system and membranes was limited to those that are commercially available, as

the re-development of these components would be extremely time-consuming. Four soluble anchors (1- and 2-branched cyclodextrins with Rink linker, pentaerithritol, DPEG) (chemical structures shown in Section 3.2.4.2) were contributed by the research partners of the MemTide consortium. Together with 2,4-didocosyloxybenzalcohol (DDBA) (Figure 3.2) which was synthesised by the author, these anchors were screened with two commercial ceramic membranes (Inopor 450 and Inopor 750) in order to select the most suitable one in terms of retention by membrane and ease of synthesis at the tens-of-grams scale. After the initial screening, DDBA was chosen for MEPS due to its relatively high retention (87.7 ± 5.3 % by Inopor 750 and 90.0 ± 3.1 % by Inopor 450) and ease of synthesis (49.02 g was synthesised in 6 days excluding the drying time).

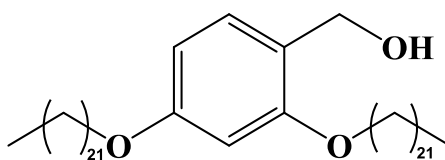


Figure 3.2. 2,4-didocosyloxybenzalcohol (DDBA) (MW = 757 g · mol⁻¹).

DDBA (Figure 3.2) was a hyper-hydrophobic anchor invented originally for LPPS (Tana et al., 2009; Abe et al., 2012; Okada et al., 2012). In traditional solution phase peptide synthesis, significant yield loss can occur during the precipitation of short peptide fragments. This problem is overcome by growing the peptide on DDBA, which can be precipitated readily by the addition of polar anti-solvents. In the original design of DDBA, each step of peptide synthesis can be carried out in tetrahydrofuran (THF) and the intermediate products can be precipitated by acetonitrile. The precipitates are then washed repeatedly with acetonitrile in order to remove impurities, before being redissolved in THF for the next reaction. The synthesis of a 20-amino-acid peptide, bivalirudin, demonstrated that the synthesis and condensation of 3 peptide fragments (each had 6 to 8 amino acid residues) on DDBA could achieve high yields (77–89 % for fragment syntheses and 85–93 % for fragment condensations) (Okada et al., 2012).

Fully deprotected Fmoc-RADA-NH₂ was first synthesised by SPPS, so that experimental results such as yield and purity could serve as the reference for comparison with MEPS. In order to study the peptide chemistry and mitigate any side-reactions before proceeding to the MEPS process, the peptide was then synthesised in liquid phase on DDBA by the precipitation of intermediate products. The MEPS of model peptide was performed several times, during which technical problems were investigated and resolved. Based on the experimental results, the performance of MEPS and SPPS were compared in terms of material cost, process time, building block utility, volumetric efficiency and environmental factor. Finally, potential areas for the further improvement of MEPS were identified and assessed.

3.2. Experimental

3.2.1. Materials

All chemicals were used as received from the commercial suppliers unless stated otherwise.

For the synthesis of DDBA, 1-bromodocosane (CAS number: 6938-66-5; product code: B0392) was purchased from TCI Europe N.V.. 2,4-dihydroxybenzaldehyde (CAS number: 95-01-2; product code: 168637), 1,3-dimethyl-2-imidazolidinone (DMI) (CAS number: 80-73-9; product code: 40725), magnesium sulphate (CAS number: 7487-88-9; product code: M7506), potassium carbonate (CAS number: 584-08-7; product code: 209619) and sodium borohydride (CAS number: 16940-66-2; product code: 71320) were purchased from Sigma-Aldrich Chemie GmbH. Chloroform (CAS number: 67-66-3; product code: P5135), n-hexane (CAS number: 110-54-3; product code: P5389) and ethanol (CAS number: 64-17-5; product code: P5314) were purchased from Romil Ltd.

Other soluble anchors, namely pentaerithritol, 1- and 2-branch cyclodextrin with Rink linker and DPEG, were supplied by other research partners of the MemTide consortium (pentaerithritol and branched cyclodextrin from the University of Turku; DPEG from IRB).

For OSN, ceramic membranes Inopor 450 and 750 (Material: $\text{TiO}_2/\text{Al}_2\text{O}_3$, 19-channel, length = 25 cm, channel diameter = 3.5 mm. Pore size = 0.9 and 1.0 nm, MWCO = 450 $\text{g} \cdot \text{mol}^{-1}$ and 750 $\text{g} \cdot \text{mol}^{-1}$ respectively) were purchased from Inopor GmbH.

For peptide synthesis, Fmoc-L-Ala-OH (CAS number: 35661-39-3; product code: 8520030250), Fmoc-L-Asp(OtBu)-OH (CAS number: 71989-14-5; product code: 8520050250), Fmoc-L-Arg(Pbf)-OH (CAS number: 154445-77-9; product code: 8520670250), HBTU (CAS number: 94790-37-1; product code: 8510060100), Fmoc-Rink linker (CAS number: 126828-35-1; product code: 8510010025) and Rink amide AM resin (100-200 mesh) (CAS number: 183599-10-2; product code: 8551300025) were

purchased from Merck KGaA. DIC (CAS number: 693-13-0; product code: D125407), DIEA (CAS number: 7087-68-5; product code: 03440), HOBt (CAS number: 123333-53-9; product code: 54802), DMAP (CAS number: 1122-58-3; product code: 107700), piperidine (CAS number: 110-89-4; product code: 104094), TFA (CAS number: 76-05-1; product code: T6508) and TIS (CAS number: 6485-79-6; product code: 233781) were purchased from Sigma-Aldrich Chemie GmbH. THF, DMF and DCM were purchased from an internal supplier at Lonza AG.

For measuring pH, pH-indicator strips (pH-measuring range: 0-14; product code: 1.09535.0001) were purchased from Merck KGaA.

For HPLC, Sunfire C18 column (150 X 4.6 mm, 3.5 μm particle size) was purchased from Waters Ltd. Hypersil C18 column (250 X 4.6 mm, 5.0 μm particle size) was purchased from Agilent Technologies Inc.. HPLC-grade acetonitrile and isopropanol were purchased from Romil Ltd. HPLC-grade water was obtained internally in Lonza AG. TFA (CAS number: 76-05-1; product number: T6508) was purchased from Sigma-Aldrich Chemie GmbH.

For NMR, deuterated chloroform (CAS number: 865-49-6; product code: 151858) was purchased from Sigma-Aldrich Chemie GmbH.

For chloranil test, chloranil (CAS number: 118-75-2; product code: 45374) and toluene (CAS number: 108-88-3; product code: 244511) were purchased from Sigma-Aldrich Chemie GmbH. Acetone was obtained from the internal supplier (Lonza AG).

3.2.2. Apparatus

3.2.2.1. Cross-flow OSN System

A cross-flow OSN system (Figure 3.3) was purchased from Natan GmbH (Switzerland). The feed tank is elevated above other major units of the system (pipe lines, pumps, membrane unit and heat exchanger). The minimum working volume is 400-500 mL (liquid only fills up pipe line, pump 2, membrane unit and heat exchanger), while the maximum working volume is 2.5 L. The system is pressurised by compressed nitrogen from the top of feed tank with a maximum working pressure of 25 bar. Pump 1 is an external device that serves to: 1) pump in fresh solvent during constant volume diafiltration (Figure 3.3 (a)); 2) recycle the permeate from the permeate tank back to the system in order to maintain a constant volume during rejection test of compounds (Figure 3.3 (b)). Pump 2 is a gear pump that circulates the test solution in the system (flow rate is approximately $1.7 \text{ L} \cdot \text{min}^{-1}$), controlling the flow direction and inducing sufficient mixing. The membrane unit can install two different membrane housings: the one for ceramic membranes can accommodate one 19-channel membrane (diameter = 2.5 cm), while the one for polymeric membrane can accommodate two flat-sheet membranes (25 cm x 5 cm each; O-ring thickness = 0.4 cm).

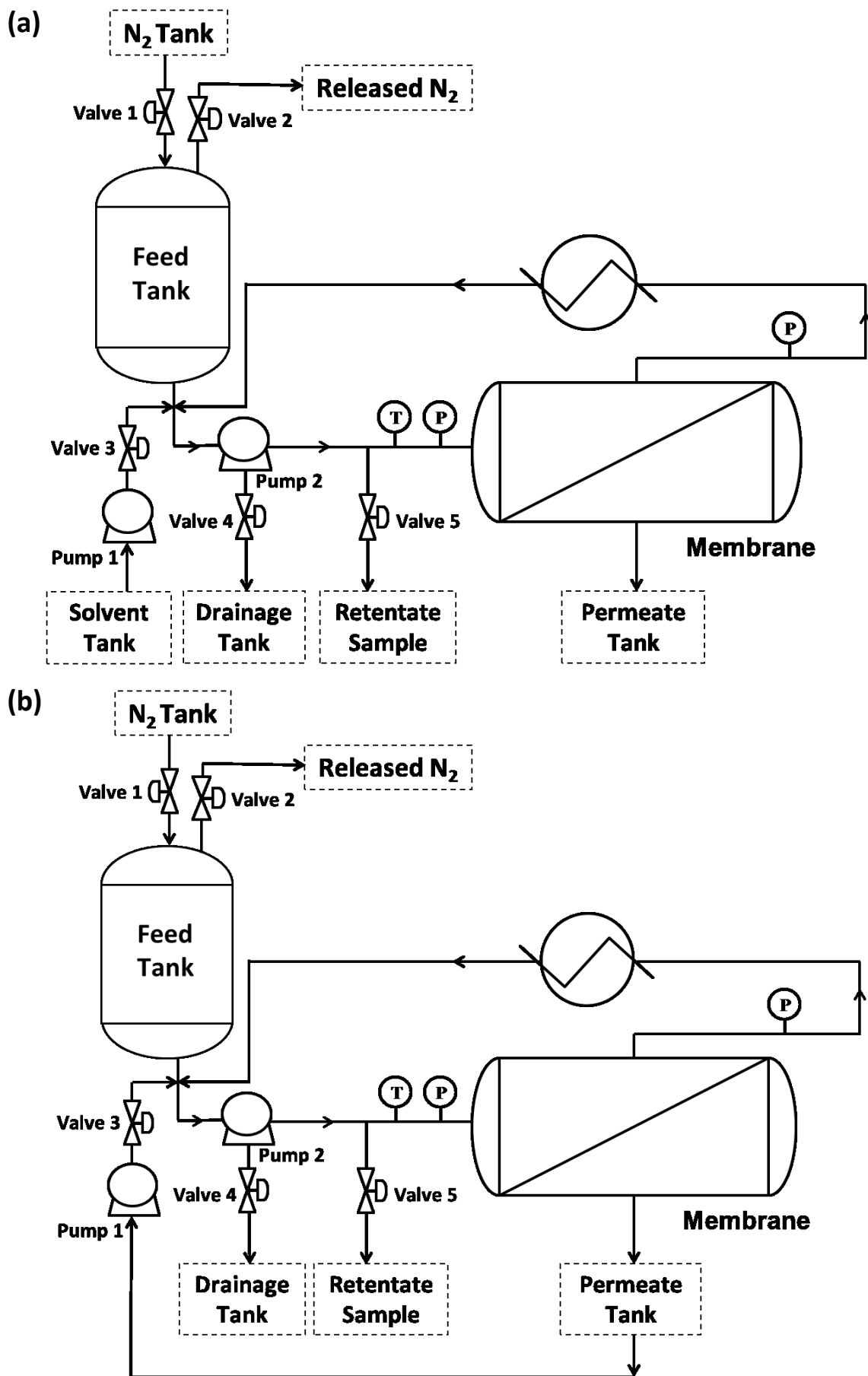


Figure 3.3. Cross-flow OSN system in (a) diafiltration mode and (b) full recycle mode.

3.2.2.2. Analytical Equipment

Solution NMR spectra were obtained with a Bruker Ascend 400. HPLC measurements were obtained by a Waters 2695 separations module and a Waters 2487 dual λ absorbance detector. LC/MS measurements were obtained by QSTAR® XL hybrid LC/MS/MS System.

3.2.3. Analytical Methods

3.2.3.1. HPLC Methods

| | | | | | |
|----------------------------------|---|--------------------------------|------|------|------|
| Name | DDBA_HPLC1* | | | | |
| HPLC Column | Sunfire, C18, 150 X 4.6 mm, 3.5 μ m particle size | | | | |
| Column Temperature (°C) | 40 | | | | |
| Detection Wavelength (nm) | 220 | | | | |
| Gradient | Time(min) | Flow (mL · min ⁻¹) | %A | %B | %C |
| | 0.00 | 1.00 | 0.0 | 40.0 | 60.0 |
| | 15.00 | 1.00 | 0.0 | 90.0 | 10.0 |
| | 17.00 | 1.00 | 0.0 | 90.0 | 10.0 |
| | 17.50 | 0.50 | 95.0 | 0.0 | 5.0 |
| | 38.50 | 0.50 | 95.0 | 0.0 | 5.0 |
| | 39.00 | 0.50 | 0.0 | 40.0 | 60.0 |
| | 42.00 | 0.50 | 0.0 | 40.0 | 60.0 |
| | 42.50 | 1.00 | 0.0 | 40.0 | 60.0 |
| | 45.00 | 1.00 | 0.0 | 40.0 | 60.0 |
| Eluent A | Isopropanol | | | | |
| Eluent B | 0.1 vol% TFA/Acetonitrile (i.e. 2 mL TFA in 2 L Acetonitrile) | | | | |
| Eluent C | 0.1 vol% TFA/Water (i.e. 2 mL TFA in 2 L Water) | | | | |
| *Note | Old name (as on HPLC results): RADA_DDBA_10Jun2013 | | | | |

| | | | | | |
|----------------------------------|---|--------------------------------|------|------|------|
| Name | Fmoc-RADA-DDBA_HPLC1* | | | | |
| HPLC Column | Sunfire, C18, 150 X 4.6 mm, 3.5 µm particle size | | | | |
| Column Temperature (°C) | 40 | | | | |
| Detection Wavelength (nm) | 220 | | | | |
| Gradient | Time(min) | Flow (mL · min ⁻¹) | %A | %B | %C |
| | 0.00 | 1.00 | 0.0 | 40.0 | 60.0 |
| | 15.00 | 1.00 | 0.0 | 90.0 | 10.0 |
| | 17.00 | 1.00 | 0.0 | 90.0 | 10.0 |
| | 17.50 | 0.50 | 85.0 | 0.0 | 15.0 |
| | 50.00 | 0.50 | 95.0 | 0.0 | 5.0 |
| | 60.00 | 0.50 | 95.0 | 0.0 | 5.0 |
| | 60.50 | 0.50 | 0.0 | 40.0 | 60.0 |
| | 64.50 | 0.50 | 0.0 | 40.0 | 60.0 |
| | 65.00 | 1.00 | 0.0 | 40.0 | 60.0 |
| 70.00 | 1.00 | 0.0 | 40.0 | 60.0 | |
| Eluent A | Isopropanol | | | | |
| Eluent B | 0.1 vol% TFA/Acetonitrile (i.e. 2mL TFA in 2L Acetonitrile) | | | | |
| Eluent C | 0.1 vol% TFA/Water (i.e. 2mL TFA in 2L Water) | | | | |
| *Note | Old name (as on HPLC results): RADA_DDDBA_1July2013 | | | | |

| | | | | | |
|----------------------------------|---|--------------------------------|-----|------|------|
| Name | Fmoc-RADA_HPLC1* | | | | |
| HPLC Column | Sunfire, C18, 150 X 4.6 mm, 3.5 µm particle size | | | | |
| Column Temperature (°C) | 40 | | | | |
| Detection Wavelength (nm) | 220 | | | | |
| Gradient | Time(min) | Flow (mL · min ⁻¹) | %A | %B | %C |
| | 0.00 | 1.00 | 0.0 | 5.0 | 95.0 |
| | 20.00 | 1.00 | 0.0 | 95.0 | 5.0 |
| | 25.00 | 1.00 | 0.0 | 95.0 | 5.0 |
| | 25.50 | 1.00 | 0.0 | 5.0 | 95.0 |
| | 30.00 | 1.00 | 0.0 | 5.0 | 95.0 |
| Eluent A | Isopropanol | | | | |
| Eluent B | 0.1 vol% TFA/Acetonitrile (i.e. 2mL TFA in 2L Acetonitrile) | | | | |
| Eluent C | 0.1 vol% TFA/Water (i.e. 2mL TFA in 2L Water) | | | | |
| *Note | Old name (as on HPLC results): Vida Anchor A_2July2013 | | | | |

3.2.3.2. Chloranil Test

The chloranil test detects the presence of piperidine in the peptide synthesis system after each post-de-Fmoc washing for SPPS and LPPS, or post-de-Fmoc diafiltration for MEPS. Chloranil (4.1 g) was added into toluene (100 mL) and the mixture was stirred for 15 minutes at room temperature. One drop of the chloranil solution (yellow) was taken with a glass Pasteur pipette and added into a 1.5 mL glass tube, followed by the addition of 1 mL acetone. The solution to be tested for the presence of piperidine was sampled with a new glass Pasteur pipette and one drop of it was added into the diluted chloranil solution. The glass tube was then capped and shaken in order to provide good mixing. Positive result: purple solution (i.e. piperidine is present). Negative result: light yellow solution.

3.2.3.3. Ninhydrin Test

The ninhydrin test detects the presence of free amine and hence the completion of coupling in SPPS. Solution A (phenol/ethanol, 76 g / 24 g), solution B (0.2 M potassium cyanide/pyridine, i.e. 3.26 g / 250 mL) and solution C (0.28 M ninhydrin/ethanol, i.e. 12.47 g / 250 mL) were prepared separately. A sample of the peptide-loaded resin (approx. 50 mg) was taken, washed with DMF (2 mL) and then filtered. The washing was repeated two more times. The peptide-loaded resin was then washed with DCM (2 mL) and then filtered. The washing was again repeated for two more times. A small amount of the peptide-loaded resin (approx. 2 mg) was taken and added into a small test tube. Three drops of solution A were added into the test tube, followed by three drops of solution B and then the same amount of solution C. The mixture was shaken for five minutes (1000 rpm, 75 °C). Positive result: blue solution (i.e. free amine exists). Negative result: light yellow solution.

3.2.4. General Procedures

This section details the general protocols for the experiments conducted in this case study.

For the chemistry experiments, the purity of dried product was measured by HPLC, taking into account all the visible peaks. The overall yield was calculated based on this purity, the mass of dried product and the quantity of starting material. The completion of reaction was monitored by HPLC and was estimated by the relative yield of the target product. The definitions and calculation methods for purity, overall yield and relative yield are given below.

A dried product may contain impurities in addition to the target component as shown in Figure 3.4. In this example, the purity is calculated by integrating all the visible peaks (the starting material, by-product 1 and 2 and the target product) and obtaining the percentage that corresponds to the target product as shown by Equation 3.1.

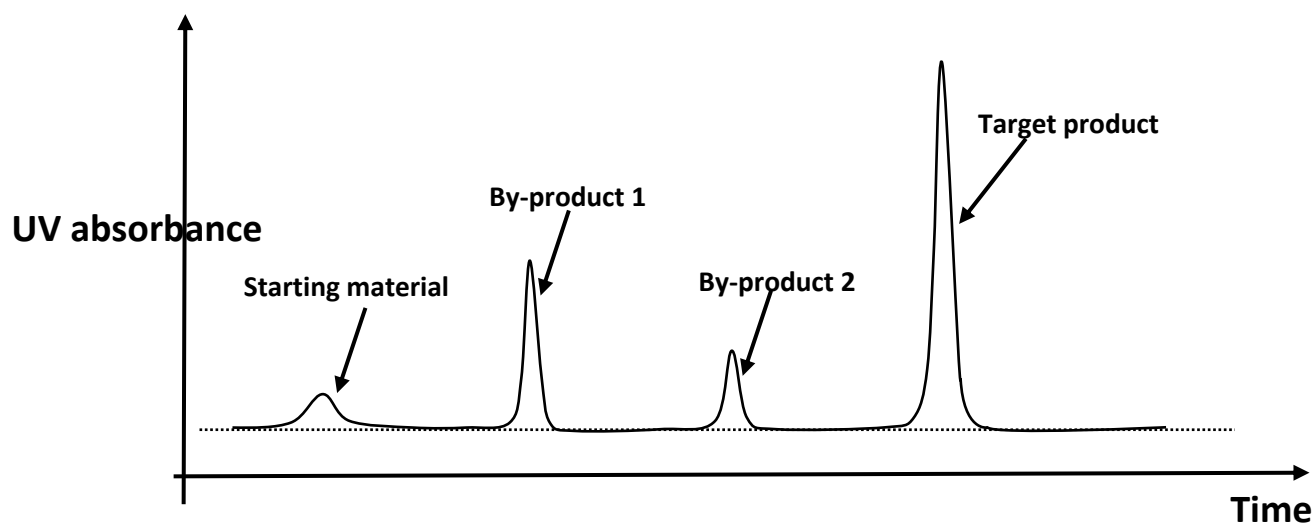


Figure 3.4. HPLC result for a dried product that contains four components.

$$\mathbf{Purity}_{dried\ product} = \frac{\mathbf{Peak\ Integration\ Area}_{target\ product}}{\mathbf{Sum\ of\ Peak\ Integration\ Areas}} \quad \mathbf{Equation\ 3.1}$$

Once the purity of the dried product is obtained, the quantity of target component is estimated based on the mass and purity of the dried product as shown by Equation 3.2, assuming that the target component and all impurities have similar correlations between UV-absorbance and concentration. The overall yield of the reaction/synthesis is then calculated based on the estimated quantity of target product, the quantity of starting material and the stoichiometric coefficient (N) as shown by Equation 3.3.

$$\mathbf{Quantity}_{target\ product} = \frac{\mathbf{Total\ Mass}_{dried\ product} \times \mathbf{Purity}_{dried\ product}}{\mathbf{Molecular\ Weight}_{target\ product}} \quad \mathbf{Equation\ 3.2}$$

$$\mathbf{Overall\ Yield} = \frac{\mathbf{Quantity}_{target\ product}}{\mathbf{Quantity}_{starting\ material} \times \mathbf{N}} \quad \mathbf{Equation\ 3.3}$$

where N is the stoichiometric coefficient of the target product (i.e. 1 mol of starting material is expected to have N mol of target product assuming all the intermediate reactions have 100% yield).

The relative yield of target product with respect to the starting material in the same reaction is used to estimate the completion of a reaction, which is calculated by integrating the peaks of the starting material and the target product according to Equation 3.4. The underlying assumption is that the target component and starting material have similar correlations between UV-absorbance and concentration.

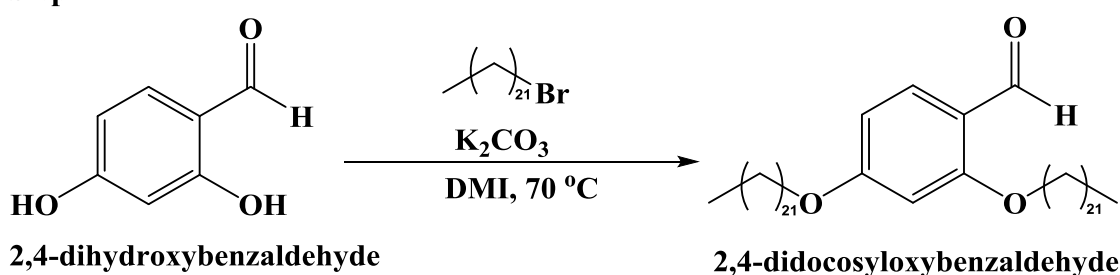
$$\mathbf{Relative\ Yield} = \frac{\mathbf{Peak\ Integration\ Area}_{target\ product}}{\mathbf{Peak\ Integration\ Area}_{starting\ material}/\mathbf{N} + \mathbf{Peak\ Integration\ Area}_{target\ product}} \quad \mathbf{Equation\ 3.4}$$

where N is the stoichiometric coefficient of the target product (i.e. 1 mol of starting material is expected to have N mol of target product assuming all the intermediate reactions have 100 % yield).

3.2.4.1. Synthesis of DDBA

DDBA was synthesised by the author for using it as a soluble anchor in MEPS. The synthesis consisted of two steps: the synthesis of 2,4-didocosyloxybenzaldehyde from 2,4-dihydroxybenzaldehyde and 1-bromodocosane, and then the reduction of 2,4-didocosyloxybenzaldehyde by sodium borohydride into DDBA (Figure 3.5). The synthesis protocols were derived from the ones for similar compounds (Morikawa et al., 2006; Chiba et al., 2009).

Step 1.



Step 2.

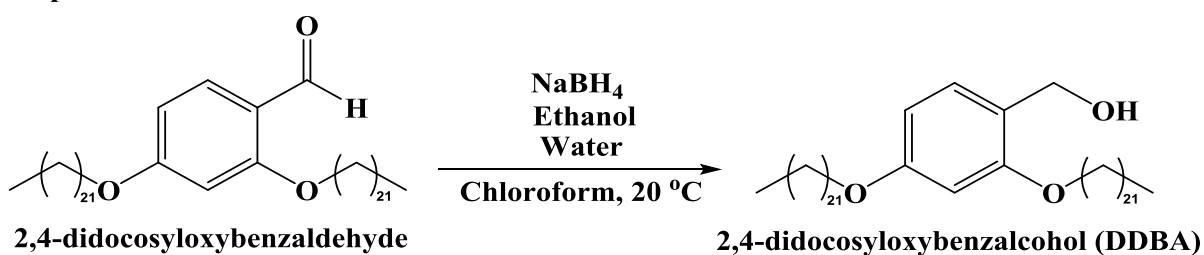


Figure 3.5. Synthesis of DDBA.

Step 1. Synthesis of 2,4-didocosyloxybenzaldehyde DMI (420 mL) was warmed to 70 °C, followed by the addition of 1-bromodocosane (100.00 g, 256 mmol, 2.2 eq), 2,4-dihydroxybenzaldehyde (15.90 g, 115 mmol, 1.0 eq) and potassium carbonate (38.40 g, 278 mmol, 2.4 eq). The reaction solution was stirred for 24 hours at 70 °C and the reaction was monitored by HPLC (analysis at the beginning of reaction and after 24 hours; method: DDBA_HPLC1). By-products and unreacted reagents were removed by 2 cycles of extraction with n-hexane (1400 mL), and then with water (700 mL). The product was dried in a vacuum oven (-80 kPa (gauge) and 30 °C) until the mass loss due to solvent evaporation became negligible.

Step 2. Synthesis of 2,4-didocosyloxybenzalcohol(DDBA) 2,4-didocosyloxybenzaldehyde (10.00 g, 13.2 mmol, 1.0 eq) was dissolved in chloroform (800 mL) at 25 °C, followed by ethanol (250 mL), sodium borohydride (0.50 g, 13.2 mmol, 1.0 eq) and lastly de-ionised water (840 µL, 46.6 mmol, 3.5 eq). The reaction solution was stirred for 8 hours at 20 °C and the reaction was monitored by HPLC (analysis after 5 and 8 hours; method: DDBA_HPLC1). By-products and unreacted reagents were removed by extractions with aqueous sodium chloride solution (38.40 g in 960 mL). The organic phase was dried with magnesium sulphate (20.00 g) and the product was obtained by evaporation of chloroform and then dried in a vacuum oven (-80 kPa (gauge) and 30 °C) until the mass loss due to solvent evaporation became negligible.

3.2.4.2. Anchor Screening

Five soluble anchors were tested with Inopor 450 and Inopor 750 membranes. DDBA was synthesised by the author and the other four were provided by research partners of the MemTide consortium as mentioned earlier in this chapter (Section 3.2.1). One of the smallest amino acids, Fmoc-Ala-OH, was also tested for the purpose of comparison.

A solution of the test compound (1.0 weight % in solvent, e.g. 1.0 g compound in 100.0 g solvent) was prepared and added into the OSN system, which was then pressurised (5 bar) for the solution to permeate through the membrane. The permeate was collected in a measuring cylinder (100 mL) and recycled back to the system, maintaining a constant external volume (50-100 mL) throughout the experiment (Figure 3.3 (b)). Samples of permeate and retentate were taken every hour and analysed by HPLC to determine the concentrations of test compound in the samples (except DDBA, whose concentration was measured by UV absorption at 289 nm as the suitable HPLC method was unavailable at that time). Rejection of the component i (R_i) was then calculated according to Equation 2.2 (Section 2.2.11).

Several measures were taken to ensure the validity of rejection data:

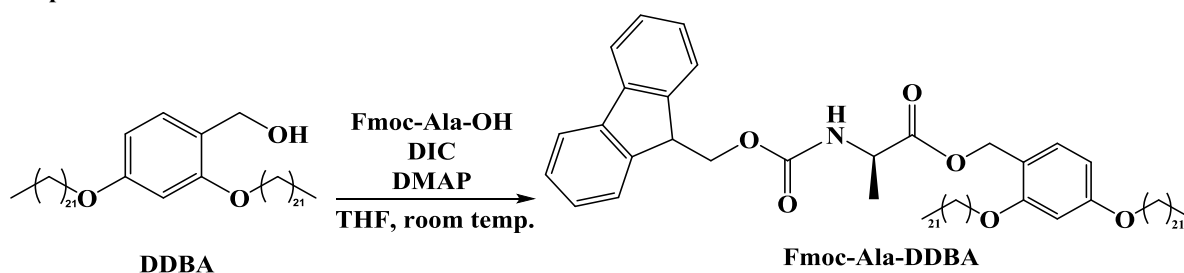
- 1) Each rejection test was run for three hours so that three sets of samples could be taken from the permeate and retentate streams at an hourly interval;
- 2) Calibration curves (between concentration and integrated peak area on chromatogram for HPLC; between concentration and absorbance for UV absorption) were made for each compound to ensure that the measured concentrations were in the linear region;
- 3) Samples of permeate and retentate were diluted by the same extent to allow direct comparison;

- 4) Due to the variability of membrane performance, four membranes (two pieces of Inopor 450 and two pieces of Inopor 750) were used repeatedly for the rejection tests so that the rejection data are comparable;
- 5) Rejection tests were carried out in this sequence: a) Fmoc-Ala-OH/THF; b) anchor A; c) Fmoc-Ala-OH/THF; d) anchor B; e) Fmoc-Ala-OH/THF etc. After each experiment, the membrane was washed repeatedly with solvent and then submerged in aqueous sodium hydroxide solution (pH ~11) overnight. The membrane was then washed repeatedly with water and dried in a vacuum (-80 kPa (gauge)) oven at 30 °C. The rejection test of Fmoc-Ala-OH served to check the consistency of membrane performance after repeated usage and washing.

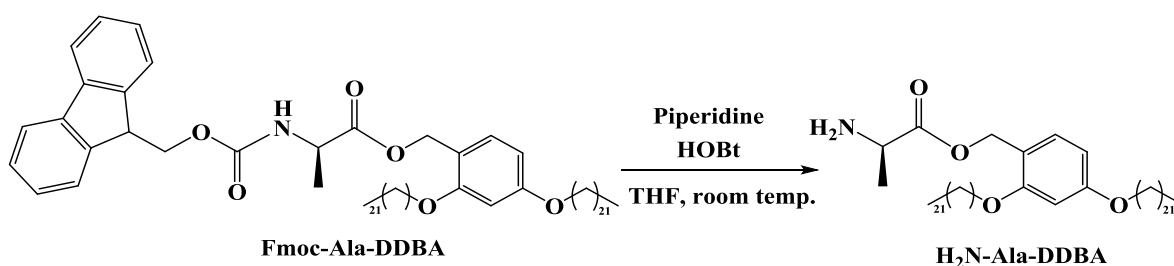
3.2.4.3. LPPS of Fully Protected Fmoc-RADA-DDBA by Precipitation

Fully protected Fmoc-RADA-DDBA was synthesised in liquid phase by the precipitation of anchored peptide after each reaction. The aim was to investigate the synthesis chemistry before attempting MEPS, which would involve scaling up the synthesis and substituting precipitation with diafiltration. The synthesis stopped at the de-Fmoc of fully protected Fmoc-DA-DDBA due to a side-reaction (the formation of DKP) (Section 3.3.5).

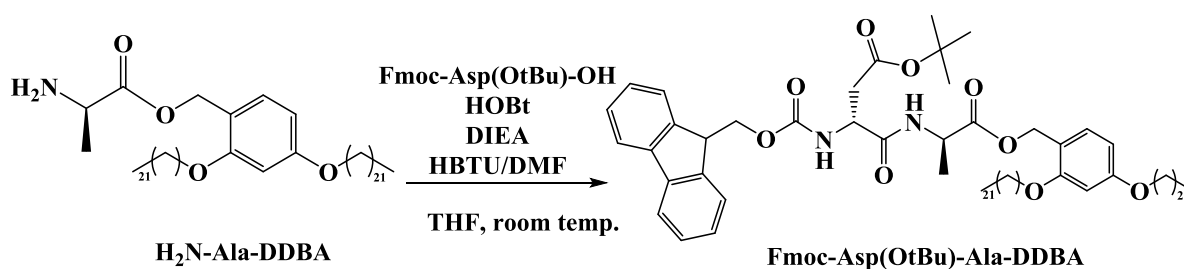
Step 1.



Step 2.



Step 3.



Step 4.

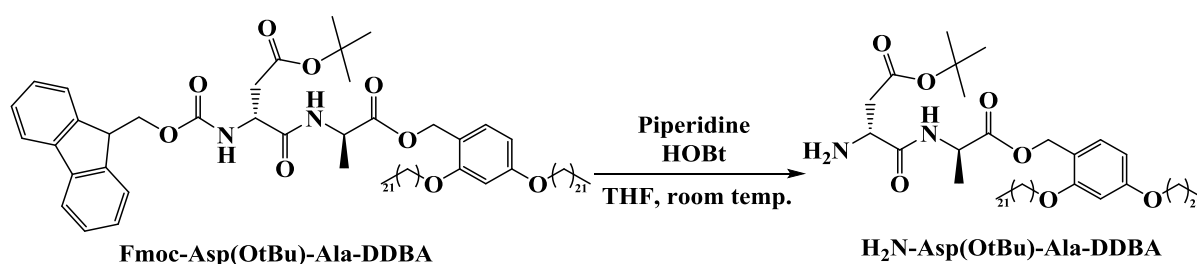


Figure 3.6. Synthesis of fully protected Fmoc-RADA-DDBA upto the de-Fmoc of Fmoc-DA-DDBA.

All the steps below were conducted at room temperature and pressure unless stated otherwise.

Step 1. Loading of Ala Fmoc-Ala-OH (4.11 g, 13.2 mmol, 2.0 eq) was dissolved in THF (50.00 g), followed by DIC (1.67 g, 13.2 mmol, 2.0 eq). The reaction solution was stirred for five minutes for activation. DDBA (5.00 g, 6.60 mmol, 1.0 eq) was then added into the solution, followed by DMAP (0.08 g, 0.655 mmol, 0.1 eq). The reaction solution was stirred at room temperature and the reaction was monitored by HPLC (analysis every 30 minutes; method: Fmoc-RADA-DDBA_HPLC1). When the reaction was complete, acetonitrile (500 mL) was added to precipitate the product. The precipitate was washed with acetonitrile (500 mL) twice and dried in a vacuum oven (-80 kPa (gauge) and 30 °C) until the mass loss due to solvent evaporation became negligible.

Step 2. De-Fmoc of Fmoc-Ala-DDBA Fmoc-Ala-DDBA (4.50 g, 4.28 mmol, 1.0 eq) was dissolved in THF (450.00 g), followed by HOBt (0.58 g, 4.28 mmol, 1.0 eq). Piperidine (22.50 g) was then added dropwise into the reaction solution while stirring. After the addition of piperidine, the reaction solution was stirred and the reaction was monitored by HPLC (analysis every 30 minutes; method: Fmoc-RADA-DDBA_HPLC1). When the reaction was complete, acetonitrile (1.5 L) was added to precipitate the product. The precipitate was washed with acetonitrile (500 mL) 3 times and the presence of piperidine in the washing acetonitrile was checked by the chloranil test. The precipitate was dried in vacuum oven (-80 kPa (gauge) and 30 °C) until the mass loss due to solvent evaporation became negligible.

Step 3. Coupling of Asp(OtBu) H₂N-Ala-DDBA (2.00 g, 2.41 mmol, 1.00 eq) was dissolved in THF (200.00 g), followed by Fmoc-Asp(OtBu)-OH (1.04 g, 2.53 mmol, 1.05 eq) and HOBt (0.34 g, 2.52 mmol, 1.05 eq). HBTU (0.96 g, 2.53 mmol, 1.05 eq) was dissolved DMF (4.30 g). HBTU/DMF solution was added into H₂N-Ala-DDBA/Fmoc-Asp(OtBu)-OH/HOBt/THF solution, followed by DIEA (2.00 g, 15.6 mmol, 6.45 eq). The reaction solution was stirred and the reaction was monitored by HPLC (analysis every 30 minutes; method: Fmoc-RADA-DDBA_HPLC1). When the reaction was complete,

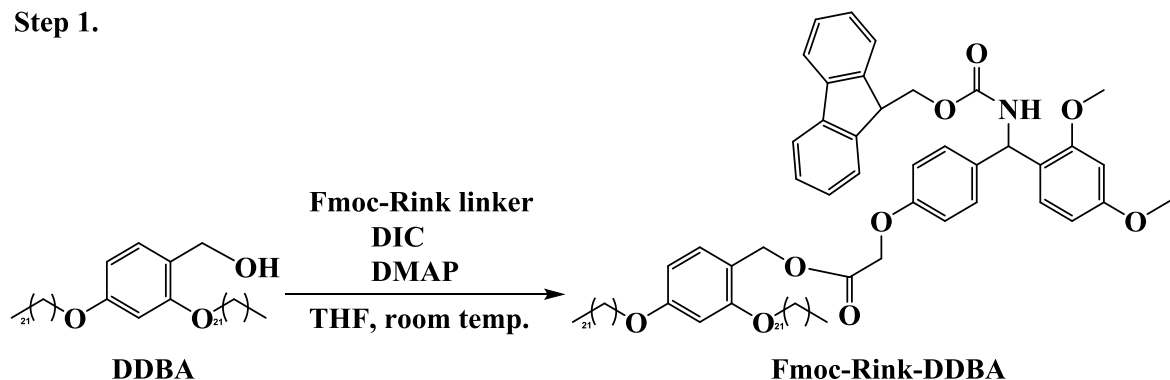
acetonitrile (1.0 L) was added to precipitate the product. The precipitate was washed with acetonitrile (100 mL) 5 times and dried in a vacuum oven (-80 kPa (gauge) and 30 °C) until the mass loss due to solvent evaporation became negligible.

Step 4. De-Fmoc of Fmoc-Asp(OtBu)-Ala-DDBA Fmoc-Asp(OtBu)-Ala-DDBA (0.2000 g, 0.164 mmol, 1.0 eq) was dissolved in THF (20.00 g), followed by HOBt (0.0222 g, 0.164 mmol, 1.0 eq). Piperidine (1.0000 g) was added dropwise into the Fmoc-Asp(OtBu)-Ala-DDBA/HOBt/THF solution. The reaction solution was stirred and the reaction was followed by HPLC (analysis every hour; method: Fmoc-RADA-DDBA_HPLC1).

3.2.4.4. Synthesis of H₂N-Rink-DDBA

The Fmoc-Rink linker was attached to DDBA in order to suppress the side-reaction that occurred during the de-Fmoc of fully protected Fmoc-DA-DDBA. The Fmoc-Rink-DDBA was then deprotected, purified and dried for the use in MEPS.

Step 1.



Step 2.

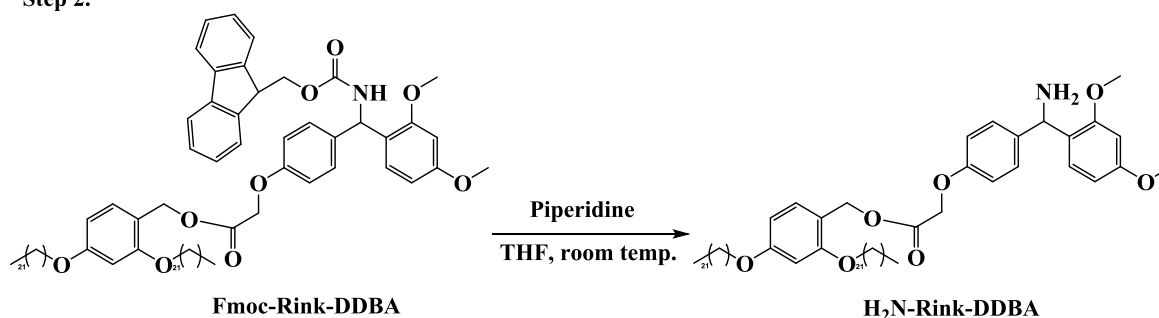


Figure 3.7. Synthesis of H₂N-Rink-DDBA.

All the steps below were conducted at room temperature and pressure unless stated otherwise.

Step 1. Loading of Fmoc-Rink Linker Fmoc-Rink-OH (14.25 g, 26.4 mmol, 2.0 eq) was dissolved in THF (100 g), followed by DIC (3.33 g, 26.4 mmol, 2.0 eq). The reaction solution was stirred for 5 minutes for activation. DDBA (10.00 g, 13.2 mmol, 1.0 eq) was then added into the solution, followed by DMAP (0.16 g, 1.31 mmol, 0.10 eq). The reaction solution was stirred for 2 hours and the reaction was monitored by HPLC (analysis every hour; method: Fmoc-RADA-DDBA_HPLC1). When the

reaction was complete, acetonitrile (300 mL) was added to precipitate the product. The precipitate was washed with acetonitrile (100 mL) for 5 times and dried in vacuum oven (-80 kPa (gauge) and 30 °C) until the mass loss due to solvent evaporation became negligible.

Step 2. De-Fmoc of Fmoc-Rink-DDBA Fmoc-Rink-DDBA was dissolved in THF (10 weight % in THF), followed by piperidine (10 weight% in THF). The reaction solution was stirred for 2.5 hours and the reaction was monitored by HPLC (analysis after 1 and 2 hours; method: Fmoc-RADA-DDBA_HPLC1). When the reaction was complete, acetonitrile (300 mL) was added to precipitate the product. The precipitate was washed with acetonitrile (100 mL) 5 times and the amount of piperidine left was checked by the chloranil test. The washed precipitate was dried in a vacuum oven (-80 kPa (gauge) and 30 °C) until the mass loss due to solvent evaporation became negligible.

3.2.4.5. SPPS of Fully Deprotected Fmoc-RADA-NH₂

Fully deprotected Fmoc-RADA-NH₂ was synthesised by SPPS, whose experimental results are compared with those of the MEPS process in the later part of this chapter (Section 3.3.9).

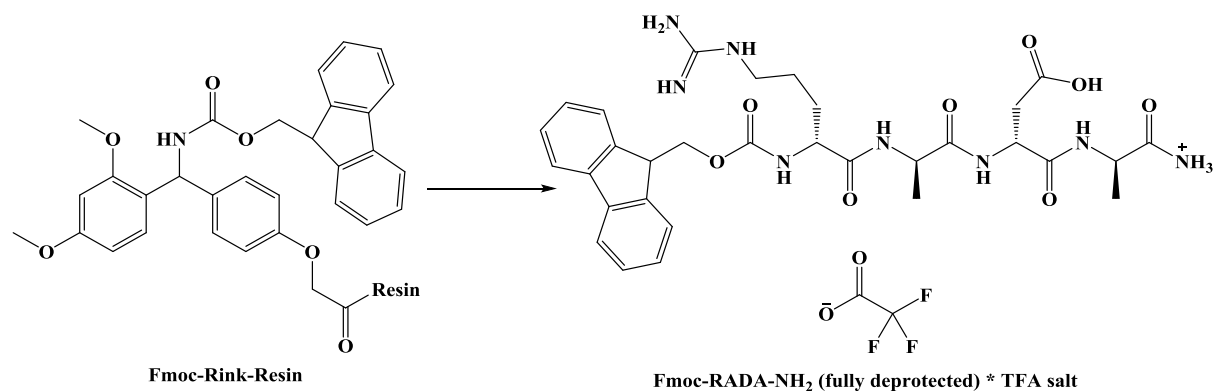


Figure 3.8. SPPS of fully deprotected Fmoc-RADA-NH₂.

All the steps below were conducted at room temperature and pressure unless stated otherwise. The equivalent of reagent was with respect to the quantity of loading site on the resin.

Step 1. Swelling of Fmoc-Rink-Resin PL-Rink resin (15.41 g) was added into a reactor (250 mL), followed by DMF (50 mL). Another portion of DMF (50 mL) was used to wash down any resin on the reactor wall. The resin was allowed to swell with the solvent at 20.0 °C for 1 hour and then drained.

Step 2. De-Fmoc of Fmoc-Rink-Resin Piperidine (40.00 g, 5.0 weight % in 200 g DMF) was added into DMF (200.00 g) and half of the solution (100 mL) was added to the reactor. The reaction mixture was stirred at 20.0 °C for 1 hour, after which the resin was drained and washed with DMF (100 mL) 6 times. The presence of piperidine in washing DMF was checked by the chloranil test to ensure the proper removal of piperidine.

Step 3, 5, 7 and 9. Coupling of Amino Acid Amino acid (16.2 mmol, 1.5 eq) was dissolved in DMF (100 mL), followed by HOBT (2.18 g, 16.1 mmol, 1.5 eq) and DIC (2.04 g, 16.2 mmol, 1.5 eq). The solution

was stirred at room temperature for 10 minutes, before it was added to the reactor. The reaction mixture was stirred at 20.0 °C and the reaction was followed by the ninhydrin test every 30 minutes. After the reaction was complete, the resin was drained and washed with DMF (100 mL) 5 times.

Step 4, 6 and 8. De-Fmoc of Fmoc-Peptide Fragment-Resin HOBt (1.43 g, 0.1M in 100 g DMF) was added into DMF (100.00 g), followed by piperidine (5.00 g, 5.0 weight % in 100 g DMF). The piperidine/HOBt/DMF solution was added into the reactor. The reaction mixture was stirred at 20.0 °C for 10 minutes and the resin was then drained. The same steps were repeated once. The resin was washed with DMF (100 mL) 5 times. The presence of piperidine in washing DMF was checked by the chloranil test to ensure the proper removal of piperidine.

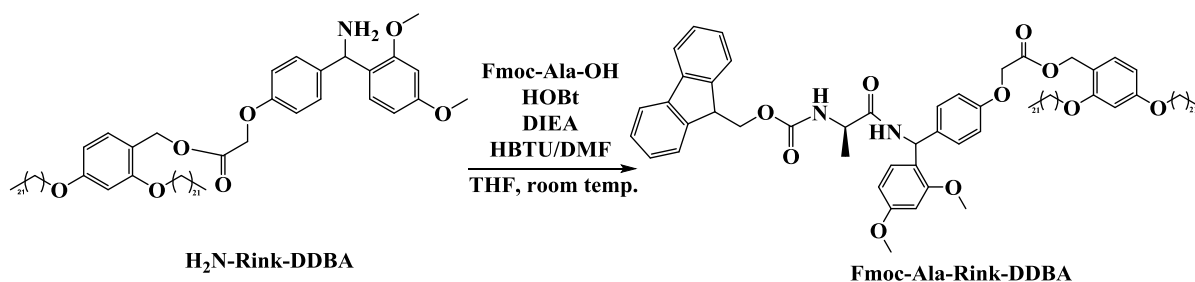
Step 10. Cleavage and Global Deprotection The peptide-bound resin was added into the cleavage cocktail (TFA/TIS/Anisole (90/8/2, v/v/v), 100 mL) and the mixture was stirred at 20.0 °C for 1 hour. The resin was then drained and the solution was added into cold diisopropylether (900 mL). These steps were repeated 3 times. All the precipitate was filtered and washed with diisopropylether (100 mL) 5 times and then dried in a vacuum oven (-80 kPa (gauge) and 30 °C) until the mass loss due to solvent evaporation became negligible.

3.2.4.6. Small-scale Coupling Tests for Fully Protected Fmoc-RADA-Rink-DDBA in Liquid Phase by

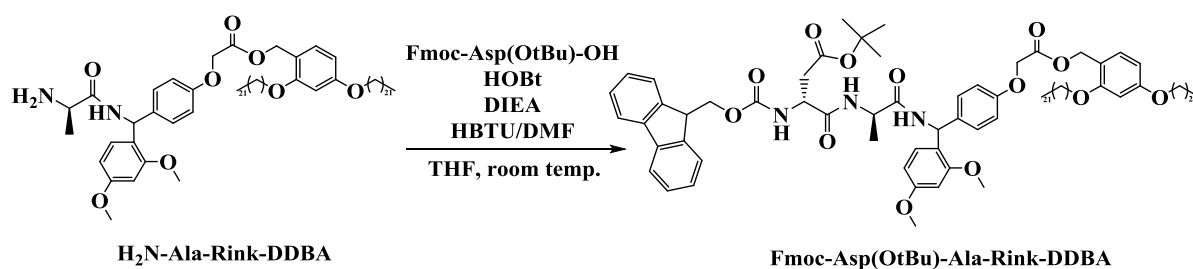
Precipitation

Numerous small-scale tests were conducted in order to investigate the best conditions for the couplings by varying reagent concentrations, reagent equivalent with respect to the anchored deprotected peptide and reaction time. The best conditions were then implemented in the MEPS.

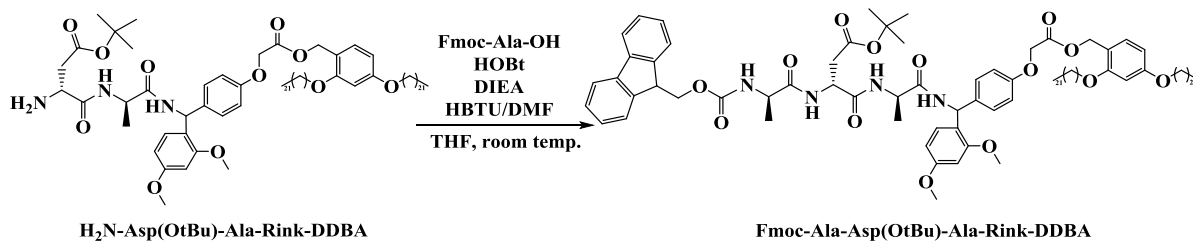
Loading



Coupling 1.



Coupling 2.



Coupling 3.

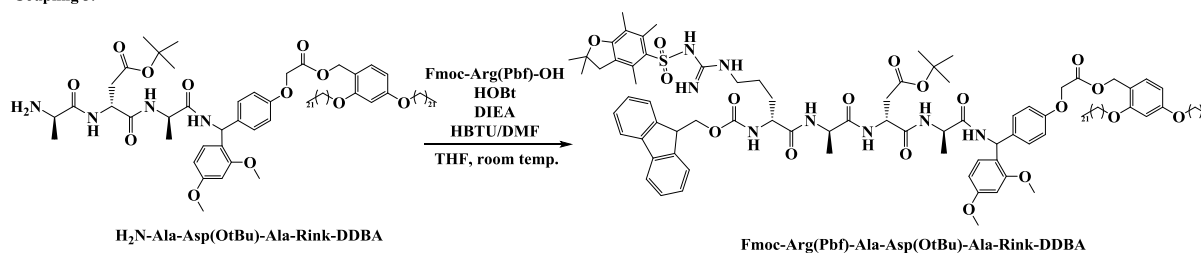


Figure 3.9. Coupling steps in the synthesis of fully protected Fmoc-RADA-Rink-DDBA.

All the steps below were conducted at room temperature and pressure unless stated otherwise.

Loading. Synthesis of Fmoc-Ala-Rink-DDBA Fmoc-Ala-OH (31.1 mg, 0.10 mmol, 1.05 eq) was dissolved in THF (10.00 g), followed by DIEA (24.6 mg, 0.19 mmol, 2.00 eq). HBTU (37.9 mg, 0.10 mmol, 1.05 eq) was dissolved separately in DMF (0.38 g). The HBTU/DMF solution was added into Fmoc-Ala-OH/DIEA/THF solution. H₂N-Rink-DDBA (100 mg, 0.095 mmol, 1.00 eq) was added into the solution. The reaction solution was stirred and the reaction was monitored by HPLC (analysis every 30 minutes; method: Fmoc-RADA-DDBA_HPLC1).

Coupling 1. Fmoc-Asp(OtBu)-Ala-Rink-DDBA Fmoc-Asp(OtBu)-OH (38.3 mg, 0.093 mmol, 1.05 eq) was dissolved in THF (10.00 g), followed by DIEA (22.9 mg, 0.18 mmol, 2.00 eq). HBTU (35.3 mg, 0.093 mmol, 1.05 eq) was dissolved separately in DMF (0.35 g). The HBTU/DMF solution was added into Fmoc-Asp(OtBu)-OH/DIEA/THF solution. H₂N-Ala-Rink-DDBA (100 mg, 0.089 mmol, 1.00 eq) was added into the solution. The reaction solution was stirred and the reaction was monitored by HPLC (analysis every 30 minutes; method: Fmoc-RADA-DDBA_HPLC1).

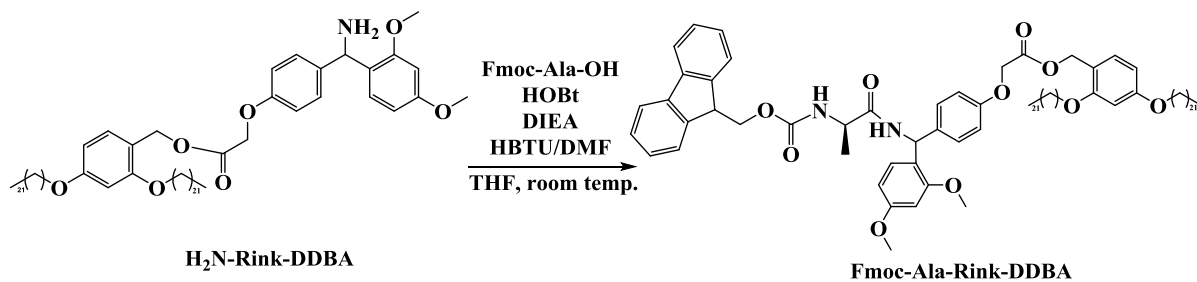
Coupling 2. Fmoc-Ala-Asp(OtBu)-Ala-Rink-DDBA Fmoc-Ala-OH (25.2 mg, 0.081 mmol, 1.05 eq) was dissolved in THF (10.00 g), followed by DIEA (19.4 mg, 0.150 mmol, 2.00 eq). HBTU (30.7 mg, 0.081 mmol, 1.05 eq) was dissolved separately in DMF (0.31 g). The HBTU/DMF solution was added into Fmoc-Ala-OH/DIEA/THF solution. H₂N-Asp(OtBu)-Ala-Rink-DDBA (100 mg, 0.077 mmol, 1.00 eq) was added into the solution. The reaction solution was stirred and the reaction was monitored by HPLC (analysis every 30 minutes; method: Fmoc-RADA-DDBA_HPLC1).

Coupling 3. Fmoc-Arg(Pbf)-Ala-Asp(OtBu)-Ala-Rink-DDBA Fmoc-Arg(Pbf)-OH (49.3 mg, 0.076 mmol, 1.05 eq) was dissolved in THF (10.00 g), followed by DIEA (18.1 mg, 0.140 mmol, 2.00 eq). HBTU (28.8 mg, 0.076 mmol, 1.05 eq) was dissolved separately in DMF (0.29 g). The HBTU/DMF solution was added into Fmoc-Arg(Pbf)-OH/DIEA/THF solution. H₂N-Ala-Asp(OtBu)-Ala-Rink-DDBA (100 mg, 0.072 mmol, 1.00 eq) was added into the solution. The reaction solution was stirred and the reaction was monitored by HPLC (analysis every 30 minutes; method: Fmoc-RADA-DDBA_HPLC1).

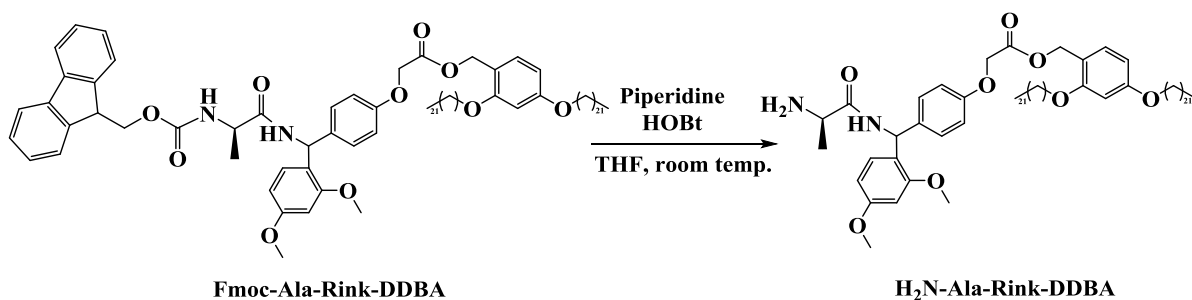
3.2.4.7. MEPS of Fully Deprotected Fmoc-RADA-NH₂ on H₂N-Rink-DDBA

Fully deprotected Fmoc-RADA-NH₂ was synthesised on H₂N-Rink-DDBA by MEPS. After each reaction, diafiltration was performed to remove the excess reagents and by-products.

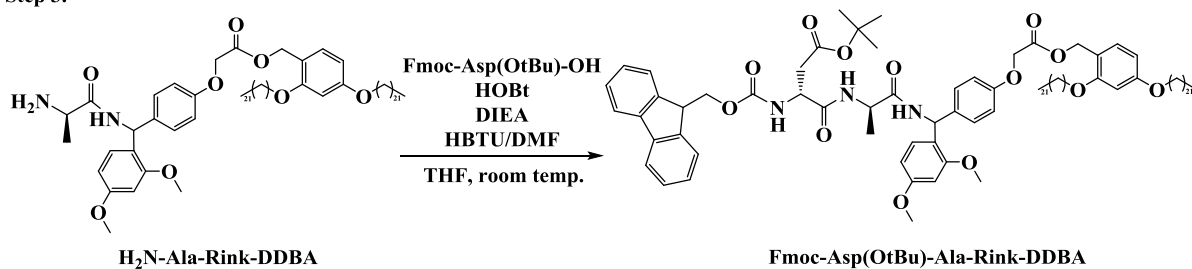
Loading



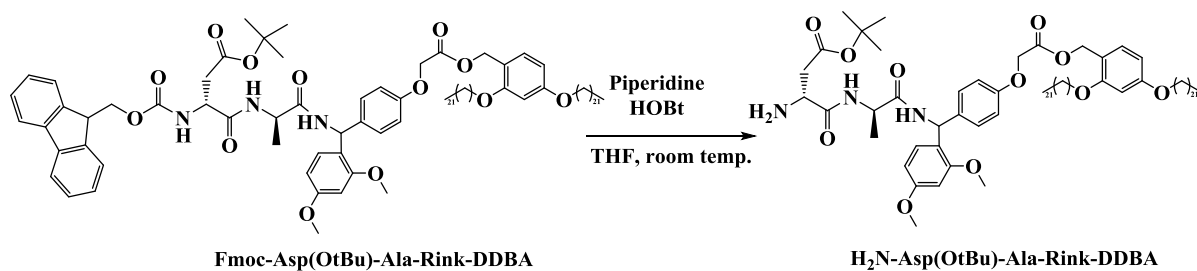
Step 2.



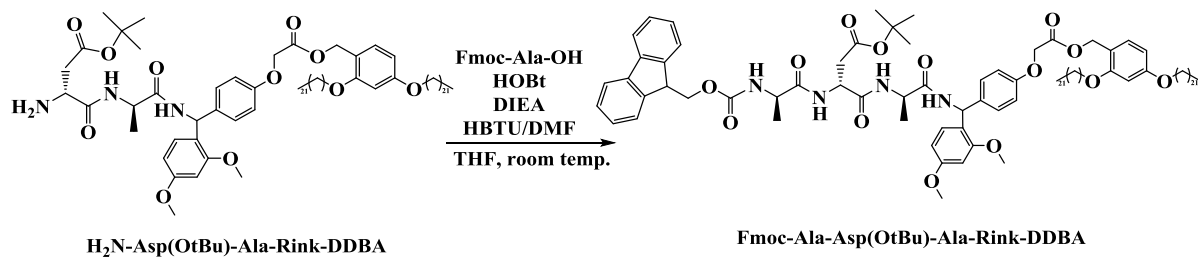
Step 3.



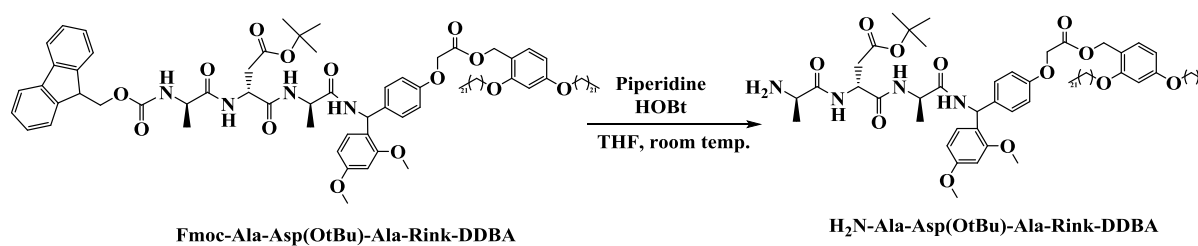
Step 4.



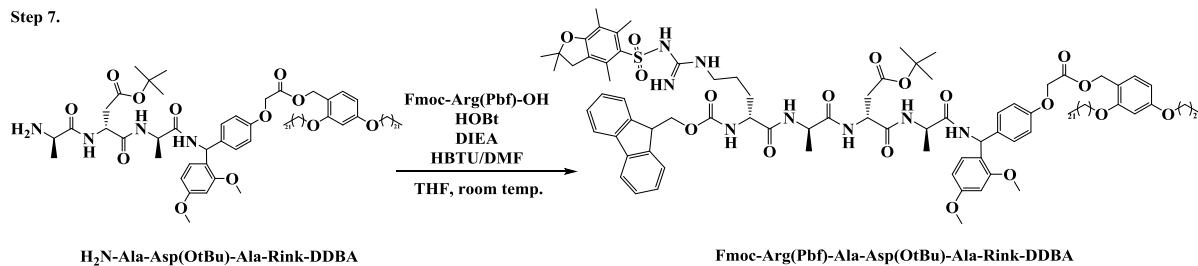
Step 5.



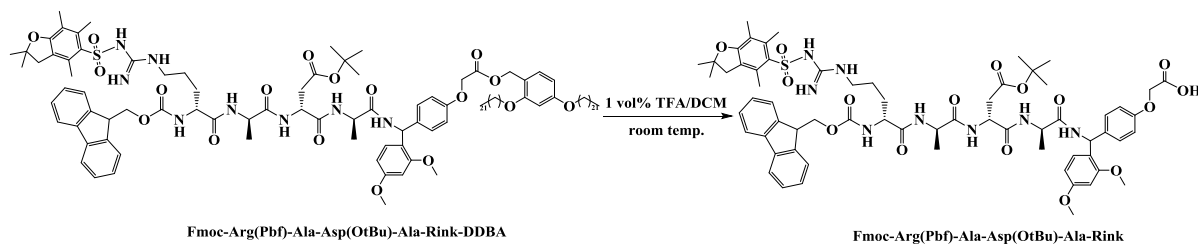
Step 6.



Step 7.



Step 8.



Step 9.

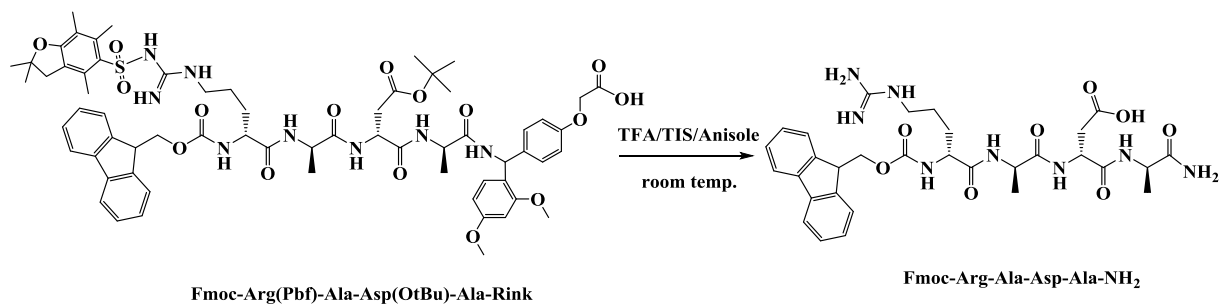


Figure 3.10. Synthesis of fully deprotected Fmoc-RADA-NH₂.

All the steps below were conducted at room temperature and pressure unless stated otherwise. The equivalent of reagent was with respect to the quantity of H₂N-Rink-DDBA in the loading step.

Step 1. Loading of Ala Fmoc-Ala-OH (3.27 g, 10.5 mmol, 1.05 eq) was dissolved in THF (105.70 g), followed by HOBt (1.42 g, 10.5 mmol, 1.05 eq) and DIEA (1.46 g). HBTU (3.98 g, 10.5 mmol, 1.05 eq) was dissolved separately in DMF (40.00 g) and the solution was added into the reaction solution. H₂N-Rink-DDBA (10.57 g, 10.0 mmol, 1.0 eq) was added into the reaction solution. The reaction solution was stirred and the reaction was monitored by HPLC (analysis every 30 minutes; method: Fmoc-RADA-DDBA_HPLC1). After the reaction was complete, the reaction solution was diluted to 500mL with more THF and then added into the OSN system for diafiltration (3 washes, 500 mL each wash).

Step 2, 4 and 6. De-Fmoc of Fmoc-Peptide Fragment-DDBA HOBt (7.32 g, 0.1 M in 500 mL THF) was added into the reaction solution, followed by piperidine (24.20 g, 5.0 weight % in 500mL THF). The reaction solution was circulated in the OSN system and the reaction was monitored by HPLC (analysis every 30 minutes; method: Fmoc-RADA-DDBA_HPLC1). After the reaction was complete, diafiltration was performed to remove the piperidine (7 washes, 1000 mL each wash). The presence of piperidine in washing DMF was checked by the piperidine test.

Step 3, 5 and 7.1. Coupling of Amino Acid Amino acid (10.5 mmol, 1.05 eq) was added into the solution, followed by HOBt (1.42 g, 10.5 mmol, 1.05 eq) and DIEA (4.85 g). HBTU (4.00 g, 10.5 mmol,

1.05 eq) was dissolved separately in DMF (40.00 g) and the solution was added into the reaction solution. The reaction solution was circulated in the OSN system and the reaction was monitored by HPLC (analysis every 30 minutes; method: Fmoc-RADA-DDBA_HPLC1). After the reaction was complete, diafiltration was performed (3 washes, 500 mL each wash).

Step 7.2. Drying of Fmoc-Arg(Pbf)-Ala-Asp(OtBu)-Ala-Rink-DDBA After the coupling of Fmoc-Arg(Pbf)-OH, the OSN system was drained and then washed with THF (500 mL) three times. The combined solution was evaporated to 150mL and then added into acetonitrile (400 mL) for precipitation of product. The white precipitate was washed with acetonitrile (100 mL) 5 times and then dried in a vacuum oven (-80 kPa (gauge) and 30 °C) over several days until the mass loss due to solvent evaporation became negligible.

Step 8. Cleavage of Peptide Dried Fmoc-Arg(Pbf)-Ala-Asp(OtBu)-Ala-Rink-DDBA was added into TFA/DCM (1 vol% TFA in DCM, 200 mL) and the mixture was stirred for 1 hour. The reaction was followed by HPLC (analysis after 1 hour; method: Fmoc-RADA-DDBA_HPLC1). When the reaction was complete, acetonitrile (500 mL) was added into the mixture and the mixture was filtered. The filtered particles were washed with TFA/DCM (1 vol% TFA in DCM, 100 mL) 6 times. The filtrate was collected and evaporated to dryness under vacuum (-80 kPa (gauge) and 30 °C).

Step 9. Global Deprotection of Peptide Dried Fmoc-Arg(Pbf)-Ala-Asp(OtBu)-Ala-Rink from the previous step was added into TFA (250 mL) and the mixture was stirred at room temperature for 1 hour. The reaction was followed by HPLC (analysis at 1st hour; method: Fmoc-RADA_HPLC1). After the disappearance of Fmoc-Arg(Pbf)-Ala-Asp(OtBu)-Ala-Rink on HPLC, TIS/Anisole (125 mL /65 mL) was added into the mixture, and the mixture was stirred for another hour. The reaction was also followed by HPLC (analysis after 1 hour; method: Fmoc-RADA_HPLC1). After the reaction was complete, the mixture was added into cooled diisopropylether (1 L) and then filtered. The filtered product was dried and then washed with diisopropylether (100 mL) 6 times. The product was dried in nitrogen until the mass loss due to solvent evaporation became negligible.

3.3. Results and Discussion

3.3.1. Synthesis of DDBA

The synthesis of DDBA was successful and highly repeatable. The first step (the synthesis of 2,4-didocosyloxybenzaldehyde) was carried out twice and both attempts achieved high yields (92.4 - 95.0 %) and purities (100.0 % for both cases) (Table 3.1).

At the beginning of the reaction, DMI was heated to high temperature (70 °C) in order to dissolve the hydrophobic 1-bromodocosane. The reaction solution was orange-red due to 2,4-dihydroxybenzaldehyde and potassium carbonate remained as a white solid even after extensive and prolonged stirring. As the reaction progressed, the solution turned black and a large amount of grey solid was observed. The grey solid was separated and washed repeatedly by water and n-hexane to give the pure product (identity of the compound was confirmed by LC/MS and NMR (Figure 3.11 and Figure 3.12); purity confirmed by HPLC and NMR). This reaction is kinetically hindered, as it required at least 24 hours to complete even with a high concentration of 1-bromodocosane in DMI (15 weight%) under reflux conditions.

Table 3.1. Summary of results for the synthesis of 2,4-didocosyloxybenzaldehyde.

| Reaction | Scale (mmol) | Purity by HPLC (%) | Yield (%) |
|----------|--------------|--------------------|-----------|
| 1 | 77 | 100.0 | 92.4 |
| 2 | 115 | 100.0 | 95.0 |

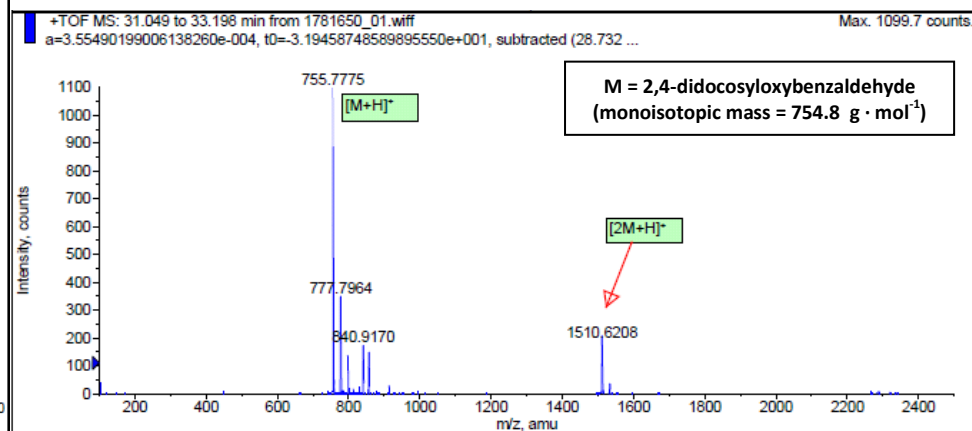
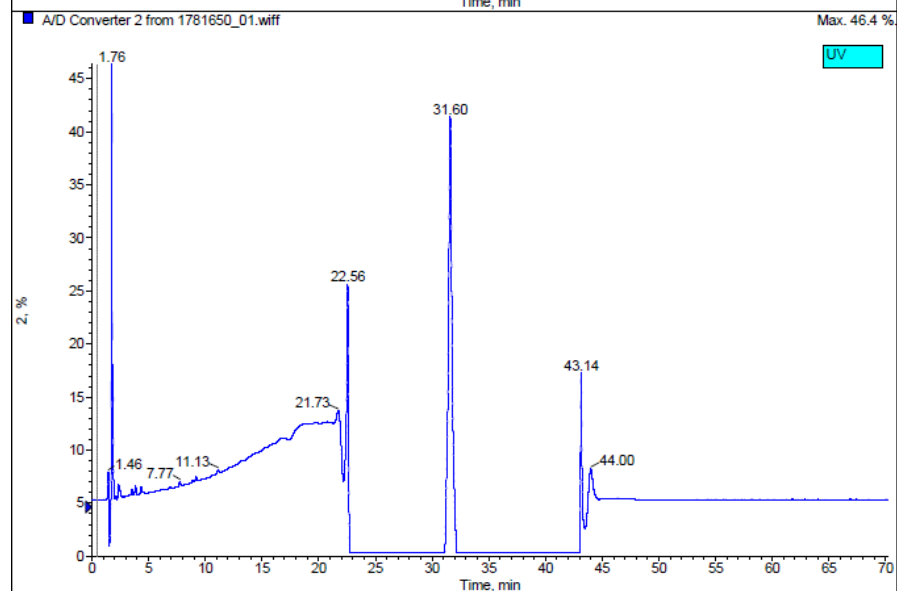
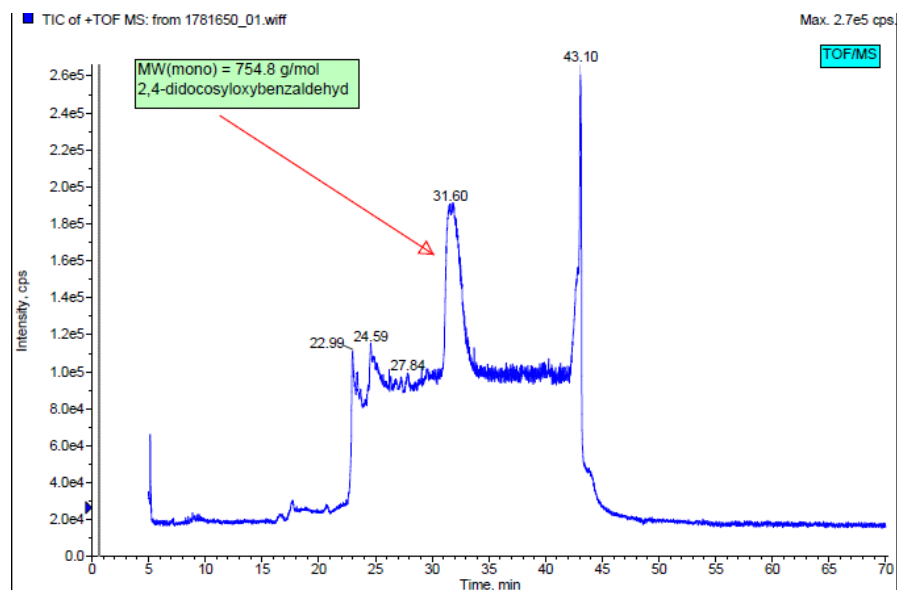


Figure 3.11. LC/MS result of 2,4-didocosyloxybenzaldehyde (dried product of Reaction 1 in Table 3.1) (HPLC method: DDBA_HPLC1).

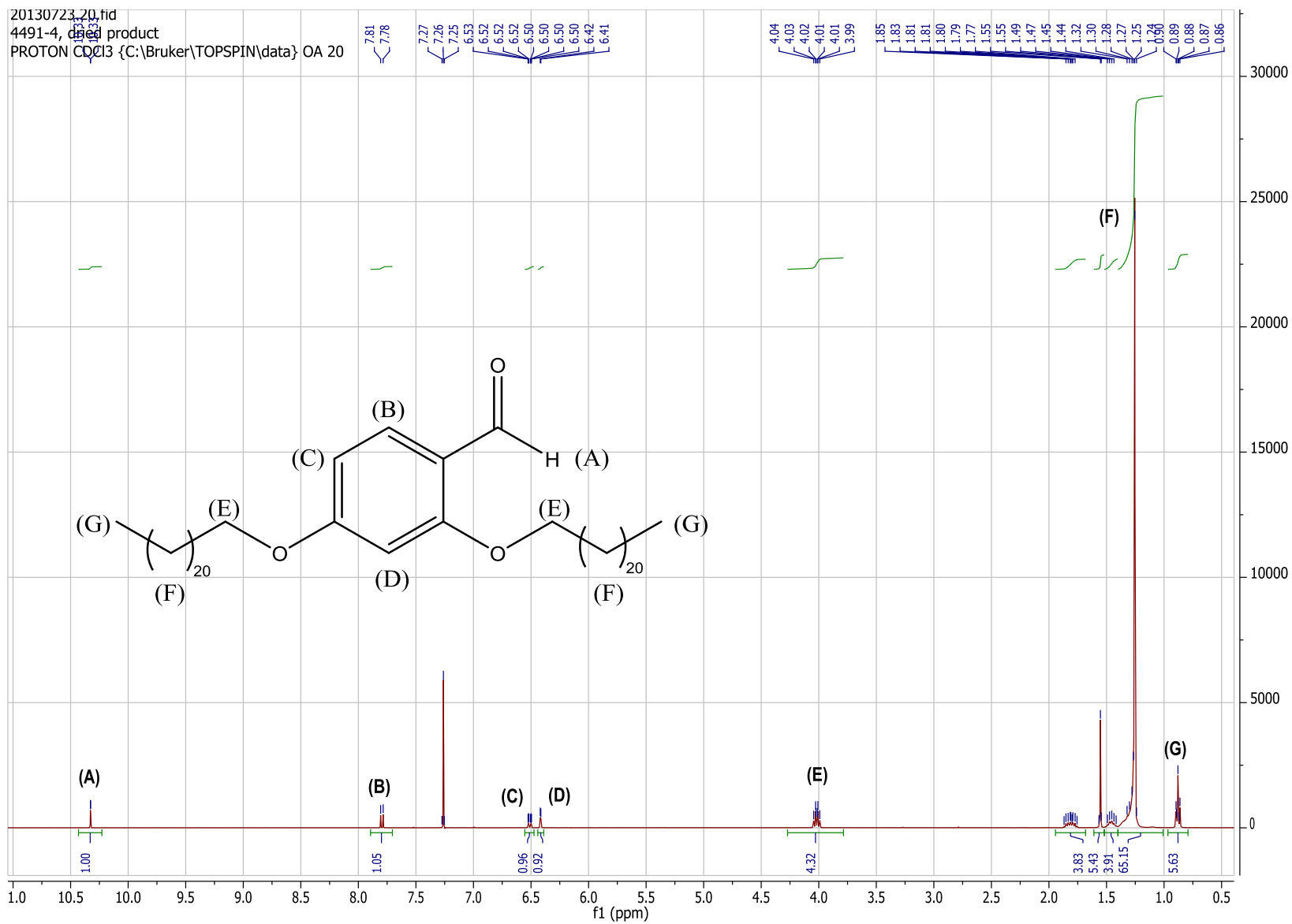


Figure 3.12. NMR result of 2,4-didocosyloxybenzaldehyde (dried product of Reaction 1 in Table 3.1).

The second step of the synthesis involves the reduction of the aldehyde group to alcohol by sodium borohydride and was repeated fourteen times, all with high yields (96.8 - 103.1%) and purities (100.0% for all cases) (Table 3.2). The identity of the compound was confirmed by LC/MS and NMR (Figure 3.13 and Figure 3.14). Some repeats of the reaction had yields slightly higher than 100%, probably due to the incomplete removal of solvent during evaporation. One consequence of using the products of these reactions in the peptide synthesis would be a lower overall yield for the final peptide, as the actual quantity of anchor to start with was in fact lower than the apparent value (i.e. with residual solvent).

Interestingly, 2,4-didocosyloxybenzaldehyde has extremely low solubility in most organic solvents, including THF which is used to dissolve DDBA for LPPS. After trial and error, chloroform was found to be the only suitable solvent, but the concentration of 2,4-didocosyloxybenzaldehyde could hardly go beyond 1 weight%. Sodium borohydride was insoluble in chloroform, but was consumed as the reaction went to completion. As compared to the synthesis of 2,4-didocosyloxybenzaldehyde, this reaction was significantly faster, as each attempt required only 8 hours to complete under room temperature. The only concern about this reaction was safety, because sodium borohydride is highly flammable and requires careful handling.

Table 3.2. Summary of results for the reduction of 2,4-didocosyloxybenzaldehyde.

| Reaction | Scale (mmol) | Purity by HPLC (%) | Yield (%) |
|----------|--------------|--------------------|-----------|
| 1 | 6.62 | 100.0 | 99.9 |
| 2 | 6.62 | 100.0 | 103.1 |
| 3 | 6.63 | 100.0 | 100.3 |
| 4 | 6.62 | 100.0 | 100.1 |
| 5 | 6.63 | 100.0 | 99.9 |
| 6 | 6.62 | 100.0 | 99.9 |
| 7 | 6.62 | 100.0 | 100.9 |
| 8 | 6.62 | 100.0 | 101.7 |
| 9 | 6.65 | 100.0 | 101.3 |
| 10 | 6.63 | 100.0 | 101.1 |
| 11 | 13.2 | 100.0 | 98.3 |
| 12 | 26.4 | 100.0 | 96.8 |
| 13 | 13.2 | 100.0 | 100.0 |
| 14 | 13.2 | 100.0 | 98.2 |

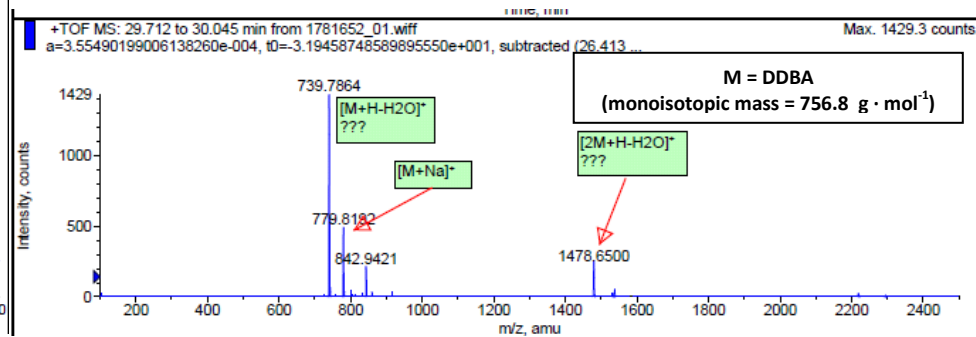
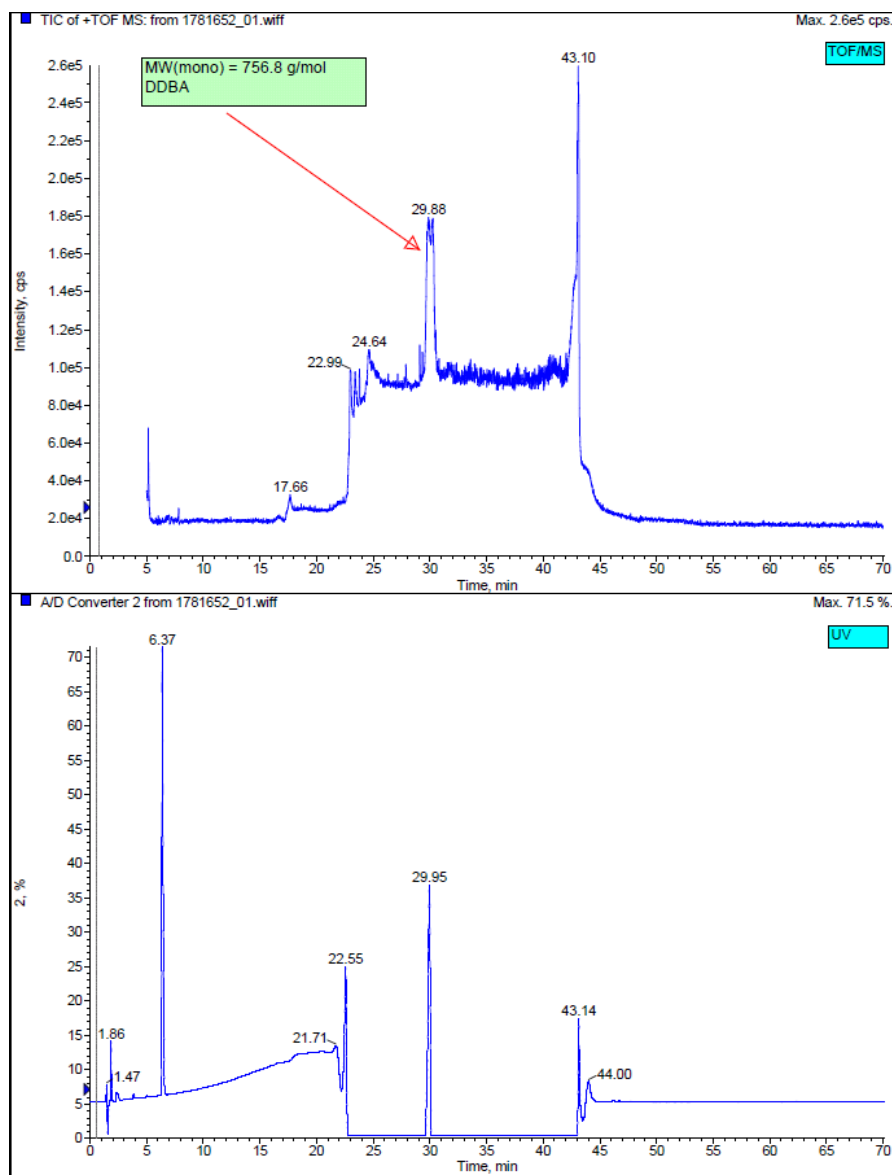


Figure 3.13. LC/MS result of DBA (dried product of Reaction 10 in Table 3.2) (HPLC method: DBA_HPLC1).

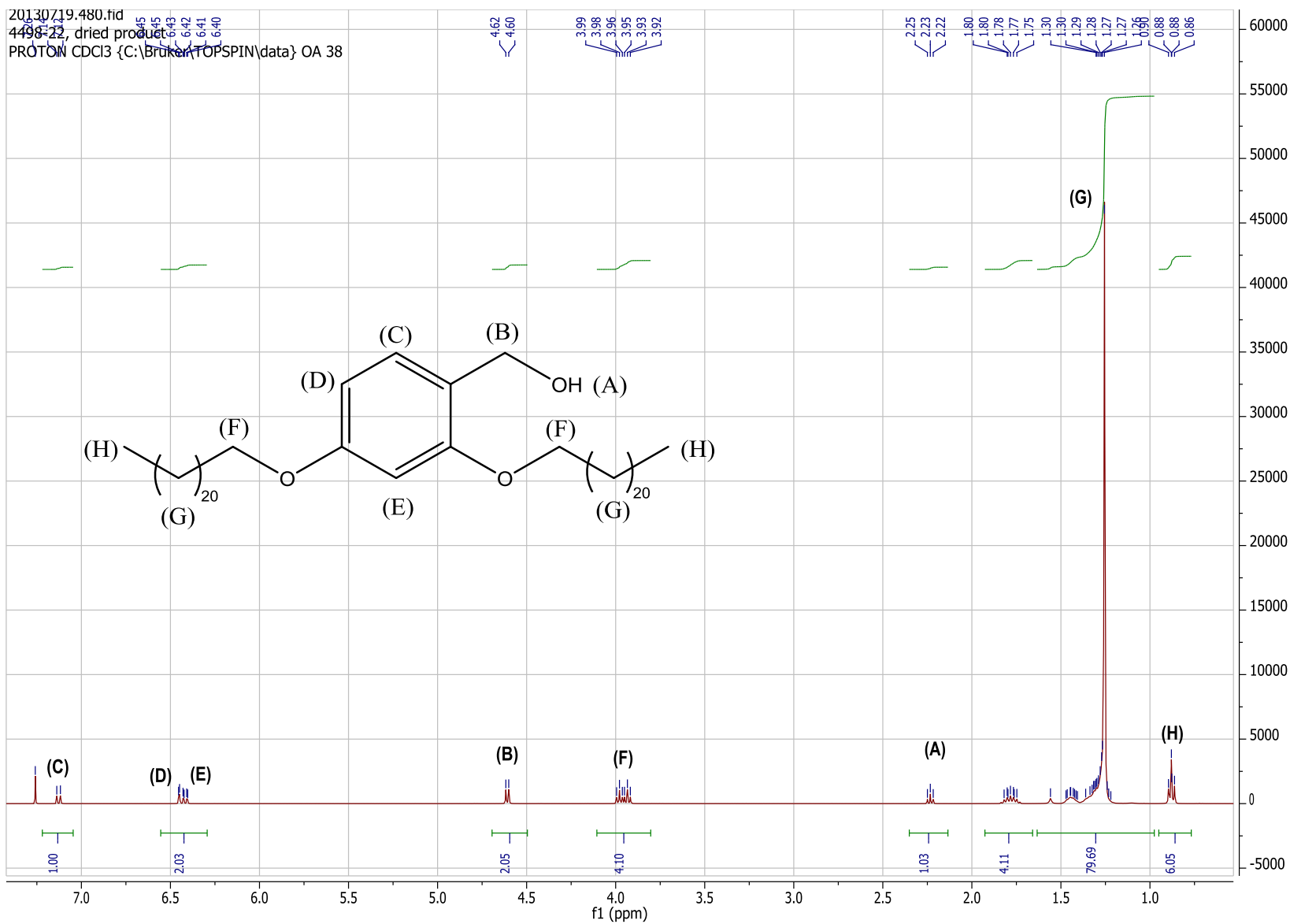


Figure 3.14. NMR result of DDBA (dried product of Reaction 10 in Table 3.2).

3.3.2. Analysis of DDBA and Related Compounds

In general, HPLC is an excellent method for both qualitative and quantitative analysis for liquid phase reactions. With a suitable method (eluent gradient, column, column temperature, flow etc), different compounds can be separated and appear as distinct peaks on the chromatogram. The identity of each compound can then be confirmed by MS, allowing the user to monitor the progress of a particular reaction. The peak integration area is proportional to the concentration of the corresponding compound, usually with a linear correlation below the saturation level, allowing the user to quantify the concentration of a particular compound with high accuracy.

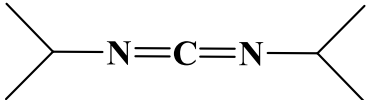
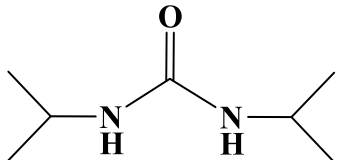
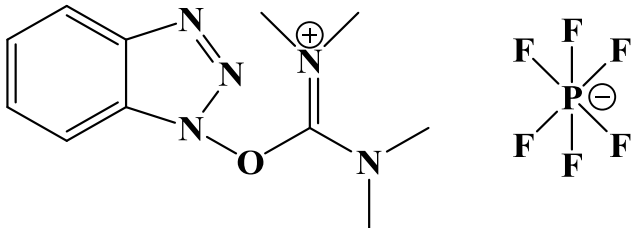
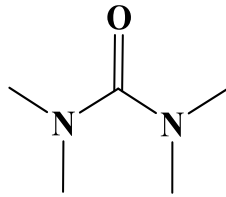
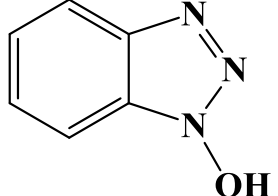
In this project, reverse phase HPLC was used as the main analysis technique, but finding a suitable method for DDBA and all the related anchored peptides was in fact a challenging task. Due to its hydrophobicity, DDBA is barely soluble in acetonitrile and water, which are the most commonly used eluents for HPLC. After extensive trial and error, methanol, ethanol and isopropanol were found to be the suitable eluents for DDBA. In order to ionise the separated compounds in MS, water must be present in the eluent, but its addition into methanol or ethanol apparently prevented the desorption of DDBA from the column (the DDBA peak was not observed in the presence of water in the eluent mixture), even at a relatively low concentration (water/alcohol, 5/95, v/v (alcohol is methanol or ethanol)).

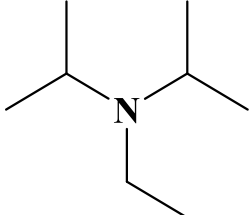
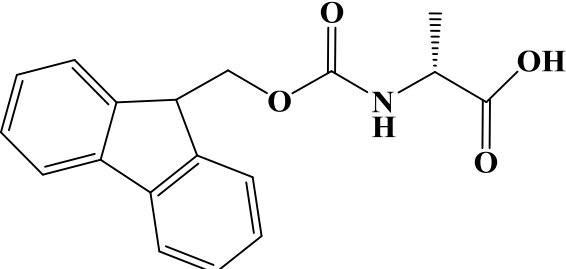
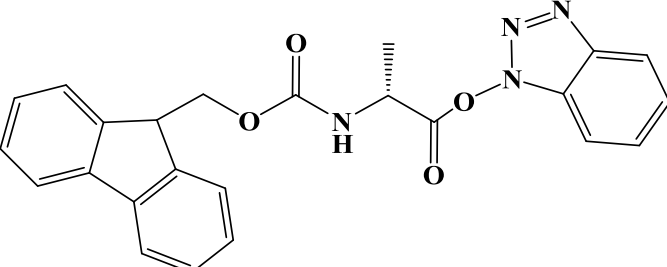
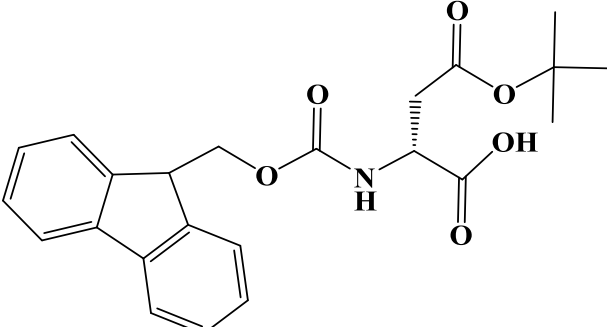
As DDBA has poor solubility in these three alcohols, the desorption of DDBA from the HPLC column was most probably caused by the competitive adsorption of these alcohols against DDBA on the C18 column. With a higher extent of hydrophobicity as compared to the other two alcohols, isopropanol could replace DDBA and adsorb on the surface of the column even in the presence of water, giving a peak of the anchor on the chromatogram. As a result, the final HPLC methods (DDBA_HPLC1 and Fmoc-RADA-DDBA_HPLC1) used a mixture of isopropanol and water as the eluent for DDBA and all related compounds.

3.3.3. Anchor Screening

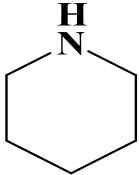
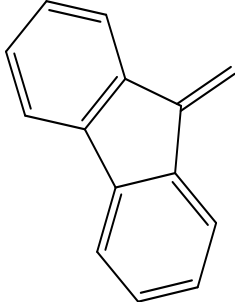
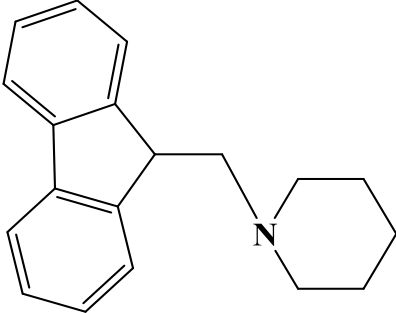
MWCO is meant to aid the selection of membrane for a particular separation process, but it is not a universal standard as it can vary with different test molecules and nanofiltration conditions. According to the supplier (Inopor GmbH (Germany)), the MWCOs of Inopor 450 and Inopor 750 had been tested by linear PEG, but these values could not be translated directly into the current context as the compounds involved (coupling and de-Fmoc reagents and anchored peptide fragment) were hardly linear in structure. In MEPS, excess coupling reagents (e.g. activated Fmoc-protected amino acids) and de-Fmoc reagents (e.g. piperidine) must be removed during diafiltration while the anchored peptide fragment must be retained by the membrane. As shown in Table 3.3, most of the compounds to be removed were small molecules, among which the relatively bulky ones contained the Fmoc group. Ideally, the Fmoc group should be tested as the reference compound for the development of the MEPS process, but it was not commercially available. Therefore, the closest available option, Fmoc-Ala-OH, was chosen as the reference compound to check the separation performance of membranes in this research project.

Table 3.3. Compounds to be removed by diafiltration during peptide synthesis.

| Compound | Role in synthesis | Structure | MW (g · mol ⁻¹) |
|--|---|---|--------------------------------|
| <u>Coupling</u> | | | |
| N,N'-diisopropylcarbodiimide (DIC) | Activator |  | 126 |
| Diisopropylurea | By-product for the activation of amino acid by DIC |  | 144 |
| O-(Benzotriazol-1-yl)-N,N,N',N'-tetramethyluronium hexafluorophosphate (HBTU) | Activator |  | 379 |
| Tetramethylurea | By-product for the activation of amino acid by HBTU |  | 116 |
| Hydroxybenzotriazole (HOBT) | Racemisation suppressor |  | 135 |

| | | | |
|---|---|---|------------|
| <p>Diisopropylethylamine (DIEA)</p> | <p>Base for facilitating activation by HBTU</p> |  | <p>129</p> |
| <p>Fmoc-Ala-OH</p> | <p>Amino acid</p> |  | <p>311</p> |
| <p>Activated Fmoc-Ala</p> | <p>Activated amino acid</p> |  | <p>428</p> |
| <p>Fmoc-Asp(OtBu)-OH</p> | <p>Amino acid</p> |  | <p>411</p> |

| | | | |
|--------------------------|----------------------|---|-----|
| Activated Fmoc-Asp(OtBu) | Activated amino acid | <p>The structure shows the Fmoc-Asp(OtBu) molecule. It consists of a fluorenylmethyl (Fmoc) group attached to the nitrogen of an aspartic acid derivative. The side chain of the aspartic acid is protected as a tert-butyl ester (OtBu). The carboxyl group of the aspartic acid is also protected as a benzotriazol-1-yl ester.</p> | 529 |
| Fmoc-Arg(Pbf)-OH | Amino acid | <p>The structure shows the Fmoc-Arg(Pbf)-OH molecule. It features a fluorenylmethyl (Fmoc) group on the nitrogen of an arginine derivative. The side chain of the arginine is protected as a 2,2,4,6,6-pentamethyl-1,3-dioxane-5-sulfonyl (Pbf) ester. The carboxyl group of the arginine is in its free hydroxyl form (OH).</p> | 649 |
| Activated Fmoc-Arg(Pbf) | Activated amino acid | <p>The structure shows the Fmoc-Arg(Pbf) molecule. It is similar to Fmoc-Arg(Pbf)-OH, but the carboxyl group of the arginine is also protected as a benzotriazol-1-yl ester.</p> | 766 |

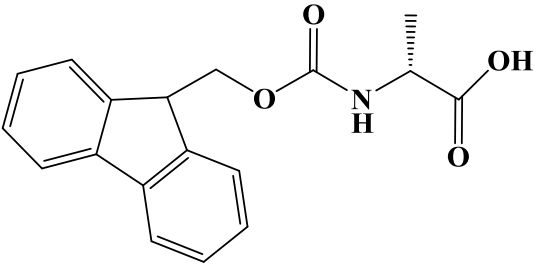
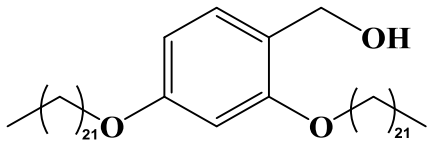
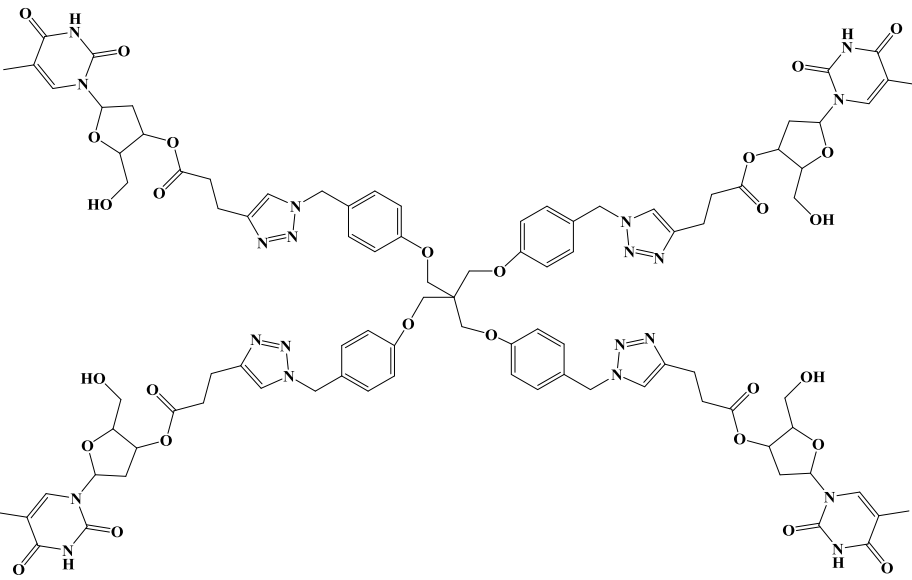
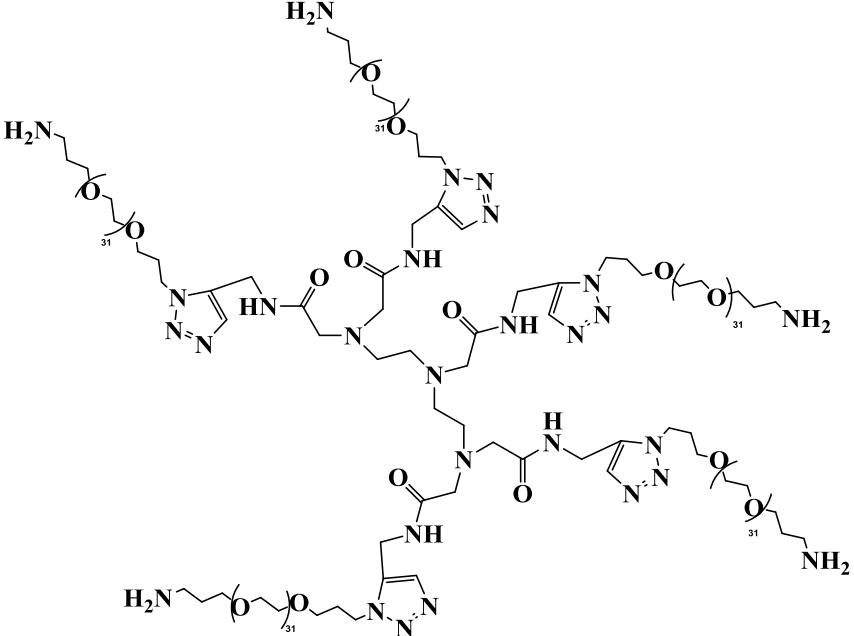
| <u>De-Fmoc</u> | | | |
|--------------------------------|-----------------------------------|--|-----|
| Piperidine | deFmoc reagent |  | 85 |
| Hydroxybenzotriazole (HOBT) | Racemisation suppressor | See above | |
| Dibenzofulvene (DBF) | By-product for the deFmoc process |  | 178 |
| DBF-piperidine | By-product for the deFmoc process |  | 263 |

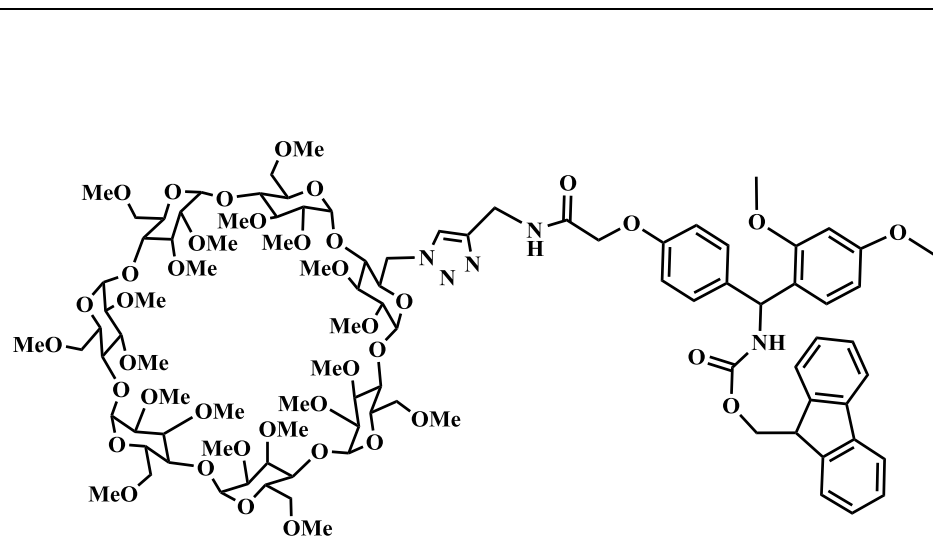
All five soluble anchors were chosen mainly due to their branched structures (Table 3.4), which were assumed to have significant resistance against permeating through the membrane pores. As expected, all anchors had high rejections ($81.4 \pm 3.9\%$ - $97.9 \pm 2.2\%$) as compared to Fmoc-Ala-OH ($29.8 \pm 5.8\%$ - $33.3 \pm 13.2\%$) (Table 3.5).

The rejection data for the anchors are statistically reliable as the standard deviations are less than or close to 5% of the average values. The rejection data of Fmoc-Ala-OH seems problematic at first glance, because the standard deviations are high compared to the average value (relative standard deviations up to 40%). A closer examination of the rejection data reveals that the rejection values of each membrane were relatively constant, but differed significantly from one membrane to another (note: two pieces of membrane were tested for both Inopor 450 and Inopor 750). This means, while the membrane performance remained consistent for all membranes throughout the tests, it could vary from one piece to another even for the same type of membrane. In other words, despite the large standard deviations of the rejection values of the reference molecule, all the data have high degree of validity.

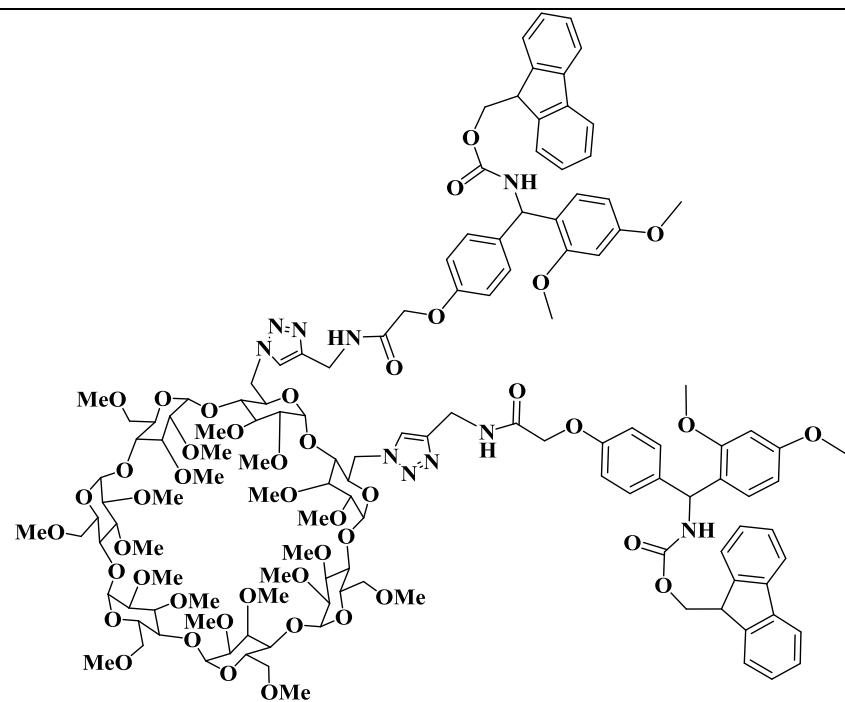
As Inopor 750 has bigger pore size than Inopor 450 (i.e. 1.0 nm as compared to 0.9 nm), it is expected to always have higher permeance, but lower rejection for the same compound. The permeance data in Table 3.5 are in agreement with this generalisation, as the permeance of Inopor 750 was always twice or higher compared to that of Inopor 450 for the same compound. However, the rejection values of Inopor 750 were comparable to those of Inopor 450 ($|\text{Rejection}_{\text{Inopor 450}} - \text{Rejection}_{\text{Inopor 750}}| < 5\%$) except for branched cyclodextrins with Fmoc-Rink linker, whose rejection values of Inopor 750 were significantly lower than those of Inopor 450 as expected.

Table 3.4. Compounds for rejection tests.

| | |
|---|---|
|  <p style="text-align: center;">Fmoc-Ala-OH</p> |  <p style="text-align: center;">DDBA</p> |
|  <p style="text-align: center;">Pentaerithritol</p> |  <p style="text-align: center;">DPEG</p> |



1-branch Cyclodextrin with Fmoc-Rink Linker



2-branch Cyclodextrin with Fmoc-Rink Linker

Table 3.5. Rejection data of Fmoc-Ala-OH and soluble anchors.

| Compound | MW ($\text{g} \cdot \text{mol}^{-1}$) | Concentration (weight %) | Inopor 450 | | Inopor 750 | |
|--|--|-----------------------------|--------------------|---|------------------|---|
| | | | Rejection (%) | Permeance ($\text{L} \cdot \text{m}^{-2} \cdot \text{h}^{-1} \cdot \text{bar}^{-1}$) | Rejection (%) | Permeance ($\text{L} \cdot \text{m}^{-2} \cdot \text{h}^{-1} \cdot \text{bar}^{-1}$) |
| Fmoc-Ala-OH | 311 | 1.0 | 33.3 ± 13.2 | 0.85 ± 0.68 | 29.8 ± 5.8 | 3.91 ± 6.13 |
| DDBA | 757 | 0.9 | 90.0 ± 3.1 | 1.40 ± 0.78 | 87.7 ± 5.3 | 2.99 ± 1.19 |
| Penthaerithritol | 1949 | 0.6 | 95.1 ± 0.3 | NA. | 97.3 ± 0.2 | NA. |
| 1-branch Cyclodextrin with Fmoc-Rink Linker | 2016 | 1.5 | 91.1 ± 1.6 | 3.51 ± 1.69 | 82.2 ± 3.2 | 8.29 ± 6.73 |
| 2-branch Cyclodextrin with Fmoc-Rink Linker | 2603 | | 91.0 ± 1.7 | | 81.4 ± 3.9 | |
| DPEG | 8209 (approx.) | 1.1 | 96.9 ± 1.1 | 0.13 ± 0.06 | 97.9 ± 2.2 | 0.21 ± 0.09 |

As shown in Figure 3.15, the rejection curve is a plateau over the range of molecular weight between $757 \text{ g} \cdot \text{mol}^{-1}$ and $8209 \text{ g} \cdot \text{mol}^{-1}$. The smallest anchor, DDBA, had similar rejection values as compared to DPEG, even though the latter is more than ten times higher in molecular weight. This is a commonly known problem in the field of nanofiltration, as the molecular weight of a compound is not reflective of the effective diameter of the compound in solution. A reliable method for determining the actual conformation and hence measuring the effective diameter is not available to date. As a result, it is always necessary to screen anchors for a new process whose specific conditions (e.g. solvents, pressure and temperature) influence the three dimensional configurations of the anchors.

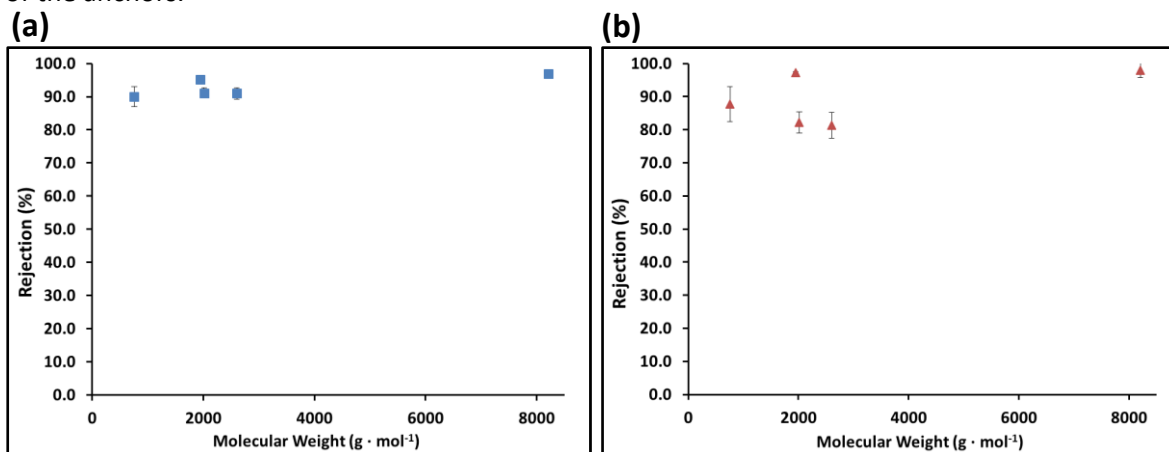


Figure 3.15. Rejection of anchor vs molecular weight for (a) Inopor 450 and (b) Inopor 750.

Among the anchors, DDBA was the only one that could be synthesised in relatively large scale (up to 26.4 mmol) for MEPS, which required at least 5 g of anchor (i.e. 6.6 mmol for DDBA) for each experiment with the present OSN system. The other three anchors were synthesised in multiple steps and were limited in terms of scale and process time as they relied on time-consuming chromatography for purification. Therefore, due to its relatively high rejection value and ease of synthesis, DDBA was chosen as the soluble anchor for the development of MEPS.

3.3.4. SPPS of Fully Deprotected Fmoc-RADA-NH₂

Fully deprotected Fmoc-RADA-NH₂ was synthesised with conventional SPPS as a reference for MEPS (Table 3.6). The scale of SPPS (11.42 mmol) was similar to that of the last attempt at MEPS (10.01 mmol (Section 3.3.8.2.4)) for comparison purpose. DIC was chosen as the coupling reagent instead of HBTU as it is frequently used in SPPS and it has a significantly lower cost than the latter (the unit prices were 150 Euro · mol⁻¹ and 569 Euro · mol⁻¹ respectively). At 1.5 eq amino acids and coupling reagents, most of the couplings went to completion without additional coupling reagents, except the loading of Fmoc-Ala-OH onto H₂N-Rink-Resin, which required additional DIC (1.37 eq) (Table 3.7 and Table 3.8).

Table 3.6. Summary of results for SPPS.

| | | Note |
|--------------------|---------------|--|
| Resin | PL Rink-Resin | |
| Scale (mmol) | 11.42* | Loading: 0.76 mmol · g ⁻¹ |
| Solvent | DMF | |
| Temperature (°C) | 20 | |
| System Volume (mL) | 100 | |
| Overall Yield (%) | 78.3** | |
| Purity (HPLC) (%) | 85.3** | Before cleavage and global deprotection. |
| Overall Yield (%) | 73.3 | After cleavage and global deprotection. |
| Purity (HPLC) (%) | 85.3 | |

*The experiment started with 15.52 g resin (11.80 mmol). After the first coupling with Fmoc-Ala-OH, 0.49 g Fmoc-Ala-Rink-Resin was taken for the loading test, leaving approximately 15.03 g resin (11.42 mmol) for further reactions.

** The overall yield and purity before cleavage and global deprotection were not measured directly as the peptide was still bound to the resin and an accurate measurement of the corresponding total mass was difficult at this scale of synthesis. According to industrial experience of Lonza AG, the yield loss during cleavage and global deprotection was normally less than 5%. The overall yield before cleavage and global deprotection was calculated based on this observation. The purity of peptide was assumed to remain constant before and after cleavage and global deprotection.

Table 3.7. Experimental data of the de-Fmoc.

| Reaction | Concentration | | Reaction Time (h) | Note |
|--|----------------------|----------|-------------------|-------------|
| | Piperidine (weight%) | HOBt (M) | | |
| De-Fmoc of Fmoc-Rink-Resin | 5.0 | | 1.0 | |
| De-Fmoc of Fmoc-Ala-Rink-Resin | 5.0 | 0.1 | 0.2 | Repeat once |
| De-Fmoc of Fmoc-Asp(OtBu)-Ala-Rink-Resin | 5.0 | 0.1 | 0.2 | Repeat once |
| De-Fmoc of Fmoc-Ala-Asp(OtBu)-Ala-Rink-Resin | 5.0 | 0.1 | 0.2 | Repeat once |

Table 3.8. Experimental data of the couplings.

| Reaction | Step | Amino Acid (eq) | DIC (eq) | HOBt (eq) | Reaction Time (h) | Ninhydrin Test* |
|-------------------------------|------|-----------------|----------|-----------|-------------------|-----------------|
| Loading of Fmoc-Ala-OH | 1 | 1.38 | 1.38 | 1.37 | 2.0 | + - |
| | 2 | | 1.37 | | 0.5 | - |
| Coupling of Fmoc-Asp(OtBu)-OH | 1 | 1.51 | 1.53 | 1.52 | 0.5 | - |
| Coupling of Fmoc-Ala-OH | 1 | 1.51 | 1.62 | 1.53 | 1.5 | - |
| Coupling of Fmoc-Arg(Pbf)-OH | 1 | 1.51 | 1.53 | 1.51 | 2.0 | - |

*Slightly positive result indicated by "+ -" and negative results indicated by "-". A complete coupling consumed all the free amine and gave positive result for the ninhydrin test (more details of the ninhydrin test can be found in section 3.2.3.3).

The global deprotection of the resin-bound protected peptide was performed with concentrated TFA solution (95 vol% TFA with scavengers). Initially, water and triisopropyl silane (TIS) were used as scavengers for the side-chain protecting groups, but were found to be ineffective in capturing the Pbf group from arginine. As a result, the integrated peak areas of the fully deprotected Fmoc-RADA-NH₂ and Fmoc-R(Pbf)-ADA-NH₂ have a ratio of 1.36 : 1.00 even after the extension of reaction time and addition of more water and TIS. This peptide mixture was precipitated, dried and then added into another cocktail that contained anisole (TFA/TIS/Anisole, 90/8/2, v/v/v). All the Fmoc-R(Pbf)-ADA-NH₂ disappeared within 30 minutes, demonstrating that anisole is an excellent scavenger for the Pbf group. The precipitation of global deprotection product gave 24.21 g Fmoc-RADA-NH₂ · TFA salt with decent overall yield and purity (by HPLC) (73.3% and 85.3% respectively). The identity of the final product was confirmed by LC/MS result (Figure 3.16).

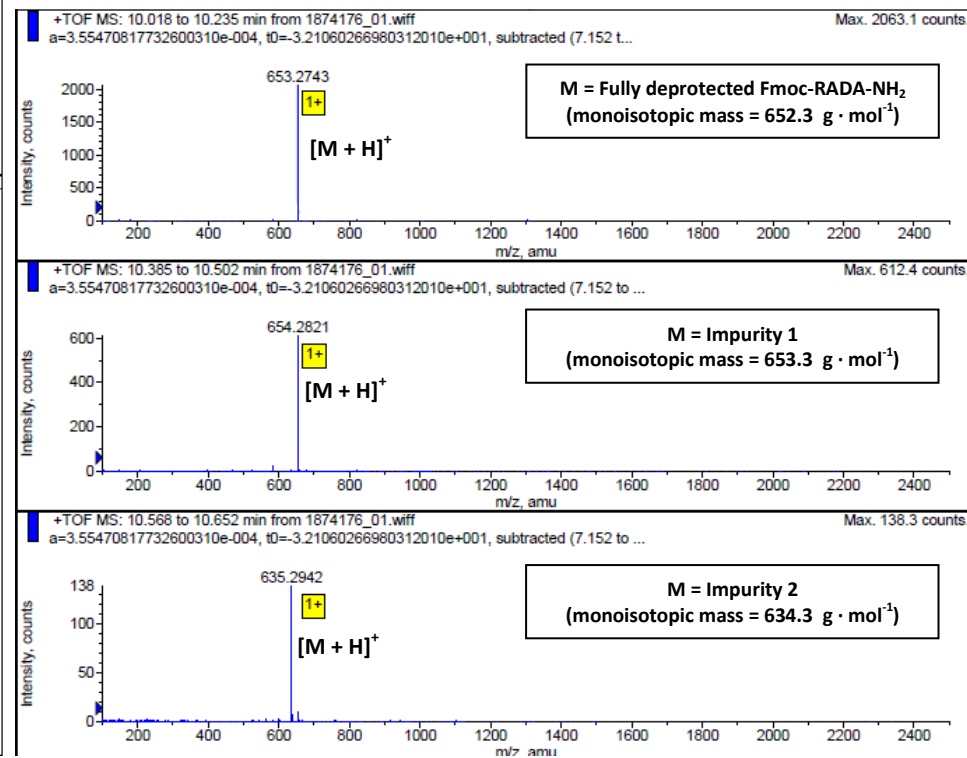
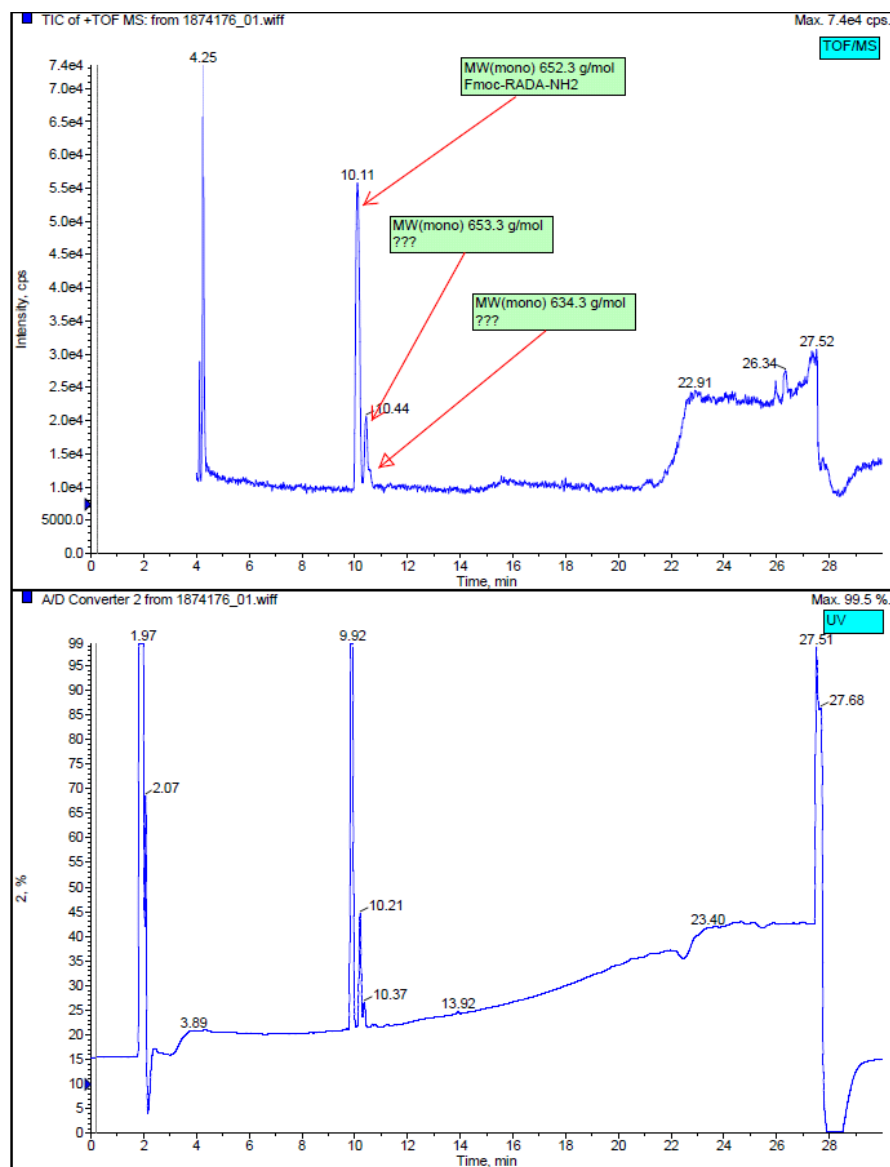


Figure 3.16. LC/MS result of the dried fully deprotected Fmoc-RADA-NH₂ (HPLC method: Fmoc-RADA_HPLC1).

3.3.5. LPPS of Fully Protected Fmoc-RADA-DDBA by Precipitation

Before moving directly onto MEPS, the target peptide was synthesised on DDBA by the precipitation of intermediate products in order to investigate the liquid phase chemistry and to develop the appropriate HPLC method for monitoring the extent of reaction/purity of the compounds.

For each step of peptide synthesis, small-scale tests (0.132 – 0.243 mmol) were first conducted for determining the best reaction conditions, followed by scaled-up reactions (2.40 – 6.60 mmol) under those conditions for validation purposes. In this context, the best reaction conditions for loading and coupling should have the lowest equivalent of amino acids and coupling reagents, while having the highest yield. The best reaction conditions for de-Fmoc should have the lowest concentration of piperidine and the shortest reaction time, while having the highest yield.

As shown in Table 3.9, the best reaction conditions for the loading of alanine onto DDBA were 10.0 weight% DDBA in THF, 2.0 eq Fmoc-Ala-OH and DIC, and 0.1 eq DMAP. After one hour of reaction, the relative yield of Fmoc-Ala-DDBA was 100.0%. A series of small-scale tests (reaction one to eight) showed that high concentration of DDBA (> 5.0 weight %) was important for driving the reaction to completion. At 1.0 weight % DDBA, the reaction was not complete even after a prolonged period (relative yield increased to 79.2 % from 52.1 % after 5 hours of reaction, as Fmoc-Ala-OH and DIC increased from 1.5 to 3.0 eq), whereas at 5.0 weight % DDBA, the reaction was nearly complete after 1 hour (99.0 % relative yield with 2.0 eq Fmoc-Ala-OH and DIC). Increasing the concentration of DDBA to 10.0 weight % improved the relative yield to 100.0 % after 1 hour of reaction with 2.0 eq Fmoc-Ala-OH and DIC, but lowering the quantities of Fmoc-Ala-OH and DIC to 1.5 eq resulted in only 95.9 % relative yield after 1 hour of reaction.

Table 3.9. Loading of Fmoc-Ala-OH under different conditions.

| Reaction | Scale (mmol) | Concentration (weight %) | | Fmoc-Ala-OH (eq) | DIC (eq) | DMAP (eq) | Reaction Time (h) | Relative Yield* (%) |
|----------|--------------|--------------------------|-------------|------------------|----------|-----------|-------------------|---------------------|
| | | DDBA | Fmoc-Ala-OH | | | | | |
| 1 | 0.132 | 1.0 | 0.6 | 1.5 | 2.3 | 0.2 | 5.0 | 52.1 |
| 2 | 0.133 | 1.0 | 1.0 | 2.5 | 2.5 | 0.1 | 5.0 | 68.2 |
| 3 | 0.132 | 1.0 | 1.2 | 3.0 | 3.1 | 0.2 | 5.0 | 79.2 |
| 4 | 0.139 | 10.3 | 6.1 | 1.4 | 1.6 | 0.1 | 5.0 | 95.9 |
| 5 | 0.134 | 9.7 | 9.9 | 2.5 | 2.6 | 0.2 | 0.5 | 100.0 |
| 6 | 0.134 | 10.0 | 12.2 | 3.0 | 3.3 | 0.1 | 1.0 | 100.0 |
| 7 | 0.134 | 5.1 | 4.1 | 2.0 | 2.1 | 0.1 | 1.5 | 99.0 |
| 8 | 0.135 | 10.0 | 8.1 | 2.0 | 2.1 | 0.1 | 1.0 | 100.0 |
| 9 | 6.60 | 10.0 | 8.3 | 2.0 | 2.0 | 0.1 | 1.0 | 100.0 |

*Note: relative yield calculated from the integrated peak areas of the product and starting material.

As shown in Table 3.10 (reaction one to nine), the best reaction conditions for the de-Fmoc of Fmoc-Ala-DDBA were 5.0 weight % piperidine in THF and 1.0 eq HOBt. After 3 hours of reaction, the relative yield of H₂N-Ala-DDBA was 100.0 %. Unlike the previous step, lowering the concentration of the reactant (Fmoc-Ala-DDBA) from 10.0 weight % to 1.0 weight % had no significant effect on the relative yield. The concentration of piperidine was the major factor affecting the relative yield (reducing the concentration of piperidine from 5.0 weight % to 2.6 weight % and further resulted in lower relative yields).

Table 3.10. De-Fmoc of Fmoc-Ala-DDBA under different conditions.

| Reaction | Scale (mmol) | Concentration (weight %) | | HOBt (eq) | Reaction Time (h) | Relative Yield* (%) |
|----------|--------------|--------------------------|------------|-----------|-------------------|---------------------|
| | | Fmoc-Ala-DDBA | Piperidine | | | |
| 1 | 0.191 | 10.0 | 5.3 | 1.0 | 2.5 | 95.0 |
| 2 | 0.194 | 10.1 | 2.6 | 1.0 | 3.0 | 64.1 |
| 3 | 0.191 | 1.0 | 5.0 | 1.0 | 3.0 | 100.0 |
| 4 | 0.192 | 1.0 | 2.6 | 1.0 | 3.0 | 84.4 |
| 5 | 0.192 | 1.0 | 0.5 | 1.0 | 5.0 | 29.3 |
| 6 | 0.191 | 1.0 | 0.08 | 1.0 | 5.0 | 3.6 |
| 7 | 0.193 | 1.0 | 0.05 | 1.1 | 3.0 | 1.2 |
| 8 | 0.192 | 1.0 | 0.03 | 1.0 | 3.0 | 0.9 |
| 9 | 0.192 | 1.0 | 0.02 | 1.0 | 3.0 | 0.9 |
| 10 | 4.29 | 1.0 | 5.0 | 1.0 | 3.0 | 98.7 |

*Note: relative yield calculated from the integrated peak areas of the product and starting material.

The next step, coupling of Fmoc-Asp(OtBu)-OH, was complete after 1 hour of reaction with only 1.05 eq Fmoc-Asp(OtBu)-OH, HBTU and HOBT, and 6.45 eq DIEA (Table 3.11).

Table 3.11. Coupling of Fmoc-Asp(OtBu)-OH under different conditions.

| Reaction | Scale (mmol) | Step | Concentration (weight %) | | Fmoc-Asp(OtBu)-OH (eq) | HBTU (eq) | HOBT (eq) | DIEA (eq) | Reaction Time (h) | Relative Yield* (%) |
|----------|--------------|------|---------------------------|-------------------|------------------------|-----------|-----------|-----------|-------------------|---------------------|
| | | | H ₂ N-Ala-DDBA | Fmoc-Asp(OtBu)-OH | | | | | | |
| 1 | 0.243 | 1 | 1.0 | 0.5 | 1.10 | 1.12 | 1.10 | 0.66 | 3.0 | 92.6 |
| | | 2 | | | | | | | 6.97 | 0.5 |
| 2 | 0.244 | 1 | 1.0 | 0.5 | 1.04 | 1.09 | 1.12 | 0.65 | 3.0 | 90.9 |
| | | 2 | | | | | | | 6.89 | 1.0 |
| 3 | 2.41 | 1 | 1.0 | 0.5 | 1.06 | 1.06 | 1.04 | 6.45 | 1.0 | 100.0 |

*Note: relative yield calculated from the integrated peak areas of the product and starting material.

Finally, the de-Fmoc of Fmoc-Asp(OtBu)-Ala-DDBA was complete within 1 hour with 5.0 weight % piperidine in THF and 1.0 eq HOBT (Table 3.12). However, HPLC results show that DDBA began to appear after 3 hours of reaction (relative yield of H₂N-Asp(OtBu)-Ala-DDBA decreased to 58.5 % with respect to DDBA) (Figure 3.17 (a) to (d)), suggesting the formation of DKP (Figure 3.19), which was confirmed by the LC/MS result (Figure 3.18). Detailed explanation of the DKP formation mechanism can be found in the literature review (Section 2.1.6.2).

Table 3.12. De-Fmoc of Fmoc-Asp(OtBu)-Ala-DDBA under different conditions.

| Reaction | Scale (mmol) | Step | Concentration (weight %) | | HOBT (eq) | Reaction Time (h) | Relative Yield* (%) | Note |
|----------|--------------|------|--------------------------|------------|-----------|-------------------|---------------------|------|
| | | | Fmoc-Asp(OtBu)-Ala-DDBA | Piperidine | | | | |
| 1 | 0.165 | 1 | 1.0 | 5.0 | 1.0 | 1.0 | 100.0 | |
| | | 2 | | | | | 3.0 | 58.5 |
| 2 | 0.166 | 1 | 1.0 | 0.05 | 1.0 | Overnight | 1.3 | |
| 3 | 0.166 | 1 | 1.0 | 2.6 | 1.0 | 1.0 | 100.0 | |
| | | 2 | | | | | Overnight | 7.5 |

*Note: relative yield calculated from the integrated peak areas of the product and starting material.

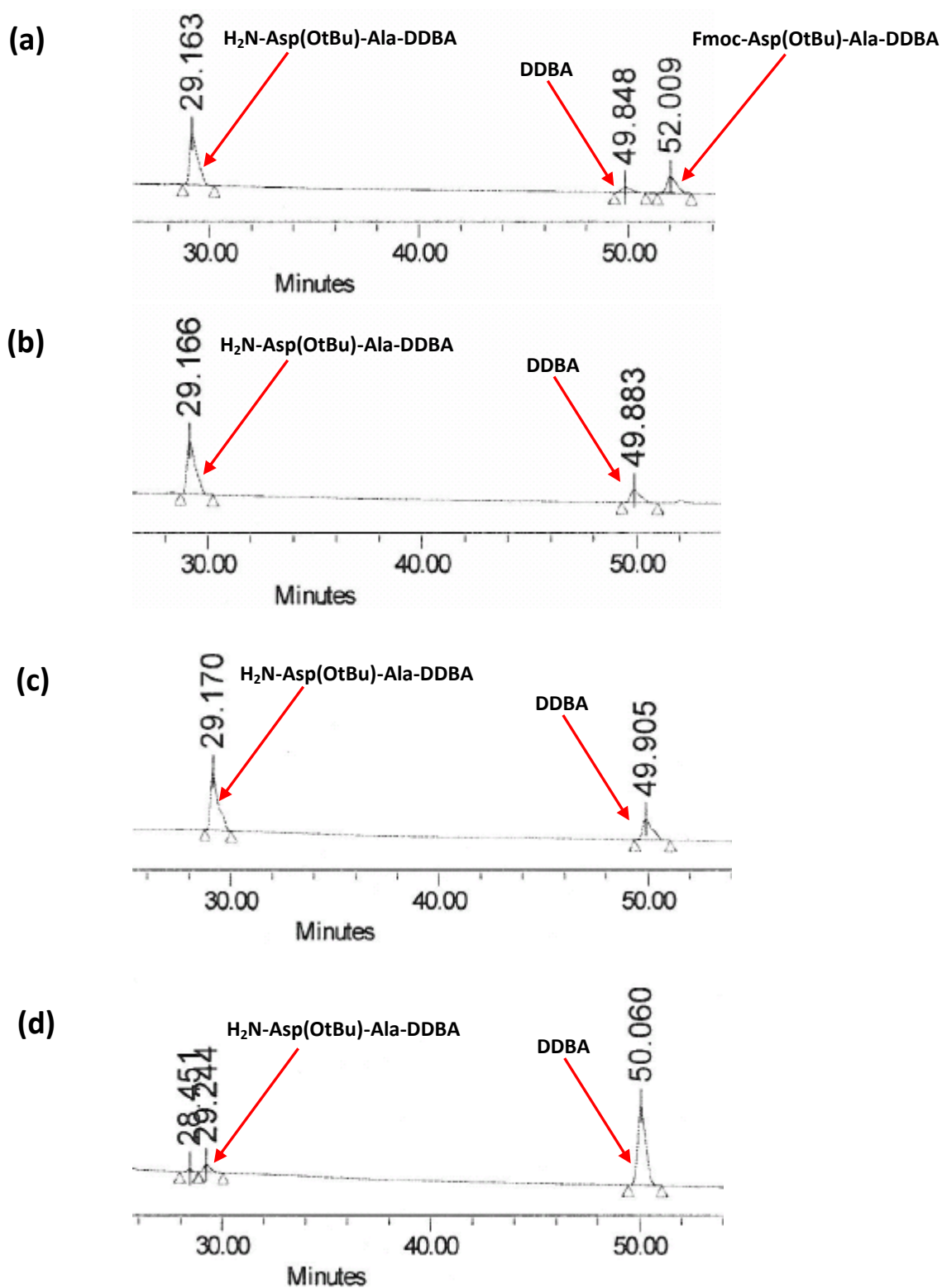


Figure 3.17. HPLC results for the de-Fmoc of Fmoc-Asp(OtBu)-Ala-DDBA: (a) 1 hour of de-Fmoc; (b) 2 hours of de-Fmoc; (c) 3 hours of de-Fmoc; (d) overnight de-Fmoc.

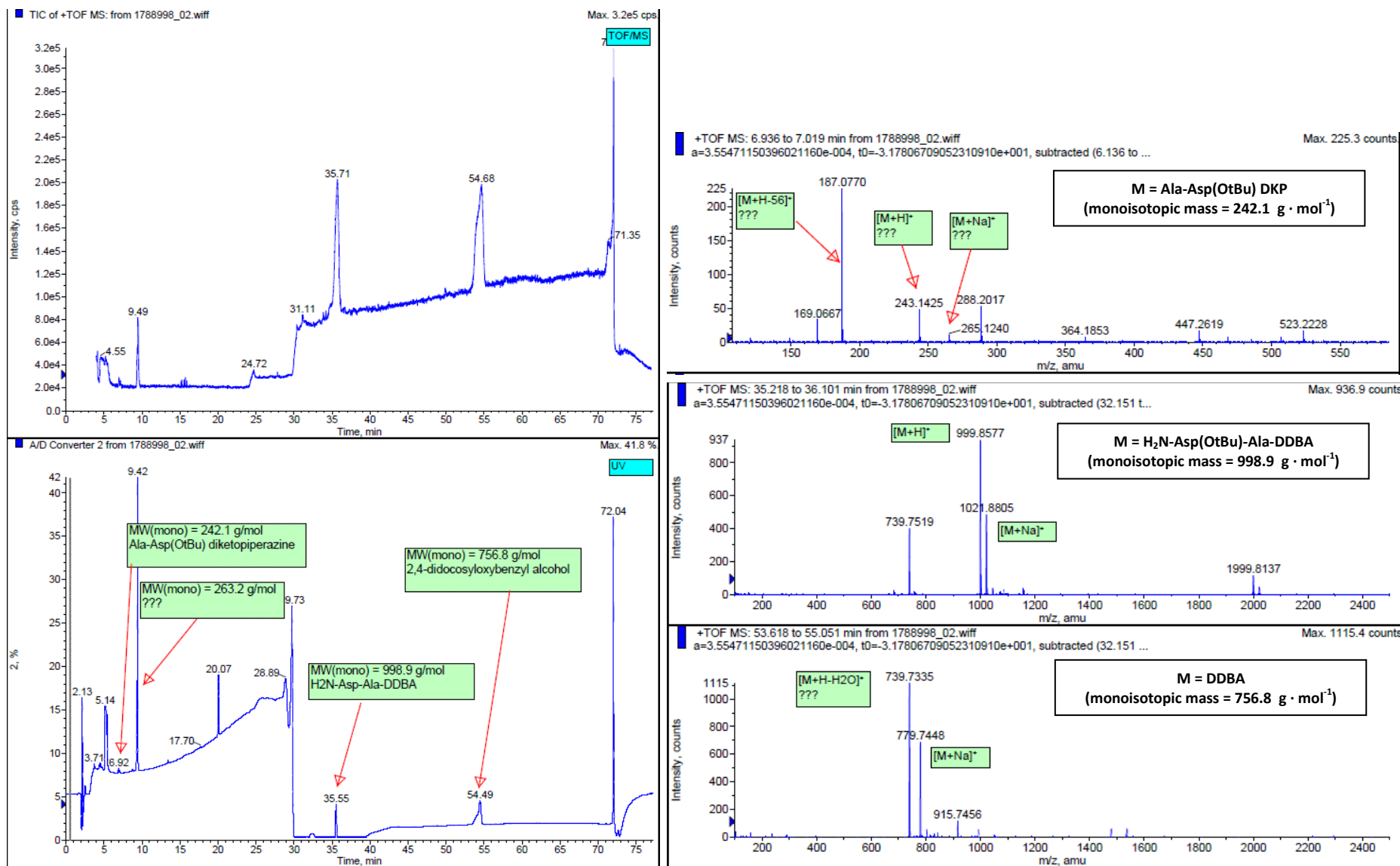


Figure 3.18. LC/MS result for the 3-hour de-Fmoc of Fmoc-Asp(OtBu)-Ala-DDBA (Table 3.12) (HPLC method: Fmoc-RADA-DDBA_HPLC1).

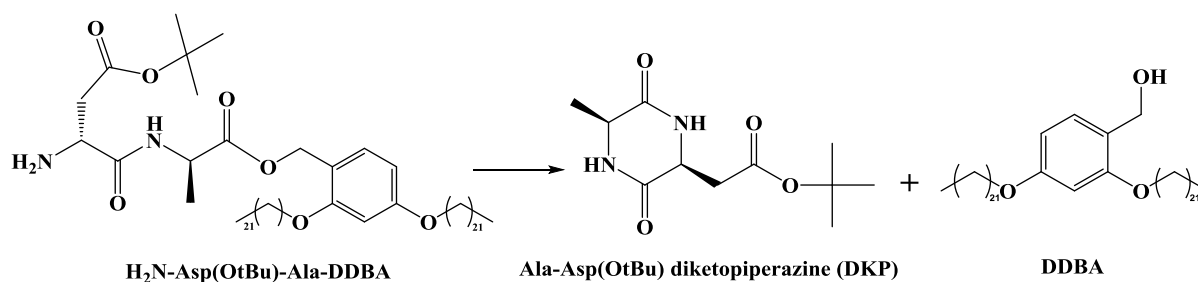


Figure 3.19. DKP formation.

The synthesis data show that the loading of the first amino acid onto DDBA requires a high concentration of DDBA to proceed to completion, probably due to the relatively low reactivity of the alcohol group. The complete de-Fmoc of amino acid or peptide fragment on DDBA can be achieved with at least 5 weight% piperidine in THF. The coupling of amino acid with deprotected peptide fragment requires only close to equivalent amount (1.05 eq) of amino acid and coupling reagents to proceed to completion, confirming the advantage of liquid phase synthesis in terms of material costs. Most importantly, the data show that peptide synthesis on DDBA is prone to the formation of DKP when aspartic acid is present in the sequence. To overcome this problem, DDBA was modified with the attachment of Fmoc-Rink linker, which is commonly incorporated on resins for SPPS. Due to the sterically hindered structure of Fmoc-Rink, the formation of DKP became less favourable. More details about the synthesis of the modified anchor and the corresponding peptide synthesis are covered in the following sections.

3.3.6. Synthesis of H₂N-Rink-DDBA

The synthesis of H₂N-Rink-DDBA was successful and repeatable (Table 3.13 and 3.14). The attachment of Fmoc-Rink linker unto DDBA went to completion with 10 weight% DDBA in THF. Fmoc-Rink-DDBA was then deprotected by piperidine, resulting in high yields (88.7 - 108.4 %) and purities (97.4 - 99.4 %). The identities of the compounds were confirmed by the LC/MS results (Figure 3.20 and Figure 3.21).

Similar to the second step in the synthesis of DDBA, the de-Fmoc of Fmoc-Rink-DDBA had a repeat with an overall yield higher than 100.0 % (i.e. 108.4 %). A possible cause was the incomplete removal of the anti-solvent (i.e. acetonitrile for precipitating the deprotected anchor) during evaporation. The implication of using the product from this repeat in the peptide synthesis would be a lower overall yield for the final peptide, as the actual quantity of anchor to start with was in fact lower than the apparent value (i.e. with the presence of trace amount of anti-solvent).

Table 3.13. Summary of results for the synthesis of Fmoc-Rink-DDBA.

| Reaction | Scale (mmol) | Purity by HPLC (%) | Yield (%) | Note |
|----------|--------------|--------------------|-----------|---|
| 1 | 13.4 | 100.0 | NA. | Yield not available as product not dried completely before proceeding to deFmoc due to time constraint. |
| 2 | 13.3 | 100.0 | | |
| 3 | 19.3 | 100.0 | | |
| 4 | 62.1 | 100.0 | | |

Table 3.14. Summary of results for the synthesis of H₂N-Rink-DDBA.

| Reaction | Scale (mmol) | Purity by HPLC (%) | Overall Yield* (%) |
|----------|--------------|--------------------|--------------------|
| 1 | 13.4 | 97.4 | 97.5 |
| 2 | 13.3 | 99.4 | 98.6 |
| 3 | 19.3 | 99.4 | 88.7 |
| 4 | 62.1 | 98.3 | 108.4 |

*Overall yield with respect to the original amount of DDBA.

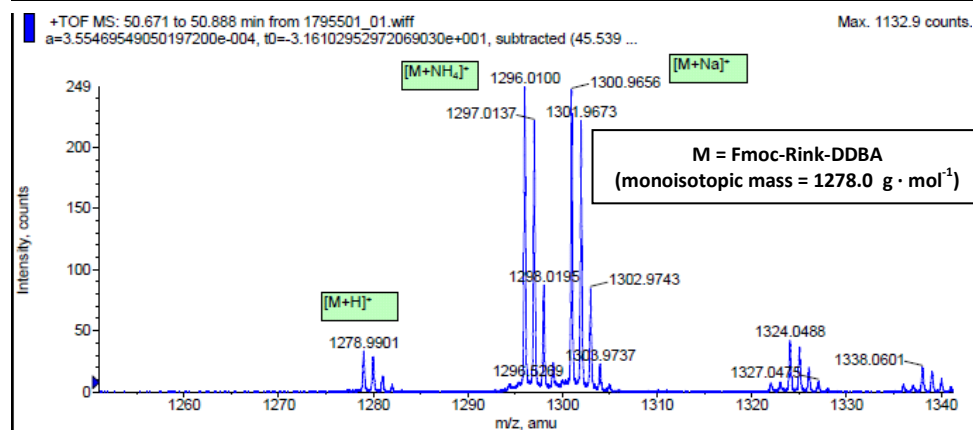
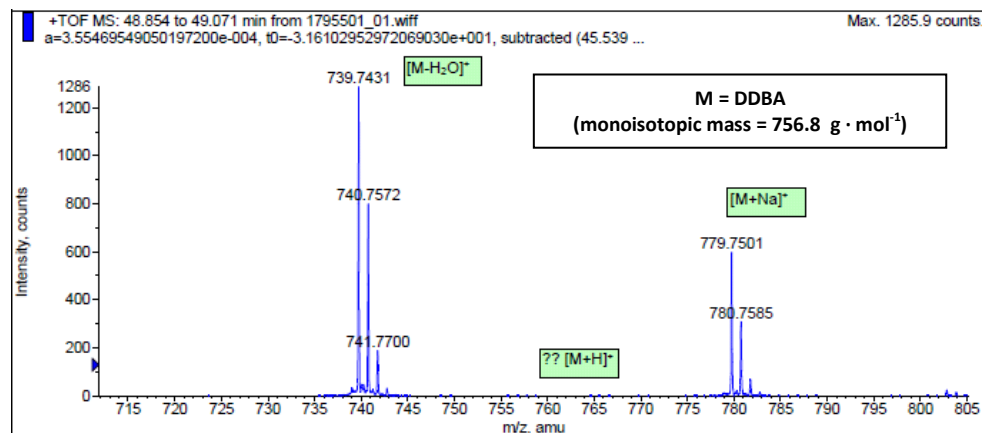
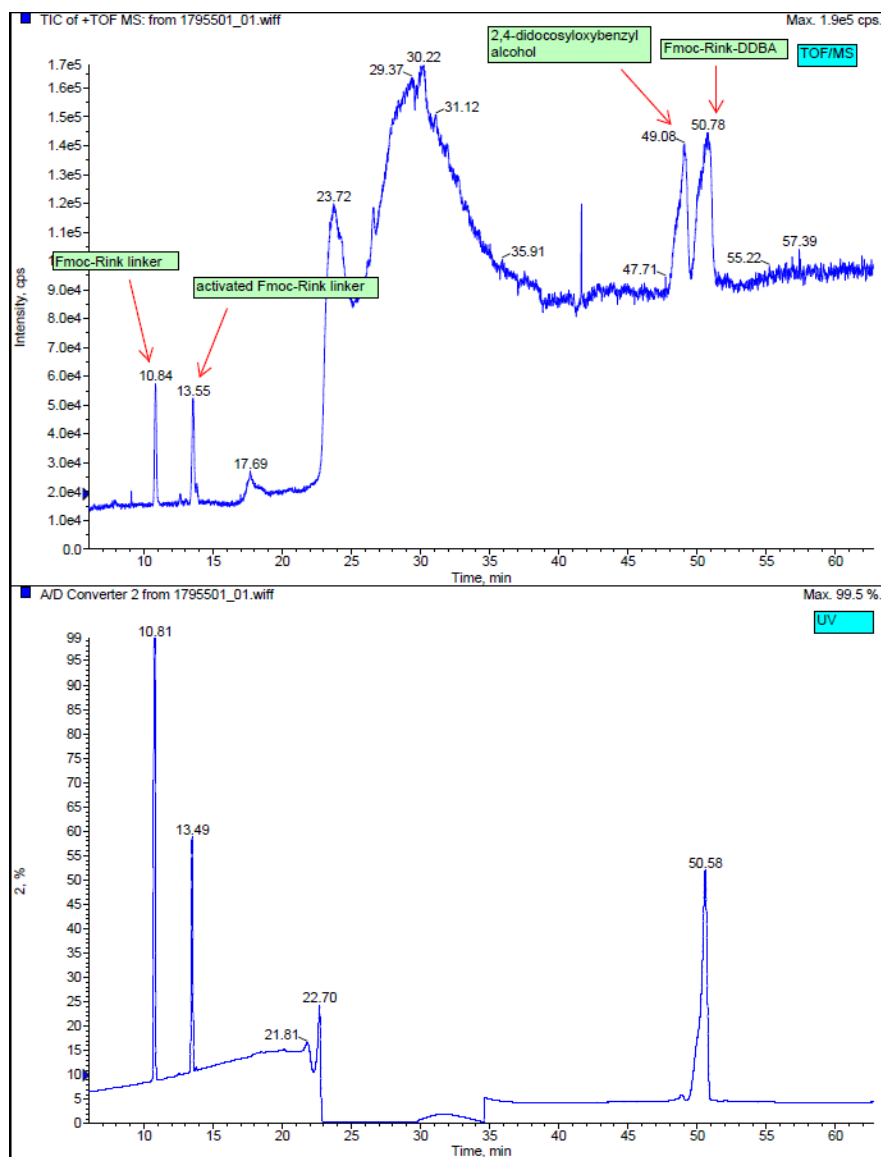


Figure 3.20. LC/MS result for the loading of Fmoc-Rink linker unto DDBA (HPLC method: Fmoc-RADA-DDBA_HPLC1).

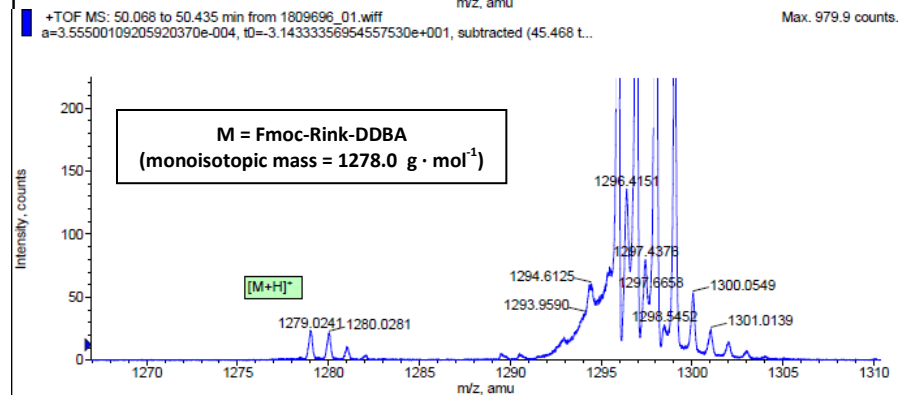
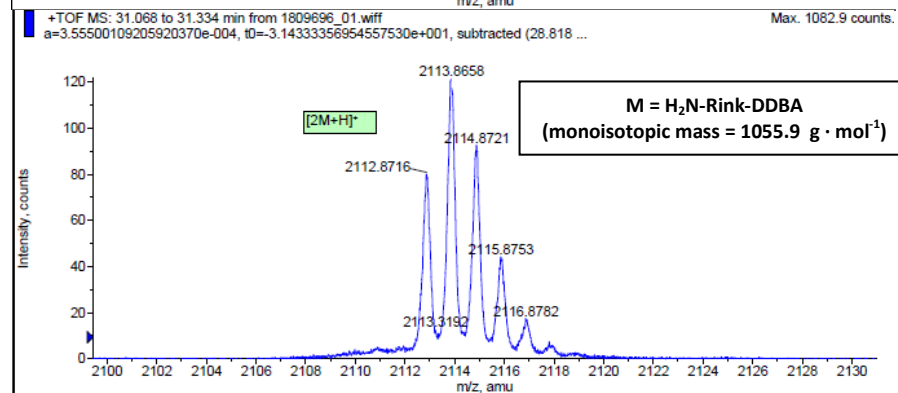
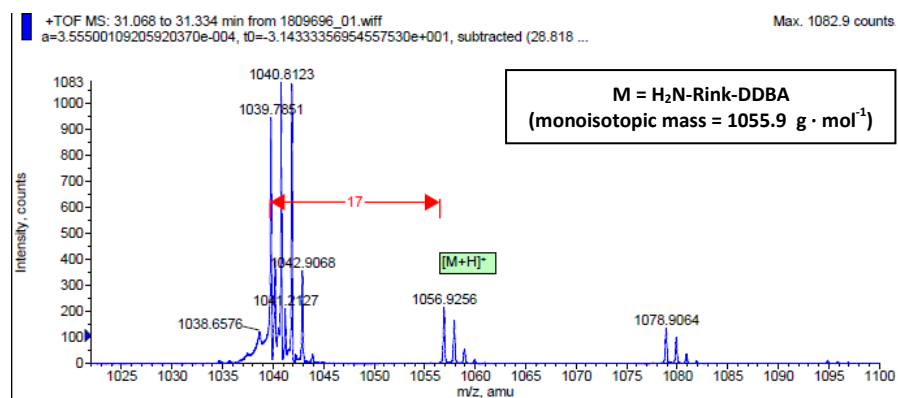
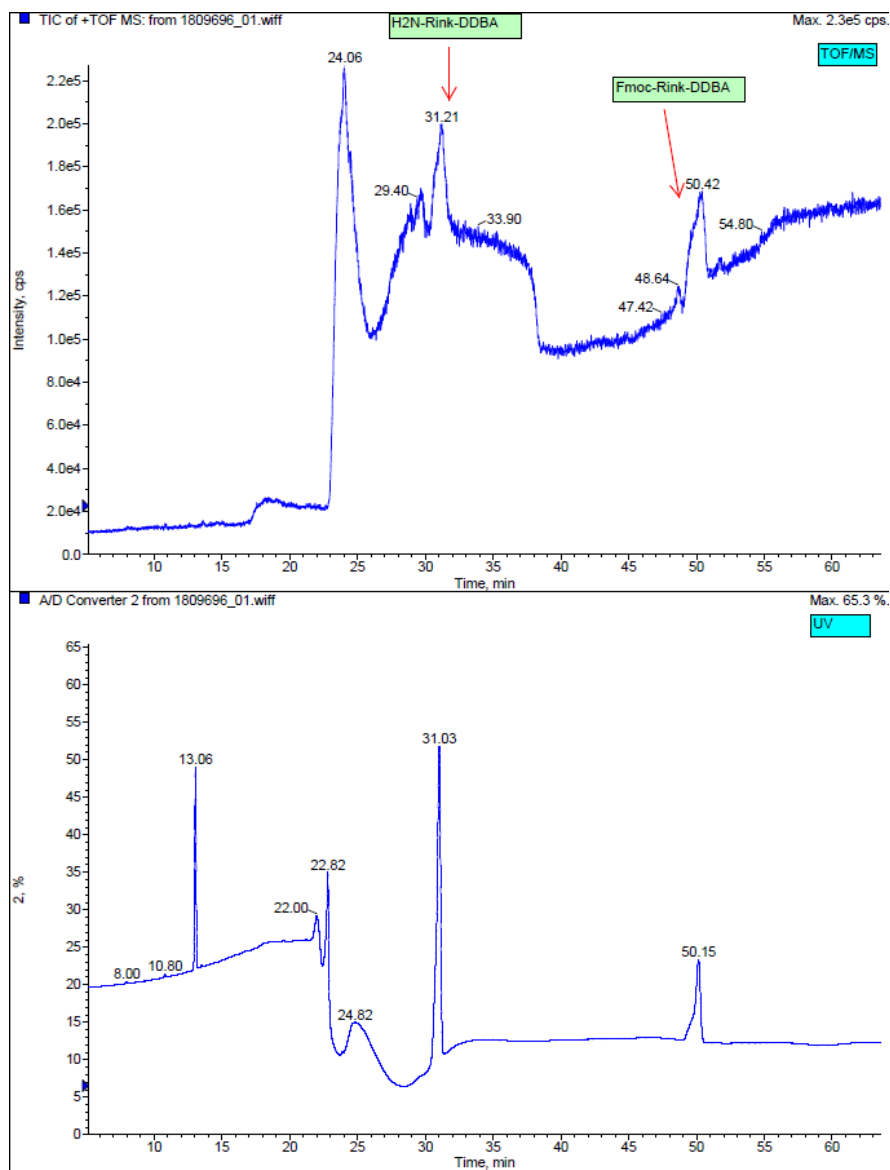


Figure 3.21. LC/MS result for the de-Fmoc of Fmoc-Rink-DBA (HPLC method: Fmoc-RADA-DBA_HPLC1).

3.3.7. Small-scale Coupling Tests for Fully Protected Fmoc-RADA-Rink-DDBA in Liquid Phase by Precipitation

For the synthesis of fully protected Fmoc-RADA-Rink-DDBA, small-scale tests (0.074 - 0.097 mmol as shown in Table 3.15) showed that all couplings went to near completion (94.3 - 99.1 %) within 30 minutes with only a slight excess (0.05 eq) of amino acid and coupling reagents. No further improvement in yield could be achieved by prolonging the reactions up to three hours, after which additional HBTU could only increase the yield slightly.

Table 3.15. Small-scale coupling tests at 1.0 weight% of deprotected peptide-anchor.

| Reaction | Scale (mmol) | Step | Reactant | Reactant Concentration (weight %) | Amino Acid (eq) | HBTU (eq) | DIEA (eq) | Reaction Time (h) | Relative Yield* (%) |
|------------|--------------|------|--|-----------------------------------|-----------------|-----------|-----------|-------------------|---------------------|
| Loading | 0.097 | 1 | H ₂ N-Rink-DDBA | 1.0 | 1.03 | 1.03 | 4.85 | 3.0 | 94.3 |
| | | 2 | | | | 1.00 | | 0.5 | 99.2 |
| Coupling 1 | 0.089 | 1 | H ₂ N-Ala-Rink-DDBA | 1.0 | 1.06 | 1.11 | 4.83 | 3.0 | 97.1 |
| | | 2 | | | | 1.07 | | 0.5 | 99.8 |
| Coupling 2 | 0.077 | 1 | H ₂ N-Asp(OtBu)-Ala-Rink-DDBA | 1.0 | 1.06 | 1.10 | 6.62 | 0.5 | 99.1 |
| Coupling 3 | 0.074 | 1 | H ₂ N-Ala-Asp(OtBu)-Ala-Rink-DDBA | 1.0 | 1.05 | 1.04 | 5.41 | 3.0 | 97.2 |
| | | 2 | | | | 1.00 | | 3.0 | 98.3 |

*Note: relative yield calculated from the integrated peak areas of the product and starting material.

Normally, liquid phase reaction should be run at high concentration (e.g. ≥ 10 weight % of limiting reactant) in order to have fast kinetics and to lower the quantity of excess reactants. In MEPS, this is even more important, because the removal of excess reagents and by-products by nanofiltration is more efficient in terms of process time and solvent consumption at high concentration. As mentioned earlier, the OSN system has a minimum working volume between 400 mL and 500 mL, meaning that about 40 to 50 g of soluble anchor is needed to run one experiment at 10 weight % anchor concentration. In reality, due to the limited scale of anchor synthesis, only 10 % of this quantity of anchor (i.e. 4 to 5 g) could be used for the majority of MEPS experiments. Therefore, the small-scale tests were also meant to investigate whether couplings could finish at 1 weight % anchor concentration. Since positive results were obtained, MEPS should proceed smoothly at the same concentration.

3.3.8. MEPS of Fully Deprotected Fmoc-RADA-NH₂ on H₂N-Rink-DDBA

3.3.8.1. Screening of Membrane with DDBA

Following the screening of anchors, eight Inopor 450 and Inopor 750 membranes (four for each type) were tested with DDBA again in order to select the best one for MEPS. On average, Inopor 450 membranes had markedly higher rejection value and lower permeance than Inopor 750 (Table 3.16). The standard deviations of rejection value are 6.8 % and 10.8 % with respect to the mean values for Inopor 450 and Inopor 750 respectively, whereas those for permeance are significantly higher (87.8 % and 84.1 % respectively), suggesting that the performance of ceramic membranes is in fact variable and a screening of membrane is always necessary for a particular process. The membrane with the highest rejection value of DDBA (Inopor 450 (A1): rejection value= 91.1 ± 0.3 %, permeance= 6.3 ± 0.1 L · m⁻² · h⁻¹ · bar⁻¹) was selected for all the MEPS experiments in the following sections.

Table 3.16. Rejection tests of DDBA by ceramic membranes.

| Inopor 450 Membrane* | Rejection (%) | Permeance (L · m ⁻² · h ⁻¹ · bar ⁻¹) | Inopor 750 Membrane** | Rejection (%) | Permeance (L · m ⁻² · h ⁻¹ · bar ⁻¹) |
|---|---------------|--|-----------------------|---------------|--|
| A1 | 90.8 | 6.4 | B1 | 75.4 | 12.1 |
| | 91.2 | 6.3 | | 74.8 | 12.8 |
| | 91.3 | 6.3 | | 75.2 | 13.0 |
| A2 | 81.2 | 19.0 | B2 | 72.1 | 28.3 |
| | 81.7 | 18.1 | | 72.1 | 27.1 |
| | 81.2 | 18.1 | | 71.3 | 27.1 |
| A3 | 87.0 | 1.5 | B3 | 61.7 | 3.4 |
| | 87.2 | 1.5 | | 65.1 | 3.2 |
| | 87.9 | 1.4 | | 65.3 | 3.1 |
| A4 | 75.5 | 4.8 | B4 | 86.5 | 4.7 |
| | 84.0 | 4.4 | | 86.3 | 4.5 |
| | 74.8 | 4.0 | | 82.3 | 4.5 |
| Mean | 84.5 | 7.7 | | 74.0 | 12.0 |
| Standard Deviation | 5.7 | 6.7 | | 8.0 | 10.1 |
| Standard Deviation as Percentage of Mean (%) | 6.8 | 87.8 | | 10.8 | 84.1 |

*Four different pieces of Inopor 450. A1: SG813-A/5th Aug2013; A3: SG1405/6th Nov2012;

A2: SG1392/5th Aug2013; A4: SG1392/21st May2012.

** Four different pieces of Inopor 750. B1: SG1391/22th July2013; B3: SG1391/21st May2012;

B2: SG1405-B/5th Aug2013; B4: SG1405-B/6th Nov2012.

(Labelling of membrane: batch number/date of first use)

3.3.8.2. MEPS

Small-scale tests of fully protected Fmoc-RADA-Rink-DDBA synthesis showed that couplings could finish within 30 minutes even with only 1.05 eq amino acids and coupling reagents at approximately 1 weight % anchor concentration. The liquid phase synthesis was then scaled up for MEPS to accommodate the minimum working volume of the available OSN system (400 - 500 mL) and, surprisingly, the couplings of amino acids were not as straightforward as in the small-scale tests.

Four attempts were made in total, in which the first two had incomplete couplings for the last two amino acid residues (Ala and Arg(Pbf)). The subsequent attempts revealed that all couplings could proceed to completion by increasing the number of wash volumes from 5 to 14 for each post-de-Fmoc diafiltration. Hence, it was hypothesised that even a minute amount of piperidine could interfere with the coupling process, but the mechanism needed to be confirmed (see the next chapter (Section 4.3.3.2)). As a result of this finding, the last two attempts achieved decent yields and high purities of the target compound (76.5 - 78.6 % and 93.8 - 98.5 % respectively before cleavage and global deprotection). The results of the fourth attempt are used to represent MEPS in deriving the various performance parameters in the later section of this chapter (Section 3.3.9).

In terms of chemistry, HBTU activation of amino acids resulted in faster coupling in liquid phase (reaction time = 30 minutes) as compared to DIC (reaction time \geq 3 hours) and the couplings proceeded little further after 30 minutes. However, the corresponding couplings seemed more susceptible to interference by residual piperidine based on observations in the first two attempts (the incomplete coupling of Fmoc-Asp(OtBu)-OH had relative yield of 90.3 % for DIC and 75.5 % for HBTU before addition of more DIC and HBTU respectively). With 14 wash volumes for each post-de-Fmoc diafiltration, all couplings went to completion in 30 minutes with close-to-equivalent quantities (1.05 eq) of amino acids and coupling reagents (HBTU/HOBt). On the other hand, all de-Fmoc went to completion in 1 hour with 5.0 weight % piperidine/THF solution.

3.3.8.2.1. MEPS (First Attempt)

In the first attempt, DIC (1.05 eq) was used as the activator so that a direct comparison with SPPS could be made. Each coupling of the first two amino acids required approximately three hours to proceed to completion. The third coupling with Fmoc-Ala-OH was incomplete (relative yield (HPLC): 30.2 %) even after the addition of a second portion of DIC (1.04 eq) and the prolongation of reaction (Figure 3.22 (a) and (b)). Without diafiltration, HBTU (1.05 eq)/DMF and DIEA (pH of reaction solution: 9 - 10) were added into the reaction solution and the relative yield (HPLC) increased to 52.2 %, but an unknown impurity appeared (relative yield (HPLC): 18.8 %) (Figure 3.22 (c)). Another portion of HBTU (1.06 eq)/DMF and DIEA (pH of reaction solution: 8 – 9) was added and the reaction was run overnight, but the relative yield (HPLC) only increased marginally to 62.7 % (relative yield of impurity: 25.0 %) (Figure 3.22 (d)).

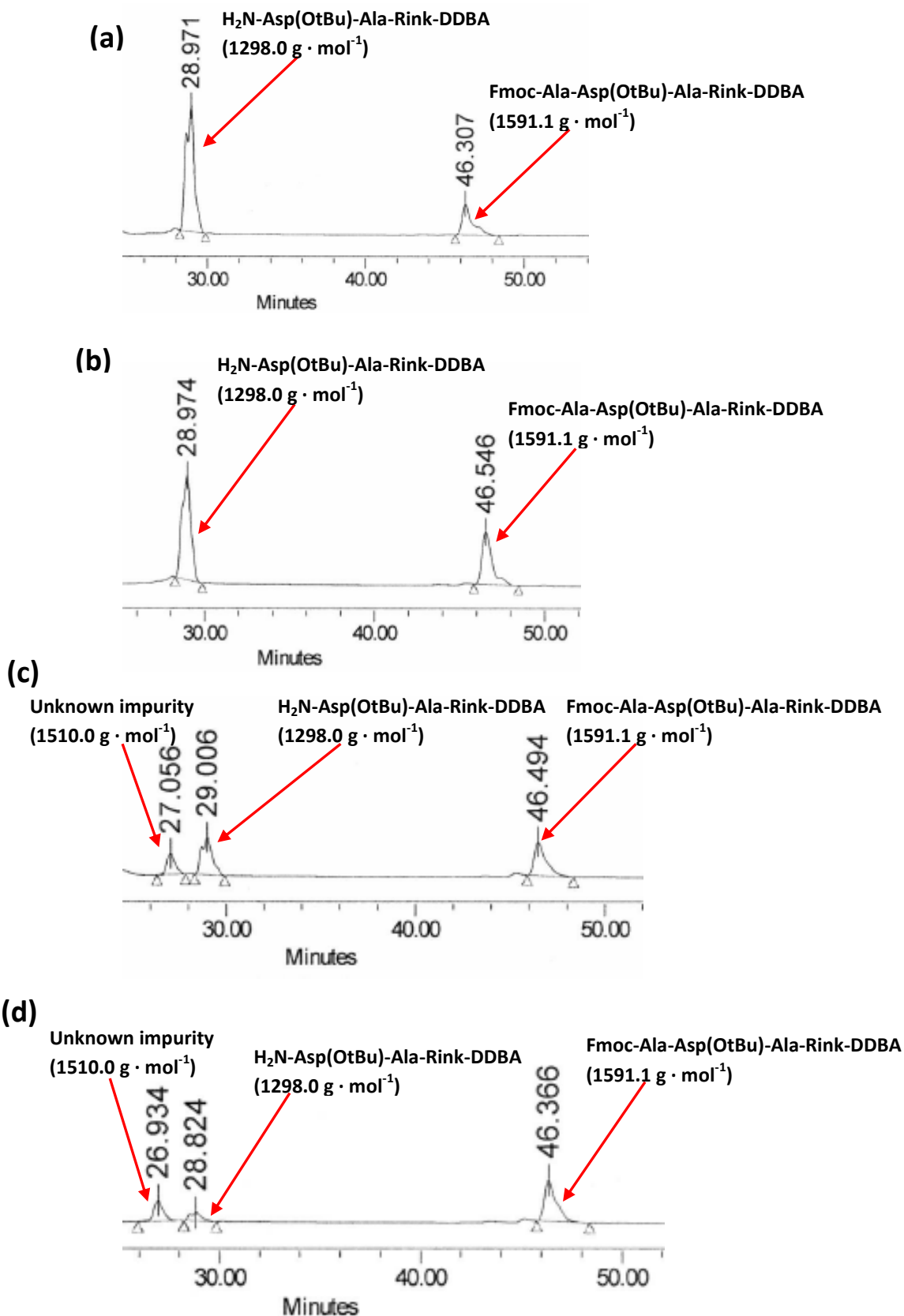


Figure 3.22. Incomplete third coupling with Fmoc-Ala-OH: (a) 2.5 hours of coupling; (b) overnight coupling after the addition of second portion of DIC; (c) 30 minutes after the addition of HBTU/DIEA; (d) overnight after the addition of second portion of HBTU/DIEA. (Monoisotopic mass of component displayed)

The last coupling with Fmoc-Arg(Pbf)-OH was performed with HBTU (1.05 eq) as the activator and the reaction was incomplete (relative yield (HPLC): 69.7 %) with the unknown impurity and unreacted H₂N-Asp(OtBu)-Ala-Rink-DDBA from the third coupling with Fmoc-Ala-OH (Figure 3.23).

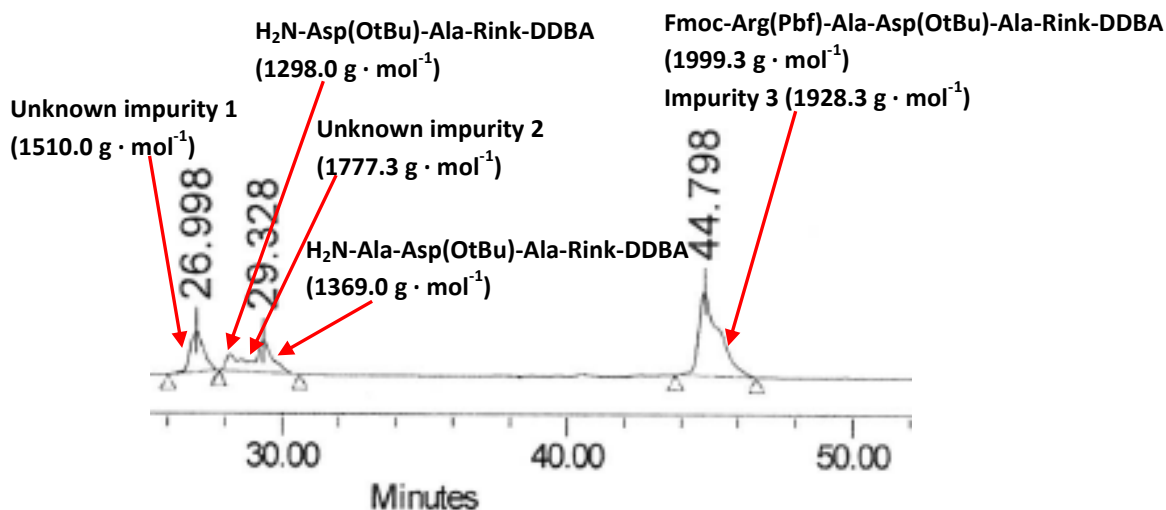


Figure 3.23. Incomplete fourth coupling with Fmoc-Arg(Pbf)-OH. (Monoisotopic mass of component displayed)

On the other hand, every de-Fmoc was complete in 1 hour with 5.0 weight % piperidine/THF solution. Diafiltration with 5 wash volumes was performed after each de-Fmoc, but not after each coupling. Chloranil tests (as used in conventional SPPS) showed that 5 wash volumes were sufficient to reduce the concentration of piperidine to the acceptable level as the colour of test solution went from dirty green to purple and subsequently to pale yellow (i.e. a negative result).

3.3.8.2.2. MEPS (Second Attempt)

In the second attempt, HBTU (1.05 eq) was used as the activator as in the small-scale tests of fully protected Fmoc-RADA-Rink-DDBA synthesis. The loading of the first amino acid was nearly complete in 30 minutes (relative yield (HPLC): 99.4 %). The next coupling with Fmoc-Asp(OtBu)-OH was incomplete (relative yield (HPLC): 75.5 %) and the second portion of Fmoc-Asp(OtBu)-OH (0.10 eq) and HBTU (0.11 eq)/DMF was added in order to drive the reaction to near completion (relative yield (HPLC): 92.3 %) (Figure 3.24).

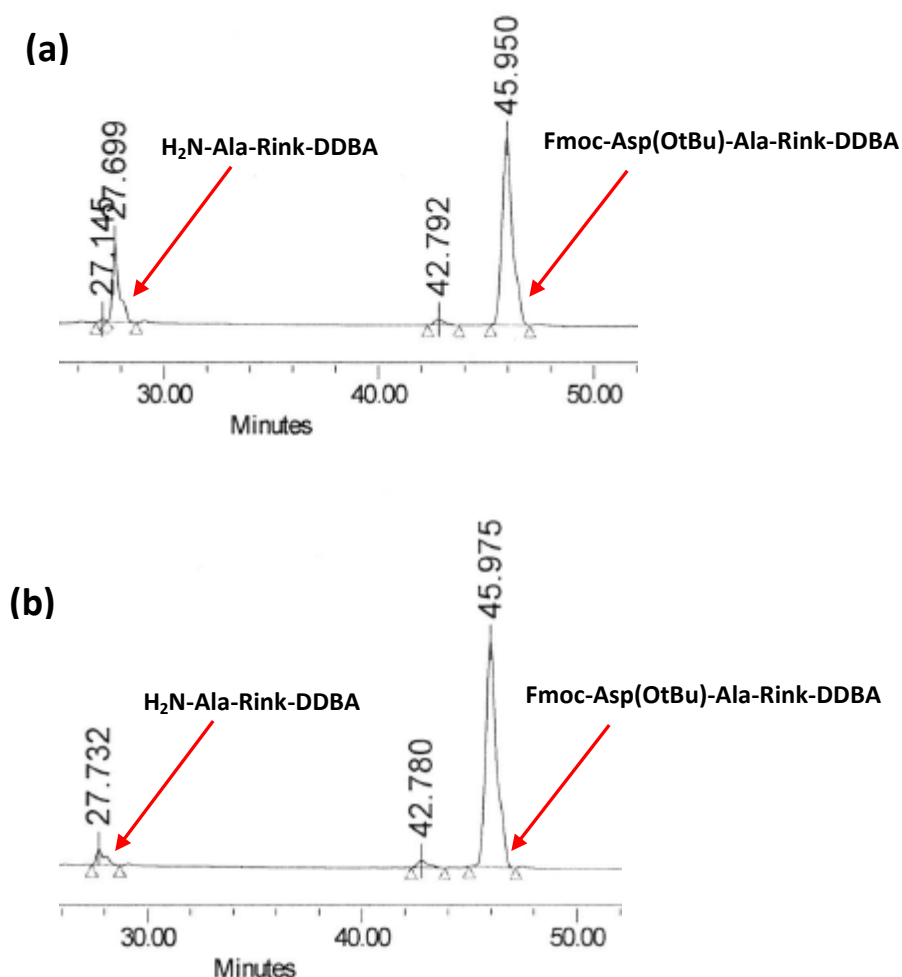
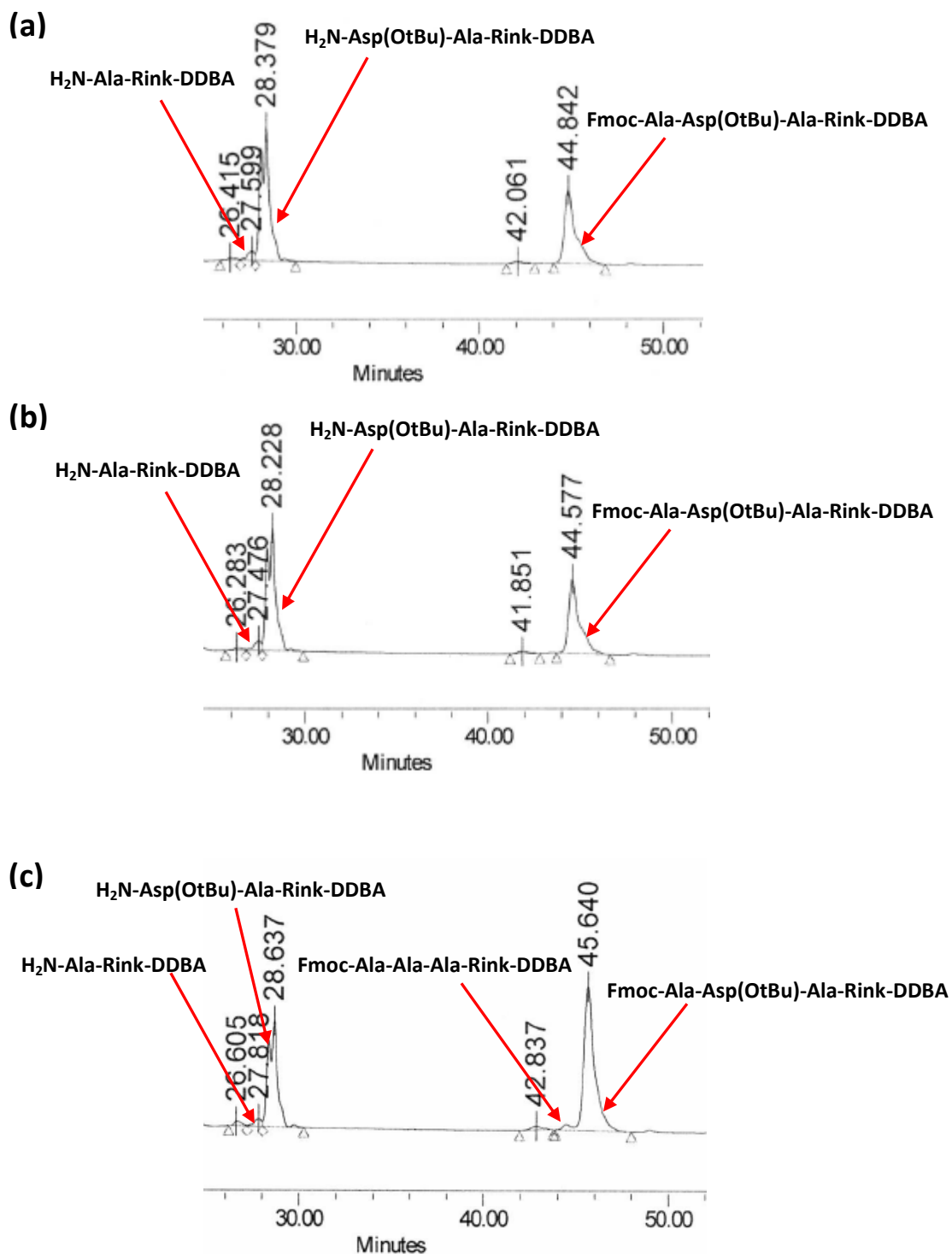


Figure 3.24. Second coupling with Fmoc-Asp(OtBu)-OH: (a) 3 hours of coupling; (b) 3 hours after the addition of second portion of Fmoc-Asp(OtBu)-OH and HBTU.

The following coupling with Fmoc-Ala-OH only had a relative yield (HPLC) of 39.4 % and the addition of second portion of Fmoc-Ala-OH (0.21 eq), HBTU (0.21 eq)/DMF and DIEA could not improve the relative yield. The improvement of relative yield was only possible with the additions of more Fmoc-Ala-OH (0.20 eq), HBTU (0.20 eq)/DMF and DIEA after diafiltrations (Figure 3.25 (c) to (f)), leading to a final relative yield of 87.3 %.



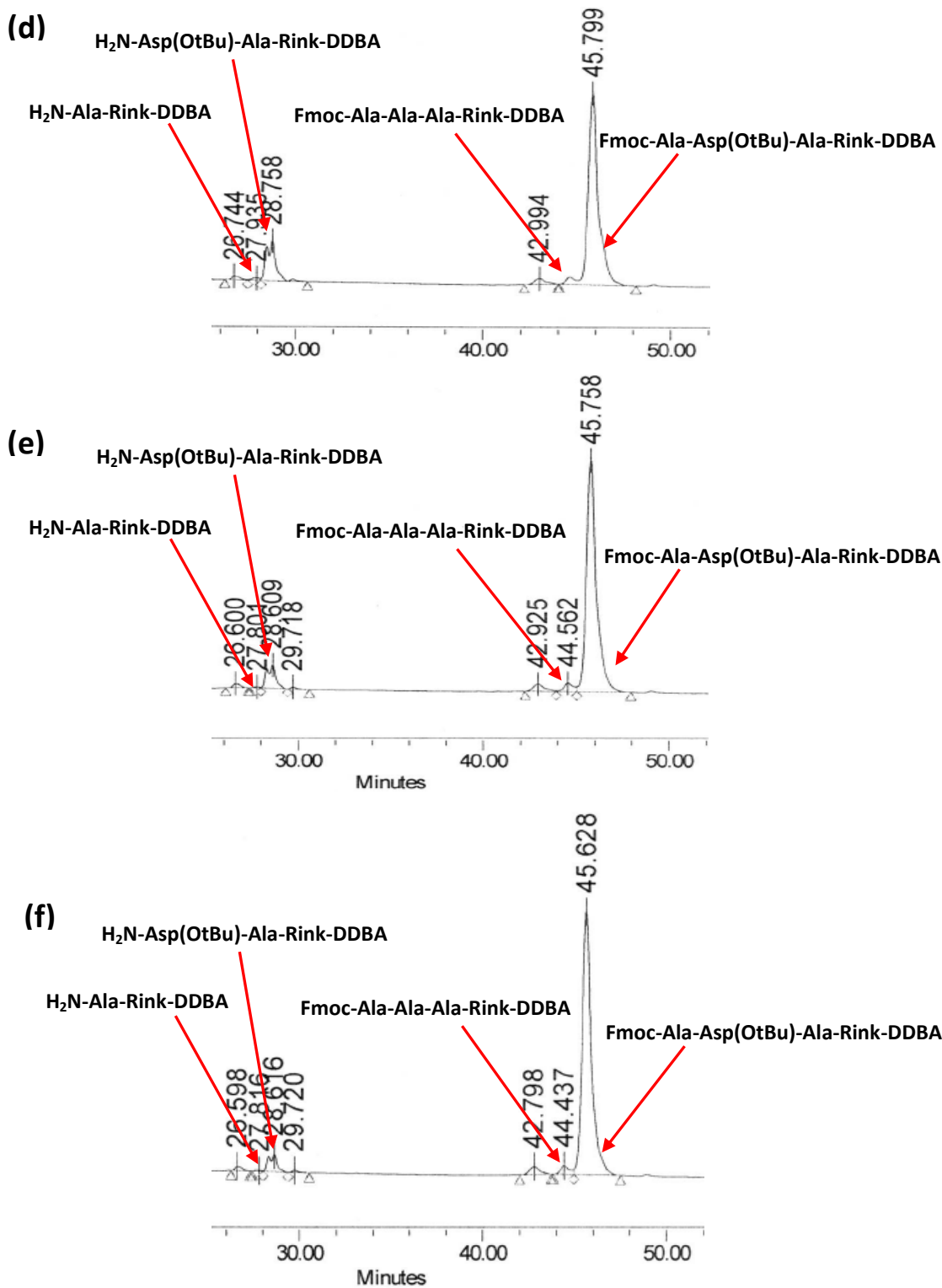


Figure 3.25. Third coupling with Fmoc-Ala-OH: (a) 3 hours of coupling; (b) 2 hours after the addition of second portion of Fmoc-Ala-OH/HBTU/DIEA; (c) 3 hours after the first diafiltration (5 wash volumes) and addition of third portion of Fmoc-Ala-OH/HBTU/DIEA; (d) 30 minutes after the second diafiltration (10 wash volumes) and addition of fourth portion of Fmoc-Ala-OH/HBTU/DIEA; (e) 30 minutes after the addition of fifth portion of Fmoc-Ala-OH/HBTU/DIEA; (f) 30 minutes after the addition of sixth portion of Fmoc-Ala-OH/HBTU/DIEA.

The last coupling had a relative yield of 75.5 % (Figure 3.26 (a)) and the addition of a second portion of Fmoc-Arg(Pbf)-OH (0.11 eq), HBTU (0.11 eq)/DMF and DIEA could not improve the relative yield (Figure 3.26 (b) and (c)). On the other hand, the de-Fmoc and diafiltrations were performed similar to the first attempt, and all de-Fmoc went to completion in one hour. Observations of the last two couplings suggested that more wash volumes were needed after each de-Fmoc for the next coupling to have high yields. This hypothesis was tested in the third attempt.

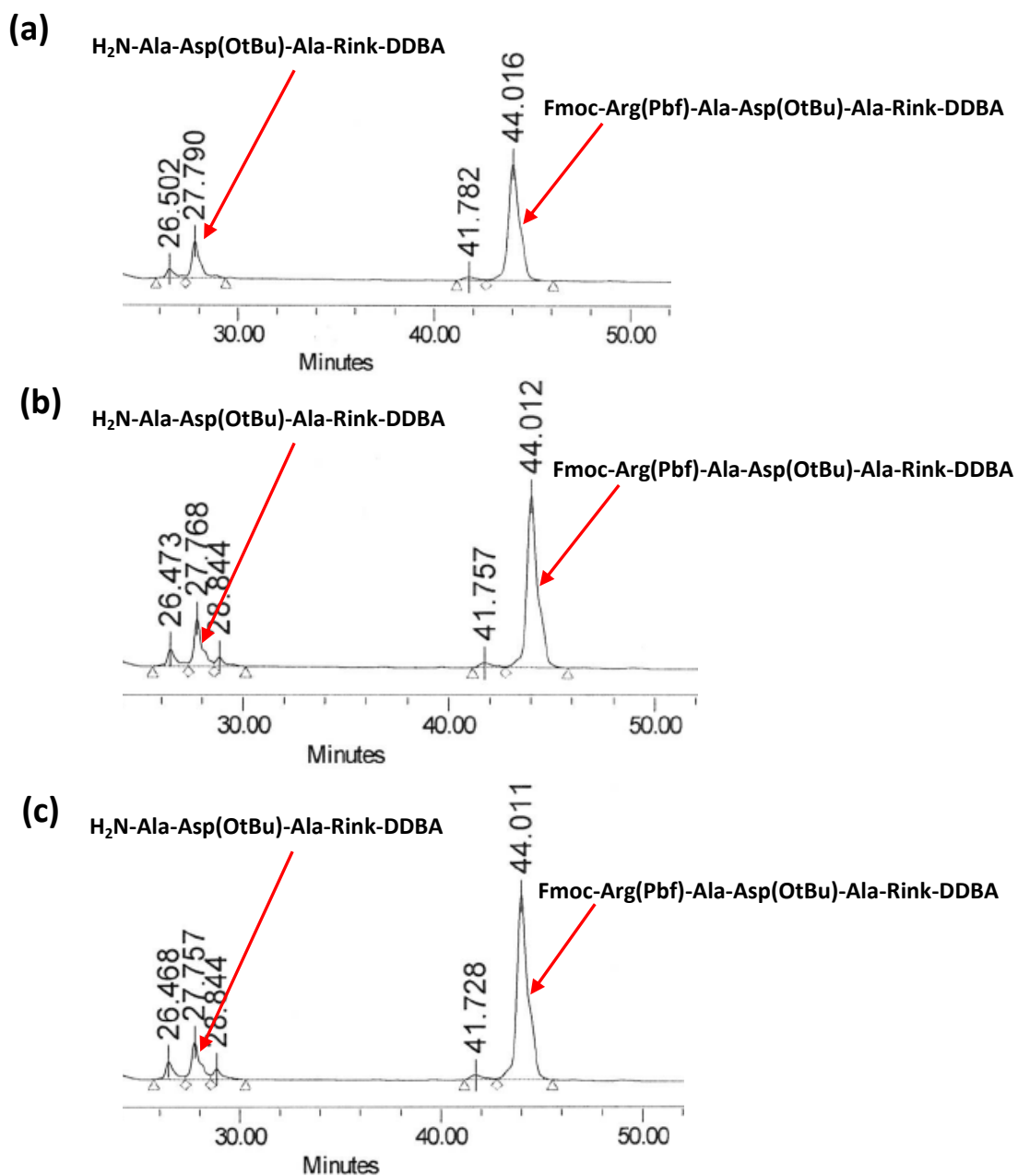


Figure 3.26. Fourth coupling with Fmoc-Arg(Pbf)-OH: (a) 1 hour of coupling; (b) 1 hour after the addition of second portion of Fmoc-Arg(Pbf)-OH/HBTU/DIEA; (c) 30 minutes after the addition of third portion of Fmoc-Arg(Pbf)-OH/HBTU/DIEA.

3.3.8.2.3. MEPS (Third Attempt)

In the third attempt, the coupling of the first Fmoc-Ala-OH went to completion in 30 minutes (relative yield (HPLC): 96.1 % as compared to that of H₂N-Rink-DDBA (0.6 %)), followed by diafiltration (3 wash volumes) and de-Fmoc with 5.0 weight % piperidine in THF, which was complete in 1 hour (relative yield (HPLC): 98.9 %). Diafiltration with 5 wash volumes was then performed.

The coupling with Fmoc-Asp(OtBu)-OH was incomplete after 30 minutes (relative yield (HPLC): 89.8 % as compared to that of H₂N-Ala-Rink-DDBA (5.5 %)) (Figure 3.27 (a)). Diafiltration with 2 wash volumes was carried out and additional Fmoc-Asp(OtBu)-OH (0.10 eq), HBTU (0.11 eq), HOBT (0.06 eq) and DIEA were added into the solution. Significant improvement was made in 30 minutes as the relative yield increased to 93.5 % (HPLC) as compared to that of H₂N-Ala-Rink-DDBA (1.7 %) (Figure 3.27 (b)). Diafiltration and the de-Fmoc of Fmoc-Asp(OtBu)-Ala-Rink-DDBA was performed under the similar conditions as the previous one and was complete in one hour (relative yield (HPLC): 99.1 %). Diafiltration with 10 wash volumes was then performed.

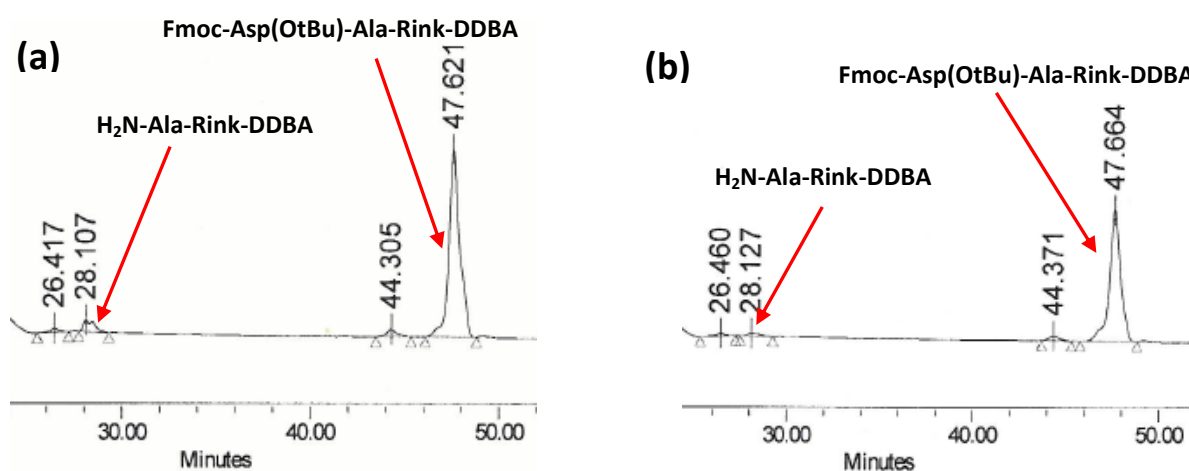


Figure 3.27. Second coupling with Fmoc-Asp(OtBu)-OH: (a) 30 minutes of coupling; (b) 30 minutes after the diafiltration and addition of second portion of Fmoc-Asp(OtBu)-OH and HBTU.

Although the wash volumes after de-Fmoc were doubled, the next coupling with Fmoc-Ala-OH was still incomplete and even had a significantly lower yield than the previous couplings (relative yield (HPLC): 76.8 % as compared to that of H₂N-Asp(OtBu)-Ala-Rink-DDBA (19.0 %)) (Figure 3.28 (a)). Diafiltration was performed with 2 wash volumes and additional amino acid and coupling reagents were added as in the previous coupling. As a result, the relative yield increased marginally to 83.4 % as compared to that of H₂N-Asp(OtBu)-Ala-Rink-DDBA (12.3 %) (Figure 3.28 (b)). Diafiltration and addition of reagents were repeated once and the relative yield increased further to 93.1 % compared to that of the deprotected peptide (1.9 %) (Figure 3.28 (c)). Diafiltration and de-Fmoc of the anchored peptide was performed as in the previous step.

Experimental results of the third coupling showed that increasing the wash volumes from 5 to 10 after de-Fmoc was still insufficient to remove the residual piperidine, leading to the accumulation of piperidine in the system and a lower initial coupling yield (76.8 % as compared to 89.9 % and 96.1 % in the previous couplings). Therefore, the diafiltration after de-Fmoc of Fmoc-Ala-Asp(OtBu)-Ala-Rink-DDBA was performed with 14 wash volumes.

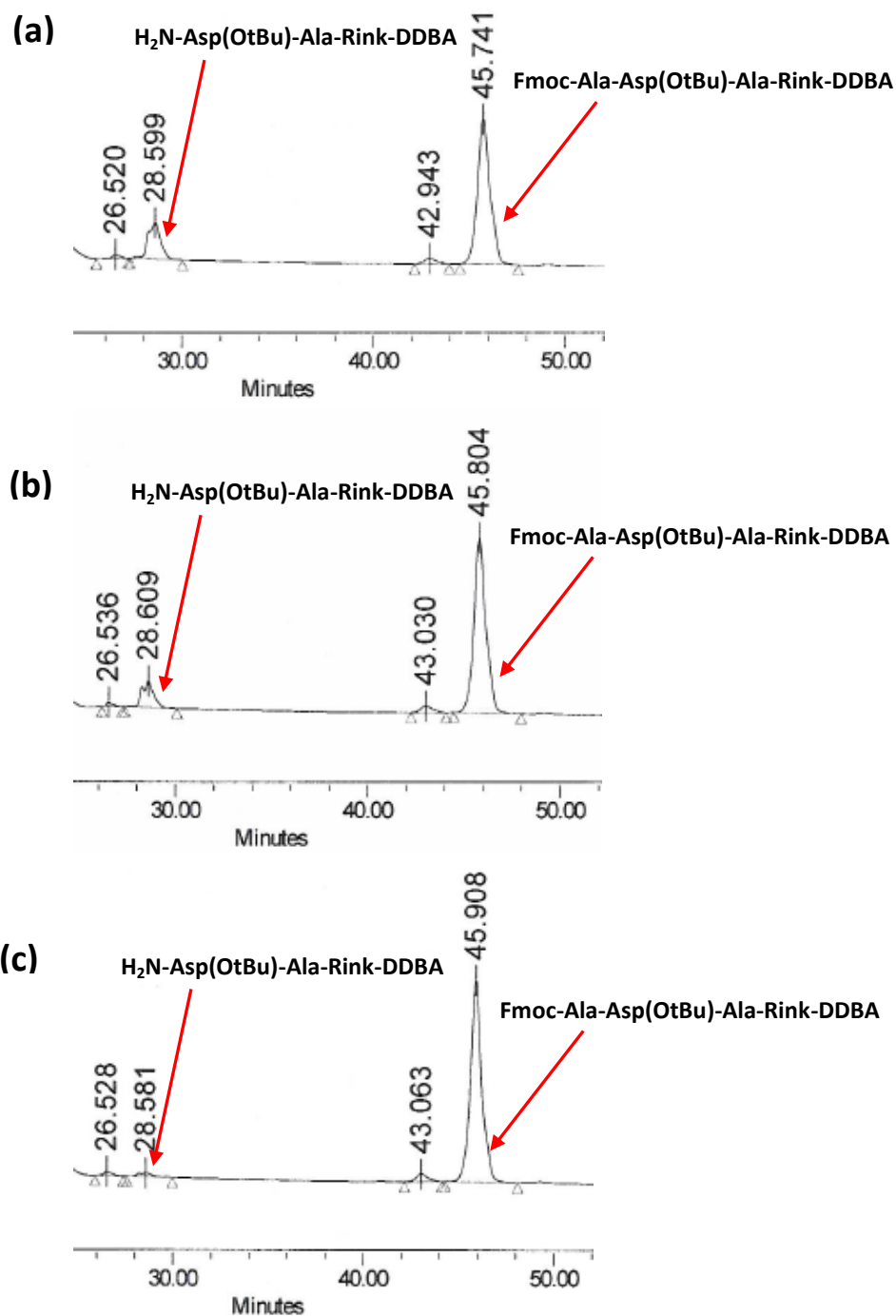


Figure 3.28. Third coupling with Fmoc-Ala-OH: (a) 30 minutes of coupling; (b) 30 minutes after the first diafiltration (2 wash volumes) and addition of second portion of Fmoc-Ala-OH/HBTU/DIEA; (c) 30 minutes after the second diafiltration (2 wash volumes) and addition of third portion of Fmoc-Ala-OH/HBTU/DIEA.

The increased wash volumes were indeed effective in removing the residual piperidine, as the last coupling with Fmoc-Arg(Pbf)-OH went to completion in 30 minutes (relative yield (HPLC): 95.9 % as compared to the deprotected anchored peptide (0.3 %)) (Figure 3.29) and then diafiltration with 4 wash volumes was performed to remove excess reagents and by-products. The OSN system was drained and washed with THF (500 mL) 3 times. The combined solution was evaporated to 100 mL and then added into acetonitrile (400 mL) for the precipitation of product. White precipitate was obtained and washed with acetonitrile (100 mL) 5 times. The precipitate was dried in a vacuum oven (8.16 g obtained). Before cleavage and global deprotection, purity (HPLC) was 93.8 % and overall yield was 76.5 %. The identity of the final product (i.e. Fmoc-Arg(Pbf)-Ala-Asp(OtBu)-Ala-Rink-DDBA) was confirmed by LC/MS (Figure 3.30).

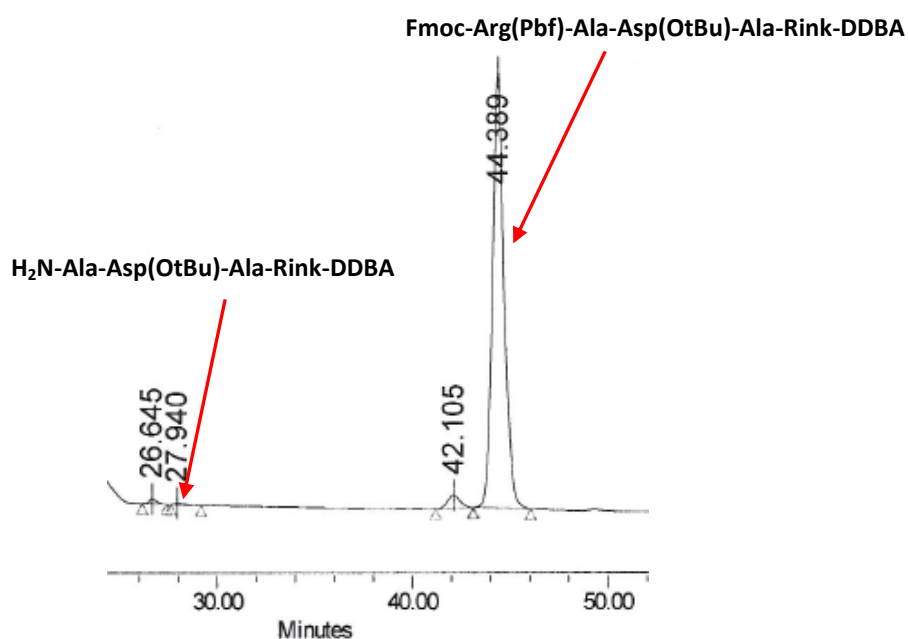


Figure 3.29. Fourth coupling with Fmoc-Arg(Pbf)-OH (30 minutes of reaction).

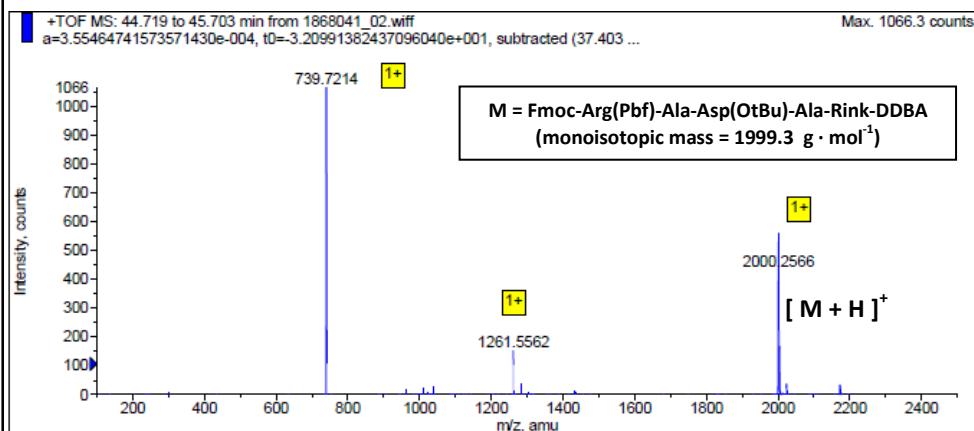
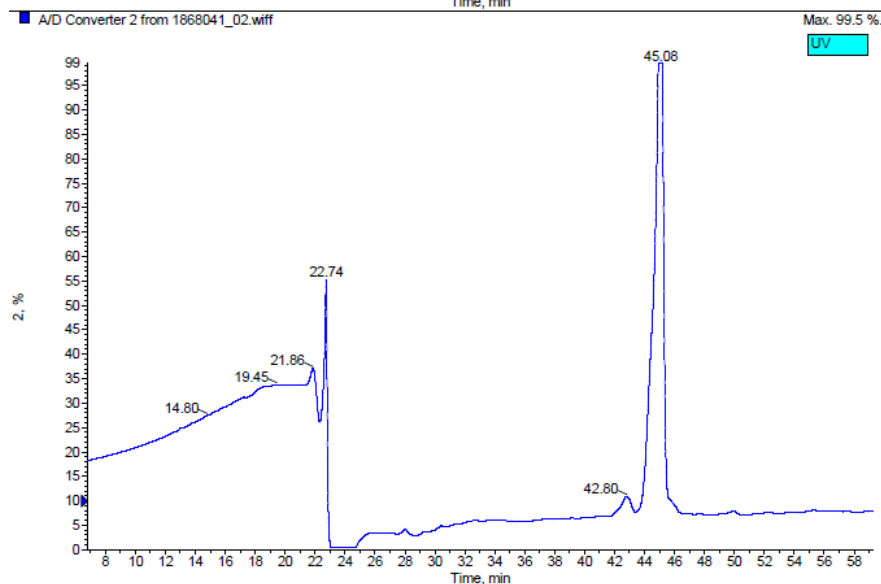
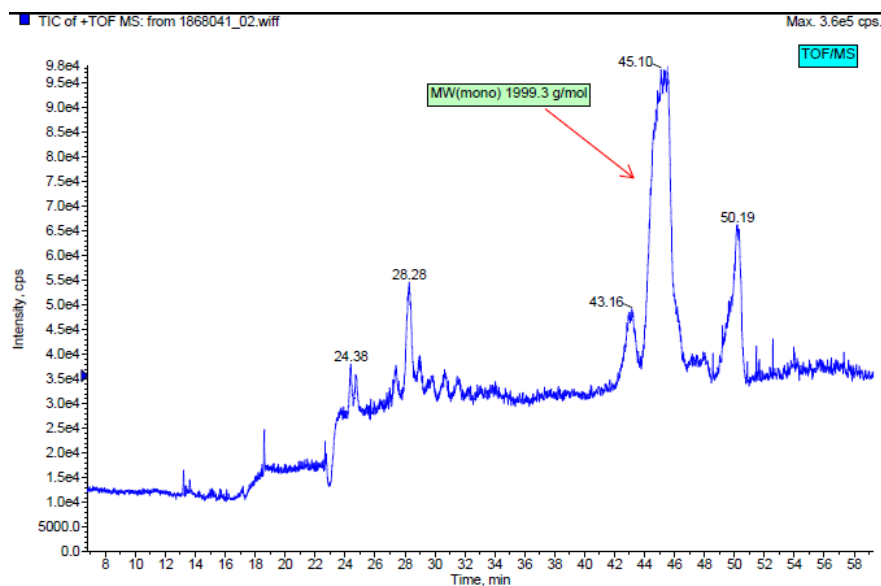


Figure 3.30. LC/MS result for dried Fmoc-Arg(Pbf)-Aal-Asp(OtBu)-Ala-Rink-DDBA (3^d attempt) (HPLC method: Fmoc-RADA-DDBA_HPLC1).

The cleavage and global deprotection of anchored peptide was performed with the same cleavage cocktail as for SPPS study, but the Rink linker unexpectedly decomposed and one fragment remained attached to the peptide (Figure 3.31). As a result, the purity of the final peptide decreased to 53.5 % (HPLC) and the major impurity was Fmoc-Arg-Ala-Asp-Ala-Rink fragment (Figure 3.32). Detailed LC/MS result of the globally deprotected product is shown in Figure 3.33.

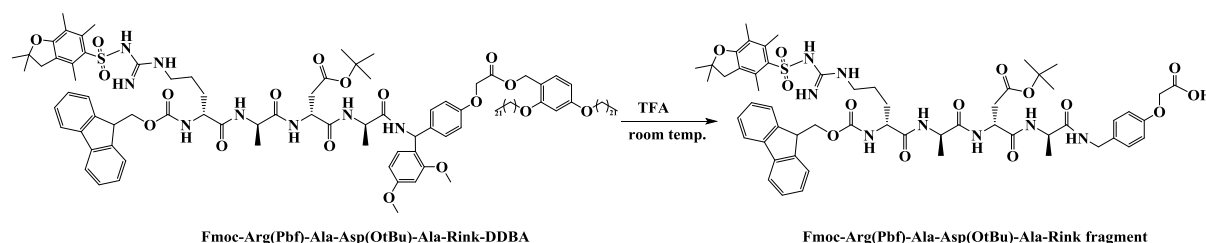


Figure 3.31. Decomposition of Rink linker during global deprotection.

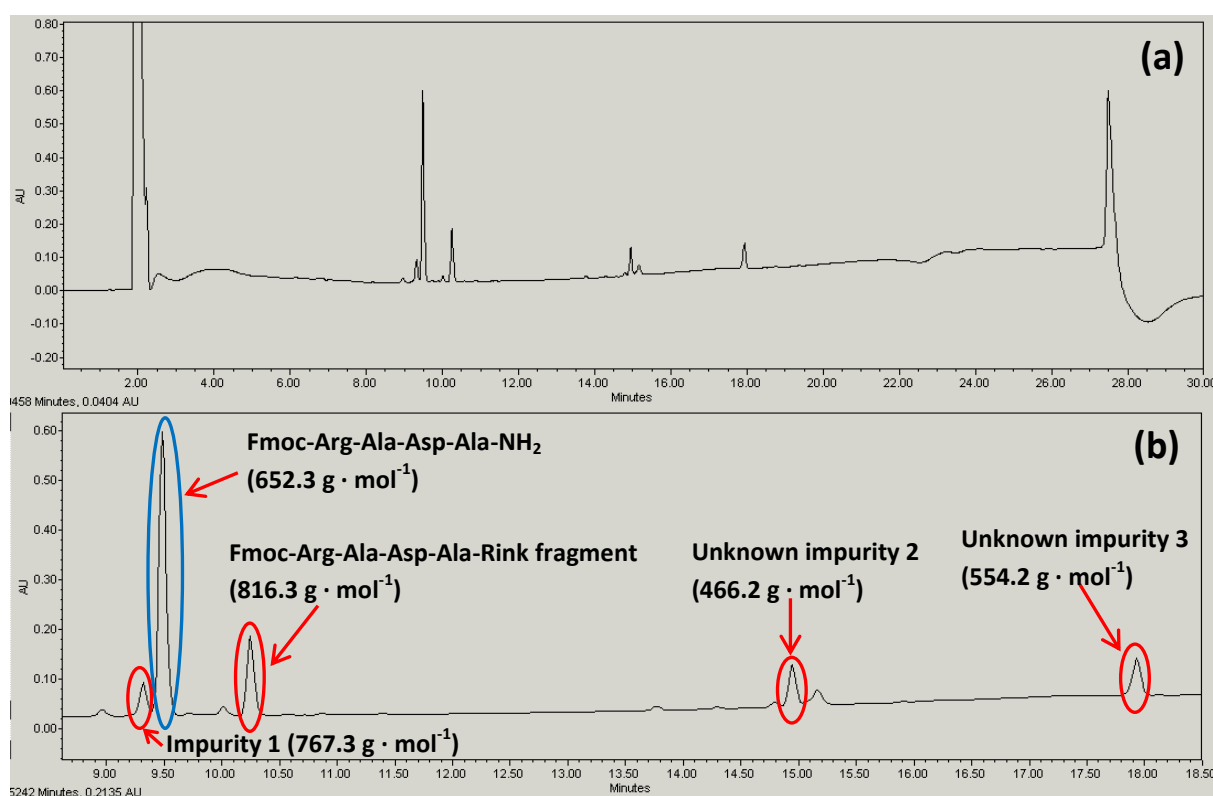


Figure 3.32. HPLC of product after cleavage and global deprotection (peak identities based on TOF/MS result). (b) is the zoom-in image of (a). (Monoisotopic mass of component displayed)

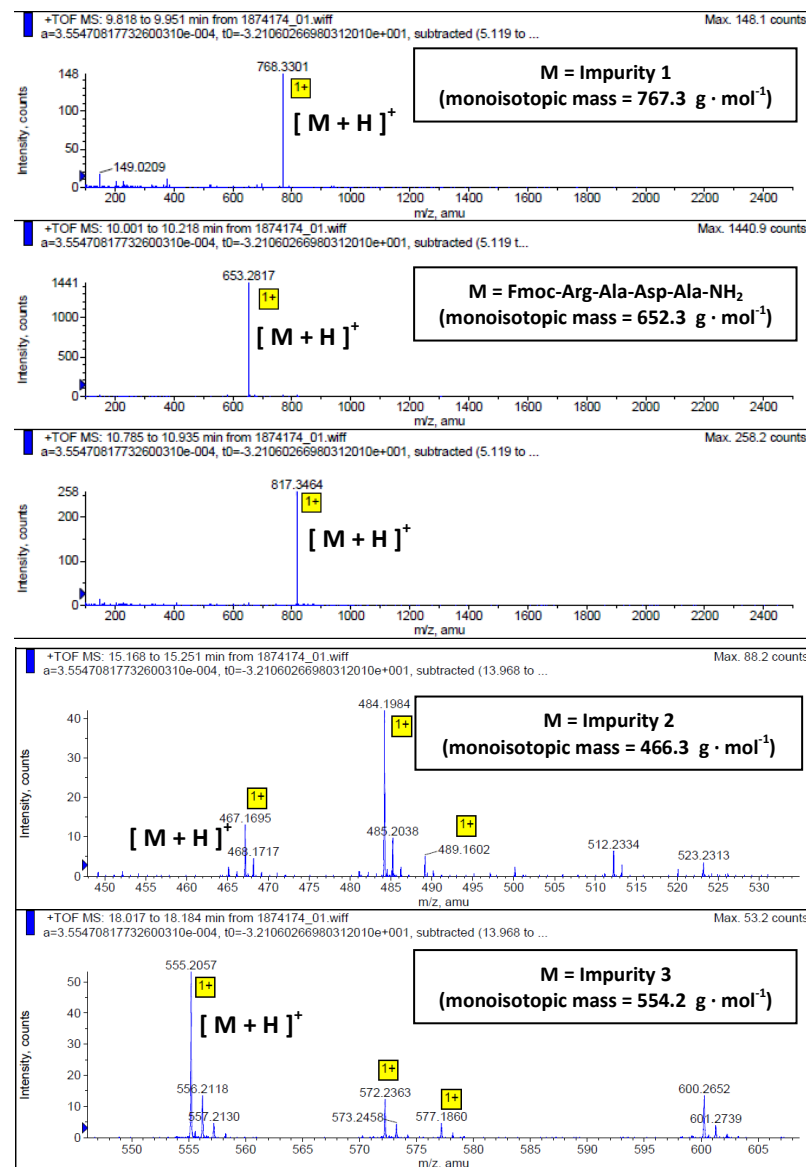
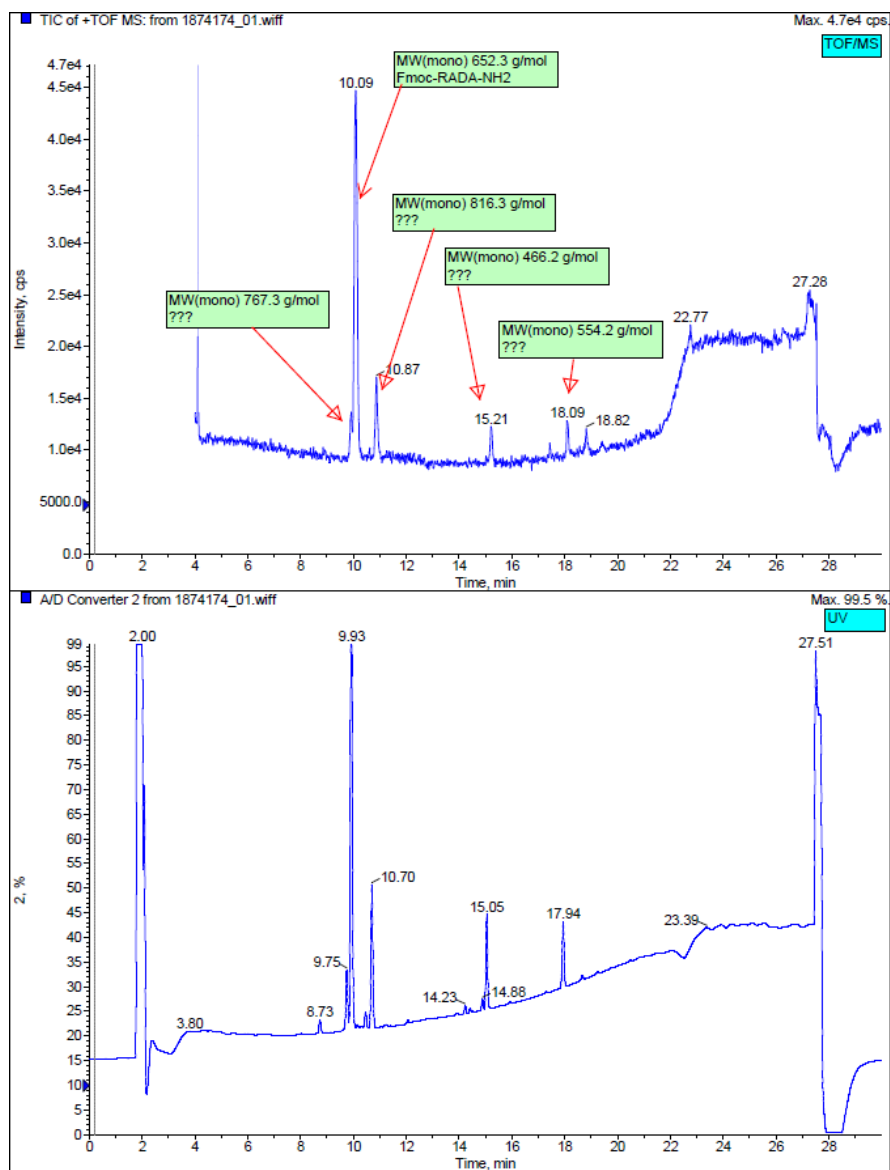


Figure 3.33. LC/MS result for globally deprotected product (3rd attempt) (HPLC method: Fmoc-RADA_HPLC1).

3.3.8.2.4. MEPS (Fourth Attempt)

With the lessons learned from the previous attempts, the last experiment served to demonstrate the technical viability of MEPS. The experimental data were summarised in Table 3.17 to 3.19. In short, all the de-Fmoc went to completion in 1 hour with 5.0 weight % piperidine/THF solution and all couplings were complete in 30 minutes with 1.05 eq of amino acids and coupling reagents (Figure 3.34). Diafiltration with 14 wash volumes was performed after each de-Fmoc and this amount of washing seemed sufficient as the couplings proceeded smoothly. A total of 55 wash volumes (27.5 L) were used for the diafiltrations. Decent overall yield and high purity (HPLC) before cleavage and global deprotection were achieved (78.6 % and 98.5 % respectively). The identity of the final product (i.e. Fmoc-Arg(Pbf)-Ala-Asp(OtBu)-Ala-Rink-DDBA) was confirmed by LC/MS (Figure 3.35).

Table 3.17. Summary of results for the fourth attempt at MEPS.

| | | Note |
|---|------------------|--|
| Anchor | DDBA | |
| Linker | Rink | |
| Scale (mmol) | 10.01 | |
| Solvent | THF | |
| Temperature (°C) | 20 | |
| Membrane | Inopor 450 | (TiO ₂ , 19-Channel, d ₅₀ = 0.9 nm, l = 250 mm, d _a = 25 mm, d _c = 3.5 mm) |
| OSN System | Natan OSN System | Minimum Working Volume: 500 mL |
| Coupling Reagents | HBTU/HOBt/DIEA | 1.05 eq for HBTU and HOBt |
| System Volume (mL) | 500 | |
| Starting Concentration (weight% anchor in THF) | 2.4 | 500 mL THF |
| Overall Yield (%) | 78.6 | Before Cleavage and Global Deprotection |
| Purity (HPLC) (%) | 98.5 | |
| Overall Yield (%) | 51.4 | After Cleavage and Global Deprotection |
| Purity (HPLC) (%) | 58.4 | |

Table 3.18. Experimental data of the de-Fmoc.

| Reaction | Concentration | | Reaction Time (h) | Relative Yield (%)* |
|---|-----------------------|----------|-------------------|---------------------|
| | Piperidine (weight %) | HOBt (M) | | |
| De-Fmoc of Fmoc-Ala-Rink-DDBA | 5.0 | 0.1 | 1.0 | 99.1 |
| De-Fmoc of Fmoc-Asp(OtBu)-Ala-Rink-DDBA | 5.0 | 0.1 | 1.0 | 99.2 |
| De-Fmoc of Fmoc-Ala-Asp(OtBu)-Ala-Rink-DDBA | 5.0 | 0.1 | 1.0 | 100.0 |

*Note: relative yield calculated from the integrated peak areas of the product and starting material.

Table 3.19. Experimental data of the couplings.

| Reaction | Amino Acid (eq) | HBTU (eq) | HOBt (eq) | pH after Addition of DIEA** | Reaction Time (h) | Relative Yield (%)* |
|-------------------------------|-----------------|-----------|-----------|-----------------------------|-------------------|-------------------------|
| Loading of Fmoc-Ala-OH | 1.05 | 1.05 | 1.05 | 9 – 10 | 0.5 | 97.0 (impurity: 3.0) |
| Coupling of Fmoc-Asp(OtBu)-OH | 1.05 | 1.05 | 1.05 | 9 – 10 | 0.5 | 97.0 (impurity: 3.0) |
| Coupling of Fmoc-Ala-OH | 1.05 | 1.06 | 1.06 | 9 – 10 | 0.5 | 96.9 (impurity: 3.1) |
| Coupling of Fmoc-Arg(Pbf)-OH | 1.05 | 1.06 | 1.06 | 9 – 10 | 0.5 | 97.3 (impurity: 2.7) |

*Note: relative yield calculated from the integrated peak areas of the product and starting material.

**Measured by pH-indicator strips.

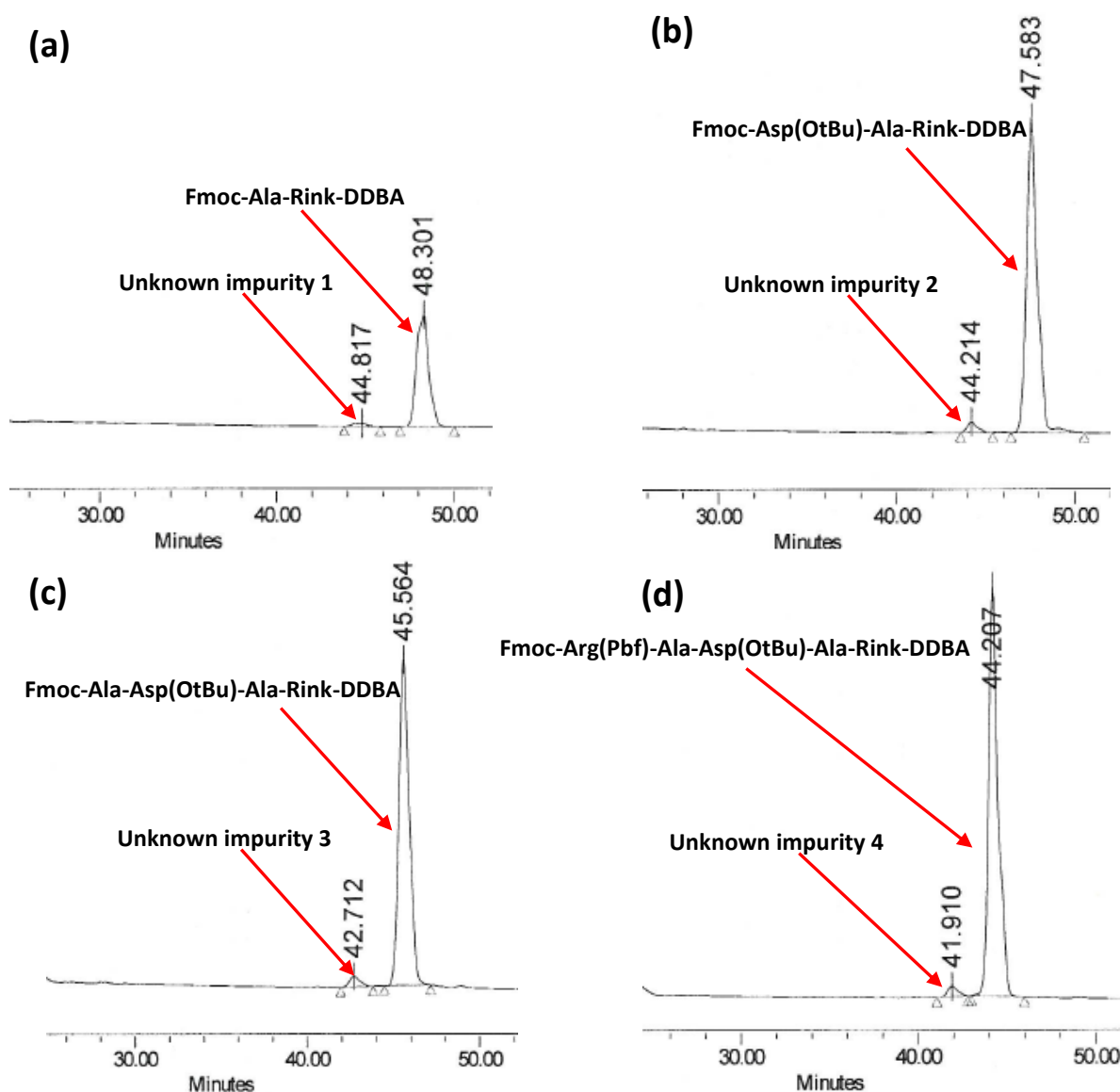


Figure 3.34. Coupling of amino acids (30 minutes of reaction): (a) First coupling with Fmoc-Ala-OH; (b) second coupling with Fmoc-Asp(OtBu)-OH; (c) Third coupling with Fmoc-Ala-OH; (d) Fourth coupling with Fmoc-Arg(Pbf)-OH.

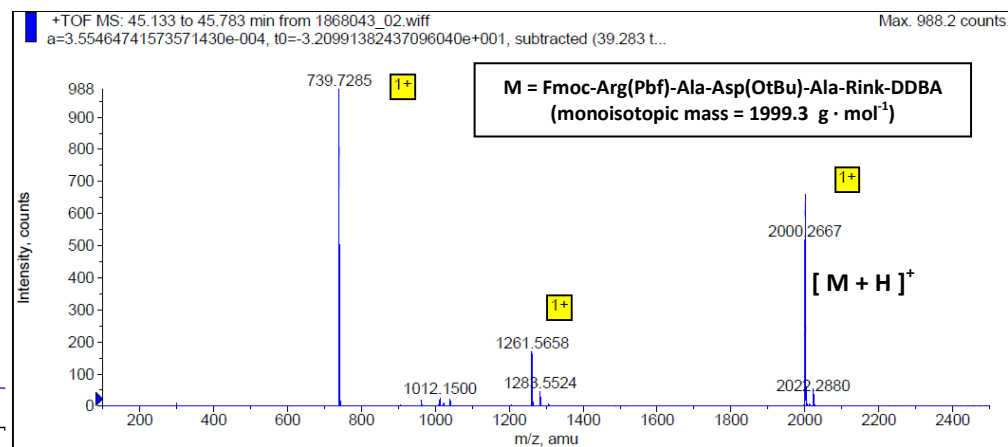
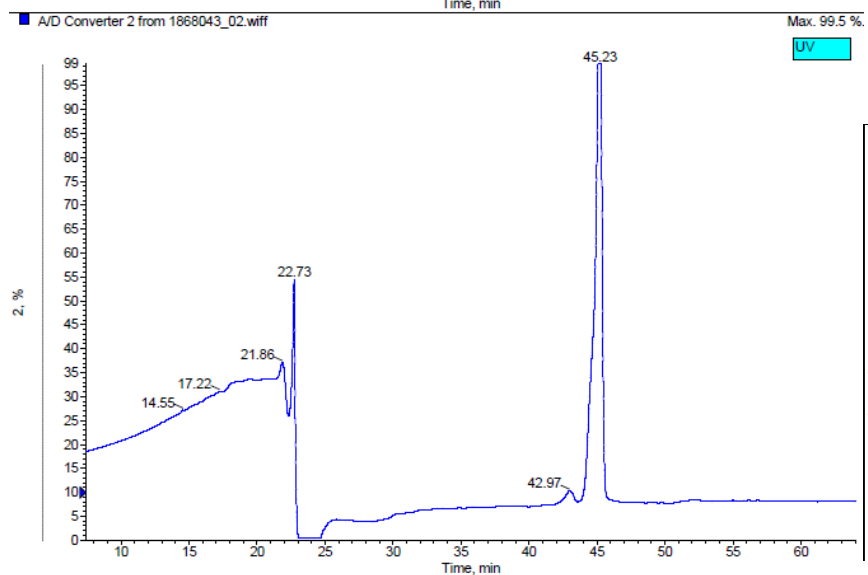
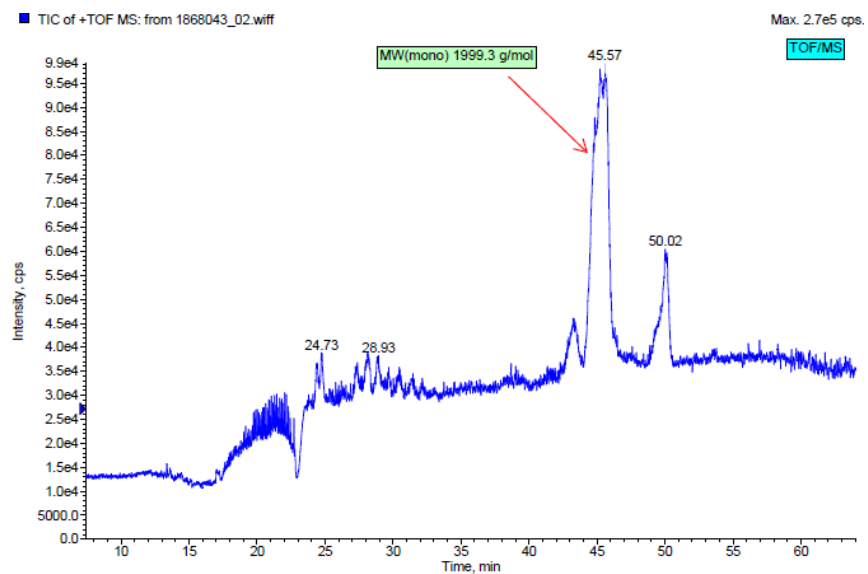


Figure 3.35. LC/MS result for dried Fmoc-Arg(Pbf)-Aal-Asp(OtBu)-Ala-Rink-DBA (4th attempt) (HPLC method: Fmoc-RADA-DBA_HPLC1).

To avoid the decomposition of Rink linker during global deprotection, Fmoc-Arg(Pbf)-Ala-Asp(OtBu)-Ala-Rink was first cleaved from the anchor (DDBA) in mild TFA/DCM solution. Dried Fmoc-Arg(Pbf)-Ala-Asp(OtBu)-Ala-Rink-DDBA (16.40 g) was added into TFA/DCM (1 vol % TFA in DCM, 200 mL) and the mixture was stirred at room temperature for 1 hour. The solid initially dissolved in the TFA solution to form a yellow liquid and then new solid started to appear and the mixture gradually turned purple. The reaction was complete in 1 hour (HPLC method: Fmoc-RADA-DDBA_HPLC1), after which acetonitrile (500 mL) was added into the mixture and the mixture was filtered. The filtered particles were washed with TFA/DCM (1 vol % TFA in DCM, 100 mL) 6 times and the filtrate was collected and evaporated to dryness in vacuum.

Small-scale tests of global deprotection were carried out for Fmoc-Arg(Pbf)-Ala-Asp(OtBu)-Ala-Rink. Experimental results showed that adding Fmoc-Arg(Pbf)-Ala-Asp(OtBu)-Ala-Rink directly into the TFA solution (TFA/TIS/Anisole, 85/10/5, v/v/v) resulted in a higher extent of Rink decomposition than reacting the compound with TFA for 1 hour before adding the scavengers (the relative yields of fully Fmoc-Arg-Ala-Asp-Ala-Rink fragment were 16.7 % and 2.7 % respectively).

Following the small-scale tests, the dried Fmoc-Arg(Pbf)-Ala-Asp(OtBu)-Ala-Rink was added into TFA (250 mL) and the mixture was stirred at room temperature for 1 hour. The mixture turned dark purple and the reaction was complete in 1 hour (HPLC method: Fmoc-RADA_HPLC1). TIS/Anisole (125 mL/65 mL) was then added into the mixture and the mixture was stirred at room temperature for another hour. The mixture turned grey and the reaction was complete in 1 hour (HPLC method: Fmoc-RADA_HPLC1). The mixture was added into cool diisopropylether (1 L) and then filtered. The filtered product was dried and then washed with diisopropylether (100 mL) 6 times. The product was dried under nitrogen over 2 days (6.75 g obtained, Figure 3.36). Purity (Fmoc-Arg-Ala-Asp-Ala-NH₂, HPLC method: Fmoc-RADA_HPLC1): 58.4 % (Fmoc-Arg-Ala-Asp-Ala-Rink fragment: relative yield = 1.8 %; Fmoc-Arg(Pbf)-Ala-Asp(OtBu)-Ala-Rink: relative yield = 0.0 %; other impurities (unknown):

relative yield = 39.8 %), overall yield: 51.4 %. Detailed LC/MS result of the globally deprotected product is shown in Figure 3.37. As compared to the third attempt at MEPS, the relative yield of peptide-Rink fragment was reduced significantly to 1.8 % by the present global deprotection method.

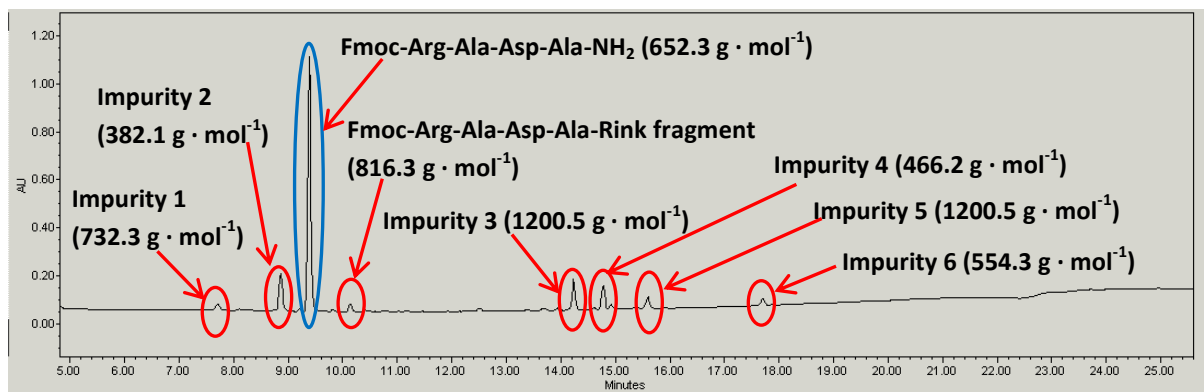
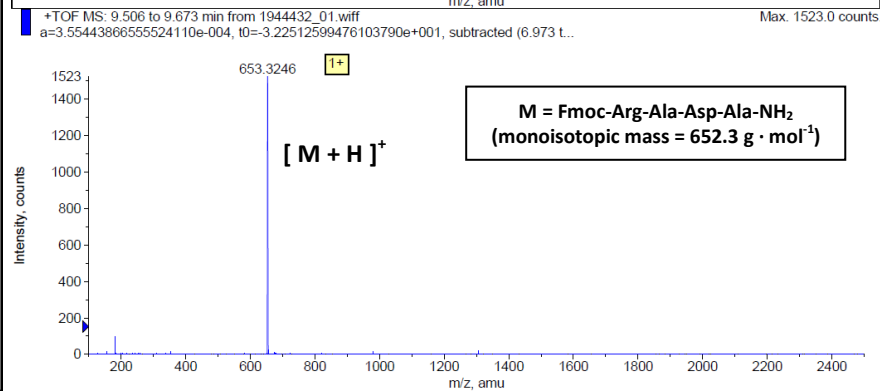
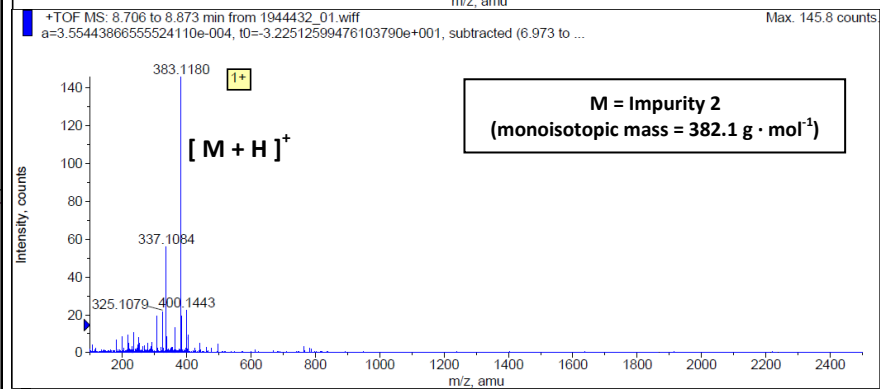
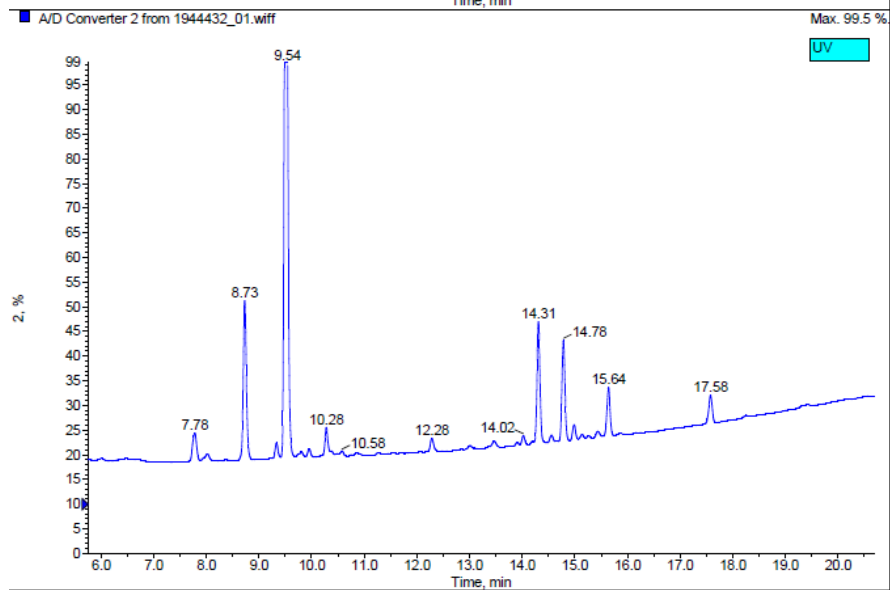
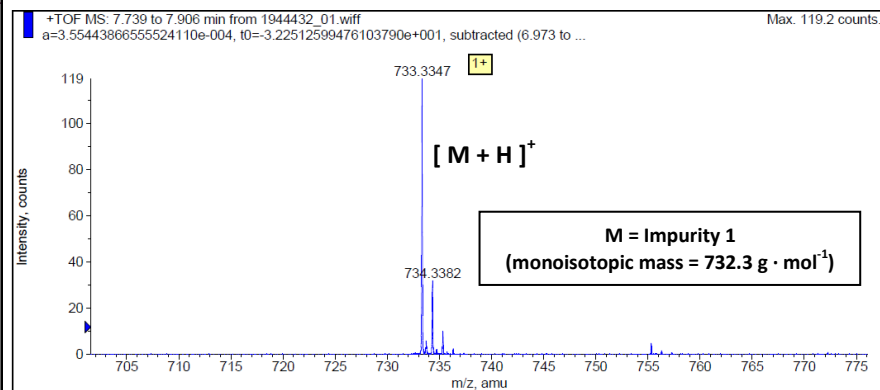
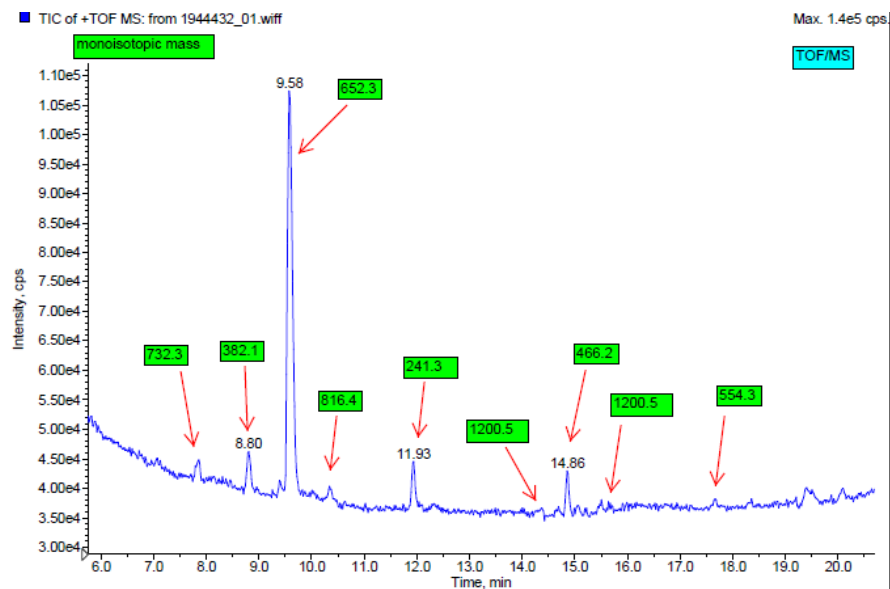


Figure 3.36. HPLC of the products of cleavage and global deprotection (peak identities based on TOF/MS result). (Monoisotopic mass of component displayed)



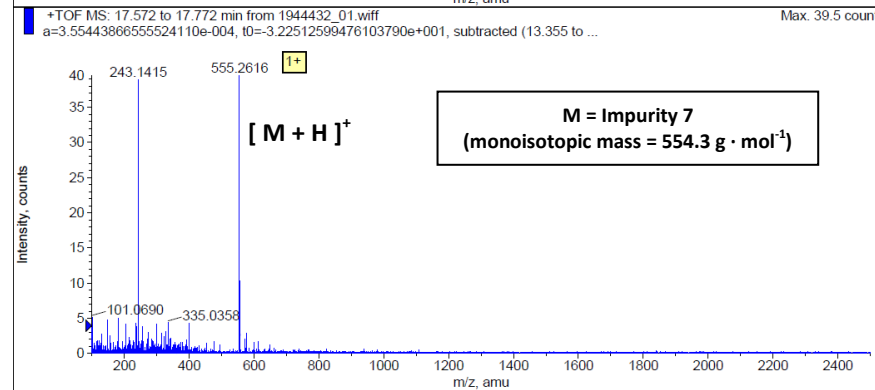
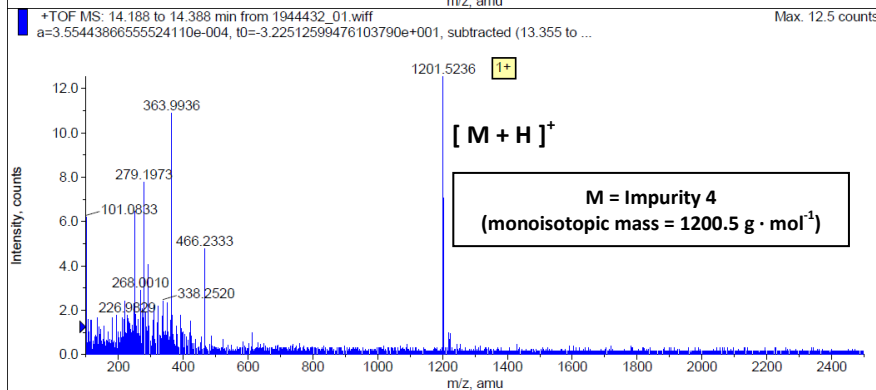
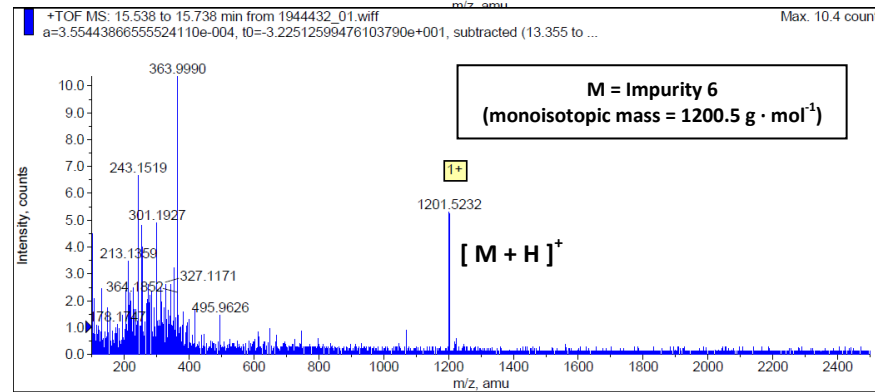
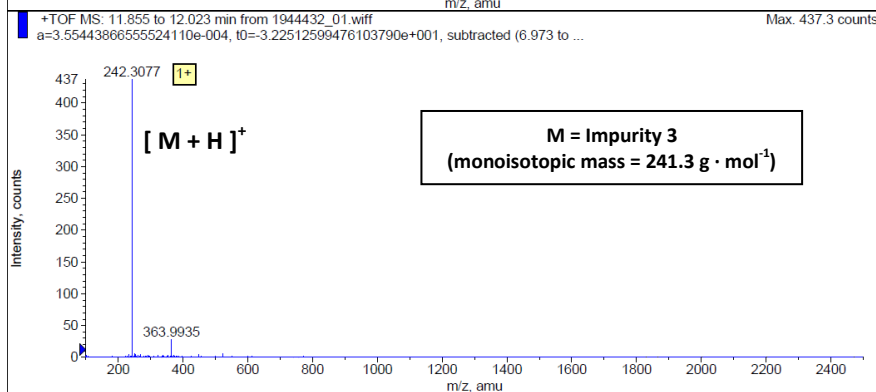
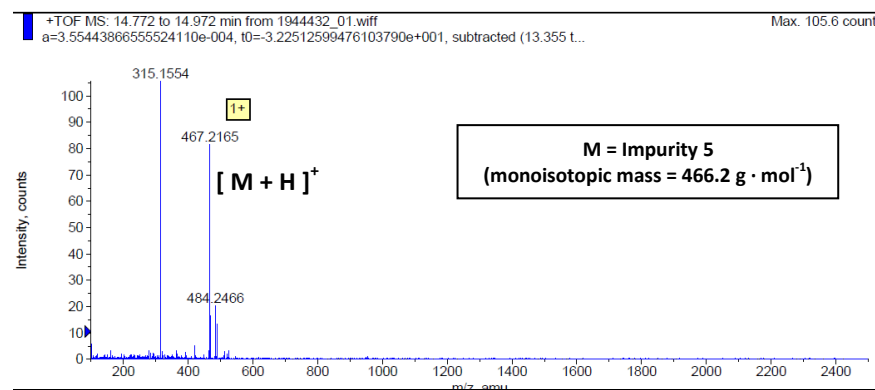
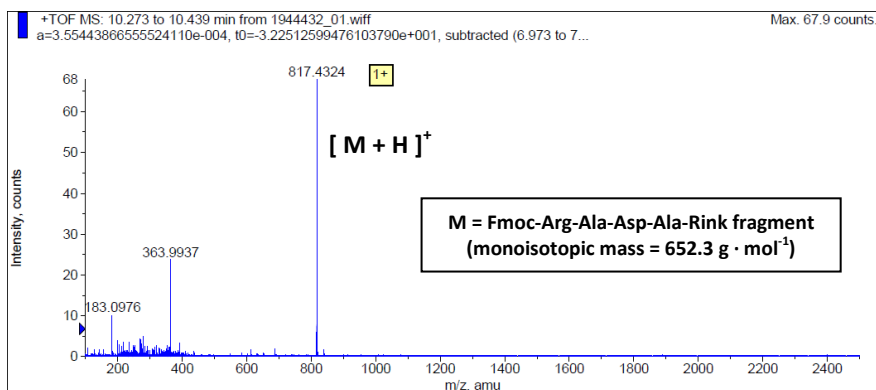


Figure 3.37. LC/MS result for globally deprotected product (4th attempt) (HPLC method: Fmoc-RADA_HPLC1).

3.3.9. Performance of MEPS in Comparison with SPPS

The performance of MEPS (based on results of the fourth attempt) is compared with SPPS in terms of product purity, overall yield, building block utility, material cost, process time, volumetric efficiency and E-factor as summarised in Table 3.20.

The calculation methods of purity and overall yield have been explained previously (Section 3.2.4).

The building block utility measures the percentage of building block that is incorporated into the final product. In peptide synthesis, the building block utility is the quotient of the total quantity of amino acid in the final peptide divided by the total quantity of amino acid used for couplings (Equation 3.5.1). Since the equivalent of amino acid was the same for every coupling in both SPPS and MEPS, the calculation of building block utility can be simplified to the division of overall yield by the equivalent of amino acid in each coupling (Equation 3.5.2).

Building Block Utility

$$= \frac{\textit{Sum of Amino Acids in the Final Peptide}}{\textit{Sum of Amino Acids used in Couplings}} \quad \text{Equation 3.5.1}$$

$$= \frac{\textit{Quantity of Final Peptide} \times n}{\textit{Sum of Amino Acids used in Couplings}}$$

$$= \frac{\textit{Quantity of Final Peptide} \times n}{\textit{Quantity of Amino Acids in each Coupling} \times n}$$

$$= \frac{\textit{Initial Quantity of Anchor} \times \textit{Overall Yield} \times n}{\textit{Initial Quantity of Anchor} \times \textit{Equivalent of Amino Acid in each Coupling} \times n}$$

$$= \frac{\textit{Overall Yield}}{\textit{Equivalent of Amino Acid in each Coupling}} \quad \text{Equation 3.5.2}$$

where n is the number of amino acid.

The material cost is the total cost of chemicals (based on the catalogue prices of anchor, amino acids, coupling reagents, de-Fmoc reagents, cleavage and global deprotection reagents, and solvents) normalised by the quantity of peptide product (Equation 3.6). The catalogue price of each chemical was obtained from its supplier's website.

$$\textit{Material Cost} = \frac{\textit{Sum of Chemical Costs}}{\textit{Quantity of Final Peptide}} \quad \text{Equation 3.6}$$

Similar to the material cost, the process time is the sum of all process time normalised by the quantity of peptide product (Equation 3.7).

$$\textit{Process Time} = \frac{\textit{Sum of Process Time}}{\textit{Quantity of Final Peptide}} \quad \text{Equation 3.7}$$

The volumetric efficiency is calculated by the division of the quantity of final product by the system volume (Equation 3.8).

$$\textit{Volumetric Efficiency} = \frac{\textit{Quantity of Final Peptide}}{\textit{System Volume}} \quad \text{Equation 3.8}$$

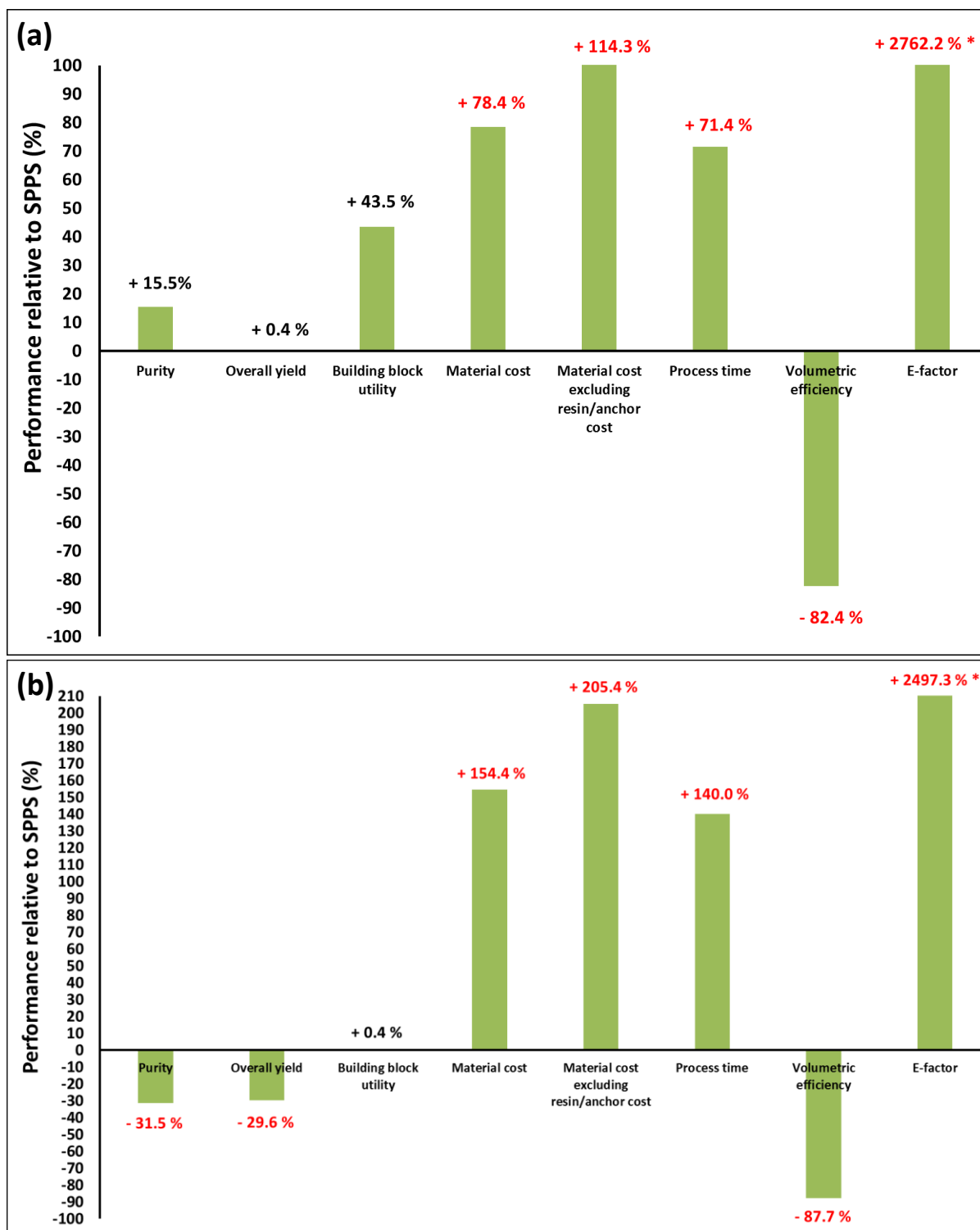
The E-factor (E stands for Environmental) is a commonly used metric for green chemistry. It is calculated by the division of the total mass of waste by the total mass of product (Equation 3.9).

$$\textit{E - factor} = \frac{\textit{Total Mass of Waste}}{\textit{Total Mass of Final Peptide}} \quad \text{Equation 3.9}$$

Table 3.20. Performance of SPPS and MEPS.

| Synthesis method | SPPS | MEPS |
|---|-------|-------|
| Scale (mmol) | 11.42 | 10.01 |
| System volume (mL) | 100 | 500 |
| <u>Before cleavage and global deprotection</u> | | |
| Purity (%) | 85.3* | 98.5 |
| Overall yield (%) | 78.3* | 78.6 |
| Building block utility (%) | 52.2 | 74.9 |
| Material cost (Euro · mmol ⁻¹) | 32.94 | 58.77 |
| Material cost excluding resin/anchor cost (Euro · mmol ⁻¹) | 10.75 | 23.04 |
| Process time (h · mmol ⁻¹) | 1.4 | 2.4 |
| Volumetric efficiency (mmol · L ⁻¹) | 89.4 | 15.7 |
| E-factor | 180 | 5152 |
| <u>After cleavage and global deprotection</u> | | |
| Purity (%) | 85.3 | 58.4 |
| Overall yield (%) | 73.3 | 51.6 |
| Building block utility (%) | 48.9 | 49.1 |
| Material cost (Euro · mmol ⁻¹) | 35.19 | 89.52 |
| Material cost excluding resin/anchor cost. (Euro · mmol ⁻¹) | 11.49 | 35.09 |
| Process time (h · mmol ⁻¹) | 1.5 | 3.6 |
| Volumetric efficiency (mmol · L ⁻¹) | 83.7 | 10.3 |
| E-factor | 329 | 8545 |

*The overall yield and purity before cleavage and global deprotection were not measured directly as the peptide was still bound to the resin and an accurate measurement of the corresponding total mass was difficult at this scale of synthesis. According to the industrial experience of Lonza AG, the yield loss during cleavage and global deprotection was normally less than 5%. The overall yield before cleavage and global deprotection was calculated based on this observation. The purity of peptide was assumed to remain constant before and after cleavage and global deprotection.



* The bar extends beyond the upper limit of the y-axis of the diagram.

Figure 3.38. Performance of MEPS relative to SPPS: (a) before cleavage and global deprotection; (b) after cleavage and global deprotection.

As shown in Figure 3.38, MEPS had a significantly higher purity than SPPS (by 15.5 %) before cleavage and global deprotection, while having a similar overall yield (0.4 % higher). These two

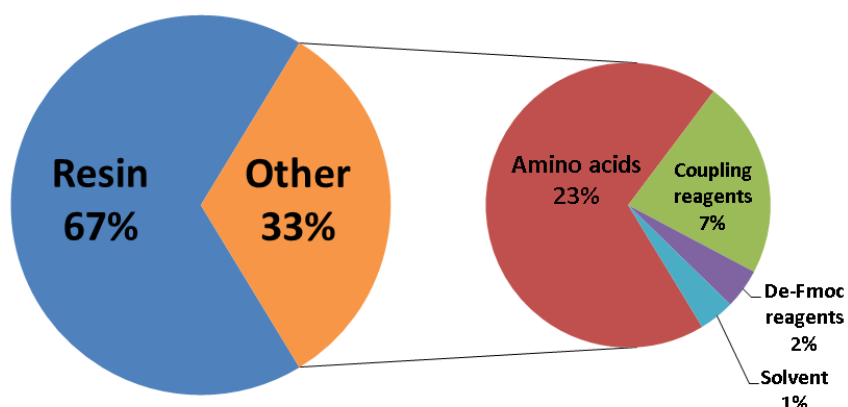
performance metrics decreased significantly after cleavage and global deprotection, putting MEPS at disadvantage as these metrics remained relatively constant for SPPS (MEPS had 31.5 % lower purity and 29.6 % lower overall yield compared to SPPS). The effects of compromised overall yield extended to all the other performance metrics except for E-factor. For example, the material cost of MEPS was 154.4 % higher than SPPS, but it was only 78.4 % higher before cleavage and global deprotection. The E-factor was an exception: the MEPS was 2762.2 % higher than SPPS before cleavage and global deprotection, but was only 2497.3 % higher after these steps. This is due to the large quantity of diisopropylether used for the precipitation of fully deprotected peptide in SPPS (3300 mL for a 100-mL system), which led to a higher E-factor of SPPS after cleavage and global deprotection. This significant drop in the overall yield of MEPS was in agreement with the previous case studies by Dr. So (Section 2.2.13.5) and confirms the fact that the cleavage and global deprotection steps are critical to the overall performance of MEPS. The effect of reducing this loss of overall yield on the performance metrics of MEPS is discussed in greater detail in the following paragraphs of this section.

One surprising observation about MEPS is that most of its performance metrics before cleavage and global deprotection were poor compared to SPPS even before the significant overall yield loss occurred. For example, the material cost and volumetric efficiency were 78.4 % higher and 82.4 % lower than SPPS. The underlying problems were the dilute concentration of anchor in solution and the cost of anchor.

Before cleavage and global deprotection, the material cost of MEPS was higher than that of SPPS due to the higher cost of anchor compared to resin (35.73 Euro · mmol⁻¹ and 22.19 Euro · mmol⁻¹ respectively) and the higher cost of washing solvent (10.81 Euro · mmol⁻¹ compared to 0.43 Euro · mmol⁻¹). Figure 3.39 shows the cost breakdown of the two processes. Surprisingly, the cost of resin/anchor accounted for more than 60% of the total material cost in both cases. For the

remaining 33 % of material cost in SPPS, the biggest component was amino acid (23 %), which was followed by coupling reagents (7 %). In MEPS, washing solvent was the main component (18 %) in the remaining 39 % material cost, while amino acid was only half of that (9 %). If the costs of resin and anchor were excluded, the difference in material cost between MEPS and SPPS was even higher (114.3 % with respect to SPPS) due to the high cost of washing solvent in MEPS, which could be reduced if the concentration of anchor was increased. In the present case study, the starting concentration of anchor was limited to 2.4 weight % (i.e. 10.58 g in 500 mL THF) due to the availability of anchor, but could increase to approximately 10.0 weight %, which is the maximum concentration of the hydrophobic anchor in THF.

SPPS



MEPS

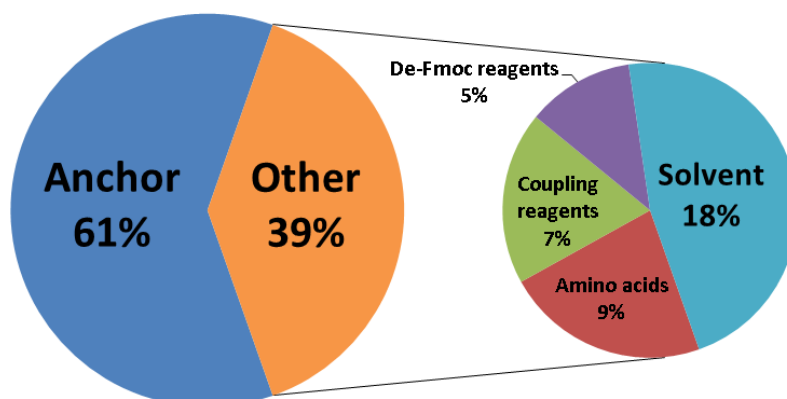


Figure 3.39. Material cost breakdown for SPPS and MEPS.

The dilute concentration of anchor in MEPS also led to longer process time (71.4 % higher than SPPS), lower volumetric efficiency for synthesis (82.4 % lower than SPPS), and a significantly higher E-factor (more than 17 times higher than SPPS), since the quantity of the final peptide product (proportional to the concentration of anchor) was the common denominator in the calculation of these metrics.

Nevertheless, Figure 3.38 shows one clear advantage of MEPS over SPPS in terms of the building block utility (43.5 % and 0.4 % higher before and after cleavage and global deprotection), as only 1.05 eq amino acid was required for the coupling to complete in MEPS whereas SPPS required 1.50 eq. Furthermore, it is common to use 2 - 3 equivalent amino acids for coupling in SPPS, making MEPS even more efficient for incorporating the building blocks into the final product. This high utility of amino acids means MEPS would be more attractive if the cost of amino acids contributes to a significant portion (e.g. ≥ 50 %) of the material cost. In this case study, however, the cost of amino acids only corresponded to 23 % and 9 % of the material cost for SPPS and MEPS respectively (Figure 3.39). These cost structures are expected to change if more expensive amino acids (generally the ones with reactive side-chains that require protection such as Fmoc-Arg(Pbf)-OH) are involved in the synthesis of a longer peptide, and if the cost of anchor can be lowered by finding a suitable substitute or by manufacturing in bulk.

Therefore, the performance of MEPS can be improved by:

1. increasing the concentration of anchor;
2. optimising the cleavage and global deprotection procedure such that the loss of overall yield is minimised or by changing the linker which will result in higher yield and purity of product after cleavage and global deprotection.

As shown in Table 3.21 and Figure 3.40, by increasing the starting concentration of H₂N-Rink-DDBA in THF from 2.4 weight % to 10.0 weight % (Improvement 1 in the table), which is approximately the

maximum concentration possible for this hydrophobic compound, significant improvements can be made for all performance parameters in comparison to the original case of MEPS. In particular, before cleavage and global deprotection, process time and E-factor decrease 75.0 % and 76.2 % respectively, while the volumetric efficiency for synthesis is more than tripled, assuming that the purity and overall yield remain the same as in the actual MEPS. The magnitude of improvement for these parameters remains similar after cleavage and global deprotection. As compared to SPPS, the new case is still disadvantageous in terms of material cost, volumetric efficiency for synthesis and E-factor, but offers significant reductions in process time (57.1% and 40.0% before and after cleavage and global deprotection). The material cost of SPPS is lower than that of the new case mainly due to the large difference between the unit prices of DIC and HBTU ($149.55 \text{ Euro} \cdot \text{mol}^{-1}$ compared to $568.88 \text{ Euro} \cdot \text{mol}^{-1}$), which are used to activate amino acids in SPPS and MEPS respectively (DIC was not used in MEPS due to incomplete couplings as discussed in Section 3.3.8.2.1).

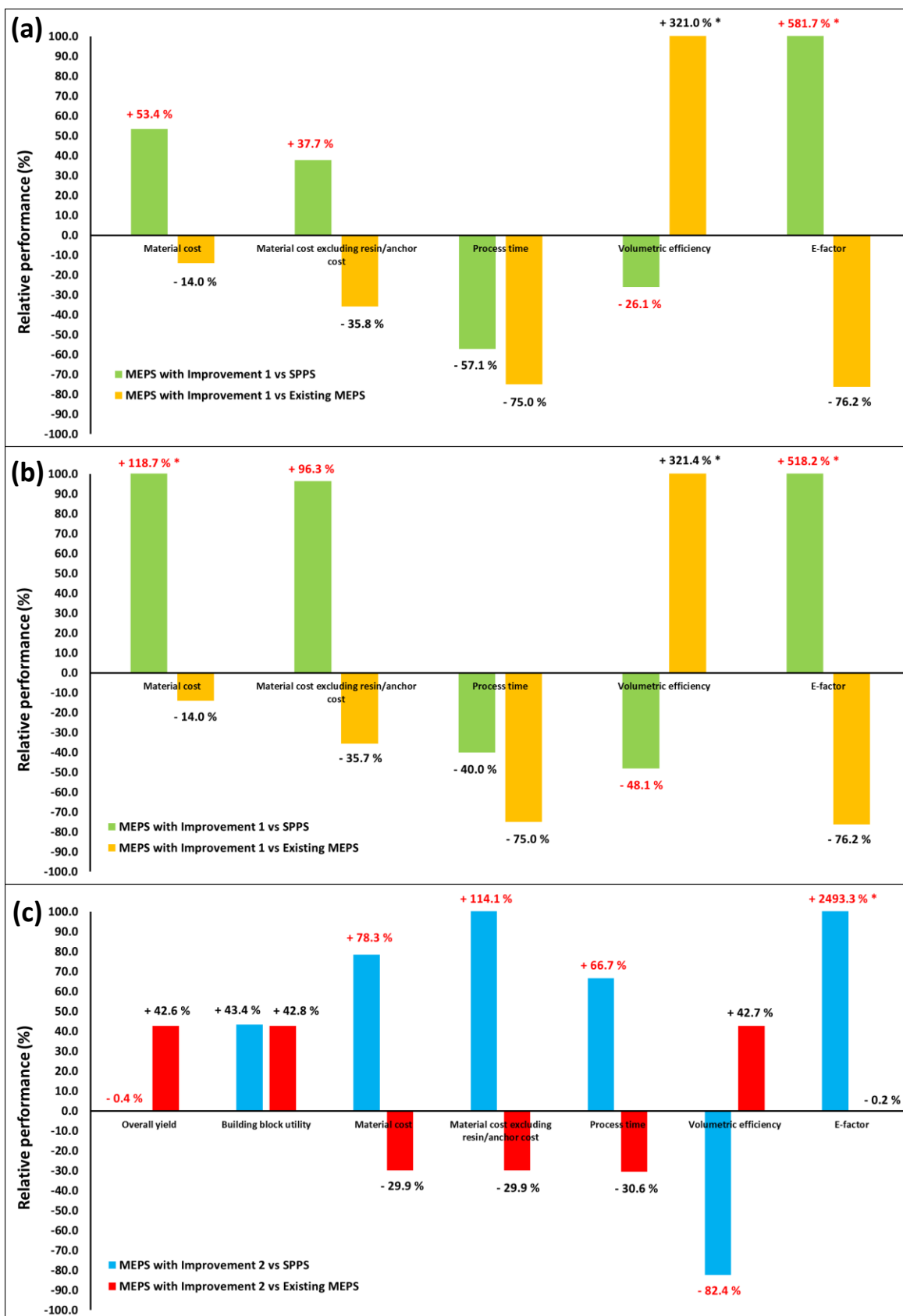
Figure 3.40 also shows that by optimising the cleavage and global deprotection procedure in order to reduce the loss of overall yield to approximately 5.0 % (Improvement 2) (as in the case of SPPS, where the yield loss during cleavage and global deprotection is normally less than 5 % based on industrial experience), improvements can be made for all parameters after cleavage and global deprotection. The magnitude of improvements is generally smaller than the first alternative, except for the total material cost (29.9 % reduction as compared to 14.0 %) and building block utility (42.8 % higher than SPPS as compared to 0.4 % (Table 3.20)). Furthermore, the current linker-anchor combination ($\text{H}_2\text{N-Rink-DDBA}$) was only a tentative option for MEPS and the optimisation of cleavage and global deprotection is case-specific (i.e. it largely depends on the peptide sequence and linker-anchor combination), rendering this option less favourable than the first one, which could be easily implemented by increasing the scale of synthesis in a fixed-volume system. In the second case study, MEPS was carried out at 10.0 weight % $\text{H}_2\text{N-Rink-DDBA}$. More details can be found in the next chapter (Section 4.3.3.5 and 4.3.4).

Table 3.21. Performance of MEPS with improvements.

| Synthesis method | SPPS | MEPS | MEPS with Improvement 1* | MEPS with Improvement 2** |
|--|-------|-------|--------------------------|---------------------------|
| Scale (mmol) | 11.42 | 10.01 | 100.1 | 10.01 |
| System volume (mL) | 100 | 500 | 500 | 500 |
| <u>Before cleavage and global deprotection</u> | | | | |
| Purity (%) | 85.3 | 98.5 | Same as MEPS | Same as MEPS |
| Overall yield (%) | 78.3 | 78.6 | | |
| Building block utility (%) | 52.2 | 74.9 | | |
| Material cost (Euro · mmol ⁻¹) | 32.94 | 58.77 | 50.53 | |
| Material cost excluding resin/anchor cost (Euro · mmol ⁻¹) | 10.75 | 23.04 | 14.8 | |
| Process time (h · mmol ⁻¹) | 1.4 | 2.4 | 0.6 | |
| Volumetric efficiency (mmol · L ⁻¹) | 89.4 | 15.7 | 66.1 | |
| E-factor | 180 | 5152 | 1227 | |
| <u>After cleavage and global deprotection</u> | | | | |
| Purity (%) | 85.3 | 58.4 | 58.4 | NA |
| Overall yield (%) | 73.3 | 51.6 | 51.6 | 73.6 |
| Building block utility (%) | 48.9 | 49.1 | 49.1 | 70.1 |
| Material cost (Euro · mmol ⁻¹) | 35.19 | 89.52 | 76.97 | 62.76 |
| Material cost excluding resin/anchor cost (Euro · mmol ⁻¹) | 11.49 | 35.09 | 22.55 | 24.6 |
| Process time (h · mmol ⁻¹) | 1.5 | 3.6 | 0.9 | 2.5 |
| Volumetric efficiency (mmol · L ⁻¹) | 83.7 | 10.3 | 43.4 | 14.7 |
| E-factor | 329 | 8545 | 2034 | 8532 |

*Improvement 1: increasing the starting concentration of anchor in THF from 2.4 weight% to 10.0 weight%.

**Improvement 2: optimising the cleavage and global deprotection procedure to reduce the loss of overall yield to 5%.



* The bar extends beyond the upper limit of the y-axis of the diagram.

Figure 3.40. Performance of MEPS: (a) with Improvement 1 before cleavage and global deprotection; (b) with Improvement 1 after cleavage and global deprotection; (c) with improvement 2 after cleavage and global deprotection.

3.4 Conclusions

The first model peptide (fully deprotected Fmoc-RADA-NH₂) was synthesised successfully by MEPS. Commercial ceramic membrane Inopor 450 was found to possess good stability in strong organic solvents such as THF which have been frequently used for peptide synthesis as well as in piperidine solution. 5 soluble anchors with molecular weights between 757 g · mol⁻¹ and 8209 g · mol⁻¹ had relatively high but similar rejections by Inopor 450 (90.0 - 96.9 %). Interestingly, even the bulkiest anchor did not have complete rejection.

Due to the ease of synthesis (tens of grams) and relatively high rejection (90.0 %), a highly hydrophobic compound (DDBA) was chosen for MEPS. Later experiments showed that peptide synthesis on DDBA alone was prone to side-reaction (DKP formation), which could be prevented by attaching the Fmoc-Rink linker to DDBA.

MEPS of the model tetrapeptide showed that all couplings could be finished with 1.05 eq amino acid/HBTU/HOBt under basic condition within 30 minutes and all de-Fmoc could proceed to completion in 5.0 weight % piperidine with 0.1 M HOBt within 1 hour. The most critical part of peptide synthesis was found to be the post-de-Fmoc diafiltration, where sufficient wash volumes of solvent had to be used to remove the piperidine in order for the next coupling to proceed to completion. With a scale of 10.01 mmol and a system volume of 500 mL, the MEPS of Fmoc-RADA-Rink-DDBA (before cleavage and global deprotection of the fully protected peptide) achieved a decent overall yield of 78.6 % with a high purity of product (98.5 %), which was similar to the SPPS (scale = 11.42 mmol; overall yield = 78.3 %; purity = 85.3 %).

Yet, due to the dilute concentration of anchor (2.4 weight % H₂N-Rink-DDBA in THF) at which MEPS was operated, the novel process underperformed in comparison to SPPS in terms of normalised material cost, process time and other areas such as volumetric efficiency and E-factor. Worse still, MEPS suffered a significant loss in overall yield and purity (51.6 % and 58.4 % respectively) after

cleavage and global deprotection, while those remained relatively constant in SPPS (73.1 % and 85.3 % respectively), rendering MEPS even more disadvantaged for all other performance parameters. The breakdown of material cost showed that more than 60 % was attributed to resin or soluble anchor for both synthesis methods (SPPS: 67 %; MEPS: 61 %) and the major component for the remaining costs was amino acids for SPPS (23 %) and solvent for MEPS (18 %). It was found that by simply increasing the concentration of anchor from 2.4 to 10.0 weight % H₂N-Rink-DDBA in THF with the same system volume (500 mL), significant improvements could be made across all performance parameters for MEPS. Therefore, this approach will be explored in the second case study which follows.

Chapter Four –

Case Study Two: MEPS of Partially Deprotected Pyr-SAFDL-NH₂

4.1. Introduction

Following the promising results of the first case study of MEPS, the established OSN system and procedure were employed for the synthesis of the second model peptide, Pyr-Ser(Bzl)-Ala-Phe-Asp-Leu-NH₂ (partially deprotected Pyr-SAFDL-NH₂, Figure 4.1). The synthesis was performed at the maximum concentration of linker-anchor (10.0 weight % H₂N-Rink-DBDA in THF) in order to improve the performance parameters such as normalised material cost and process time as predicted in the previous chapter (Section 3.3.9). For a more thorough comparison of process performance, the model peptide was also synthesised with SPPS and LPPS (by precipitation). Feasible improvement methods were discussed and assessed based on their implications on the performance parameters.

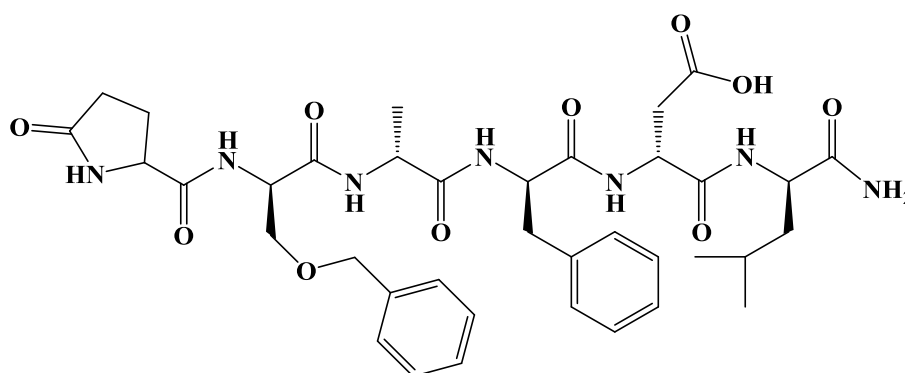


Figure 4.1. Pyr-Ser(Bzl)-Ala-Phe-Asp-Leu-NH₂ (partially deprotected Pyr-SAFDL-NH₂) (MW = 752 g · mol⁻¹).

For the purpose of direct comparison, SPPS of the model peptide was performed twice with the same activator (HBTU) as in MEPS. The first attempt employed the standard SPPS procedure, in which 1.50 eq amino acids/HBTU/HOBt were used for couplings. In order to show the advantage of liquid phase synthesis over SPPS in terms of reducing the required amounts of coupling reagents, the second attempt used 1.05 eq amino acids and coupling reagents as in MEPS (such a low excess was

expected to result in incomplete couplings and hence loss of yield and purity in SPPS). LPPS of the model peptide was performed with 1.05 eq amino acids and coupling reagents by the precipitation of intermediate products in order to study any side reactions that could occur and to assess its performance for comparison purposes. MEPS was then performed at 1.5 weight % anchor in THF with the system and procedure that were developed in the first case study, such that any technical difficulty could be identified and resolved before increasing the concentration of H₂N-Rink-DDBA to 10.0 weight % in THF, which is the maximum concentration of anchor. Based on their experimental results, the performances of SPPS, LPPS (by precipitation) and MEPS are compared and further improvements are proposed.

4.2. Experimental

The materials and equipment for peptide synthesis were generally the same as described in the Chapter Three (Section 3.2). For peptide synthesis, the amino acids (H-Pyr-OH (CAS number: 98-79-3; product code: 8540020100), Fmoc-L-Ser(Bzl)-OH (CAS number: 83792-48-7; product code: 8520180025), Fmoc-L-Phe-OH (CAS number: 35661-40-6; product code: 8520160250) and Fmoc-L-Leu-OH (CAS number: 35661-60-0; product code: 8520110250)) were purchased from Merck KGaA.

4.2.1. Analytical Methods

HPLC Methods

| | | | | | |
|----------------------------------|---|--------------------------------|----|----|----|
| Name | Pyr-SAFDL_HPLC1* | | | | |
| HPLC Column | Sunfire, C18, 150 X 4.6 mm, 3.5 µm particle size | | | | |
| Column Temperature (°C) | 40 | | | | |
| Detection Wavelength (nm) | 220 | | | | |
| Gradient | Time (min) | Flow (mL · min ⁻¹) | %A | %B | %C |
| | 0.0 | 1.00 | 0 | 10 | 90 |
| | 15.0 | 1.00 | 0 | 90 | 10 |
| | 17.0 | 1.00 | 0 | 90 | 10 |
| | 17.5 | 1.00 | 0 | 10 | 90 |
| | 20.0 | 1.00 | 0 | 10 | 90 |
| Eluent A | Isopropanol | | | | |
| Eluent B | 0.1 vol% TFA/Acetonitrile (i.e. 2 mL TFA in 2 L Acetonitrile) | | | | |
| Eluent C | 0.1 vol% TFA/Water (i.e. 2 mL TFA in 2 L Water) | | | | |
| *Note | Old name (as on HPLC results): Pyr_SAFDL_4Oct2013 | | | | |

| | | | | | |
|----------------------------------|---|--------------------------------|----|----|----|
| Name | AA_HPLC1* | | | | |
| HPLC Column | Sunfire, C18, 150 X 4.6 mm, 3.5 µm particle size | | | | |
| Column Temperature (°C) | 40 | | | | |
| Detection Wavelength (nm) | 220 | | | | |
| Gradient | Time(min) | Flow (mL · min ⁻¹) | %A | %B | %C |
| | 0.0 | 1.00 | 0 | 10 | 90 |
| | 5.0 | 1.00 | 0 | 35 | 65 |
| | 15.0 | 1.00 | 0 | 90 | 10 |
| | 20.0 | 1.00 | 0 | 90 | 10 |
| | 20.5 | 1.00 | 0 | 10 | 90 |
| | 25.0 | 1.00 | 0 | 10 | 90 |
| Eluent A | Isopropanol | | | | |
| Eluent B | 0.1 vol% TFA/Acetonitrile (i.e. 2 mL TFA in 2 L Acetonitrile) | | | | |
| Eluent C | 0.1 vol% TFA/Water (i.e. 2 mL TFA in 2 L Water) | | | | |
| *Note | Old name (as on HPLC results): AA_8Jan2014 | | | | |

4.2.2. General Procedures

4.2.2.1. SPPS of Partially Deprotected Pyr-SAFDL-NH₂

Partially deprotected Pyr-SAFDL-NH₂ was synthesised by SPPS, whose experimental results served as the reference for the MEPS process.

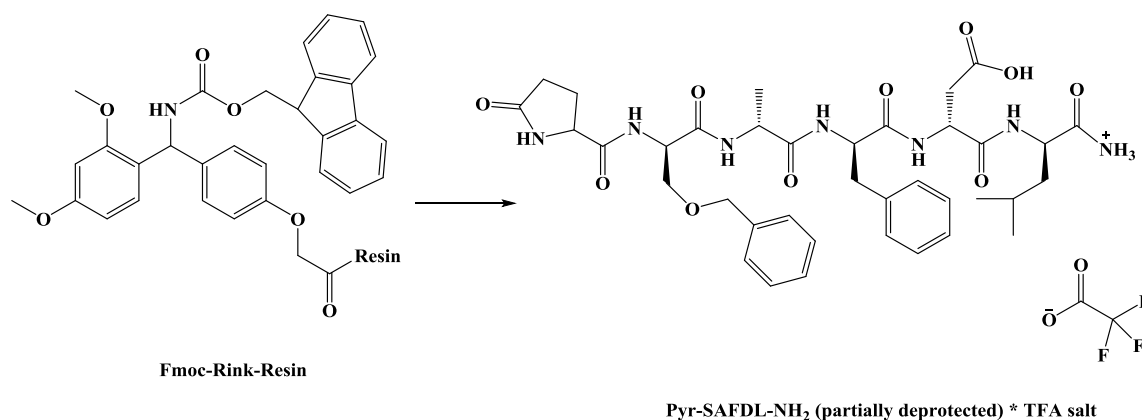


Figure 4.2. SPPS of partially deprotected Pyr-SAFDL-NH₂ on Fmoc-Rink resin

All the steps below were conducted at 20.0 °C and atmospheric pressure unless stated otherwise. The equivalent of reagent was with respect to the resin.

Step 1. Swelling of Fmoc-Rink-Resin PL-Rink resin (6.94 g, loading = 0.72 mmol · g⁻¹ according to supplier) was added into a 125-mL reactor, followed by the addition of DMF (60 mL). Another portion of DMF (50 mL) was used to wash down any resin on the reactor wall. The resin was allowed to swell with the solvent for 1 hour and then drained.

Step 2. deFmoc of Fmoc-Rink-Resin Piperidine (13.22 g, 155 mmol, 20 weight % in 70 mL DMF) was added into DMF (70 mL), followed by HOBt (10.49 g, 15.5 eq (0.5 eq with respect to piperidine*)). The solution was added to the reactor. The reaction mixture was stirred for 20 minutes, after which the resin was drained and the deprotection was repeated twice. The resin was then washed with DMF (70 mL) 6 times. The presence of piperidine in the washing DMF was checked by the chloranil test to ensure the proper removal of piperidine.

Step 3, 5, 7, 9, 11 and 13. Coupling of Amino Acid Amino acid (1.05 eq or 1.50 eq) was dissolved in DMF (70 mL), followed by HOBt (1.05 eq or 1.50 eq), DIEA (1.94 g, 15.00 mmol, 3.00 eq) and HBTU (1.05 eq or 1.50 eq). The solution was stirred at room temperature for 5 minutes, before it was added into the reactor. The reaction mixture was stirred and the reaction was followed by the ninhydrin test every 30 minutes. After the reaction was complete, the system was drained and washed with DMF (70 mL) 5 times.

Step 4, 6, 8, 10 and 12. De-Fmoc of Fmoc- Peptide Fragment-Resin Piperidine (13.22 g, 155 mmol, 20 weight % in 70 mL DMF) was added into DMF (70 mL), followed by HOBt (10.49 g, 15.5 eq (0.5 eq with respect to piperidine*)). The solution was added to the reactor and the mixture was stirred for 20 minutes. The reactor was drained and the deprotection was repeated twice with similar piperidine solutions. The resin was then washed with DMF (70 mL) 5 times. The presence of piperidine in the washing DMF was checked by the chloranil test to ensure the proper removal of piperidine.

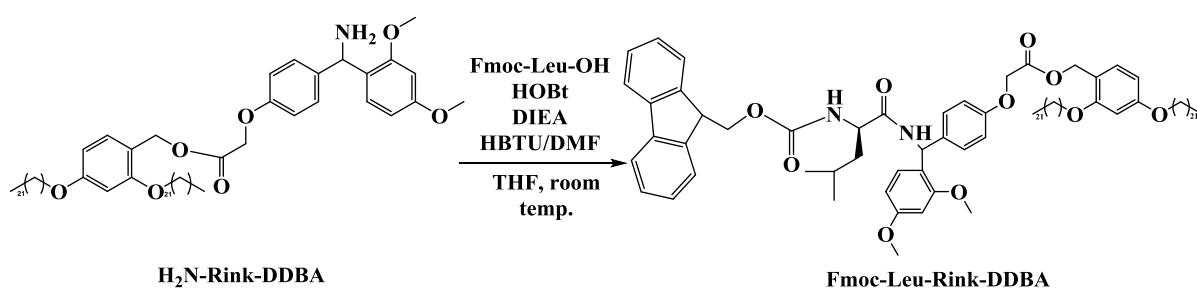
Step 14. Cleavage and Global Deprotection The peptide-bound resin was washed with DCM (100 mL) and dried under vacuum. This was repeated once more. The cleavage cocktail solution (TFA/H₂O, 95/5, v/v, 70 mL) was added to the reactor and the mixture was stirred for 1 hour, after which the system was drained and the filtrate was added into cold diisopropylether (700 mL). The cleavage and global deprotection was repeated once more to ensure complete cleavage of peptide from the resin. The precipitated product was filtered, washed with diisopropylether (100 mL) 5 times and then dried in a vacuum oven (-80 kPa (gauge) and 30 °C) until the mass loss due to solvent evaporation became negligible.

* 0.5 eq HOBt with respect to piperidine was added into the de-Fmoc solution in order to suppress the formation of aspartimide according to the study by Michels et al. (2012).

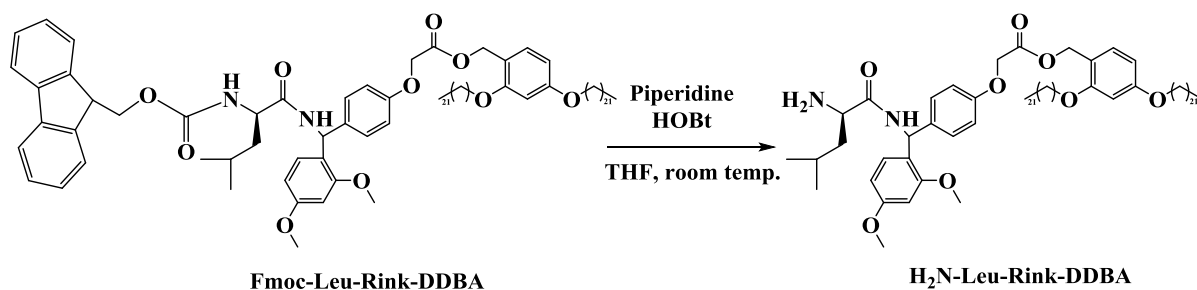
4.2.2.2. LPPS of Partially Deprotected Pyr-SAFDL-NH₂ on H₂N-Rink-DDBA by Precipitation

Partially deprotected Pyr-SAFDL-NH₂ was synthesised on H₂N-Rink-DDBA by LPPS, in which anchored peptide was precipitated after each reaction. The aim was to investigate the synthesis chemistry before attempting MEPS and to obtain experimental data that served as a reference for LPPS (by precipitation) for the comparison with MEPS.

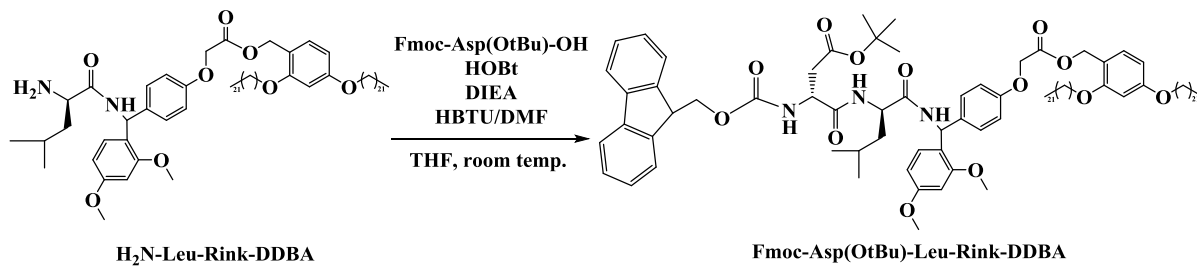
Step 1.



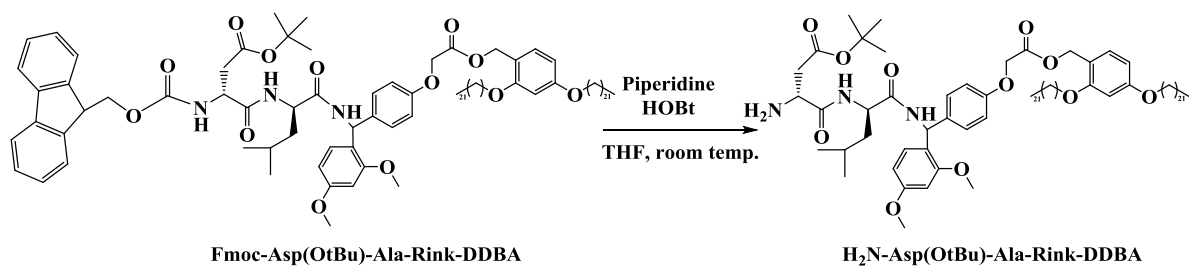
Step 2.



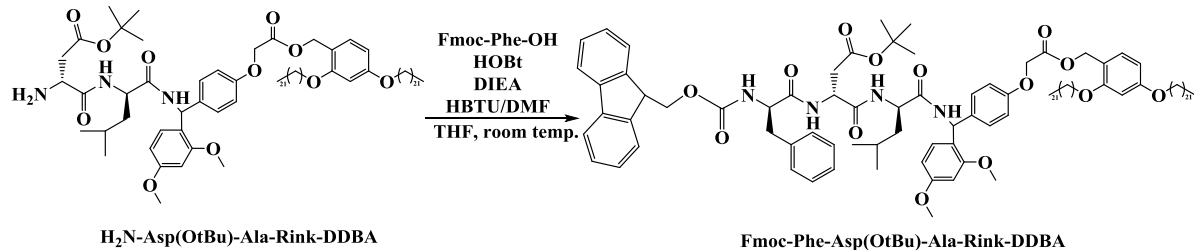
Step 3.



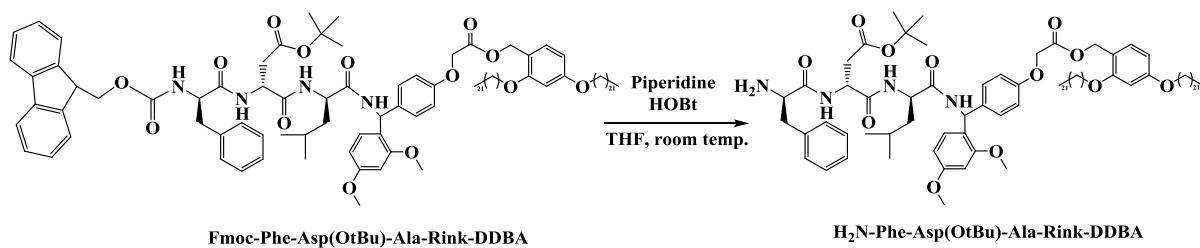
Step 4.



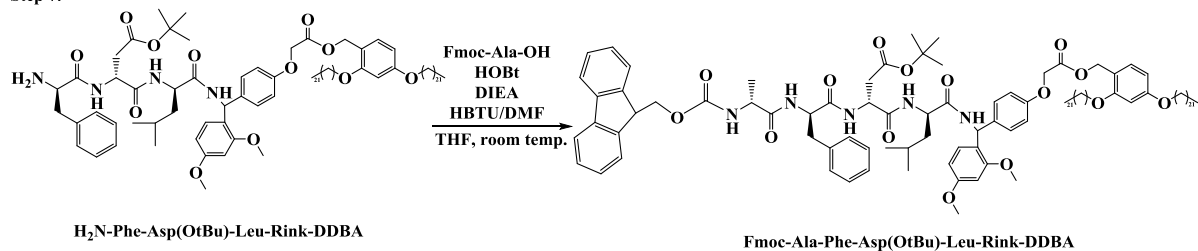
Step 5.



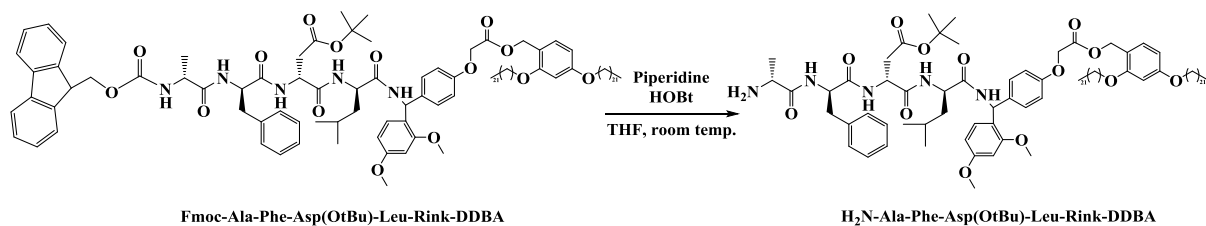
Step 6.



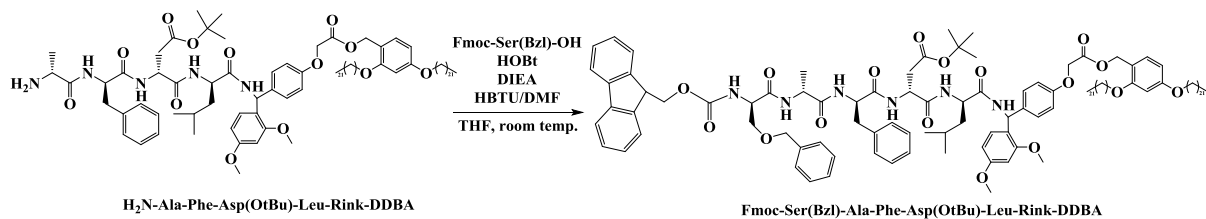
Step 7.



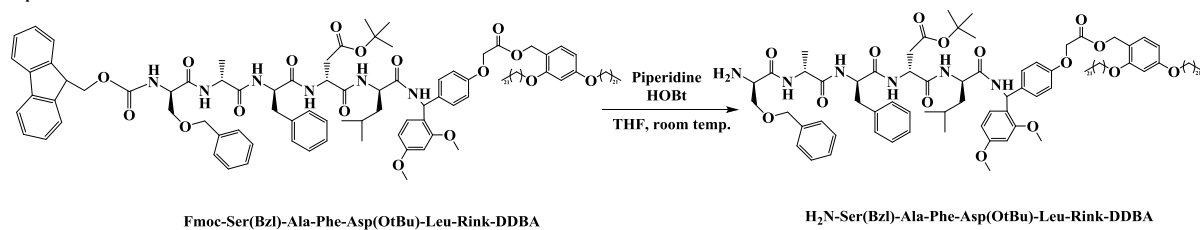
Step 8.



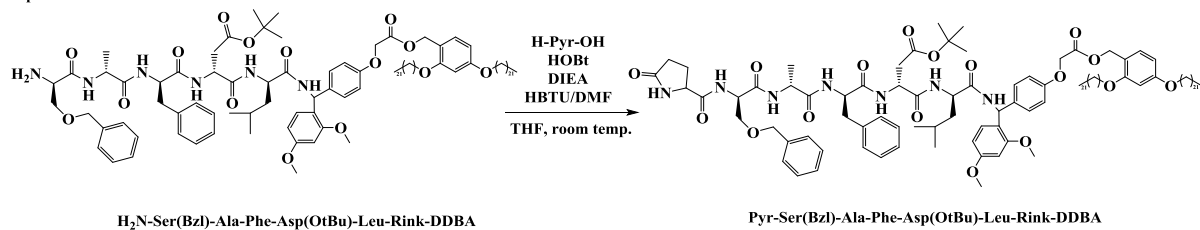
Step 9.



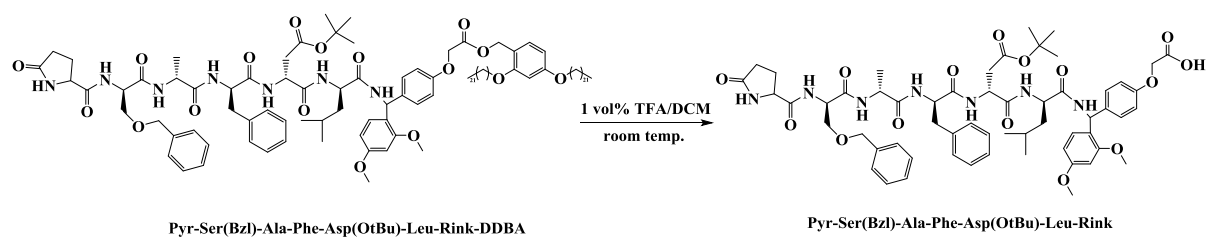
Step 10.



Step 11.



Step 12.



Step 13.

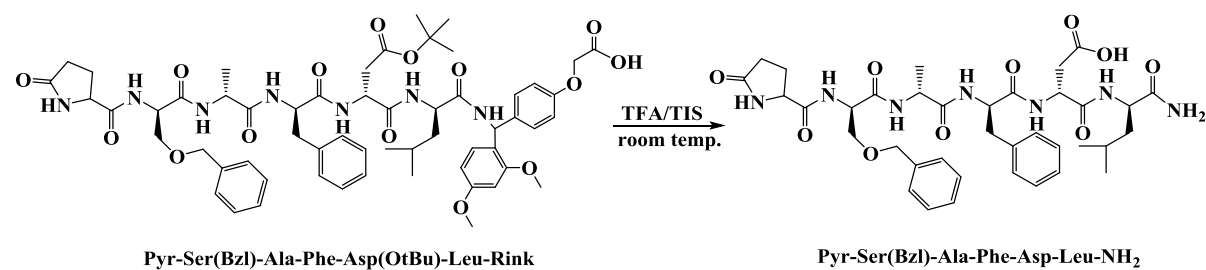


Figure 4.3. LPPS of partially deprotected Pyr-SAFDL-NH₂ on H₂N-Rink-DDBA.

All the steps below were conducted at room temperature and pressure unless stated otherwise. The equivalent of reagent was with respect to the quantity of H₂N-Rink-DDBA.

Step 1. Loading of Leu Fmoc-Leu-OH (1.86 g, 5.26 mmol, 1.05 eq) was dissolved in THF (52.80 g), followed by HOBt (0.71 g, 5.25 mmol, 1.05 eq) and DIEA (1.29 g, 9.98 mmol, 2.00 eq). HBTU (1.99 g, 5.25 mmol, 1.05 eq) was dissolved separately in DMF (40.00 g) and the solution was added to the reaction solution. H₂N-Rink-DDBA (5.28 g, 5.00 mmol, 1.0 eq) was added to the reaction solution. The reaction solution was stirred at room temperature for 1 hour and the reaction was followed by HPLC (analysis at 30 minutes; method: Fmoc-RADA-DDBA_HPLC1). After the reaction was complete, the reaction solution was added to acetonitrile (900 mL). White precipitate was obtained, filtered and washed with acetonitrile (100 mL) 5 times. The precipitate was dried in a vacuum oven (-80 kPa (gauge) and 30 °C) until the mass loss due to solvent evaporation became negligible.

Step 2, 4, 6, 8 and 10. deFmoc of Fmoc-Peptide Fragment-DDBA HOBt (0.68 g, 0.1M in 50 mL THF) and piperidine (2.22 g, 5.0 weight % in 50 mL THF) were added into THF (50 mL), followed by the dry anchored peptide. The reaction solution was stirred at room temperature for 2 hours and the reaction was monitored by HPLC (analysis after 1 and 2 hours; method: Fmoc-RADA-DDBA_HPLC1). After the reaction was complete, the reaction solution was added to acetonitrile (900 mL). White precipitate was obtained, filtered and washed with acetonitrile (100 mL) 5 times. The presence of piperidine in the washing acetonitrile was checked by the chloranil test. The precipitate was then dried in a vacuum oven (-80 kPa (gauge) and 30 °C) until the mass loss due to solvent evaporation became negligible.

Step 3, 5, 7, 9 and 11. Coupling of Amino Acid Amino acid (5.37 mmol, 1.05 eq) was added into the solution, followed by HOBt (0.72 g, 5.33 mmol, 1.05 eq) and DIEA (1.32 g, 10.21 mmol, 2.00 eq). HBTU (2.03 g, 5.35 mmol, 1.05 eq) was dissolved separately in DMF (20.00 g) and the solution was added to the reaction solution. The reaction solution was stirred at room temperature for 1 hour

and the reaction was monitored by HPLC (analysis after 30 minutes; method: Fmoc-RADA-DDBA_HPLC1). After the reaction was complete, the reaction solution was added to acetonitrile (900 mL). White precipitate was obtained, filtered and washed with acetonitrile (100 mL) 5 times. The presence of piperidine in the washing acetonitrile was checked by the chloranil test. The precipitate was then dried in a vacuum oven (-80 kPa (gauge) and 30 °C) until the mass loss due to solvent evaporation became negligible.

Step 12. Cleavage Pyr-Ser(Bzl)-Ala-Phe-Asp(OtBu)-Leu-Rink-DDBA was added into 1 vol % TFA solution (TFA/DCM, 2 mL/200 mL, 200 mL) and the mixture was stirred at room temperature for 1 hour. The reaction was monitored by HPLC (analysis after 1 hour; method: Fmoc-RADA-DDBA_HPLC1). After the reaction was complete, acetonitrile (700 mL) was added into the mixture and the mixture was filtered. The filtered solid was washed with 1 vol % TFA solution (100 mL) 6 times. The filtrate was collected and then dried under vacuum (-80 kPa (gauge) and 30 °C) until the mass loss due to solvent evaporation became negligible.

Step 13. Global Deprotection Pyr-Ser(Bzl)-Ala-Phe-Asp(OtBu)-Leu-Rink was added into the global deprotection cocktail solution (TFA/TIS, 85/15, v/v, 55 mL) and the mixture was stirred at room temperature for 1 hour and the reaction was monitored by HPLC (analysis after 1 hour; method: Fmoc-RADA-DDBA_HPLC1). After the reaction was complete, cold diisopropylether (500 mL) was added into the mixture and the mixture was filtered. The filtered solid was dried, washed with diisopropylether (100 mL) 5 times and then dried in a vacuum oven (-80 kPa (gauge) and 30 °C) until the mass loss due to solvent evaporation became negligible.

4.2.2.3. MEPS of Partially Deprotected Pyr-SAFDL-NH₂ on H₂N-Rink-DDBA

Partially deprotected Pyr-SAFDL-NH₂ was synthesised on H₂N-Rink-DDBA by MEPS following the same chemistry as in the LPPS by precipitation (as shown in Figure 4.3, Section 4.2.2.2). After each reaction, diafiltration was performed to remove excess reagents and by-products.

All the steps below were conducted at room temperature and pressure unless stated otherwise. The equivalent of reagent was with respect to the quantity of H₂N-Rink-DDBA.

Step 1. Loading of Leu Fmoc-Leu-OH (12.49 g, 35.34 mmol, 1.05 eq) was dissolved in THF (400 mL (355.60 g)), followed by HOBt (4.78 g, 35.38 mmol, 1.05 eq) and DIEA (21.74 g, 168.21 mmol 5.00 eq). HBTU (13.40 g, 35.33 mmol, 1.05 eq) was dissolved separately in DMF (134.00 g) and the solution was added to the reaction solution. H₂N-Rink-DDBA (35.56 g, 33.65 mmol, 1.00 eq) was added to the reaction solution. The reaction solution was stirred for 1 hour and the reaction was followed by HPLC (analysis after 30 minutes; method: Fmoc-RADA-DDBA_HPLC1). After the reaction was complete, the reaction solution was added to the OSN system for diafiltration (2 washes, 800 mL each wash).

Step 2, 4, 6, 8 and 10. deFmoc of Fmoc-Peptide Fragment-DDBA HOBt (5.40 g, 0.1 M in 400 mL THF) was added into the reaction solution, followed by piperidine (35.56 g, 10.0 weight % in 400 mL THF). The reaction solution was circulated in the OSN system for two hours and the reaction was followed by HPLC (analysis after 1 and 2 hours; method: Fmoc-RADA-DDBA_HPLC1). After the reaction was complete, diafiltration was performed to remove the piperidine (7 washes, 800 mL each wash). DIEA (4.35 g, 33.64 mmol, 1.00 eq) was added into the system after the 4th, 5th and 6th wash. The presence of piperidine in retentate and permeates was checked by the chloranil test to ensure proper removal of piperidine.

Step 3, 5, 7, 9 and 11.1. Coupling of Amino Acid Amino acid (35.34 mmol, 1.05 eq) was added to the solution, followed by HOBt (4.77 g, 35.30 mmol, 1.05 eq) and DIEA (21.74 g, 168.21 mmol, 5.00 eq). HBTU (13.40 g, 35.33 mmol, 1.05 eq) was dissolved separately in DMF (134.00 g) and the solution was added into the reaction solution. The reaction solution was circulated in the OSN system for 1 hour and the reaction was monitored by HPLC (analysis after 30 minutes; method: Fmoc-RADA-DDBA_HPLC1). After the reaction was complete, diafiltration was performed (2 washes, 800 mL each wash).

Step 11.2. Drying of Pyr-Ser(Bzl)-Ala-Phe-Asp(OtBu)-Leu-Rink-DDBA After the coupling of H-Pyr-OH, the system was drained and washed with THF (400 mL) twice. All the solution was combined and dried in vacuum. Acetonitrile (800 mL) was added to the dried compound for precipitation. The precipitated product was washed with acetonitrile (200 mL) 5 times and then dried in a vacuum oven (-80 kPa (gauge) and 30 °C) until the mass loss due to solvent evaporation became negligible.

Step 12. Cleavage Pyr-Ser(Bzl)-Ala-Phe-Asp(OtBu)-Leu-Rink-DDBA was added into 1 vol % TFA solution (TFA/DCM, 10 mL/1 L, 1 L) and the mixture was stirred for 1 hour. The reaction was monitored by HPLC (analysis after 1 hour; method: Fmoc-RADA-DDBA_HPLC1). After the reaction was complete, the reaction solution was reduced to 500 mL by solvent evaporation under vacuum. The concentrated solution was added to acetonitrile (100 mL into 700 mL) and the mixture was filtered. The filtered solid was washed with 1 vol% TFA solution (100 mL) 6 times. The filtrate was collected and then dried under vacuum (-80 kPa (gauge) and 30 °C) until the mass loss due to solvent evaporation became negligible.

Step 13. Global Deprotection Pyr-Ser(Bzl)-Ala-Phe-Asp(OtBu)-Leu-Rink was added into TFA (340 mL) and the mixture was stirred at room temperature for one hour. After 1 hour, TIS (360 mL) was added and the reaction was monitored by HPLC. After another hour, the mixture was allowed to settle. The top and middle layers were removed and diisopropylether (600 mL) was added into the bottom layer. Precipitate was filtered and washed with diisopropylether (100 mL) 6 times, before drying in flowing nitrogen until the mass loss due to solvent evaporation became negligible.

4.3. Results and Discussion

4.3.1. SPPS of Partially Deprotected Pyr-SAFDL-NH₂

The solid phase synthesis of partially deprotected Pyr-SAFDL-NH₂ (Pyr-Ser(Bzl)-Ala-Phe-Asp-Leu-NH₂) was conducted twice with the PL-Rink resin that was also used for the synthesis of fully deprotected Fmoc-RADA-NH₂ (Chapter Three, Section 3.2.4.5). DIC was replaced by HBTU so that a direct comparison could be made between SPPS and MEPS (available later in this chapter (Section 4.3.4)). Details of the two syntheses are summarised in Table 4.1.

Table 4.1. Summary of results for SPPS.

| | | | Note |
|---|-----------------|-----------------|---|
| Attempt | 1 st | 2 nd | |
| Resin | PL Rink-Resin | | Loading: 0.72 mmol · g ⁻¹ resin according to supplier. |
| Scale (mmol) | 5.00 | 5.02 | |
| Amino Acids and Coupling Reagents (eq) | 1.50 | 1.05 | |
| Solvent | DMF | | |
| Temperature (°C) | 20 | | |
| System Volume (mL) | 70 | | |
| Overall Yield (%) | 72.6* | 53.9* | Before cleavage and global deprotection. |
| Purity (HPLC) (%) | 98.6* | 66.8* | |
| Overall Yield (%) | 67.6 | 48.9 | After cleavage and global deprotection. |
| Purity (HPLC) (%) | 98.6 | 66.8 | |

*The overall yield and purity before cleavage and global deprotection were not measured directly as the peptide was still bound to the resin and an accurate measurement of the corresponding total mass was difficult at this scale of synthesis. According to the industrial experience of Lonza AG, the yield loss during cleavage and global deprotection was normally less than 5%. The overall yield before cleavage and global deprotection was calculated based on this observation. The purity of peptide was assumed to remain constant before and after cleavage and global deprotection.

In the first attempt, 1.50 eq of amino acids and coupling reagents were used, resulting in fast couplings (all went to completion within 30 minutes), a decent overall yield (67.6 %) and a high purity (98.6 %) (after global deprotection, Figure 4.4 (a)). The identity of the partially globally deprotected product was confirmed by LC/MS result (Figure 4.5). In the second attempt, the amount of amino acids and coupling reagents was deliberately decreased to 1.05 eq as in MEPS, in order to quantify the advantage of liquid phase synthesis over SPPS in terms of yield and purity with the same

excess of starting materials. The conventional amount of amino acids and coupling reagents used in SPPS is two to three equivalent with respect to the loading capacity of the resin, so that the concentrations of these reactants are sufficiently high to diffuse through the polymeric matrix and reach the reactive sites. Decreasing the equivalent to 1.05 was hence expected to result in sluggish coupling, unlike the liquid phase synthesis, where couplings went to completion within 30 minutes as shown in the first MEPS case study. In contrast, all couplings up to Fmoc-Ser(Bzl)-OH (inclusive) were completed within 30 minutes. Surprisingly, even though H-Pyr-OH and its activated form are relatively small as compared to other amino acids in the sequence, the last coupling could not finish after four hours of reaction, suggesting that an amino acid with a bulky protected side-chain like Fmoc-Ser(Bzl)-OH is likely to hinder the attachment of the next amino acid. Consequently, the overall yield decreased to 48.9 % with a purity of 66.8 %. The uncoupled peptide ($\text{H}_2\text{N-Ser(Bzl)-Ala-Phe-Asp-Leu-NH}_2$) accounted for the other 27.9 % purity (approximately 20.4 % yield) (Figure 4.4 (b)). The identities of peaks were confirmed by LC/MS results (Figure 4.6).

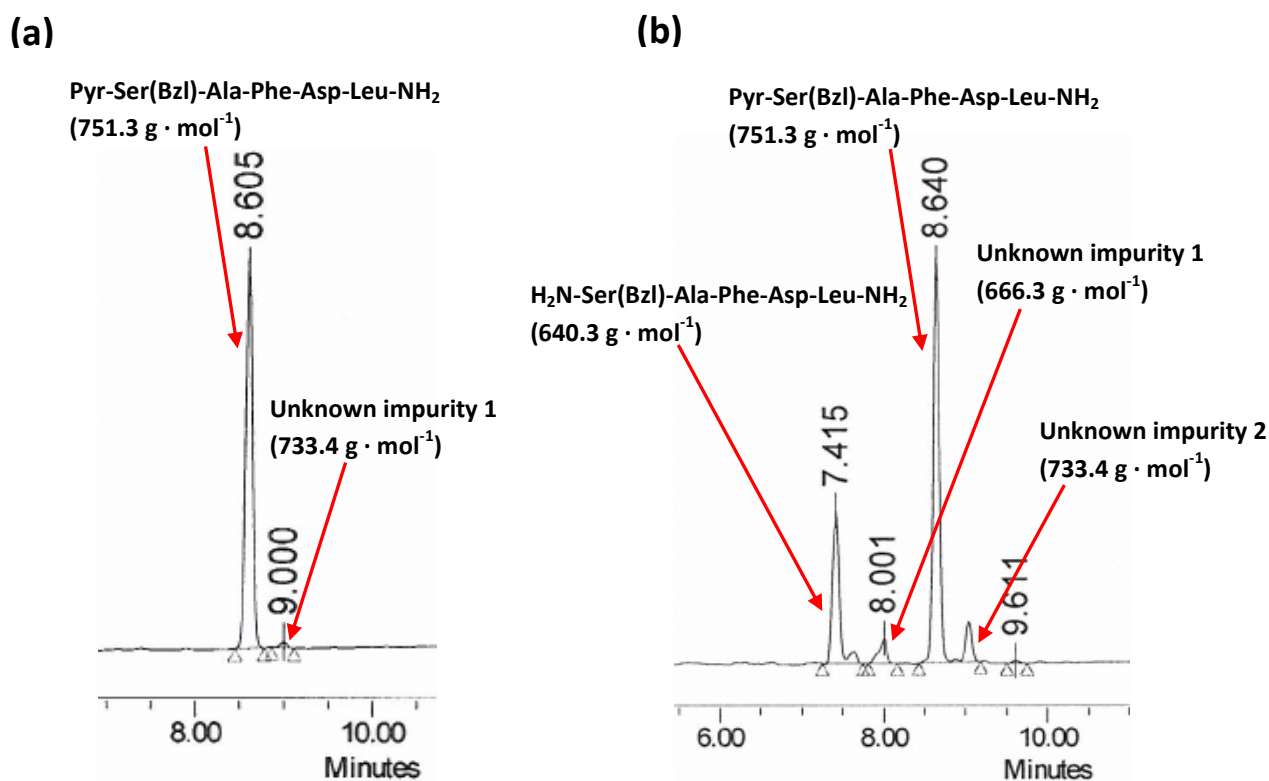
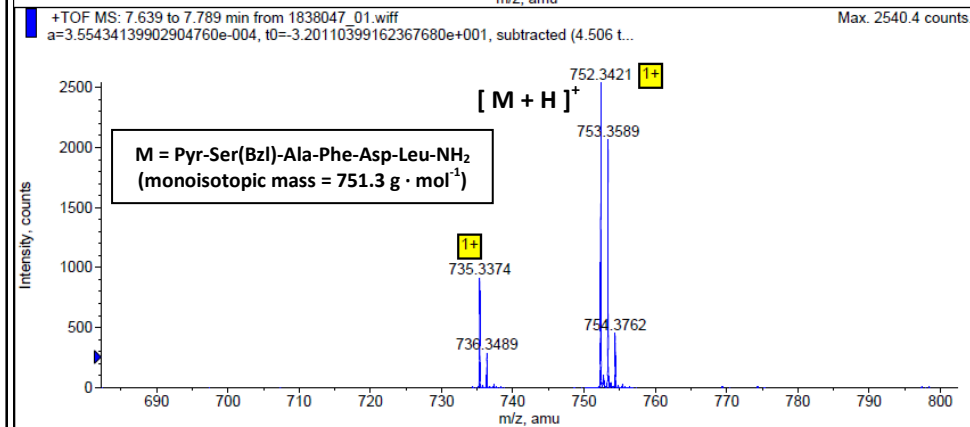
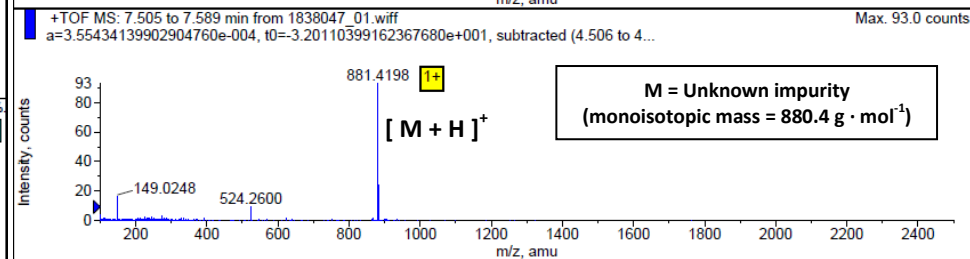
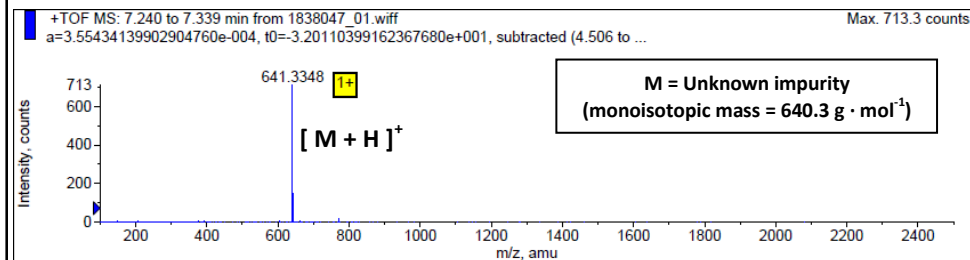
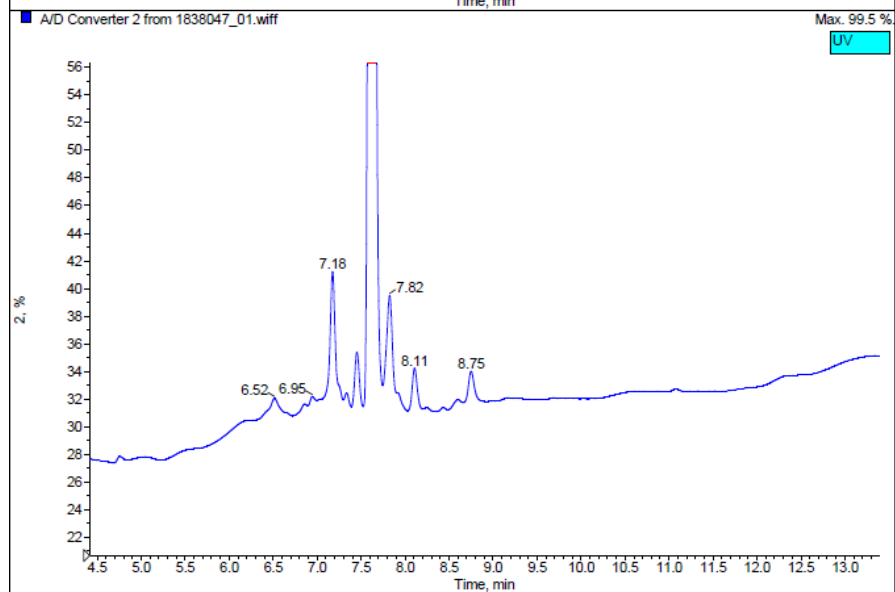
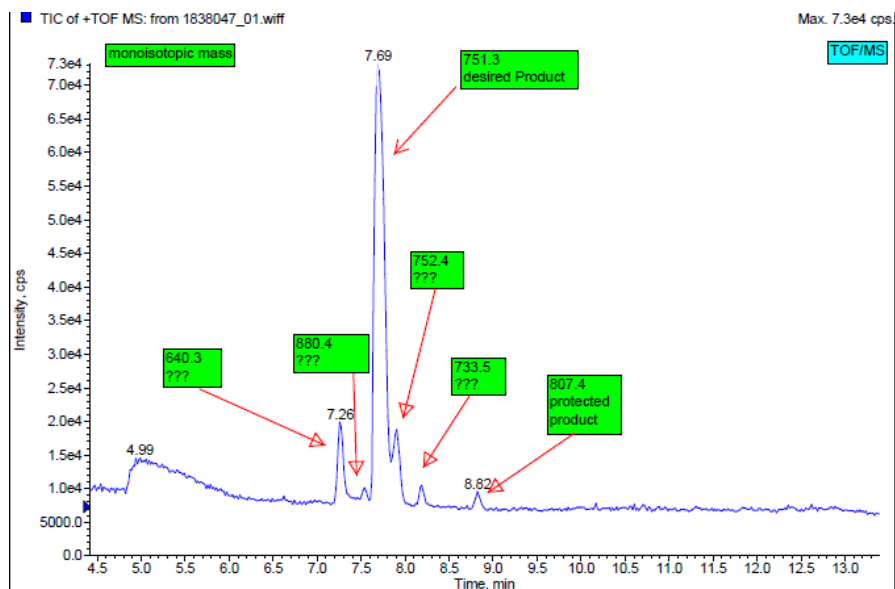


Figure 4.4. HPLC results of cleaved and global deprotected products of SPPS: (a) 1st attempt (1.50 eq amino acid for coupling); (b) 2nd attempt (1.05 eq amino acid for coupling). (Monoisotopic mass of component displayed)



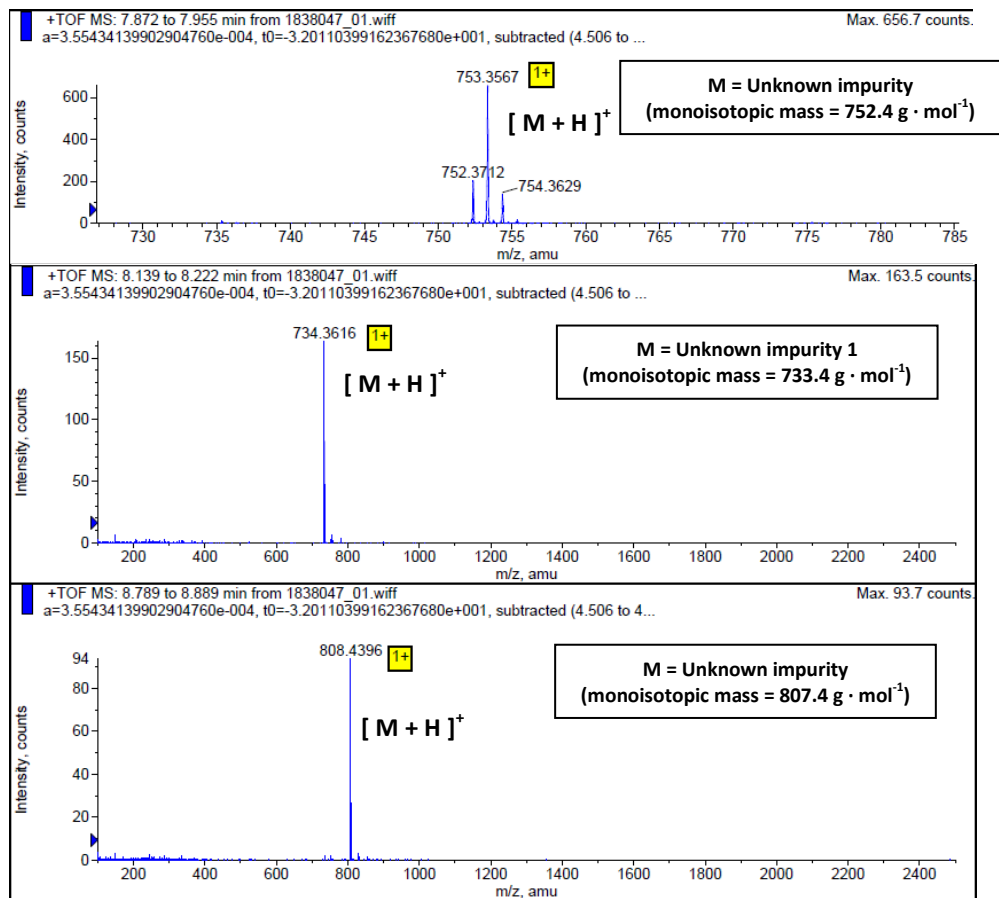
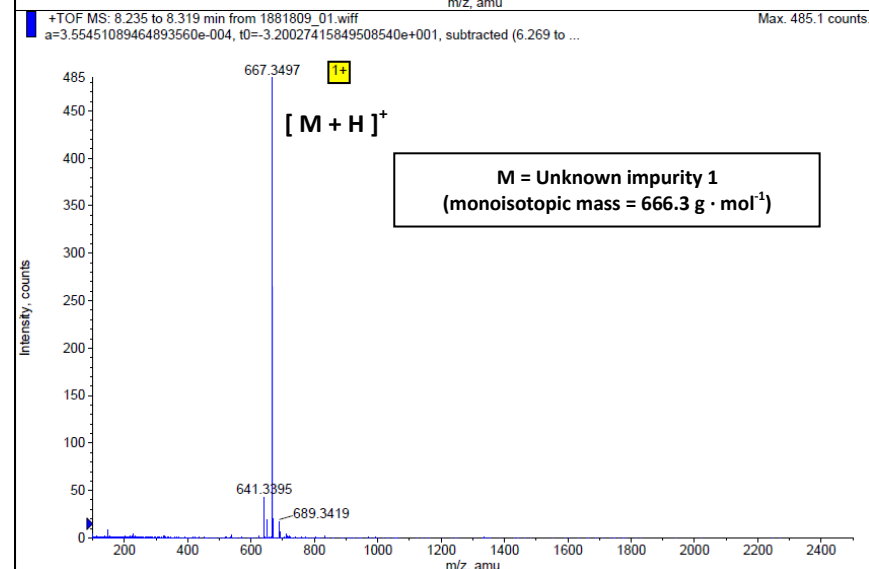
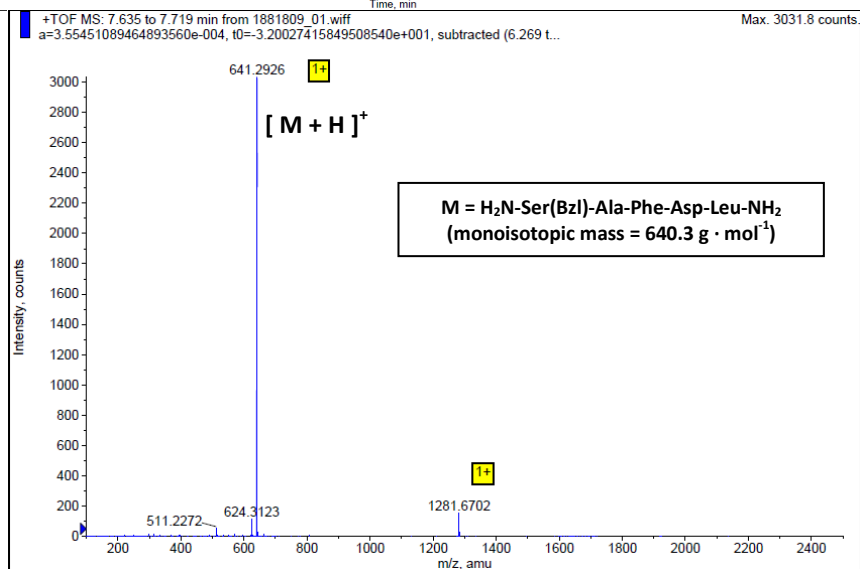
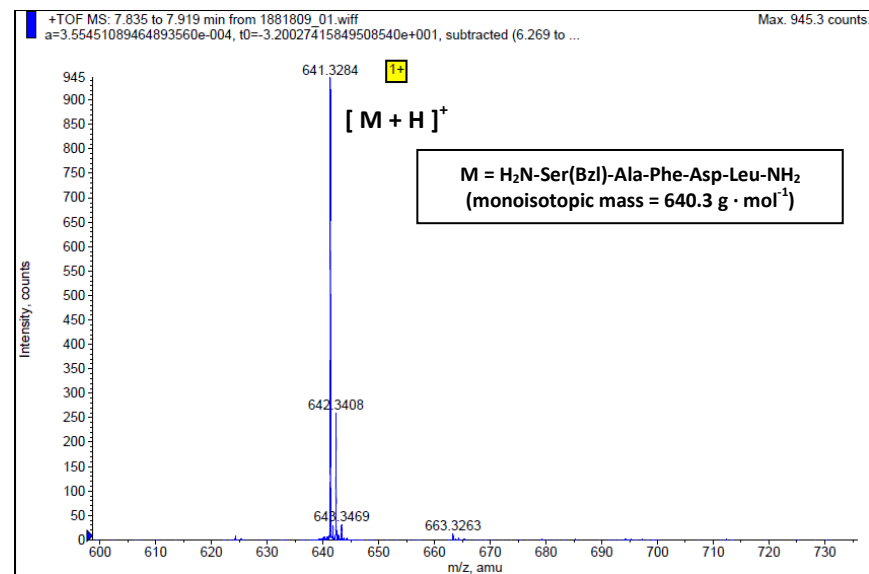
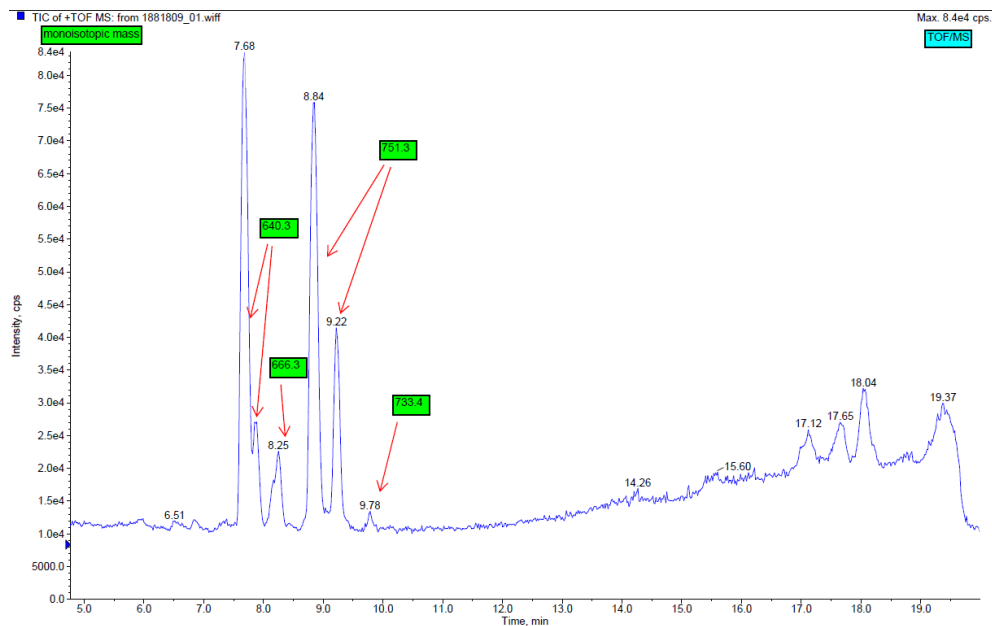


Figure 4.5. LC/MS result of the partially deprotected product (1st attempt) (HPLC method: Pyr-SAFDL_HPLC1).



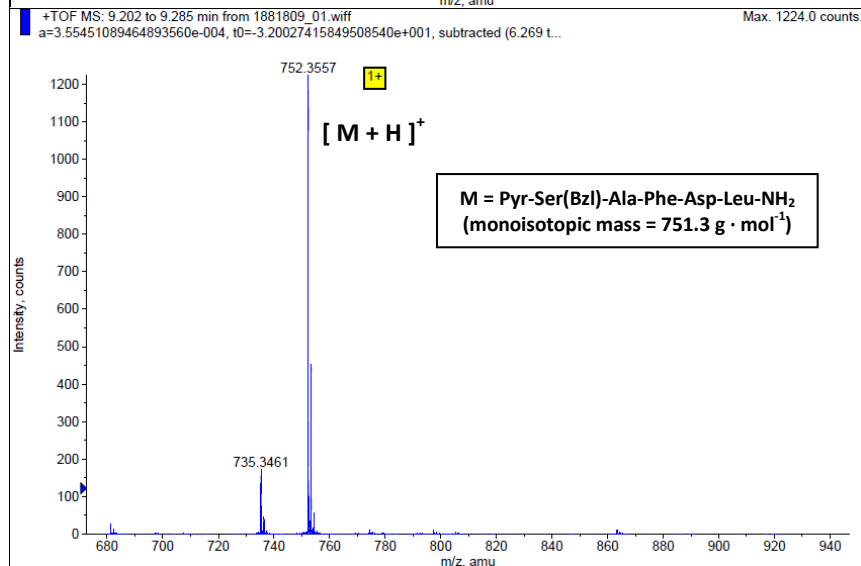
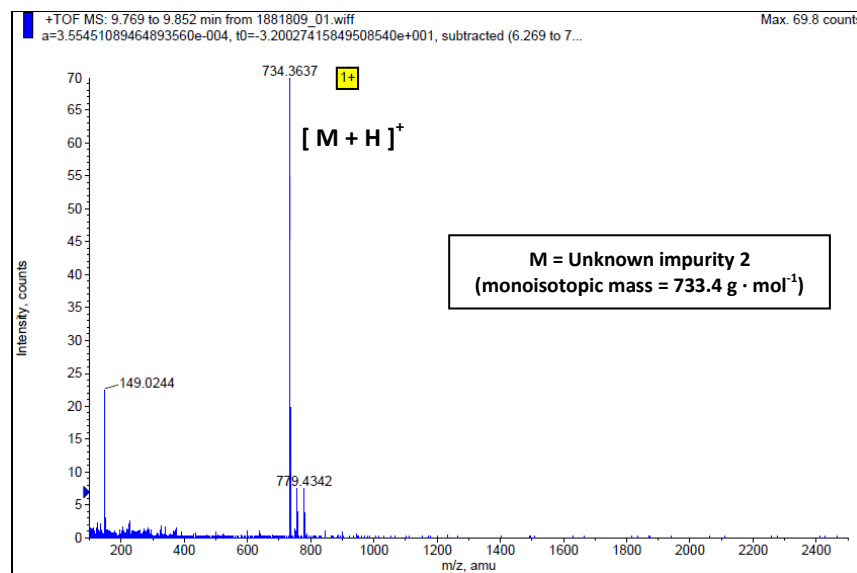
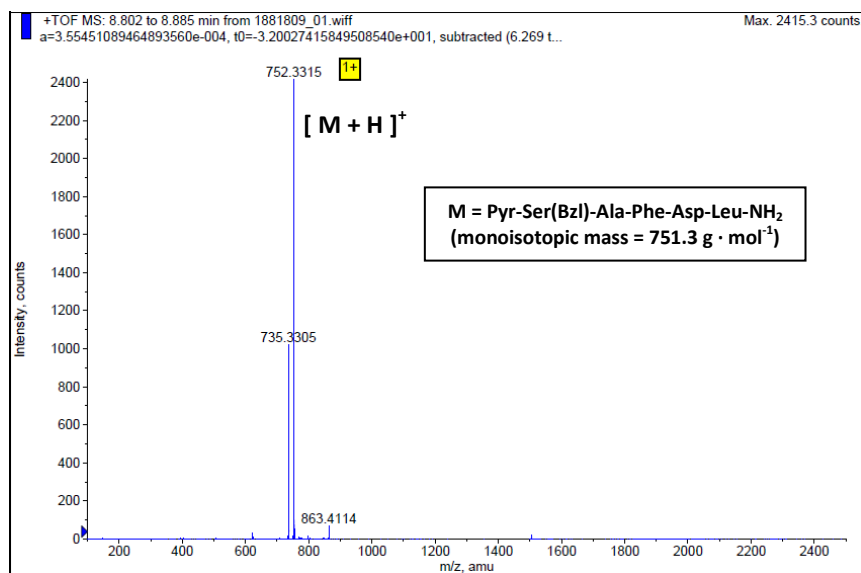


Figure 4.6. LC/MS result of the partially deprotected product (2nd attempt) (HPLC method: Pyr-SAFDL_HPLC1).

Similar to the SPPS of fully deprotected Fmoc-RADA-NH₂, the decomposition of the Rink linker was not observed during the cleavage and global deprotection in both experiments, since the side product of decomposition (partially deprotected Pyr-SAFDL-Rink-fragment, Figure 4.7) was not detected in the final products.

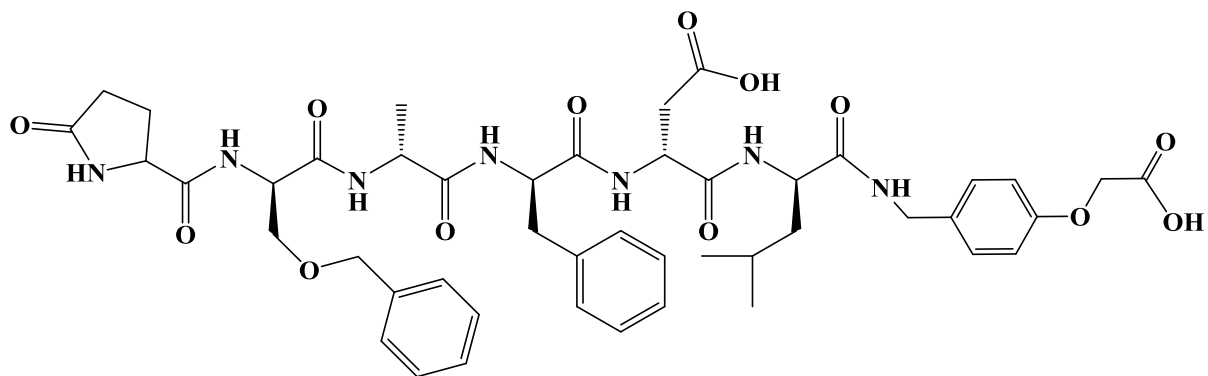


Figure 4.7. Partially deprotected Pyr-SAFDL-Rink-fragment (monoisotopic mass = 915.4 g · mol⁻¹).

4.3.2. LPPS of Partially Deprotected Pyr-SAFDL-NH₂ on H₂N-Rink-DDBA by Precipitation

LPPS of Pyr-Ser(Bzl)-Ala-Phe-Asp-Leu-NH₂ was performed by the precipitation of intermediate products (Table 4.2) in order to check the chemistry, which would be repeated for the subsequent MEPS experiments. The starting concentration of H₂N-Rink-DDBA was 10.2 weight % in THF. 1.05 eq amino acid and coupling reagents were used for each coupling and all couplings went to completion within 30 minutes, showing that the removal of piperidine was satisfactory by washing the precipitated anchored peptide with acetonitrile.

Table 4.2. Summary of results for LPPS by precipitation.

| | | Note |
|---|------------------|---|
| Anchor | DDBA | |
| Linker | Rink | |
| Scale (mmol) | 5.10 | |
| Solvent | THF | |
| Temperature (°C) | Room temperature | 20 – 25 °C |
| Amino Acids and Coupling Reagents (eq) | 1.05 | |
| Starting Concentration (weight% anchor in THF) | 10.2 | |
| Overall Yield (%) | 71.0 | Before Cleavage and Global Deprotection |
| Purity (HPLC) (%) | 100.0 | |
| Overall Yield (%) | 38.7 | After Cleavage and Global Deprotection |
| Purity (HPLC) (%) | 63.1 | |

The major drawback of this approach was the long process time as each intermediate product had to be dried before being dissolved again for the next reaction. Drying was necessary for removing the amount of anti-solvent (acetonitrile) that was trapped in the precipitate, so that the intermediate product could be redissolved in the minimum quantity of solvent (THF). The following reaction could then be performed at the maximum possible concentration, which was advantageous in terms of reaction kinetics and precipitation yield. However, significant loss of material still occurred during precipitations, leading to an overall yield of 71.0 %.

Another critical issue for the process was the decomposition of Rink linker during global deprotection of peptide. As in the case of Fmoc-RADA-NH₂, this resulted in a large yield loss, from

71.0 % to 38.7 %. The fully protected Pyr-SAFDL-Rink was first cleaved from DDBA in mild TFA solution (1 vol % TFA/DCM) and then added into the cleavage cocktail (TFA/TIS, 85/15, v/v), where the cleavage of Rink linker from peptide and its decomposition occurred simultaneously. The addition of more scavenger (TIS) did not improve the relative composition of the target peptide compared to the side product (partially deprotected Pyr-SAFDL-Rink-fragment). Therefore, the purity of the final product was only 63.1 % and partially deprotected Pyr-SAFDL-Rink-fragment counted for the other 19.8 % (Figure 4.8). The identities of the peaks were confirmed by LC/MS results (Figure 4.9).

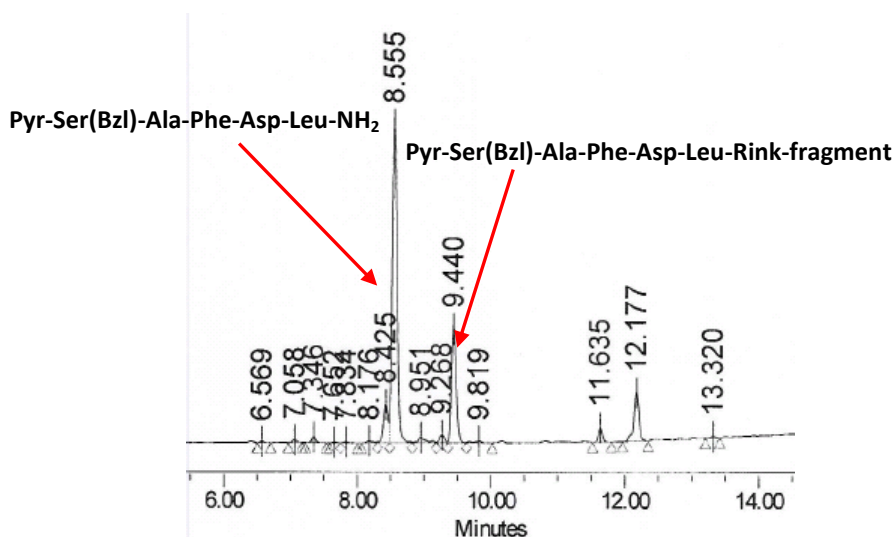
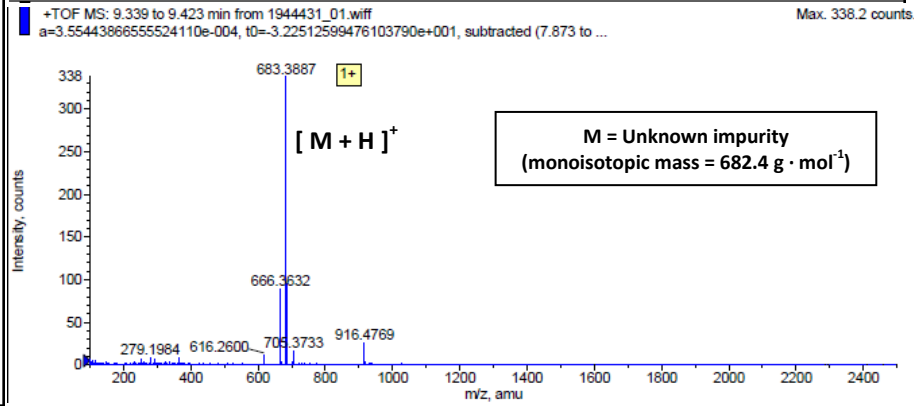
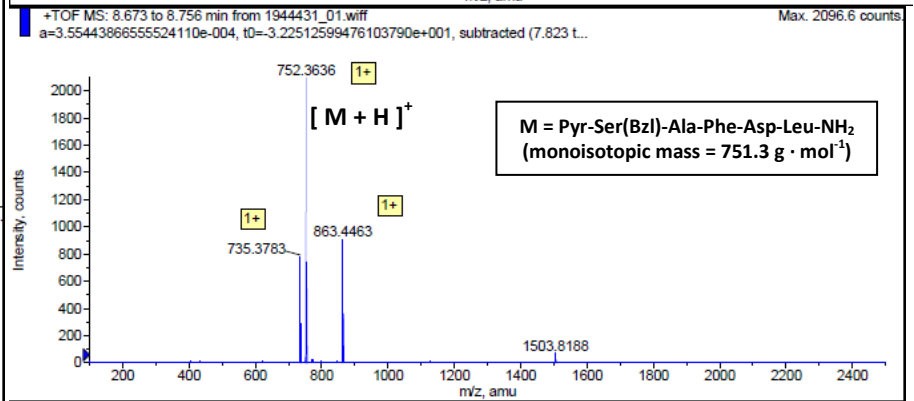
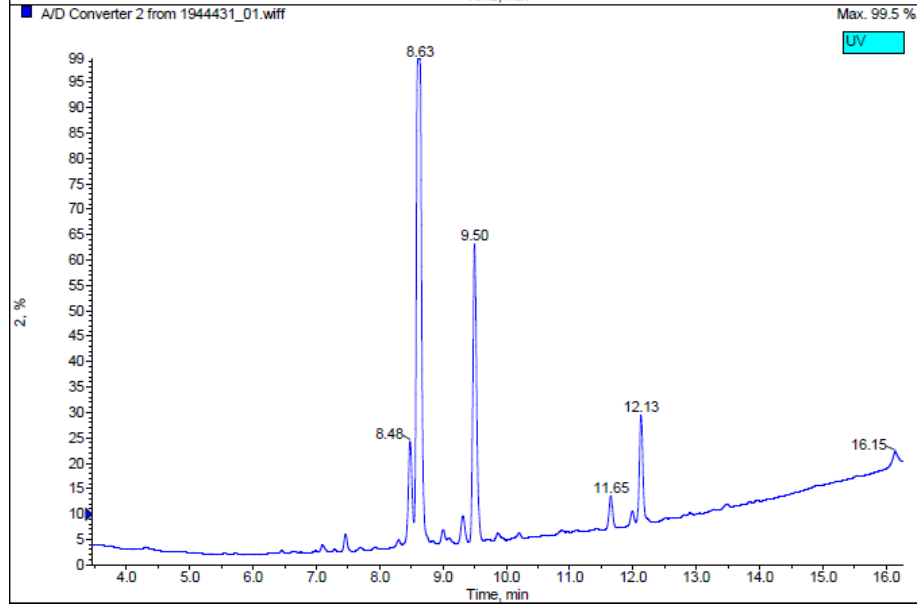
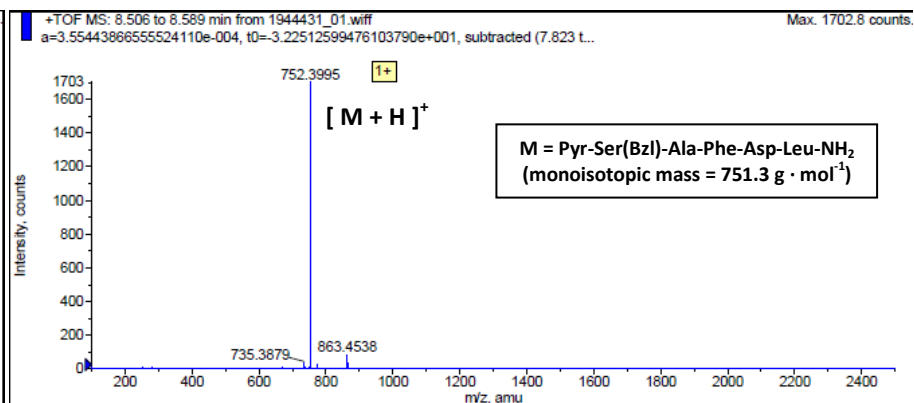
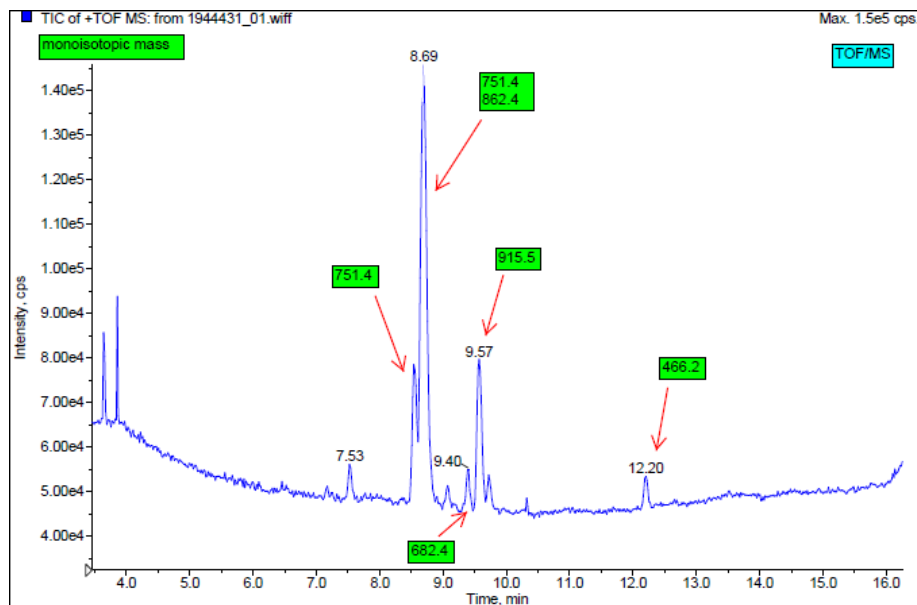


Figure 4.8. HPLC result of the partially deprotected product.



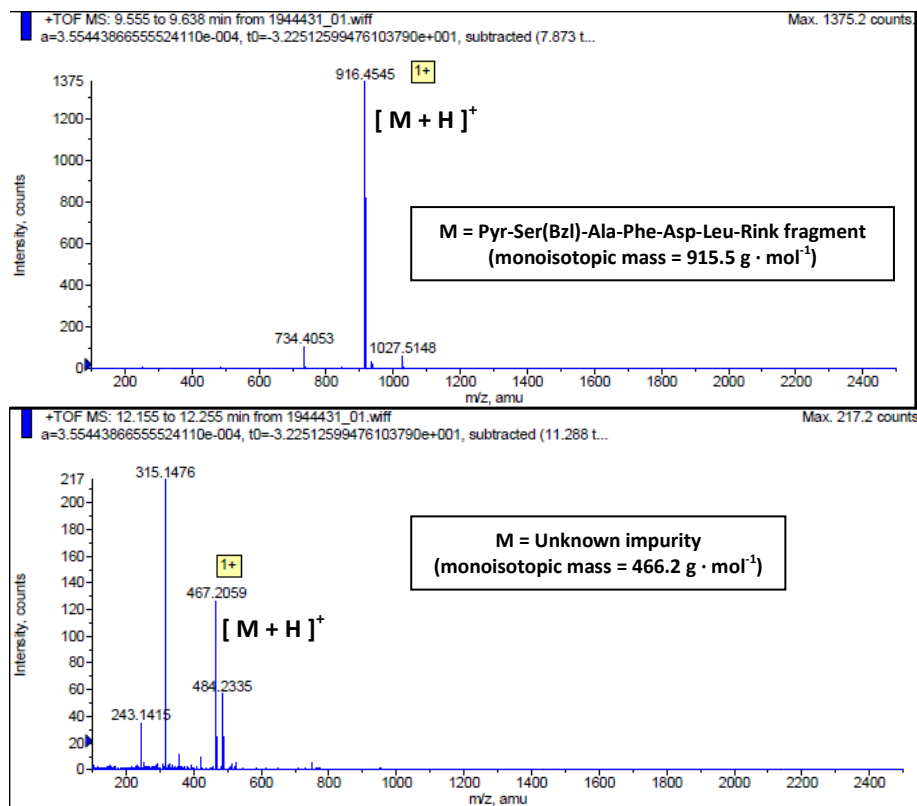


Figure 4.9. LC/MS result of the partially deprotected product (HPLC method: Pyr-SAFDL_HPLC1).

4.3.3. MEPS of Partially Deprotected Pyr-SAFDL-NH₂ on H₂N-Rink-DDBA

Successful LPPS of partially deprotected Pyr-SAFDL-NH₂ and MEPS of the previous tetrapeptide (fully deprotected Fmoc-RADA-NH₂) paved the way for the MEPS of the target hexapeptide. In total, three attempts at MEPS were made (Table 4.3). The peptide was first synthesised with the same chemistry and experimental conditions as the MEPS of fully deprotected Fmoc-RADA-NH₂, and then the synthesis was repeated at a higher concentration of anchor (the starting concentration of anchor increased from 1.5 weight % (first and second attempt) to 10.4 weight % (third attempt)) in order to lower the cost of solvent (normalised by the quantity of product) and to improve the volumetric efficiency for synthesis. The first and second attempt encountered the problem of incomplete couplings and a significant amount of time and effort was invested in understanding and solving this problem. As a result, the reactions proceeded smoothly in the last attempt, which had achieved a decent yield and a high purity before cleavage and global deprotection.

Table 4.3. Summary of results for MEPS.

| | | | | Note |
|--|-----------------|-----------------|-----------------|------|
| Attempt | 1 st | 2 nd | 3 rd | |
| Anchor | DDBA | | | |
| Linker | Rink | | | |
| Scale (mmol) | 5.01 | 4.99 | 33.65 | |
| Solvent | THF | | | |
| Temperature (°C) | 20 | | | |
| System Volume (mL) | 400 | | | |
| Amino Acids and Coupling Reagents (eq) | 1.05 | | | |
| Starting Concentration (weight% anchor in THF) | 1.5 | 1.5 | 10.4 | |
| Overall Yield (%) | NA. | 37.6 | 71.2 | |
| Purity (HPLC) (%) | 54.3 | 90.7 | 88.1 | |
| Overall Yield (%) | NA. | NA. | 32.8 | |
| Purity (HPLC) (%) | NA. | NA. | 47.1 | |

4.3.3.1. MEPS (First Attempt)

In the first attempt, couplings and de-Fmoc were performed with the same chemistry as the MEPS of fully deprotected Fmoc-RADA-NH₂ (1.05 eq amino acid and coupling reagents (HBTU/HOBt); 5.0 weight % piperidine in THF), but the volume of reaction was decreased slightly from 500 mL to 400 mL in order to reduce the volume of solvent used for diafiltrations (e.g. 10 wash volumes would require only 4 L of fresh solvent instead of 5 L). Each de-Fmoc proceeded to completion in 1 hour according to the HPLC results, but the couplings suffered decreasing yields.

After the first de-Fmoc, diafiltration was performed with 14 wash volumes (as for the first MEPS case study) in order to remove piperidine. However, the next coupling only achieved 91.5 % relative yield (Figure 4.10 (a)), which could not be improved even after the diafiltration with 3 more wash volumes and the addition of more reagents (0.1 eq Fmoc-Asp(OtBu)-OH/HBTU/HOBt) (Figure 4.10 (b)).

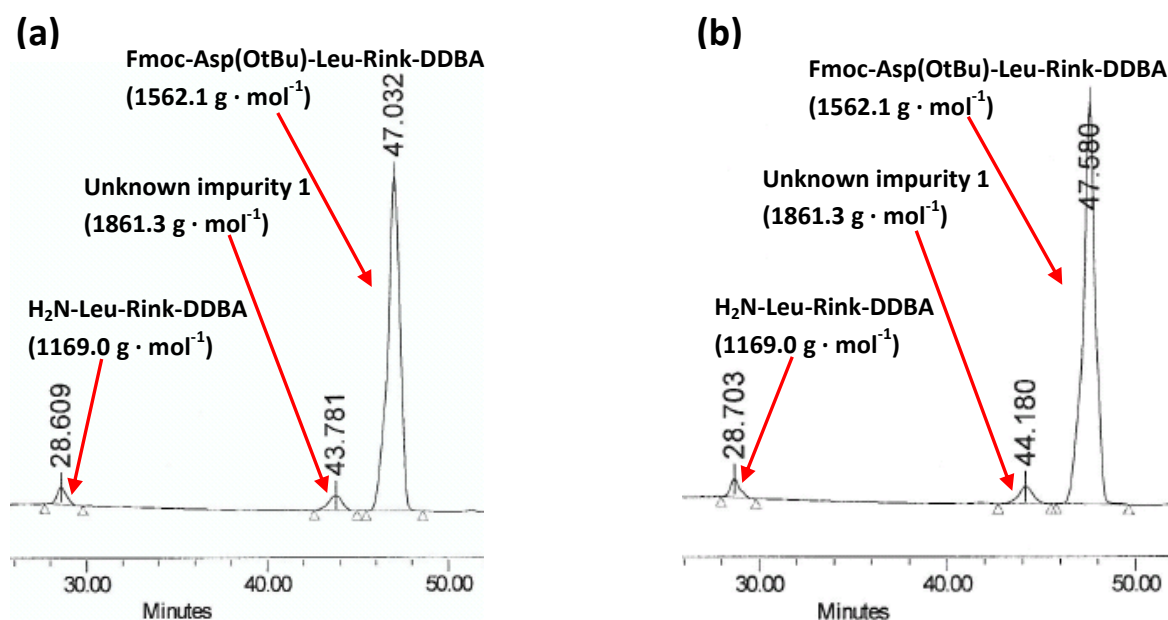


Figure 4.10. Coupling with Fmoc-Asp(OtBu)-OH: (a) 1 hour of reaction; (b) 30 minutes after the diafiltration and addition of reagents. (Monoisotopic mass of component displayed)

The relative yield of the next coupling decreased further to 82.3% after the diafiltration with 14 wash volumes (Figure 4.11). The consistent decrease in coupling yields suggested that 14 wash volumes were not sufficient for the removal of piperidine, which probably interfered with the couplings. Increasing the number of wash volumes seemed ineffective as the yield of coupling of Fmoc-Asp(OtBu)-OH had no significant improvement after the additional diafiltration with 3 wash volumes and recoupling. Therefore, other methods had to be applied in order to facilitate the removal of piperidine at a dilute concentration (since the concentration of piperidine after the fifth wash volume as shown in the first attempt of MEPS of fully deprotected Fmoc-RADA-NH₂ (Section 3.3.8.2.1)) or to reduce the reactivity of residual piperidine.

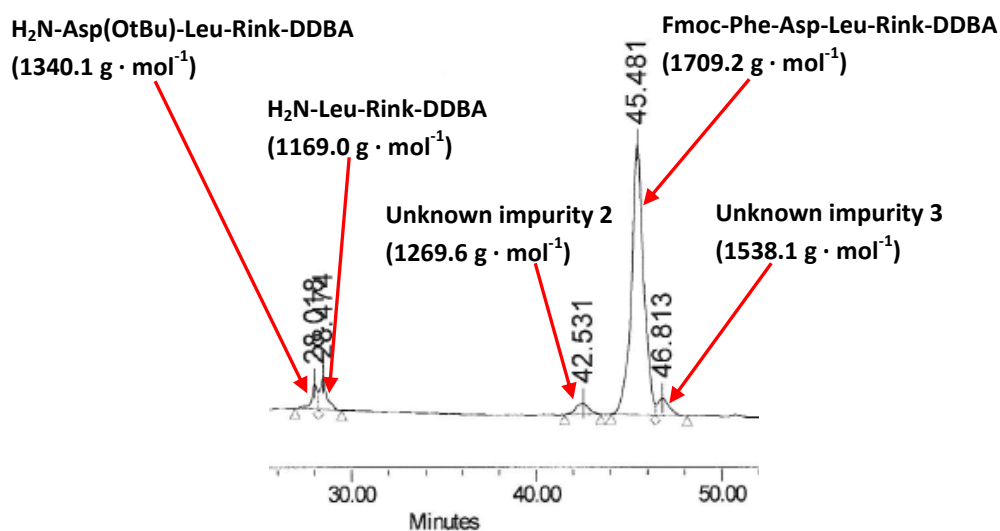


Figure 4.11. Coupling with Fmoc-Phe-OH (30 minutes of reaction). (Monoisotopic mass of component displayed)

As piperidine is a base, its retention may be due to charge effects on the membrane surface. The removal of piperidine might be enhanced by neutralising it with an acidic compound such as HOBT, which was used as the racemisation suppressor in both coupling and de-Fmoc. Based on this hypothesis, after the de-Fmoc of Fmoc-Phe-Asp(OtBu)-Leu-Rink-DDBA, HOBT was added into the system during diafiltration (14 wash volumes). One portion of HOBT (same quantity as in de-Fmoc) was added after the 2nd, 4th, 6th and 8th wash volume, but the relative yield of the next coupling continued to decrease. Worse still, the extent of reduction (from 82.3% to 59.9%) was even greater than the previous two couplings (from 95.5% to 91.5%; from 91.5% to 82.3%). The deprotected peptide fragments (H₂N-Phe-Asp(OtBu)-Leu-Rink-DDBA and H₂N-Asp(OtBu)-Leu-Rink-DDBA) were not consumed by side reactions and counted for the other 35.5% of relative yield (Figure 4.12). The additions of HOBT apparently increased the retention of piperidine, probably due to the size of the salt (piperidine · OBt).

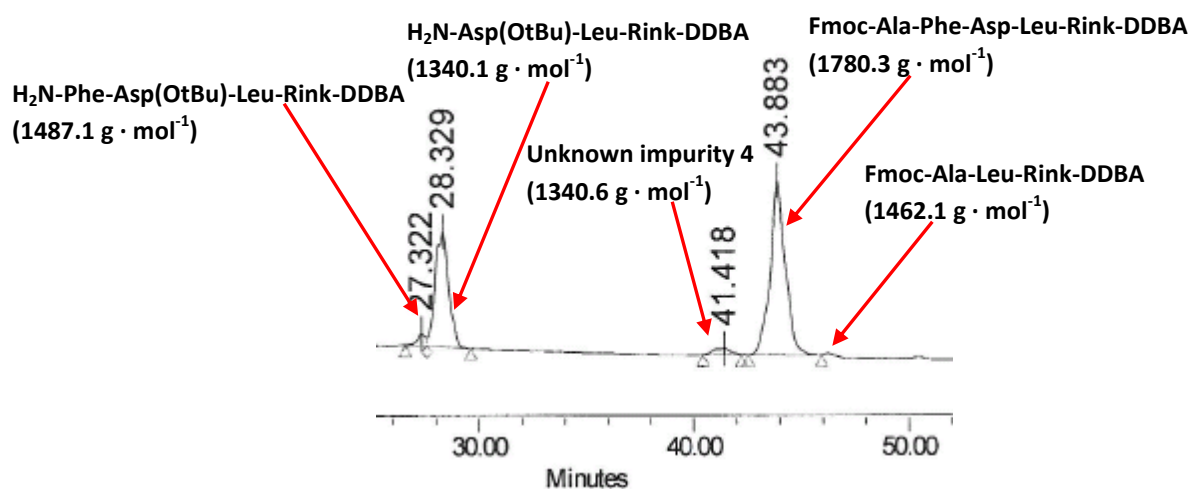


Figure 4.12. Coupling with Fmoc-Ala-OH (30 minutes of reaction). (Monoisotopic mass of component displayed)

Another mitigation method was tested during the diafiltration (12 wash volumes) after the next de-Fmoc (the de-Fmoc of Fmoc-Ala-Phe-Asp(OtBu)-Leu-Rink-DDBA). Aqueous hydrochloric acid (concentration = 1 M) was added into the system after the 6th, 8th and 10th wash volume in order to create an acidic environment for the removal of piperidine (overall pH was adjusted to the range between 4 and 7). However, the relative yield of the next coupling (with Fmoc-Ser(Bzl)-OH) decreased further to 44.1% (Figure 4.13 (a)). The relative yield of truncated sequence (Fmoc-Ser(Bzl)-Phe-Asp(OtBu)-Leu-Rink-DDBA) was 15.9% and the deprotected anchor fragments (H₂N-Ala-Phe-Asp(OtBu)-Leu-Rink-DDBA, H₂N-Phe-Asp(OtBu)-Leu-Rink-DDBA; H₂N-Asp(OtBu)-Leu-Rink-DDBA) counted for the other 37.8 %. Diafiltration with 3 wash volumes and recoupling (1.00 eq Fmoc-Ser(Bzl)-OH and coupling reagents) were performed. The relative yield of the desired product and the truncated sequence increased to 54.3 % and 26.6 % respectively, while that of the deprotected peptide fragments decreased to 15.0 % (Figure 4.13 (b)). These results showed that making the system acidic was not effective in the removal of piperidine. Furthermore, deprotected peptide fragments were not completely consumed even after recoupling, suggesting that the mere presence of piperidine significantly hindered the coupling step. The mechanism of piperidine interference was studied in depth and is discussed in the following section of this chapter. Lastly, the coupling kinetics seemed to be similar for both H₂N-Ala-Phe-Asp(OtBu)-Leu-Rink-DDBA and its shorter predecessor (H₂N-Phe-Asp(OtBu)-Leu-Rink-DDBA), as the relative yield of the corresponding products with Ser(Bzl) increased by the same extent after the recoupling.

(a)

$\text{H}_2\text{N-Ala-Phe-Asp(OtBu)-Leu-Rink-DDBA}$ ($1558.1 \text{ g} \cdot \text{mol}^{-1}$)

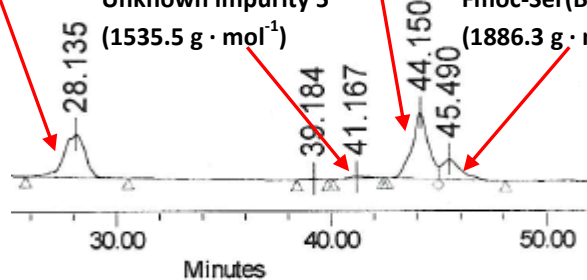
$\text{H}_2\text{N-Phe-Asp(OtBu)-Leu-Rink-DDBA}$ ($1487.1 \text{ g} \cdot \text{mol}^{-1}$)

$\text{H}_2\text{N-Asp(OtBu)-Leu-Rink-DDBA}$ ($1340.1 \text{ g} \cdot \text{mol}^{-1}$)

$\text{Fmoc-Ser(Bzl)-Ala-Phe-Asp-Leu-Rink-DDBA}$ ($1957.3 \text{ g} \cdot \text{mol}^{-1}$)

Unknown impurity 5
($1535.5 \text{ g} \cdot \text{mol}^{-1}$)

$\text{Fmoc-Ser(Bzl)-Phe-Asp-Leu-Rink-DDBA}$
($1886.3 \text{ g} \cdot \text{mol}^{-1}$)



(b)

$\text{H}_2\text{N-Ala-Phe-Asp(OtBu)-Leu-Rink-DDBA}$ ($1558.1 \text{ g} \cdot \text{mol}^{-1}$)

$\text{H}_2\text{N-Phe-Asp(OtBu)-Leu-Rink-DDBA}$ ($1487.1 \text{ g} \cdot \text{mol}^{-1}$)

$\text{H}_2\text{N-Asp(OtBu)-Leu-Rink-DDBA}$ ($1340.1 \text{ g} \cdot \text{mol}^{-1}$)

$\text{Fmoc-Ser(Bzl)-Ala-Phe-Asp-Leu-Rink-DDBA}$ ($1957.3 \text{ g} \cdot \text{mol}^{-1}$)

Unknown impurity 5
($1535.5 \text{ g} \cdot \text{mol}^{-1}$)

$\text{Fmoc-Ser(Bzl)-Phe-Asp-Leu-Rink-DDBA}$
($1886.3 \text{ g} \cdot \text{mol}^{-1}$)

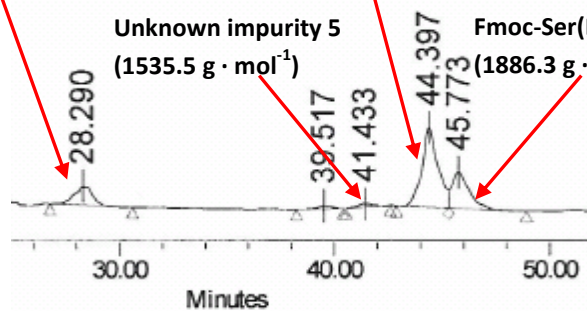


Figure 4.13. Coupling with Fmoc-Ser(Bzl)-OH: (a) 30 minutes of reaction; (b) 30 minutes after the diafiltration and addition of reagents. (Monoisotopic mass of component displayed)

4.3.3.2. Side Reaction Induced by Piperidine and Tests of Mitigation Method

The effect of piperidine on the activated amino acids was studied in small-scale tests (Table 4.4). All amino acids in the target sequence except H-Pyr-OH were UV-active and hence the reactions could be tracked with HPLC. Each amino acid was activated with HBTU (0.5 - 1.3 eq) and HOBT (0.6 - 1.3 eq) in the presence of DIEA (1.8 - 3.0 eq) for 10 minutes before the addition of piperidine (1.0 - 1.4 eq). The concentration of amino acid was kept at 0.9 weight % in order to mimic the conditions of the first attempt. The corresponding concentration of piperidine was only 0.2 weight % in order to show the effect of residual piperidine on the activated amino acids.

HPLC results showed that both amino acid and its activated form (Fmoc-X-OBt, X=Ala, Leu, Phe, Asp(OtBu) and Ser(Bzl)) coexisted after activation and the relative yield of the activated form depended on the quantity of the activator. For example, 0.5 eq of HBTU resulted in only 29.8 % relative yield of Fmoc-Ala-OBt, while the relative yield of Fmoc-Leu-OBt was significantly higher (75.4 %) in the presence of 1.1 eq HBTU. Upon the addition of piperidine, all the amino acid and its activated form were consumed to give the side product, Fmoc-X-piperidine (Figure 4.14), as in the case of Fmoc-Leu-OH, Fmoc-Phe-OH and Fmoc-Ser(Bzl)-OH, where 1.0 eq or more HBTU was present. For Fmoc-Ala-OH and Fmoc-Asp(OtBu)-OH, the yields of the piperidine-induced side product relative to the amino acid (56.9 and 62.9 %) corresponded well to the quantities of HBTU (0.5 and 0.6 eq). Furthermore, deprotection of the amino acid by equivalent amount of piperidine was not observed in the HPLC results for Fmoc-Phe-OH, which would otherwise have a UV-active H₂N-Phe-OH.

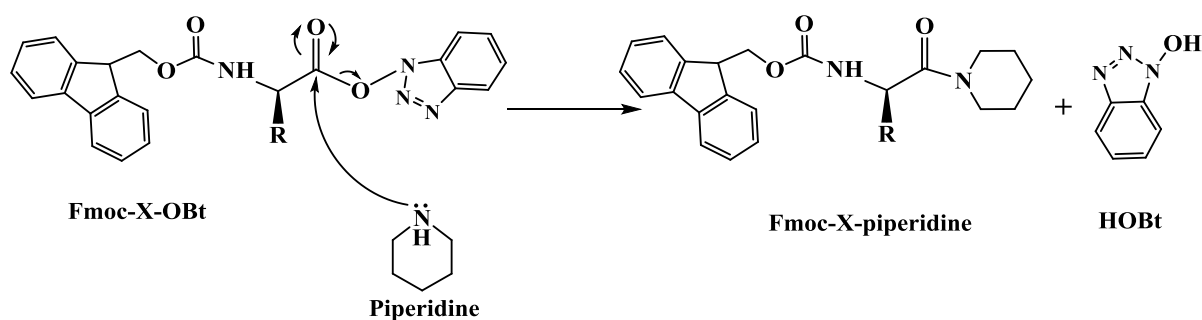


Figure 4.14. Formation of Fmoc-X-piperidine.

Table 4.4. Summary of results for the small-scale tests.

| Activation of Fmoc-Ala-OH, followed by the addition of piperidine | | | | | | | | | |
|--|------|--------------------------|------------------------|---------------------|------------------------------|--------------------|---------------------------|------------------------------|--------------------|
| Scale*(mmol) | Step | Concentration (weight %) | Fmoc-Ala-OH (eq) | HBTU (eq) | HOBT (eq) | DIEA (eq) | Reaction Time (min) | Relative Yield (%) (by HPLC) | |
| 0.32 | 1 | Fmoc-Ala-OH | 1.0 | 0.5 | 0.6 | 2.3 | 10 | Fmoc-Ala-OH | Fmoc-Ala-OBt |
| | | 0.9 | | | | | | 70.2 | 29.8 |
| | 2 | Concentration (weight %) | Piperidine (eq) | Reaction Time (min) | Relative Yield (%) (by HPLC) | | | | |
| | | Piperidine | | | Fmoc-Ala-OH | Fmoc-Ala-OBt | Fmoc-Ala-piperidine | | |
| 0.2 | 1.0 | 10 | 43.1 | 0.0 | 56.9 | | | | |
| Activation of Fmoc-Leu-OH, followed by the addition of piperidine | | | | | | | | | |
| Scale*(mmol) | Step | Concentration (weight %) | Fmoc-Leu-OH (eq) | HBTU (eq) | HOBT (eq) | DIEA (eq) | Reaction Time (min) | Relative Yield (%) (by HPLC) | |
| 0.28 | 1 | Fmoc-Leu-OH | 1.0 | 1.1 | 1.1 | 2.5 | 10 | Fmoc-Leu-OH | Fmoc-Leu-OBt |
| | | 0.8 | | | | | | 24.5 | 75.4 |
| | 2 | Concentration (weight %) | Piperidine (eq.) | Reaction Time (min) | Relative Yield (%) (by HPLC) | | | | |
| | | Piperidine | | | Fmoc-Leu-OH | Fmoc-Leu-OBt | Fmoc-Leu-piperidine | | |
| 0.2 | 0.9 | 10 | 0.0 | 0.0 | 100.0 | | | | |
| Activation of Fmoc-Phe-OH, followed by the addition of piperidine | | | | | | | | | |
| Scale*(mmol) | Step | Concentration (weight %) | Fmoc-Phe-OH (eq) | HBTU (eq) | HOBT (eq) | DIEA (eq) | Reaction Time (min) | Relative Yield (%) (by HPLC) | |
| 0.24 | 1 | Fmoc-Phe-OH | 1.0 | 1.3 | 1.3 | 3.0 | 10 | Fmoc-Phe-OH | Fmoc-Phe-OBt |
| | | 0.8 | | | | | | 48.3 | 51.7 |
| | 2 | Concentration (weight %) | Piperidine (eq) | Reaction Time (min) | Relative Yield (%) (by HPLC) | | | | |
| | | Piperidine | | | Fmoc-Phe-OH | Fmoc-Phe-OBt | Fmoc-Phe-piperidine | | |
| 0.2 | 1.3 | 10 | 0.0 | 0.0 | 100.0 | | | | |
| Activation of Fmoc-Asp(OtBu)-OH, followed by the addition of piperidine | | | | | | | | | |
| Scale*(mmol) | Step | Concentration (weight %) | Fmoc-Asp(OtBu)-OH (eq) | HBTU (eq) | HOBT (eq) | DIEA (eq) | Reaction Time (min) | Relative Yield (%) (by HPLC) | |
| 0.24 | 1 | Fmoc-Asp(OtBu)-OH | 1.0 | 0.6 | 0.8 | 1.8 | 10 | Fmoc-Asp(OtBu)-OH | Fmoc-Asp(OtBu)-OBt |
| | | 0.9 | | | | | | 81.0 | 19.1 |
| | 2 | Concentration (weight %) | Piperidine (eq) | Reaction Time (min) | Relative Yield (%) (by HPLC) | | | | |
| | | Piperidine | | | Fmoc-Asp(OtBu)-OH | Fmoc-Asp(OtBu)-OBt | Fmoc-Asp(OtBu)-piperidine | | |
| 0.2 | 1.1 | 10 | 37.1 | 0.0 | 62.9 | | | | |
| Activation of Fmoc-Ser(Bzl)-OH, followed by the addition of piperidine | | | | | | | | | |
| Scale*(mmol) | Step | Concentration (weight %) | Fmoc-Ser(Bzl)-OH (eq) | HBTU (eq) | HOBT (eq) | DIEA (eq) | Reaction Time (min) | Relative Yield (%) (by HPLC) | |
| 0.24 | 1 | Fmoc-Ser(Bzl)-OH | 1.0 | 1.3 | 1.3 | 3.0 | 10 | Fmoc-Ser(Bzl)-OH | Fmoc-Ser(Bzl)-OBt |
| | | 0.9 | | | | | | 31.6 | 68.4 |
| | 2 | Concentration (weight %) | Piperidine (eq) | Reaction Time (min) | Relative Yield (%) (by HPLC) | | | | |
| | | Piperidine | | | Fmoc-Ser(Bzl)-OH | Fmoc-Ser(Bzl)-OBt | Fmoc-Ser(Bzl)-piperidine | | |
| 0.2 | 1.4 | 10 | 0.0 | 0.0 | 100.0 | | | | |

*With respect to the amino acid.

These results suggested that equivalent amount of piperidine tend to react with all the activated amino acid available to form Fmoc-X-piperidine (Figure 4.14) even at dilute concentration (0.2 weight%) within 10 minutes. Unlike activated amino acid, which seemed to be in equilibrium with the unactivated form, the formation of the piperidine-induced side product was apparently irreversible (hence the 100 % relative yield in the case of Fmoc-Leu-OH, Fmoc-Phe-OH and Fmoc-Ser(Bzl)-OH).

In the first attempt at MEPS, close-to-equivalent amount of amino acids (1.05 eq) were used and couplings proceeded with decreasing yields, implying that only some of the activated amino acids were consumed by piperidine. In other words, the quantity of piperidine remaining in the system after each diafiltration was less than 5.26 mmol (amount of amino acid added into the system for each coupling) in 400 mL (the system volume), corresponding to a maximum concentration of only 0.01 M. At such a dilute concentration, further removal of piperidine by increasing the wash volume was ineffective as the diafiltration required relatively large quantity of solvent to remove only a small percentage of this critical impurity. A better strategy was therefore the removal of minute amounts of piperidine by the addition of compounds that could react selectively with piperidine, but not with the deprotected peptide fragment.

Four small-scale tests were performed (Table 4.5). In the first test, Fmoc-Phe-OH was first activated with HBTU and HOBt, followed by the addition of piperidine. As a result, all the activated Fmoc-Phe-OH was consumed by piperidine to form the side product. H₂N-Leu-Rink-DDBA was then added into this mixture, but no formation of Fmoc-Phe-Leu-Rink-DDBA was observed after one hour of reaction. Instead, H₂N-Leu-Rink-DDBA apparently underwent a side reaction in the presence of excess HBTU (approx. 2.9 eq) and base (18.2 eq DIEA) to give guanidine (Figure 4.15). The addition of more DIEA (35.6 eq) failed to promote the desired coupling, but resulted in more guanidine (relative yield increased from 13.9 to 22.3%). Aqueous hydrochloric acid was then added into the mixture to lower the pH (4 - 5), but the relative yield of guanidine remained unchanged overnight, showing that the formation of guanidine could not be reversed even in acidic conditions.

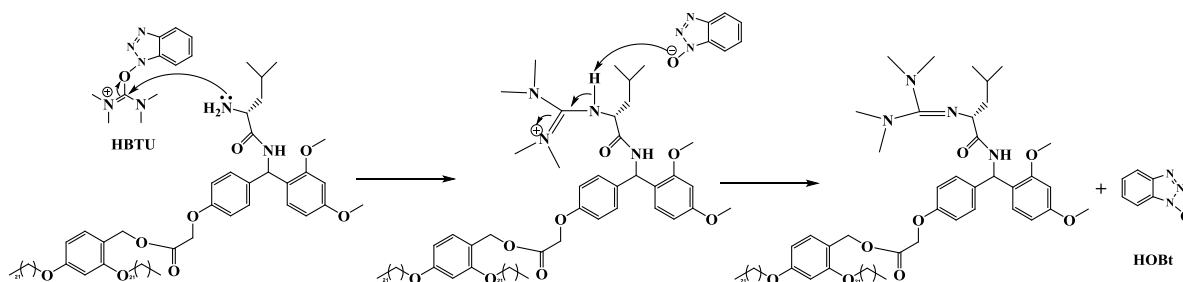


Figure 4.15. Formation of guanidine.

Table 4.5. Summary of results for the tests of mitigation method.

| Test 1: Addition of more DIEA. | | | | | | | | | |
|---|--|--|-------------------------------------|--------------------------------|--------------------------------|---------------------|------------------------------|------------------------------|---------------------|
| Scale (mmol) | Step | Concentration of Fmoc-Phe-OH (weight %) | Fmoc-Phe-OH (eq) | HBTU (eq) | HOBT (eq) | DIEA (eq) | Reaction Time (min) | Relative Yield (%) (by HPLC) | |
| | | | | | | | | Fmoc-Phe-OH | Fmoc-Phe-OBt |
| 0.045* | 1 | 0.9 | 5.8 | 8.7 | 8.9 | 18.2 | 10 | 47.4 | 52.6 |
| | 2 | Concentration of Piperidine (weight %) | Piperidine (eq) | Reaction Time (min) | Relative Yield (%) (by HPLC) | | | | |
| | | | | | Fmoc-Phe-OH | Fmoc-Phe-OBt | Fmoc-Phe-piperidine | | |
| | | 0.3 | 7.8 | 10 | 0.0 | 0.0 | 100.0 | | |
| | 3 | Concentration of H ₂ N-Leu-Rink-DDBA (weight %) | H ₂ N-Leu-Rink-DDBA (eq) | Reaction Time (min) | Relative Yield (%) (by HPLC) | | | | |
| | | | | | H ₂ N-Leu-Rink-DDBA | Guanidine | Fmoc-Phe-piperidine | | |
| | | 0.5 | 1.0 | 60 | 18.1 | 13.9 | 68.0 | | |
| | 4 | | DIEA (eq) | Reaction Time (min) | Relative Yield (%) (by HPLC) | | | | |
| | | | | | H ₂ N-Leu-Rink-DDBA | Guanidine | Fmoc-Phe-piperidine | | |
| | | | 35.6 | 60 | 11.4 | 22.3 | 66.3 | | |
| 5 | | HCl/H ₂ O (eq) | Reaction Time | Relative Yield (%) (by HPLC) | | | | | |
| | | | | H ₂ N-Leu-Rink-DDBA | Guanidine | Fmoc-Phe-piperidine | | | |
| | | 3.0** | Overnight | 9.7 | 23.9 | 66.4 | | | |
| Test 2: Addition of 1-methyl-1-cyclohexene | | | | | | | | | |
| Scale (mmol) | Step | Concentration (weight %) | Fmoc-Phe-OH (eq) | HBTU (eq) | HOBT (eq) | DIEA (eq) | Reaction Time (min) | Relative Yield (%) (by HPLC) | |
| | | | | | | | | Fmoc-Phe-OH | Fmoc-Phe-OBt |
| 0.044# | 1 | 0.9 | 5.9 | 8.9 | 9.2 | 19.0 | 10 | 46.4 | 53.6 |
| | | | | | | | | Relative Yield (%) | |
| | 2 | | 1-methyl-1-cyclohexene (eq) | Reaction Time (min) | Relative Yield (%) | | | | |
| | | | | | Fmoc-Phe-OH | Fmoc-Phe-OBt | | | |
| | | | 9.5 | 10 | 44.2 | 55.9 | | | |
| | 3 | Concentration of Piperidine (weight %) | Piperidine (eq) | Reaction Time (min) | Relative Yield (%) (by HPLC) | | | | |
| Fmoc-Phe-OH | | | | | Fmoc-Phe-OBt | Fmoc-Phe-piperidine | | | |
| | 0.2 | 6.0 | 10 | 0.0 | 0.0 | 100.0 | | | |
| 4 | Concentration of H ₂ N-Leu-Rink-DDBA (weight %) | H ₂ N-Leu-Rink-DDBA (eq) | Reaction Time (min) | Relative Yield (%) (by HPLC) | | | | | |
| | | | | H ₂ N-Leu-Rink-DDBA | Guanidine | Fmoc-Phe-piperidine | | | |
| | 0.4 | 1.0 | 60 | 43.5 | 21.6 | 34.8 | | | |
| Test 3: Addition of Methylene-cyclopentane | | | | | | | | | |
| Scale (mmol) | Step | Concentration (weight %) | Piperidine (eq) | Methylene-cyclopentane (eq) | | | Reaction Time (min) | Relative Yield (%) (by HPLC) | |
| | | | | Fmoc-Phe-OH (eq) | HBTU (eq) | HOBT (eq) | | DIEA (eq) | Fmoc-Phe-OBt |
| 0.25 | 1 | Piperidine | 1.6 | 1.7 | | | 10 | Relative Yield (%) (by HPLC) | |
| | | | | 0.3 | | | | | |
| | 2 | Concentration (weight %) | Fmoc-Phe-OH (eq) | HBTU (eq) | HOBT (eq) | DIEA (eq) | Relative Yield (%) (by HPLC) | | |
| | | | | | | | Fmoc-Phe-OH | Fmoc-Phe-OBt | Fmoc-Phe-piperidine |
| | 0.9 | 1.0 | 1.6 | 4.5 | 3.6 | 3.3 | 96.7 | | |

| Test 4: Addition of Chloranil | | | | | | | | | |
|--------------------------------------|------------|--------------------------|------------------|----------------|---------------------|------------------------------|---------------------|------------------------------|--------------|
| Scale (mmol) | Step | Concentration (weight %) | Fmoc-Phe-OH (eq) | HBTU (eq) | HOBt (eq) | DIEA (eq) | Reaction Time (min) | Relative Yield (%) (by HPLC) | |
| | | Fmoc-Phe-OH | | | | | | Fmoc-Phe-OH | Fmoc-Phe-OBt |
| 0.26 | 1 | 0.8 | 1.0 | 1.5 | 1.6 | 3.3 | 10 | 48.1 | 51.9 |
| | | Concentration (weight %) | Piperidine (eq) | Chloranil (eq) | Reaction Time (min) | Relative Yield (%) (by HPLC) | | | |
| | Piperidine | | | | Fmoc-Phe-OH | Fmoc-Phe-OBt | Fmoc-Phe-piperidine | | |
| | 0.2 | 1.1 | 1.1 | 10 | 12.4 | 0.0 | 87.6 | | |

*H₂N-Leu-Rink-DDBA

**pH = 4 – 5

#H₂N-Leu-Rink-DDBA

Three compounds (Figure 4.16) were tested in an attempt to find a suitable candidate, with which piperidine could react preferentially over the activated amino acid. The first two compounds were alkenes, which were inspired by the reaction between piperidine and dibenzofulvene (Figure 2.11 in the literature review (Section 2.1.4)). The last one was chloranil, which is frequently used to detect low concentration of piperidine in the washing solvent in standard SPPS procedure. In the presence of these compounds (1.0 - 1.6 eq with respect to piperidine), the formation of Fmoc-Phe-piperidine could not be suppressed significantly (relative yields were 87.6 %, 96.7 % and 100.0 % for chloranil, methylenecyclopentane and 1-methyl-1-cyclohexene respectively), showing that this approach was ineffective for the mitigation of the piperidine-induced side reaction.

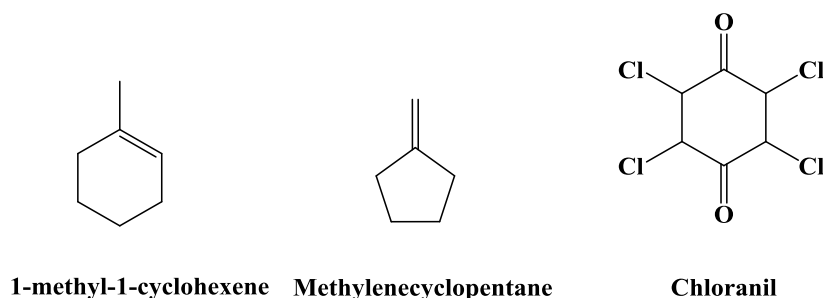


Figure 4.16. Compounds tested for the mitigation of piperidine-induced side reaction (Test 2 to 4 in Table 4.5).

4.3.3.3. Replacement of Piperidine with Diethylamine (DEA) for De-Fmoc

Since the problem of residual piperidine was the reactive nature of the base towards activated amino acids, a milder base that could also be used for the de-Fmoc of peptide was tested, in the hope that its affinity to the activated amino acid was less than that of piperidine.

Diethylamine (DEA) was chosen as the potential candidate to replace piperidine in MEPS, as it is another commonly used base for de-Fmoc and is milder than piperidine ($pK_b = 11.09$ as compared to 11.22). Consequently, DEA is not reactive towards dibenzofulvene, which would otherwise be consumed by piperidine immediately upon its formation as a by-product of the de-Fmoc step. Small-scale tests were carried out for the deprotection of Fmoc-Leu-Rink-DDBA by DEA and then its reaction in the presence of activated Fmoc-Phe-OH.

Each deprotection of anchored peptide (starting concentration = 1.0 weight % H_2N -Rink-DDBA in THF) by piperidine (5.0 weight %) was complete within 1 hour as in the first MEPS of partially deprotected Pyr-SAFDL- NH_2 , but the deprotection of Fmoc-Leu-Rink-DDBA by DEA was significantly slower (Figure 4.17). At 1.0 weight % Fmoc-Leu-Rink-DDBA and 5.7 weight % DEA, de-Fmoc was complete only after 3 hours. Increasing the concentration of the base to 8.2 - 10.2 weight % reduced the time to 2 hours, but increasing the concentration of Fmoc-Leu-Rink-DDBA from 1.0 to 7.8 weight % made no observable improvement in the kinetics. The longer deprotection confirmed that DEA was indeed milder than piperidine.

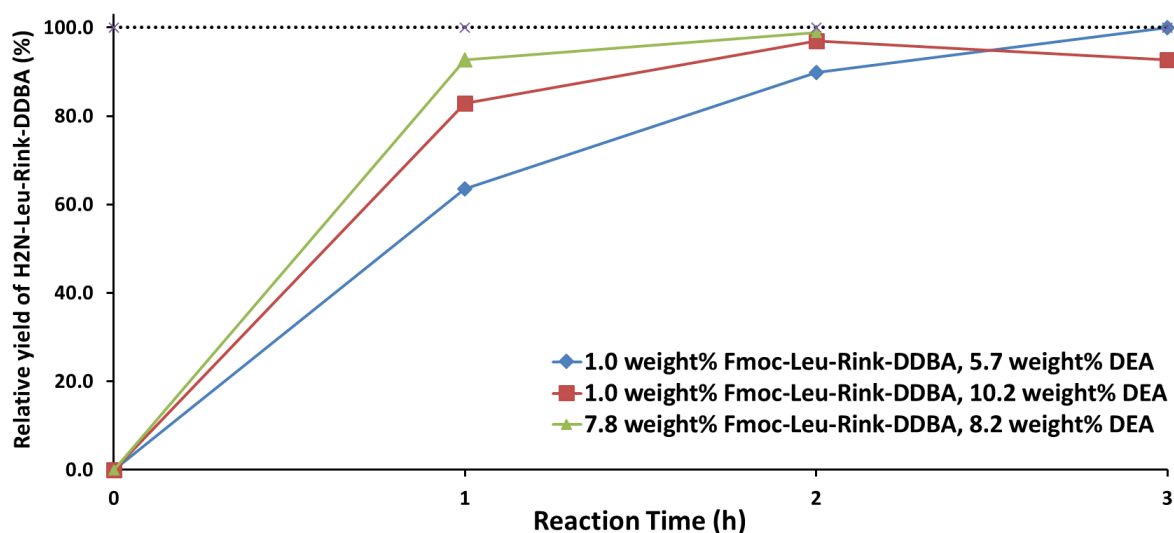


Figure 4.17. Deprotection of Fmoc-Leu-Rink-DDBA by DEA.

When added into a solution of activated Fmoc-Phe-OH (Table 4.6), DEA readily consumed all the activated amino acid to form the side product (relative yield = 100.0 %), which remained stable in the presence of H₂N-Leu-Rink-DDBA.

Table 4.6. Effect of diethylamine on activated Fmoc-Phe-OH.

| Scale* (mmol) | Step | Concentration (weight %) | Fmoc-Phe-OH (eq) | HBTU (eq) | HOBt (eq) | DIEA (eq) | Reaction Time (min) | Relative Yield (%) (by HPLC) | |
|---------------|------|--------------------------------|--------------------------------------|---------------------|------------------------------|--------------------------------|-----------------------|------------------------------|--------------|
| | | | | | | | | Fmoc-Phe-OH | Fmoc-Phe-OBt |
| 0.26 | 1 | Fmoc-Phe-OH | 1.0 | 1.5 | 1.6 | 4.5 | 10 | 47.9 | 52.1 |
| | | 0.8 | | | | | | | |
| | 2 | Concentration (weight %) | Diethylamine (eq) | Reaction Time (min) | Relative Yield (%) (by HPLC) | | | | |
| | | Diethylamine | | | Fmoc-Phe-OH | Fmoc-Phe-OBt | Fmoc-Phe-diethylamide | | |
| | | 0.2 | 1.2 | 10 | 0.0 | 0.0 | 100.0 | | |
| | 3 | Concentration (weight %) | H ₂ N-Leu-Rink-DDBA (eq.) | DIEA (eq) | Reaction Time (min) | Relative Yield (%) (by HPLC) | | | |
| | | H ₂ N-Leu-Rink-DDBA | | | | H ₂ N-Leu-Rink-DDBA | Guanidine | Fmoc-Phe-diethylamide | |
| | | NA. | 1.0 | 28.9 | 60 | 40.7 | 27.1 | 32.2 | |

*With respect to amino acid.

In summary, all the tests of mitigation method did not lead to a solution to the problem of residual base (piperidine) and hence the removal of the base had to still rely on diafiltration. As DEA has a linear structure as compared to the ring structure of piperidine, it might be removed more efficiently by diafiltration as linear compounds are known to permeate through membrane more readily than their branched counterparts (Zheng, Li, Yuan, & Vriesekoop, 2008). Therefore, DEA was used for de-Fmoc in the next attempt of MEPS.

4.3.3.4. MEPS (Second Attempt)

In the second attempt at MEPS, the first de-Fmoc was performed with 15.9 weight % DEA and was complete after 2 hours. A significant amount of white solid appeared due to the formation of dibenzofulvene. Diafiltration was then performed with 16 wash volumes. Chloranil tests for the samples of retentate and permeate had negative results after the 10th wash volume. Small-scale coupling tests showed that the yield of coupling after the 10th wash volume remained relatively constant (91.6 - 93.3 %) with 1.07 - 1.51 eq Fmoc-Aps(OtBu)-OH (Figure 4.18 (a) to (e)). These results suggested that the removal of DEA by diafiltration was inefficient after the 10th wash volume and minute amounts of the base remained persistently in the system. This is similar to the results for piperidine, and suggests that the initial assumption of better removal of DEA through the same membrane was incorrect. Together with the problem of solid formation and longer reaction, this rendered DEA unsuitable for MEPS as compared to piperidine. The relative yield of the next coupling with Fmoc-Asp(OtBu)-OH decreased to 89.2 % from 95.5 % (loading of Fmoc-Leu-OH).

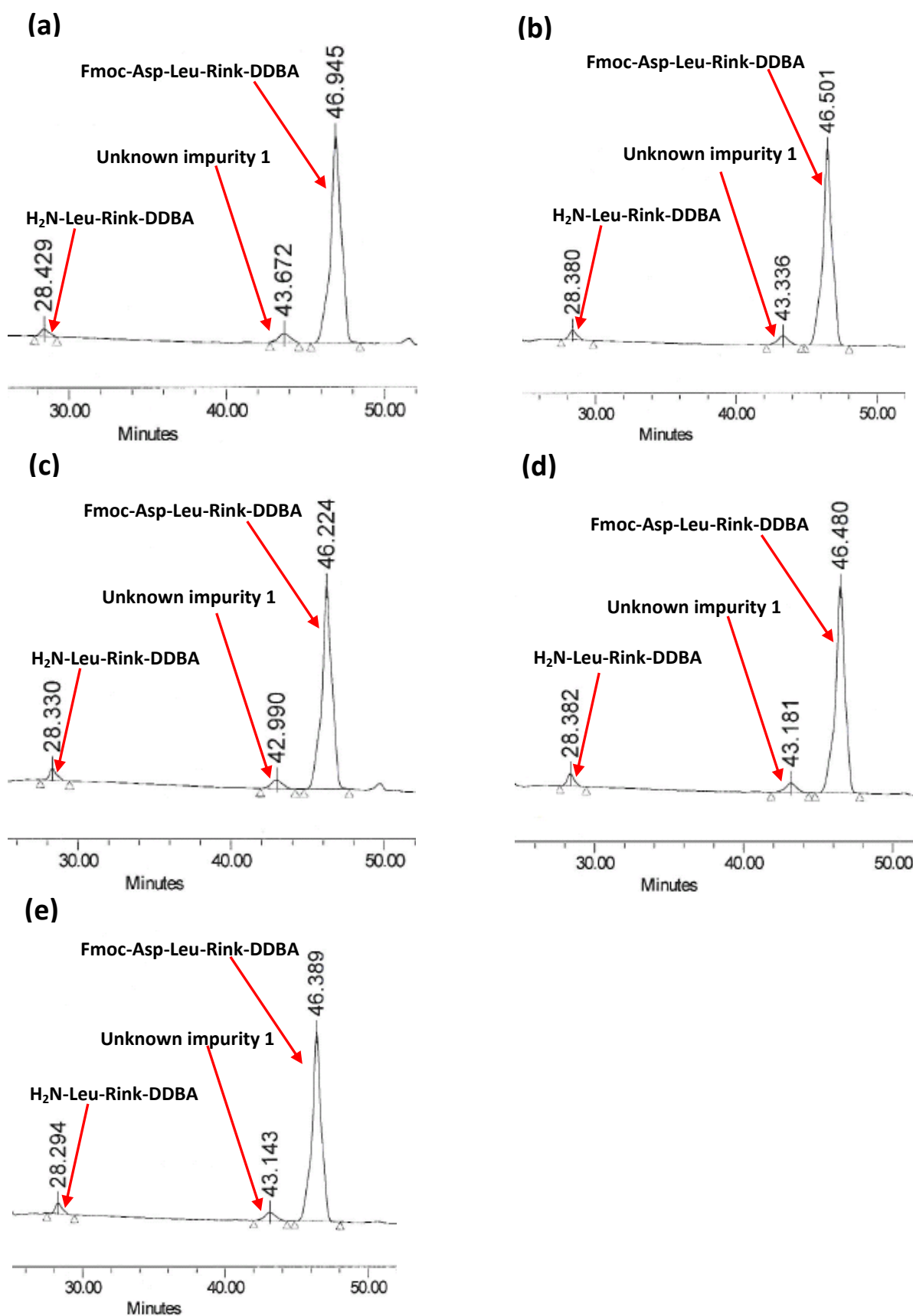


Figure 4.18. Small-scale coupling test during diafiltration: (a) After 10 wash volumes; (b) after 12 wash volumes; (c) after 14 wash volumes; (d) after 16 wash volumes with 1.2 eq coupling reagents; (e) after 16 wash volumes with 1.5 eq coupling reagents.

The second de-Fmoc was performed with piperidine and reached completion in 1 hour. Diafiltration was performed with 10 wash volumes and chloranil tests had negative results after the 10th wash volume for both retentate and permeate. Small-scale test showed that the coupling with Fmoc-Phe-OH had a yet lower yield (79.4 %), but the actual yield of MEPS was even lower (56.2 %) (Figure 4.19 (a)). Diafiltration with 4 wash volumes and recoupling were carried out with 1.05 eq Fmoc-Phe-OH to increase the yield to 79.1 % (Figure 4.19 (b)). After the third de-Fmoc, diafiltration was carried out with 10 wash volumes and the following coupling had a relative yield of 85.1 %. Coupling was repeated with 1.07 eq Fmoc-Ala-OH after diafiltration with 4 wash volumes, but the yield only had slight improvement (increased to 89.5 %).

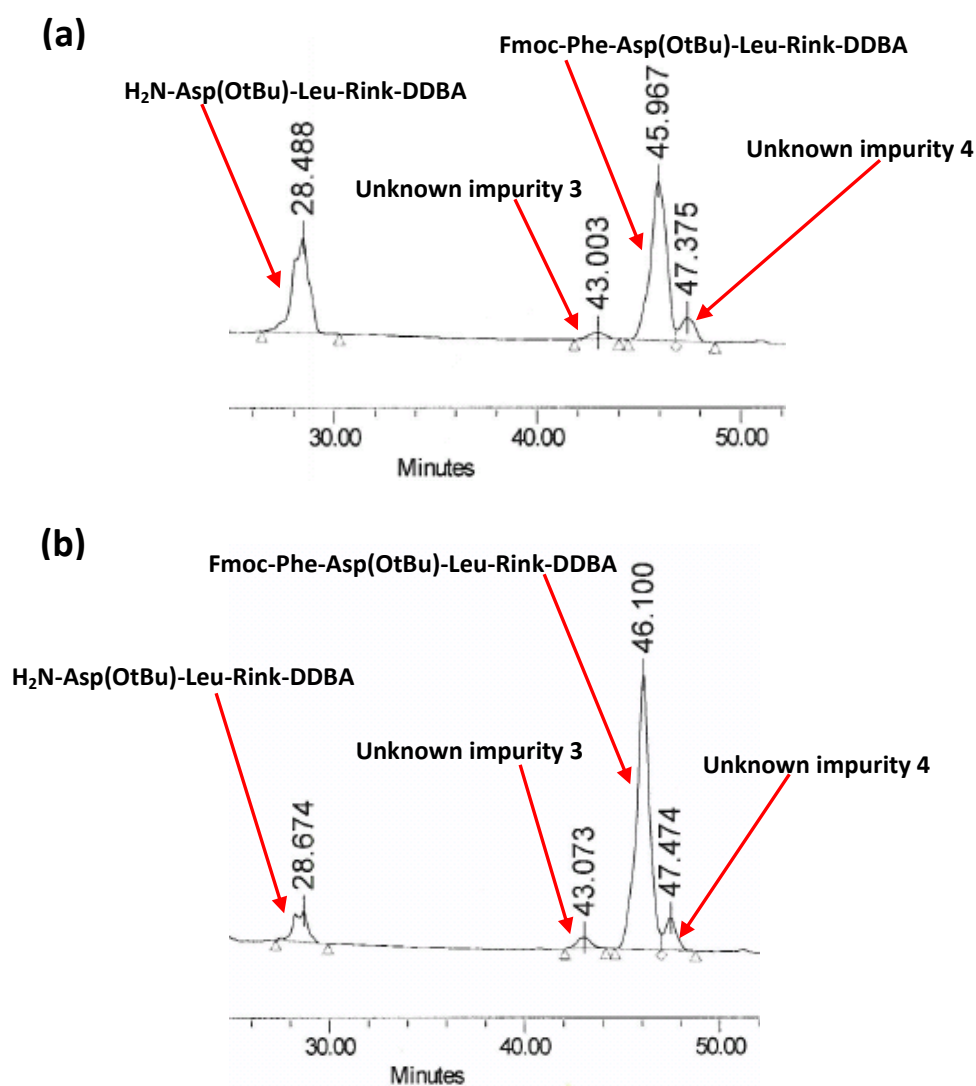


Figure 4.19. Coupling with Fmoc-Phe-OH: (a) 30 minutes of reaction; (b) recoupling after diafiltration.

The couplings of Fmoc-Phe-OH and Fmoc-Ala-OH showed that residual piperidine still remained in the system after diafiltrations with 10 wash volumes. Apparently, the residual piperidine not only consumed the activated amino acid as shown by the small-scale tests, but somehow also hindered the coupling of deprotected peptide fragments with excess activated amino acids as in the case of recoupling, as the relative yield of deprotected peptide fragments remained relatively constant (9.3 % and 6.3 % respectively). In contrast, the problem of residual piperidine was not observed in SPPS, because piperidine was removed completely with the washing solvent by suction through the microfilter, which retained the resin-bound peptide (detailed washing procedure can be found in Section 4.2.2.1).

In the first attempt at MEPS, adding acidic compounds (HOBt or HCl) into the system during diafiltrations worsened the problem of incomplete coupling. It was hence logical to test the opposite measure (i.e. adding basic compound into the system) to see if the removal of residual piperidine could be enhanced by such manipulation of pH. For the next two de-Fmoc, a portion of DIEA (quantity same as the one used in coupling) was added into the system during diafiltration (also with 10 wash volumes) after the 4th, 6th and 8th wash volume. The subsequent couplings achieved relative yields (90.2 and 90.7 %) similar to the ones after the recoupling of Fmoc-Phe-OH and Fmoc-Ala-OH (79.1 and 89.5 %), showing that the addition of DIEA was beneficial for the removal of piperidine, probably by manipulating the surface charge of the ceramic membrane. This mitigation method was subsequently employed in the third attempt of MEPS and proved to be effective.

4.3.3.5. MEPS (Third Attempt)

All the knowledge and experience that was gained from the previous attempts were put to good use in the final attempt at the MEPS of partially deprotected Pyr-SAFDL-NH₂ (Table 4.3). The starting concentration of H₂N-Rink-DDBA was 10.4 weight % in THF, which was approximately the maximum level for the hydrophobic compound, so that impurities could be removed efficiently by diafiltration after each reaction. Close-to-equivalent amount (1.05 eq) of amino acid and activators (HBTU/HOBt) were used for each coupling and de-Fmoc was performed with 10.0 weight % piperidine.

All couplings were finished within 30 minutes with relative yields between 88.1 % and 95.5 % (Figure 4.20 (a) to (f)) and all de-Fmoc went to completion in 1 or 2 hours (relative yield between 97.6 % and 98.2 %). The identity of the final anchored peptide was confirmed by the LC/MS result (Figure 4.21). DIEA was added into the system during diafiltration after each de-Fmoc (after the 8th, 10th and 12th wash volume) to enhance the removal of piperidine and the high yields of coupling confirmed that this was an effective mitigation method for the problem caused by residual piperidine. The overall yield and purity of the desired product were 71.2 % and 88.1 % respectively before cleavage and global deprotection, proving the technical viability of MEPS in comparison with the conventional SPPS, whose overall yield and purity after cleavage and global deprotection were 67.6 % and 98.6 % respectively (Table 4.3). The overall yield and purity before cleavage and global deprotection for SPPS were estimated based on values after cleavage and global deprotection, as the peptide was still attached to the resin and the accuracy of weighing was undermined by the amount of solvent trapped in the resin.

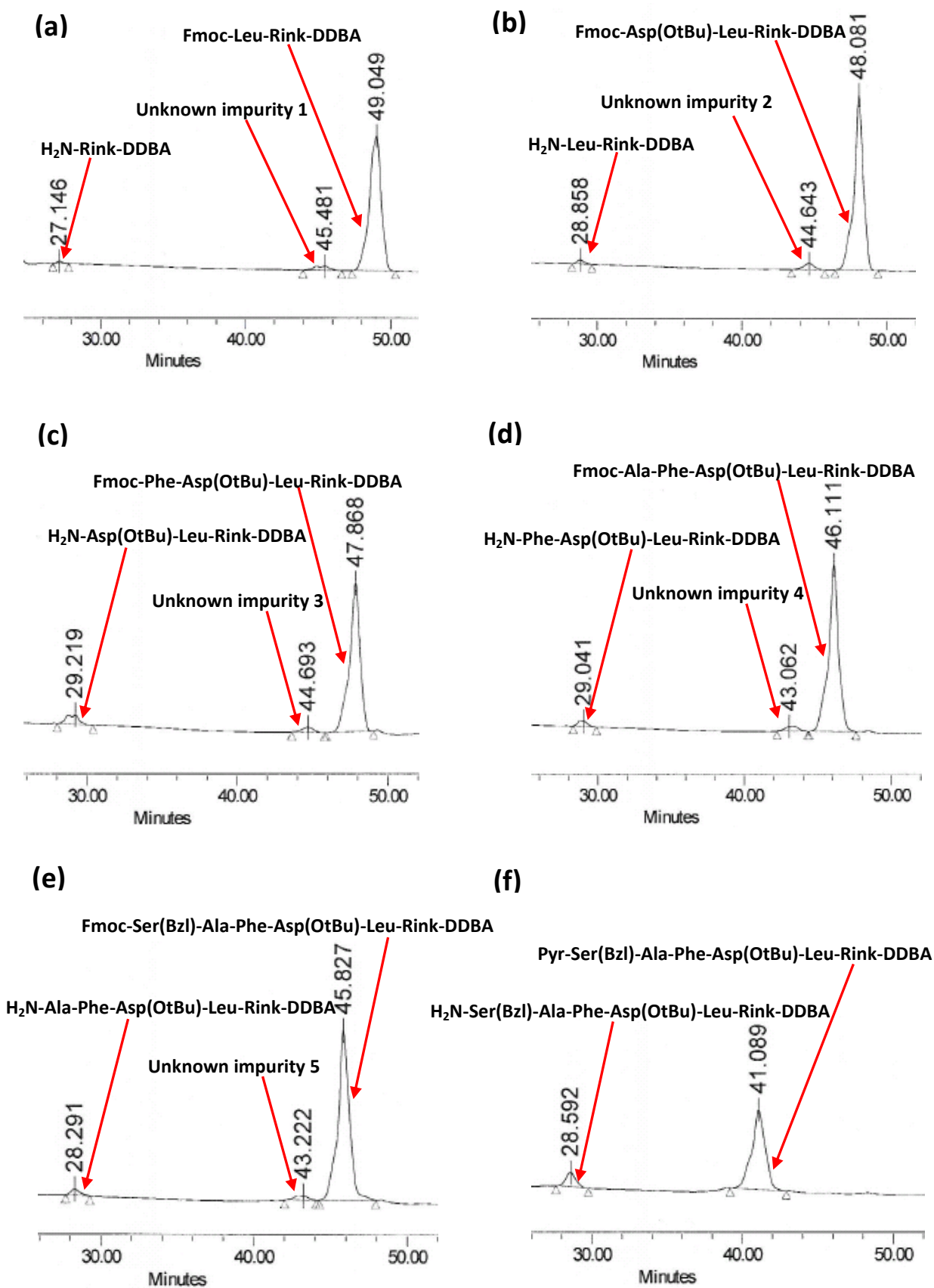


Figure 4.20. Synthesis of Pyr-SAFDL-Rink-DDBA: (a) coupling with Fmoc-Leu-OH; (b) coupling with Fmoc-Asp(OtBu)-OH; (c) coupling with Fmoc-Phe-OH; (d) coupling with Fmoc-Ala-OH; (e) coupling with Fmoc-Ser(Bzl)-OH; (f) coupling with Pyr-OH.

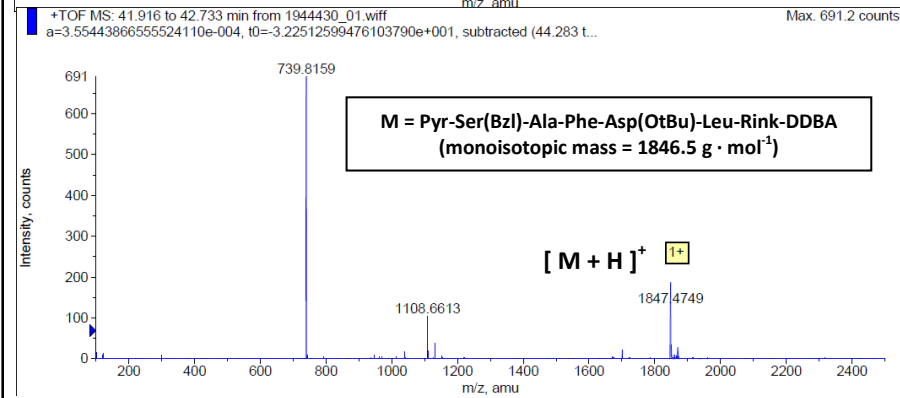
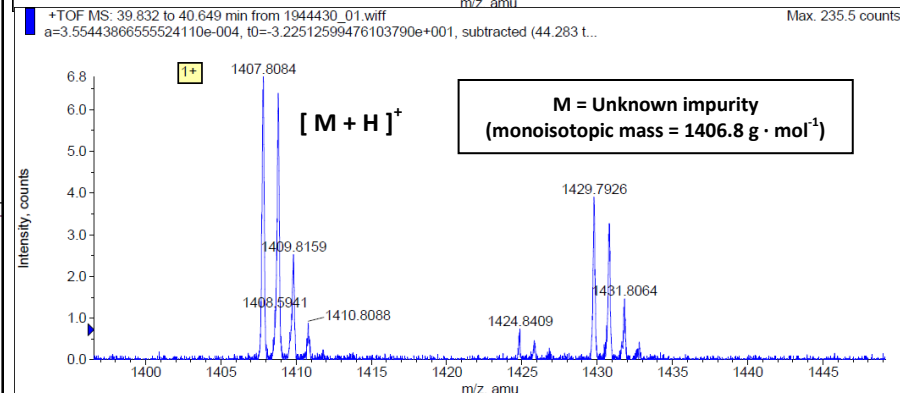
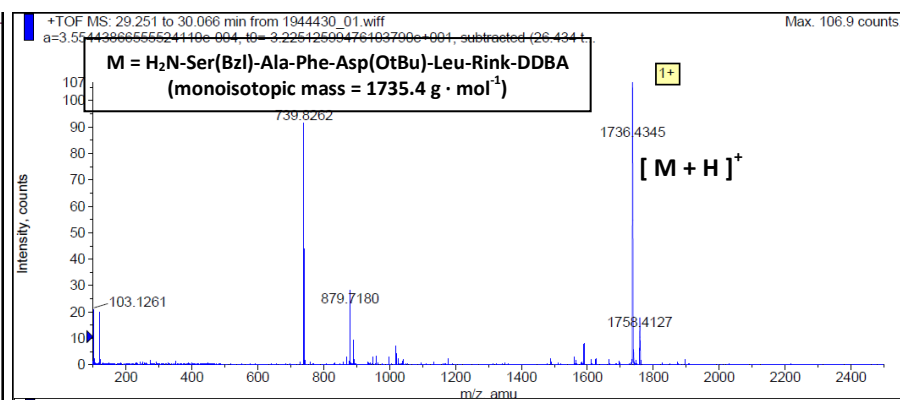
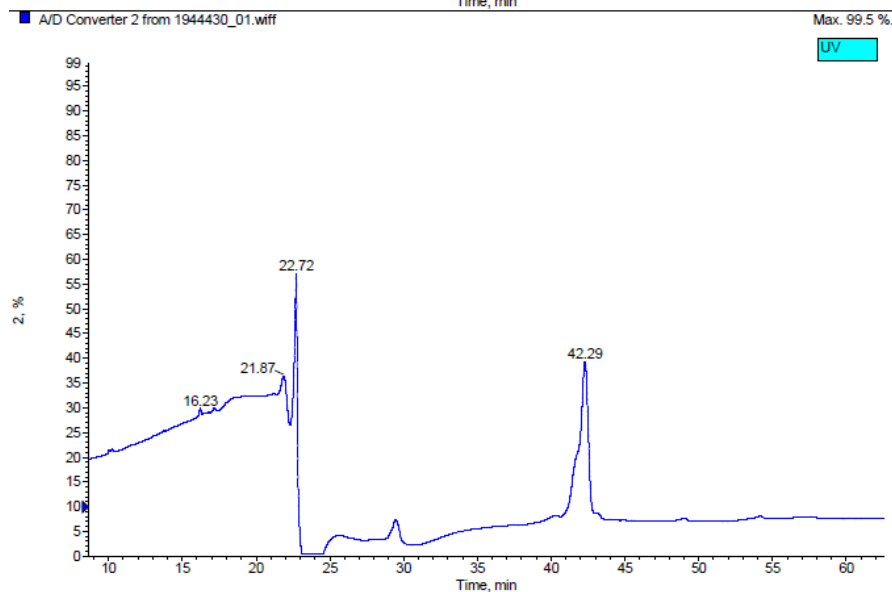
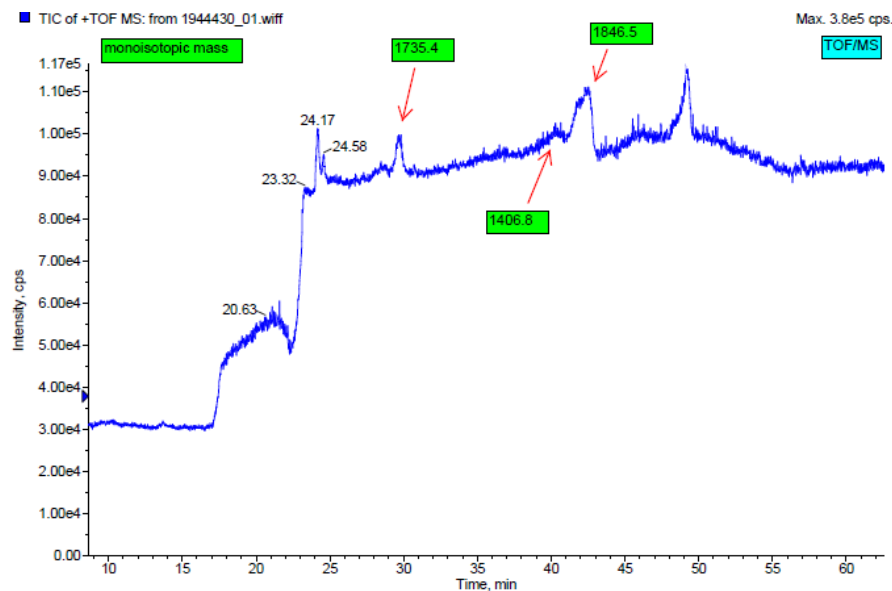


Figure 4.21. LC/MS result of the dried fully protected Pyr-SAFDL-Rink-DBA (HPLC method: Fmoc-RADA-DDBA_HPLC1).

4.3.3.6. Stability of Fmoc-Rink Linker in TFA Solution

One critical issue in the MEPS of the first peptide was the decomposition of Rink linker during global deprotection, causing significant decrease in overall yield and purity. Therefore, it was necessary to investigate, through small-scale tests, whether it was possible to prevent or reduce the extent of this side reaction.

The addition of DMB (5.0 - 7.5 vol %) was reported to be effective for the suppression of the decomposition of Rink (Stathopoulos, Papas, & Tsikaris, 2006), but the opposite results were obtained in the current research work (Table 4.7), as the linker decomposed completely upon addition to the mixture of TFA and DMB (DMB: 10 - 50 vol %). On the other hand, Fmoc-Rink linker decomposed completely within 30 minutes in TFA/H₂O (95/5). Decreasing the ratio of TFA/H₂O to 70/30 and 50/50 reduced the extent of decomposition significantly to 17.4 % and 0.0 %, probably due to the insolubility of the compound in these diluted TFA solutions (Table 4.7). Therefore, it might be wiser to first cleave peptide-Rink from DDBA and then perform global deprotection in a TFA solution, in which Rink would not decompose (e.g. TFA/H₂O = 70/30 and 50/50, v/v), in the hope that global deprotection of side chains would occur simultaneously with the cleavage of Rink from the final peptide product without any decomposition of Rink.

Table 4.7. Stability tests of Fmoc-Rink linker in TFA solution.

| TFA Solution | Mass (g)* | Concentration (weight %) | Time (min) | Relative Yield (%) (by HPLC) | Note |
|---|-----------|--------------------------|------------|------------------------------|---|
| TFA/DMB, 90/10, v/v, 1mL (i.e. 1.3946 g) | 0.0207 | 1.5 | 0 | 0.0 | Turned orange immediately |
| TFA/DMB, 70/30, v/v, 1mL (i.e. 1.3094 g) | 0.0080 | 0.6 | 0 | 0.0 | Turned orange immediately |
| TFA/DMB, 50/50, v/v, 1mL (i.e. 1.2261 g) | 0.0127 | 1.0 | 0 | 0.0 | Turned orange immediately |
| TFA/H ₂ O, 95/5, v/v, 1mL (i.e. 1.4808 g) | 0.1004 | 6.3 | 30 | 0.0 | Turned red immediately |
| TFA/H ₂ O, 70/30, v/v, 1mL (i.e. 1.5569 g) | 0.0156 | 1.0 | 30 | 82.6 | Not fully dissolved and turned orange immediately |
| TFA/H ₂ O, 50/50, v/v, 1mL (i.e. 1.4803 g) | 0.0225 | 1.5 | 30 | 100.0 | Not fully dissolved and turned pink immediately |

*Mass of Fmoc-Rink linker

4.3.3.7. Small-scale Tests for Cleavage and Global Deprotection of Fully Protected Pyr-SAFDL-Rink

The aim of the cleavage tests was to search for a suitable cleavage solution, in which fully protected Pyr-SAFDL-Rink would cleave from DDBA without any decomposition of Rink and DDBA would precipitate due to its hydrophobicity, so that the fully protected Pyr-SAFDL-Rink in solution could be separated from DDBA by microfiltration. As the fully protected Pyr-SAFDL-Rink solution would then be concentrated by vacuum distillation for precipitation or direct drying of the compound, the cleavage solution should be a dilute TFA solution (probably < 10 vol %), so that the concentration of TFA would not be too high during the evaporation of solvent.

Cleavage was tested in various solutions that contained anti-solvents of DDBA (e.g. water, DMSO, DCM and acetonitrile). TFA/H₂O/DMSO solutions were first tested, but fully protected Pyr-SAFDL-Rink-DDBA remained undissolved overnight and cleavage did not occur in solutions with less than 66.5 vol % TFA (Table 4.8). On the other hand, TFA/DCM solutions seemed suitable for the purpose, as cleavage of fully protected Pyr-SAFDL-Rink from DDBA was complete within 30 minutes in just 1 vol % TFA in DCM. Switching from 1 vol % TFA in DCM to 1 vol % TFA in acetonitrile resulted in no cleavage overnight.

Table 4.8. Cleavage tests of fully protected Pyr-SAFDL-Rink from DDBA.

| TFA Solution | Mass (g)* | Time (min) | Relative Yield (%) (by HPLC)** | Note |
|--|-----------|------------|--------------------------------|--|
| TFA/H ₂ O/DMSO, 25/25/50, v/v, 1mL | 0.0157 | 60 | 0.0 | Solid remained insoluble overnight. |
| TFA/H ₂ O/DMSO, 35/35/30, v/v, 1mL | 0.0208 | 30 | 0.0 | Solid remained insoluble overnight. |
| TFA/H ₂ O/DMSO, 35/15/50, v/v, 1mL | 0.0164 | 30 | 0.0 | Solid remained insoluble overnight. |
| TFA/H ₂ O/DMSO, 47.5/2.5/50, v/v, 1mL | 0.0184 | 30 | 0.0 | Solid remained insoluble overnight. |
| TFA/H ₂ O/DMSO, 66.5/3.5/30, v/v, 1mL | 0.0141 | 60 | 100.0 | Solid was not fully soluble and turned red after 30 minutes. |
| TFA/DCM, 50/50, v/v, 1mL (i.e. 1.2005g) | 0.0167 | 20 | 0.0 | Four unknown impurities detected instead of Pyr-SAFDL-Rink. |
| TFA/DCM, 10/90, v/v, 1mL | 0.0158 | 5 | 100.0 | Solid dissolved and turned red immediately. |
| TFA/DCM, 1/99, v/v, 1mL | 0.0173 | 30 | 100.0 | Solid dissolved and turned red slowly. |
| TFA/ACN, 1/99, v/v, 1mL | 0.0163 | Overnight | 0.0 | Solid was not fully soluble and remained yellow overnight. |

*Mass of fully protected Pyr-SAFDL-Rink

**Top liquid layer of reaction mixture sampled and analysed by HPLC.

After finding the most suitable cleavage solution (1 vol % TFA in DCM), the recovery of cleaved Pyr-SAFDL-Rink (fully protected) was investigated. Results showed that the fully protected Pyr-SAFDL-Rink was soluble in DCM and acetonitrile, while the cleaved anchor was not and hence could be filtered off to give a highly pure fully protected Pyr-SAFDL-Rink in solution (purity = 100 % by HPLC).

Finally, a small-scale test was conducted for global deprotection. The synthesis of the first peptide (Fmoc-RADA-NH₂) showed that adding the cleaved peptide-Rink directly into a global deprotection cocktail solution resulted in higher extent of Rink decomposition as compared to the addition into pure TFA followed by the addition of scavengers. The small-scale test confirmed this, as the purities of Pyr-Ser(Bzl)-Ala-Phe-Asp-Leu-NH₂ after the addition of fully protected Pyr-SAFDL-Rink into TFA and the addition of TIS (scavenger for the -OtBu group from aspartic acid) were similar (43.4 % and 31.8 % respectively) and the decomposition of Rink linker was not observed (Pyr-Ser(Bzl)-Ala-Phe-Asp-Leu-Rink-fragment not detected by HPLC).

4.3.3.8. Cleavage and Global Deprotection for Fully Protected Pyr-SAFDL-Rink-DDBA

After drying, the fully protected Pyr-SAFDL-Rink-DDBA (50.21 g, 23.96 mmol) was added into 1 vol % TFA solution (1 L) for the cleavage of fully protected Pyr-SAFDL-Rink from the hydrophobic anchor. The dried peptide fragment was then added into pure TFA (340 mL) for 1 hour, followed by TIS (180 mL × 2) for another hour. The formation of undesired product, Pyr-Ser(Bzl)-Ala-Phe-Asp-Leu-Rink-fragment, was not observed in all HPLC results, but four major unknown impurities appeared during global deprotection. When allowed to settle, the mixture separated into three layers, which from top to bottom were a TIS-rich solution, a white precipitate and a TFA-rich solution. The composition of Pyr-Ser(Bzl)-Ala-Phe-Asp-Leu-NH₂ in the first 2 layers was 5.8 - 6.1 %, while that in the bottom layer was higher (15.7 %). The bottom layer was separated and diisopropylether (600 mL) was added into it in order to precipitate the product. The precipitate was washed repeatedly with diisopropylether and dried. The final product (20.32 g TFA salt of Pyr-Ser(Bzl)-Ala-Phe-Asp-Leu-NH₂) had a purity of 47.1 % based on the HPLC result (H₂N-Ser(Bzl)-Ala-Phe-Asp-Leu-NH₂ accounted for another 8.6 %) (Figure 4.22) and an overall yield of 32.8 %. The identities of the peaks were confirmed by LC/MS results (Figure 4.23).

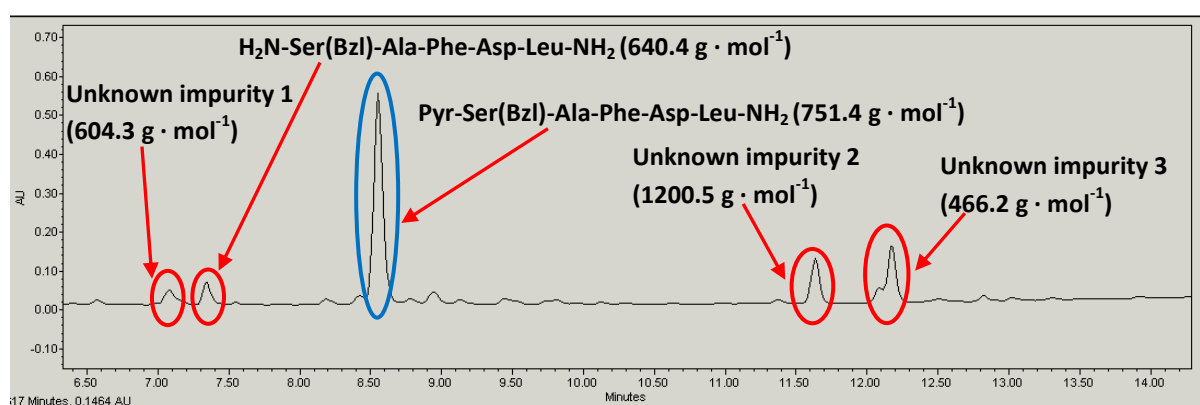
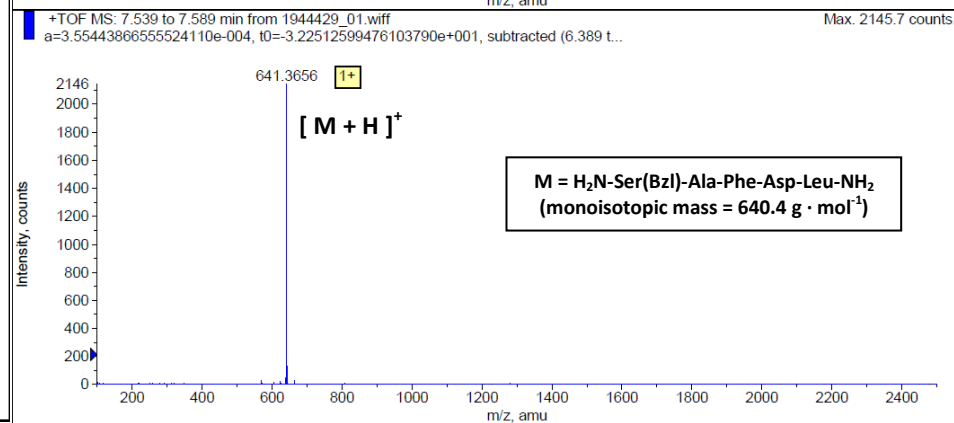
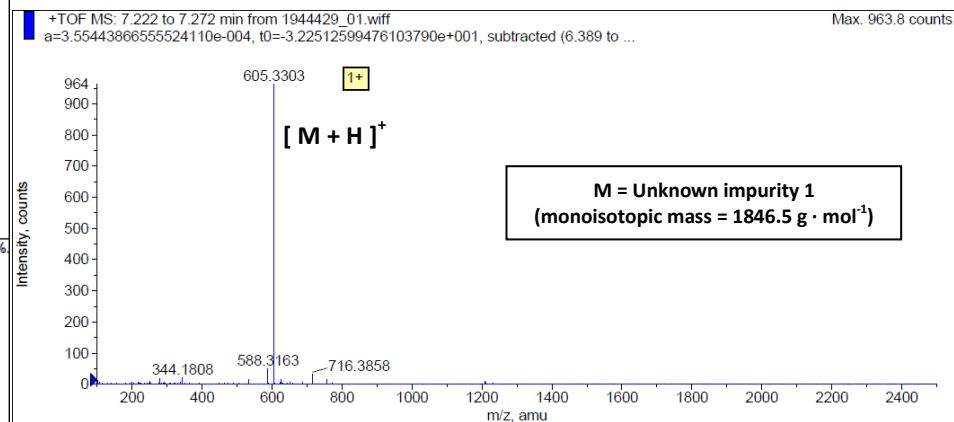
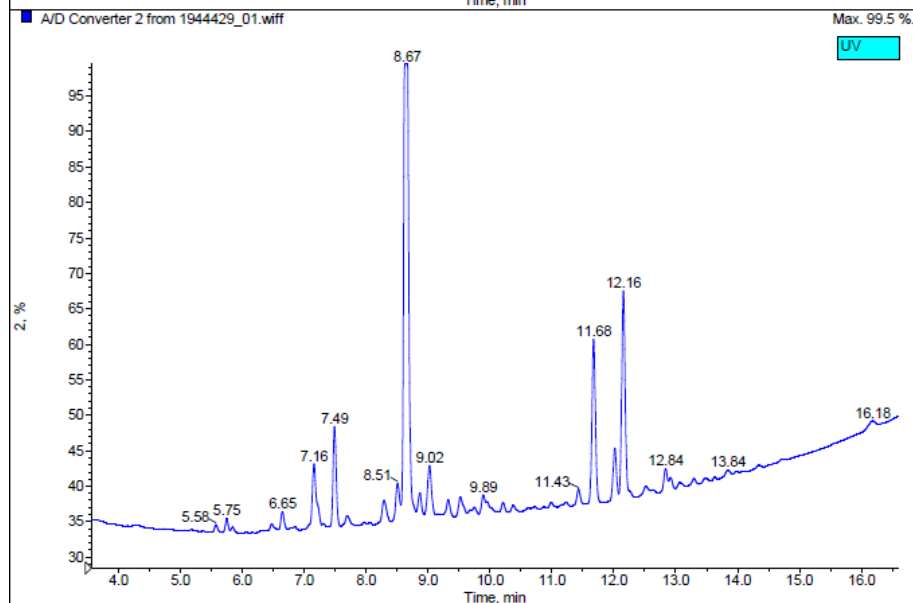
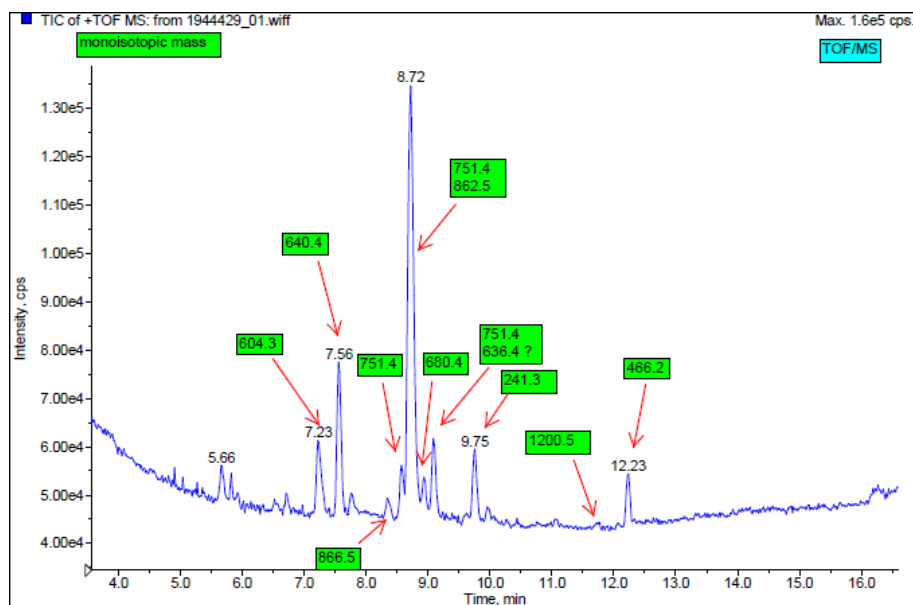


Figure 4.22. HPLC result of the global deprotection product. (Monoisotopic mass of component displayed)



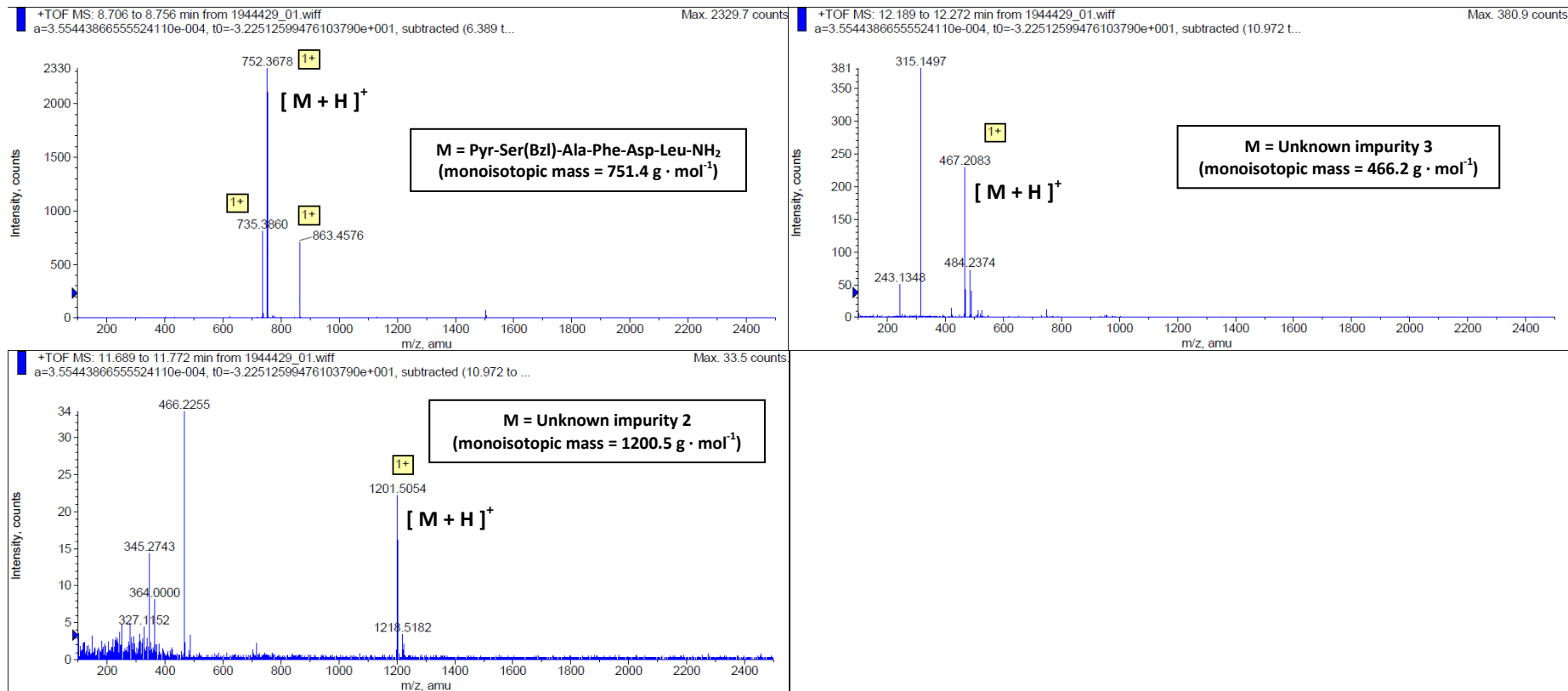


Figure 4.23. LC/MS result of the partially deprotected Pyr-SAFDL-NH₂ (HPLC method: Pyr-SAFDL_HPLC1).

4.3.4. Comparison between MEPS, SPPS and LPPS

The performance metrics of the four peptide synthesis processes (SPPS 1, SPPS 2, LPPS and MEPS) are summarised in Table 4.9.

As shown in Figure 4.24, both before and after cleavage and global deprotection, MEPS had better performance than LPPS (by precipitation) except for purity (11.9 % and 16.3 % lower respectively), overall yield (1.7 % and 6.8 % lower respectively) and building block utility (1.7 % and 6.8 % lower respectively). MEPS was advantageous over LPPS as it had substantially shorter process time than the latter (91.7 % and 91.0 % shorter before and after cleavage and global deprotection), in which the precipitated anchored peptide had to be dried before being redissolved again for the next reaction. In LPPS, the precipitation and washing of the anchored peptide generated a large quantity of waste (i.e. the anti-solvent), which resulted in a significantly higher E-factor than MEPS (68.8 % and 66.0 % higher before and after cleavage and global deprotection).

The similar overall yields and material costs of MEPS and LPPS before cleavage and global deprotection show that: 1) the yield loss of anchored peptide during diafiltration was similar to the yield loss during the precipitation of anchored peptide in LPPS; 2) the cost of anti-solvent (acetonitrile) used for the precipitation of anchored peptide in LPPS was similar to that of the solvent used for the diafiltrations in MEPS. Together with the other over-performing metrics, this shows that MEPS was definitely a better alternative to the existing LPPS technology.

The results of SPPS 2 (1.05 eq amino acid used for coupling) show that couplings required higher equivalent of amino acid in the solid phase synthesis than in the liquid phase synthesis (1.50 eq as compared to 1.05 eq), otherwise the purity of product would be compromised due to incomplete coupling (as in the coupling of H-Pyr-OH in SPPS 2). As a result, MEPS had better performance metrics than SPPS 2 before cleavage and global deprotection.

Table 4.9. Performance of SPPS, LPPS and MEPS.

| Synthesis method * | SPPS1 | SPPS2 | LPPS | MEPS |
|--|--------|--------|--------|--------|
| Scale (mmol) | 5.00 | 5.00 | 5.00 | 33.65 |
| System volume (mL) | 70 | 70 | 50 | 400 |
| <u>Before cleavage and global deprotection</u> | | | | |
| Purity (%) | 98.6 | 66.8 | 100 | 88.1 |
| Overall yield (%) | 72.6** | 53.9** | 72.4 | 71.2 |
| Building block utility (%) | 48.4 | 51.3 | 69 | 67.8 |
| Material cost (Euro · mmol ⁻¹) | 70.84 | 121.13 | 67.52 | 61.65 |
| Material cost excluding resin/anchor cost (Euro · mmol ⁻¹) | 45.57 | 86.99 | 27.96 | 22.21 |
| Process time (h · mmol ⁻¹) | 3.3 | 5.7 | 26.5 | 2.2 |
| Volumetric efficiency (mmol · L ⁻¹) | 51.9 | 38.5 | 51.7 | 59.9 |
| E-factor | 1294 | 1742 | 2929 | 915 |
| <u>After cleavage and global deprotection</u> | | | | |
| Purity (%) | 98.6 | 66.8 | 56.3 | 47.1 |
| Overall yield (%) | 67.6 | 48.9 | 35.2 | 32.8 |
| Building block utility (%) | 45.1 | 46.6 | 33.5 | 31.2 |
| Material cost (Euro · mmol ⁻¹) | 76.08 | 133.52 | 138.88 | 133.82 |
| Material cost excluding resin/anchor cost (Euro · mmol ⁻¹) | 48.94 | 95.89 | 57.51 | 48.22 |
| Process time (h · mmol ⁻¹) | 3.6 | 6.3 | 54.5 | 4.9 |
| Volumetric efficiency (mmol · L ⁻¹) | 48.3 | 34.9 | 25.1 | 27.6 |
| E-factor | 1928 | 2664 | 14430 | 4913 |

* SPPS1: first attempt at SPPS; SPPS2: second attempt at SPPS; MEPS: third attempt at MEPS.

**The overall yield before cleavage and global deprotection was not measured directly as the peptide was still bound to the resin and an accurate measurement of the corresponding total mass was difficult at this scale of synthesis. According to the industrial experience of Lonza AG, the yield loss during cleavage and global deprotection was normally less than 5%. The overall yield before cleavage and global deprotection was calculated based on this observation.

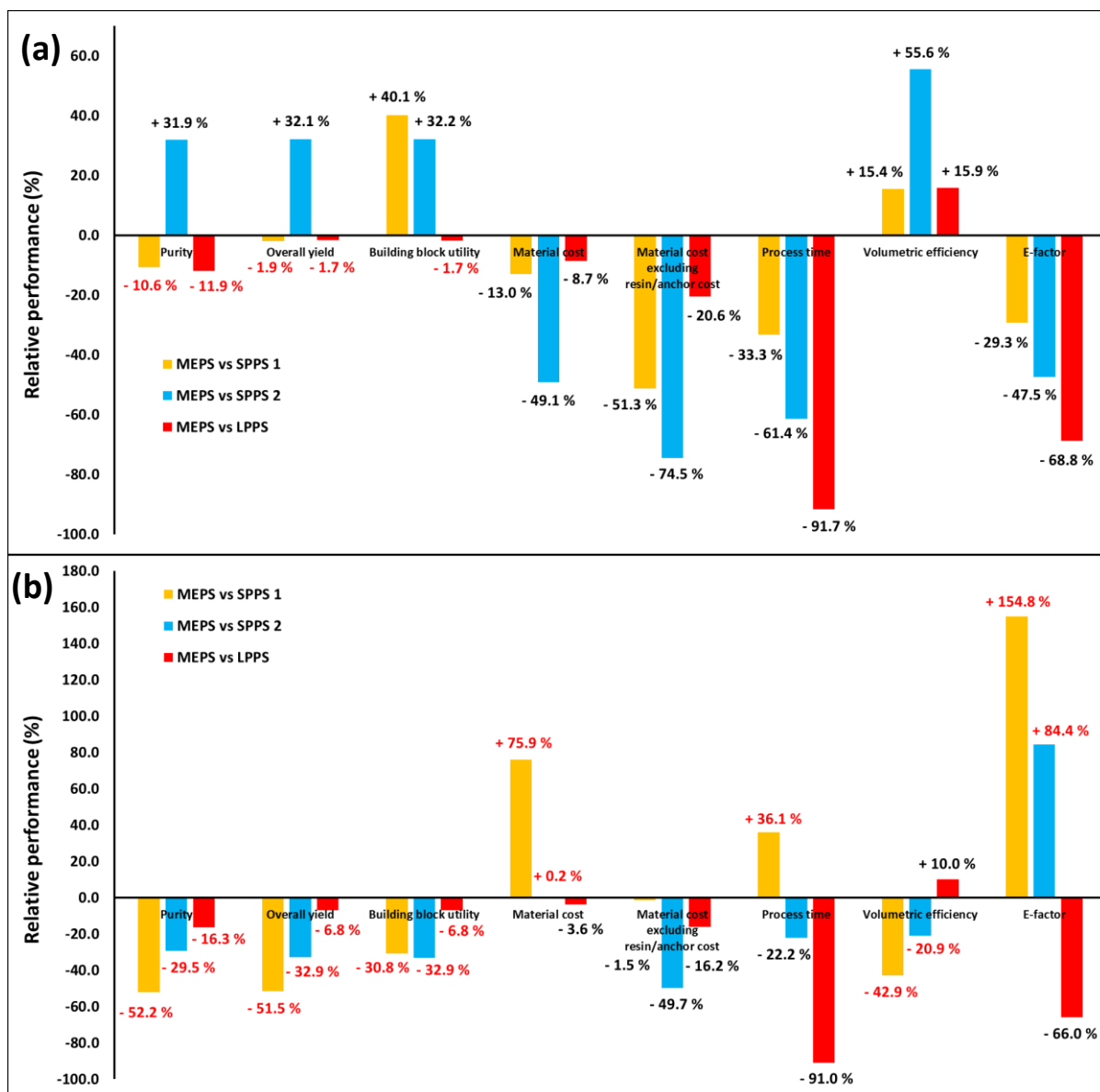


Figure 4.24. Performance of MEPS relative to SPPS (1 & 2) and LPPS: (a) before cleavage and global deprotection; (b) after cleavage and global deprotection.

Before cleavage and global deprotection, MEPS had similar overall yield (1.9 % lower) and lower purity (10.6 % lower) compared to SPPS 1 (1.50 eq amino acid used for coupling) as in the first case study. Performing MEPS at the highest concentration of soluble anchor (10.4 weight % H₂N-Rink-DBA in THF) indeed resulted in a significant improvement in the overall performance of MEPS (in particular, the process time (normalised by quantity of final product), volumetric efficiency and E-factor), since all the other performance metrics of MEPS were better than those of its solid phase counterpart. The material cost of MEPS was 40.1 % lower than SPPS, partly due to the fact that the percentage of solvent cost was reduced to 7 % (Figure 4.25) from 18 % in the MEPS of the first case study (Section 3.3.9). The main reason was the change in material cost structure for SPPS (Figure 4.25), as the portion of de-Fmoc reagents increased substantially to 36 % from 2 % in the first case study. This increase was attributed to the large quantity of HOBt added into the piperidine solution for suppressing the formation of aspartimide (0.5 eq HOBt is required to suppress this side reaction according to Michels et al. (2012)).

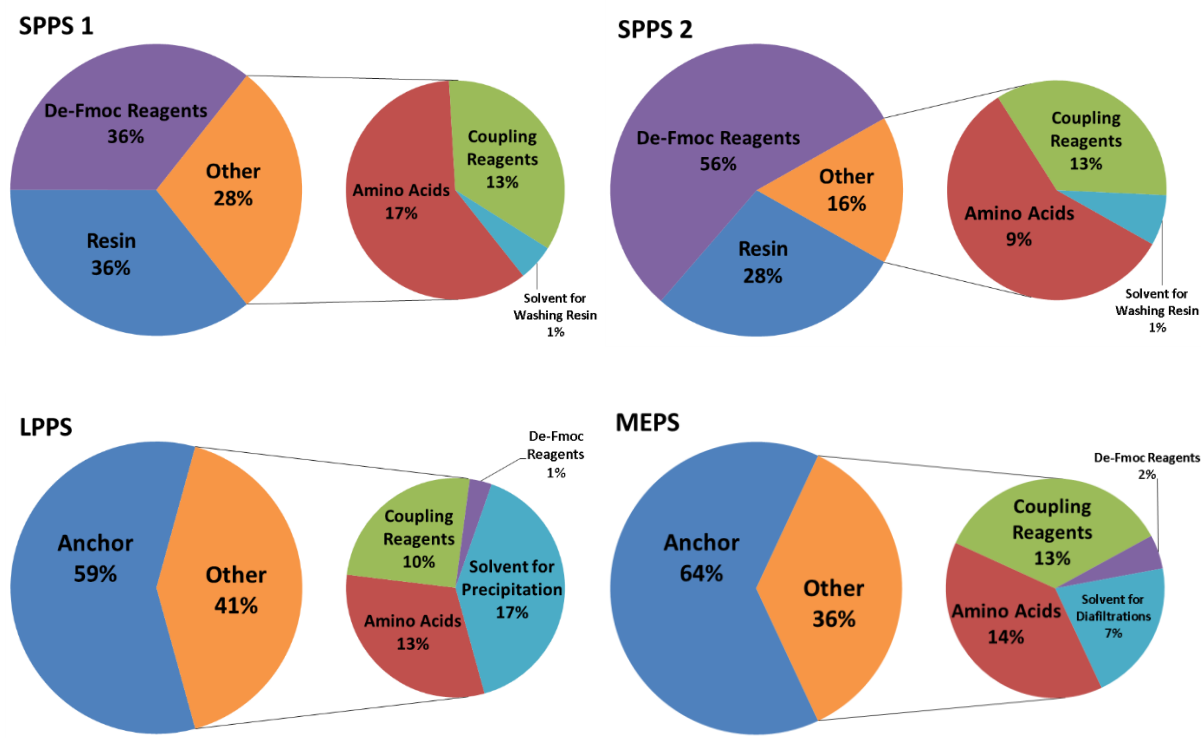


Figure 4.25. Cost breakdown for the four processes.

As in the first case study (MEPS of fully deprotected Fmoc-RADA-NH₂), significant yield loss occurred during cleavage and global deprotection (from 71.2 % to 32.8 %). Consequently, MEPS underperformed across all metrics (except material cost excluding resin/anchor cost) compared to SPPS 1, which had only 5.0 % overall yield loss after cleavage and global deprotection.

The MEPS results before cleavage and global deprotection fulfilled the aim of the study, which was to show the scalability of the new technology (from the original scale of 0.9 - 1.8 mmol in Dr. So's study) and its technical viability as compared to existing technologies (SPPS and LPPS). The mitigation of yield loss during cleavage and global deprotection involves the optimisation of the chemistry and recovery procedure (currently by precipitation), which are dependent on the soluble anchor and were therefore beyond the scope of the current study.

To further improve MEPS, the yield loss of anchored peptide during diafiltration (28.8 %) should be minimised by identifying anchors that have higher rejections than H₂N-Rink-DDBA and by performing the process in a two-stage membrane cascade system. These improvement methods were explored and will be discussed in depth in the following chapter.

4.4. Conclusions

MEPS of the second model peptide (Pyr-Ser(Bzl)-Ala-Phe-Asp-Leu-NH₂) was successful, showing the reproducibility of the new process. At a scale of 33.65 mmol and a concentration of 10.4 weight % H₂N-Rink-DDBA in THF, MEPS was performed with the same OSN system and ceramic membrane (Inopor 450) that were used in the first case study. All couplings went to completion within 30 minutes (relative yield: 88.1 - 95.5 %) with 1.05 eq amino acid/HBTU/HOBt in the presence of DIEA (5.0 eq) and all de-Fmoc were finished within 2 hours (relative yield: 97.6 - 98.2 %) in 10.0 weight % piperidine and 0.1 M HOBt solution. After each coupling and de-Fmoc, diafiltration was performed to remove the excess reagents with 4 and 14 wash volumes respectively. Experiments showed that the presence of residual piperidine after diafiltration was detrimental to the subsequent couplings as it readily consumed the activated amino acids and, for unknown reasons, hindered the coupling even in the presence of excess activated amino acids. As opposed to the addition of acid or acidic compound (HCl and HOBt), the addition of base (DIEA) during post-de-Fmoc diafiltration was found to be effective for the removal of residual piperidine. The purity and overall yield before cleavage and global deprotection (for Pyr-Ser(Bzl)-Ala-Phe-Asp(OtBu)-Leu-Rink-DDBA) were 88.1 % and 71.2 % respectively.

As a result of the high concentration of anchor and the decent overall yield, MEPS had better performance metrics than SPPS (1 and 2) and LPPS except for purity, overall yield and building block utility. However, similar to the first case study, significant yield loss occurred during cleavage and global deprotection of the anchored peptide (final overall yield: 32.8 %), undermining the general performance of MEPS. Yet, it was interesting to note that the performance of MEPS was still better than LPPS except for purity, overall yield and building block utility (16.3 %, 6.8 % and 6.8 % lower respectively) before cleavage and global deprotection, showing that MEPS was definitely a better alternative to the existing LPPS technology. Furthermore, MEPS had similar overall yield and better performance across other metrics (except for purity which was 10.6 % lower) compared to SPPS

(1.50 eq amino acid used for coupling), showing that performing MEPS at the highest concentration of anchor could indeed improve the process performance significantly as predicted in the first case study.

However, after cleavage and global deprotection, MEPS underperformed in general compared to the two attempts at SPPS, which had only 5.0 % overall yield loss. The only way to solve the problem of yield loss during cleavage and global deprotection is to optimise the recovery method (currently by precipitation), which are dependent on the soluble anchor and is therefore beyond the scope of the current study. Nevertheless, the MEPS results before cleavage and global deprotection fulfilled the aim of the study, which was to show the scalability of the new technology and its technical viability as compared to the existing ones (SPPS and LPPS).

Chapter Five –

Alternative Anchors and OSN System for Better Performance

5.1. Introduction

The second MEPS case study showed that significant yield loss occurred during the diafiltration steps even though the anchored peptides had rejections higher than 99 %. Minimising such yield loss is of paramount importance in order to make MEPS an attractive alternative to the existing peptide synthesis methods.

One approach is to continue the search for the ideal anchor, which has complete rejection by the membrane. Two alternative anchors (amine-functionalised silica nanoparticles and a branched compound with PEG arms (PyPEG) (Figure 5.1)) were tested for the synthesis of the first model peptide (fully deprotected Fmoc-RADA-NH₂) with the same chemistry which was used in the case studies.

Extensive research shows that nanoparticles are promising supports for homogeneous catalysts (Fan, & Gao, 2006; Schätz, Reiser, & Stark, 2010). More interestingly, peptide synthesis on nanoparticles is possible with the conventional chemistry that is used in SPPS (Stutz, Bilecka, Thünemann, Niederberger, & Börner, 2012; Stutz, Meszynska, Lutz, & Börner, 2013). For example, a tetrapeptide (H₂N–Phe-Lys-Leu-Gly–NH₂) was synthesised on superparamagnetic core–shell nanoparticles (core: Fe₃O₄; shell: SiO₂; particle diameter: 69 ± 8 nm; core diameter: 9 ± 3 nm) that is surface-functionalised with amino group (0.11 mmol · g⁻¹ nanoparticles). Couplings were conducted with PyBOP/DIEA and de-Fmoc were performed with 20 % piperidine/NMP solution. The resulting yield and purity (70 % and 95 % respectively) were comparable to those of SPPS (Stutz et al., 2012). For MEPS, the peptide synthesis can be performed on nanoparticles, which, with diameters substantially

larger than the pore size of membrane (0.9 nm and 1.0 nm for Inopor 450 and Inopor 750 respectively), can be retained completely by the membrane during diafiltration.

The second alternative anchor, PyPEG (Figure 5.1), is a bulky branched molecule, whose structure was expected to possess significant steric hindrance that would result in the complete retention of this anchor by the membrane during diafiltration.

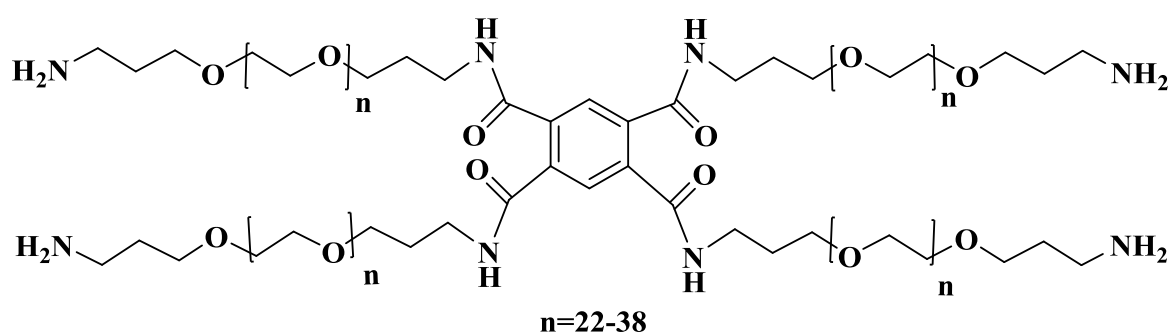


Figure 5.1. PyPEG ($M_n = 6182 \text{ g} \cdot \text{mol}^{-1}$).

In addition to the search for new anchors, another option for minimising the yield loss during diafiltration is to perform the MEPS process in a membrane cascade system, which has been studied previously for solute fractionation (Pathare, & Agrawal, 2010; Vanneste et al., 2011; Vanneste et al., 2013; Siew, Livingston, Ates, & Merschaert, 2013; Kim, Freitas da Silva, Valtcheva, & Livingston, 2013). In a study of the separation of PEG 2000 (molecular weight = $2000 \text{ g} \cdot \text{mol}^{-1}$; rejection by membrane: 92 %) from PEG 400 (molecular weight = $400 \text{ g} \cdot \text{mol}^{-1}$; rejection by membrane: 51 %) by constant volume diafiltration (Kim et al., 2013), the two-stage membrane cascade (Figure 5.2) could reduce the yield loss of PEG 2000 significantly as compared to the single-stage system (the yield of PEG 2000 increased from 59 % (single-stage) to 94 % (two-stage) while maintaining the same purity (94 %)). In short, the second-stage membrane served to recover most of the PEG 2000 that permeated through the first-stage membrane and recycle it back to the feed tank. Performing MEPS in a two-stage membrane cascade, therefore, is expected to avoid the substantial yield loss of anchored peptide during diafiltrations. In the later part of this chapter, the MEPS of the second

model peptide before cleavage and global deprotection (i.e. up till the synthesis of fully protected Pyr-SAFDL-Rink-DDBA) was modelled using Aspen Customer Modeller and its performance was compared with the experimental values of SPPS and single-stage MEPS from the second case study.

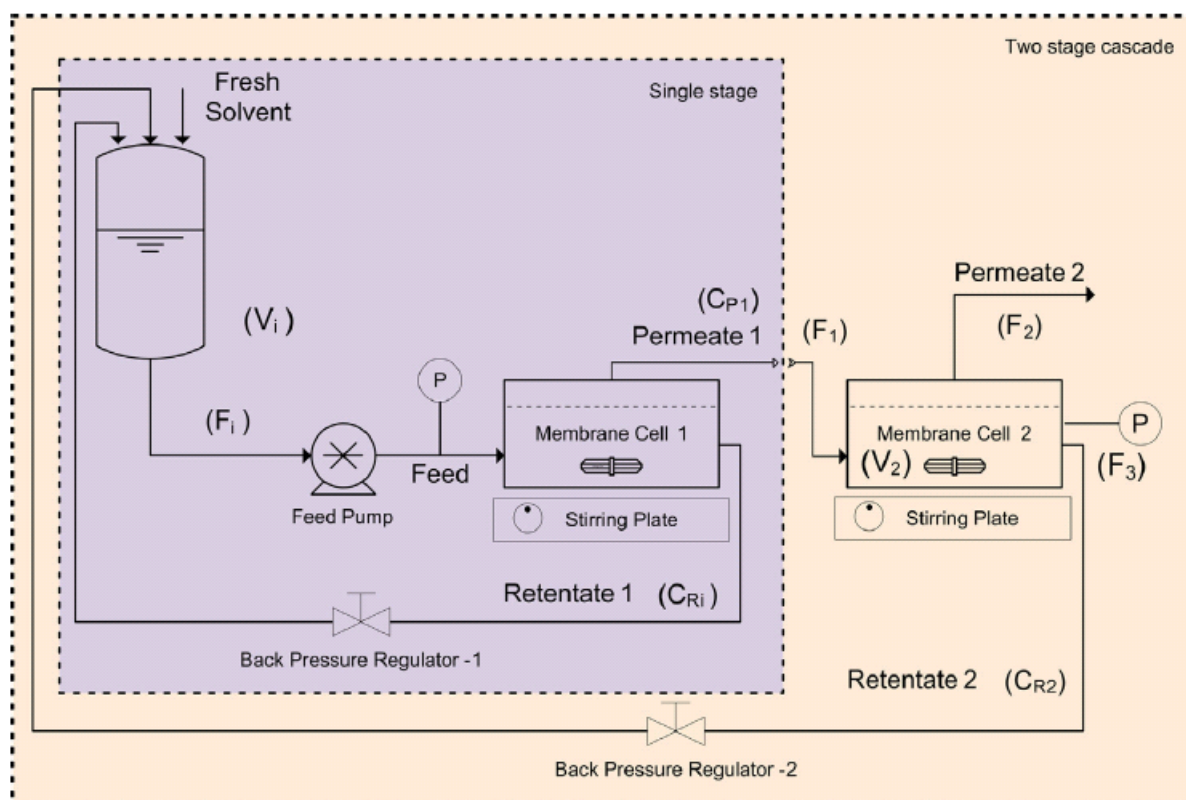


Figure 5.2. Two-stage membrane cascade (Kim et al., 2013).

For the tests of new anchors, the loading of free amine groups on the silica nanoparticles was first quantified, in order to calculate the quantity of reagents needed for reactions. The nanoparticles were then loaded with Fmoc-Rink linker and tested for peptide synthesis. The second anchor, PyPEG, was supplied by IRB (more details in Section 5.3.2.1) as a crude product with excess PEG. The anchor was first purified through diafiltration, before Fmoc-Rink linker was attached and MEPS of the first model peptide (i.e. fully deprotected Fmoc-RADA-NH₂) was attempted.

For the modelling of two-stage MEPS, a summary of the experimental data from the second study case was used to define the model parameters (e.g. system volume and membrane permeance), operating variables (e.g. reaction time and diafiltration time) and the target variables (e.g. yield and

purity of final fully protected anchored peptide). The mass balance of each chemical component (e.g. amino acid, piperidine and anchored fully protected peptide) in each part of the system (e.g. membrane and pipe) was then modelled in Aspen Customer Modeller and a single-stage system was constructed. The MEPS of the second-case-study peptide (up till the formation of full protected Pyr-SAFDL-Rink-DDBA) was then simulated and the modelled results (yield and purity of final anchored peptide) were compared with the experimental values for validation purposes. Based on the validated model of the single-stage system, a two-stage membrane cascade was constructed and the same MEPS process was modelled with only the modification of the operation variables. The yield and purity of the final anchored peptide of the two-stage MEPS was obtained and the corresponding performance parameters (e.g. normalised material cost and process time) were compared with those of SPPS and single-stage MEPS from the second case study.

5.2. Experimental

5.2.1. Materials

The materials and equipment for peptide synthesis were generally the same as described in Chapter Three (Section 3.2).

In addition, amine-functionalised silica nanoparticles (SiO_2 , purity = 99.8 %, size = 10-20 nm, product code: 6851HN) were purchased from Reade International Corp. Hydrochloric acid solution (0.1 M) (product code: 38280) was purchased from Sigma-Aldrich Chemie GmbH. Sodium hydroxide (CAS number: 1310-73-2; product code: 1064621000) was purchased from Merck KGaA.

PyPEG was synthesised by the MemTide research partner, IRB (Miss Vida de la Paz Castro under the supervision of Professor Fernando Albericio).

5.2.2. Apparatus

For the quantification of free amine groups on silica nanoparticles, pH measurement was made with Metrohm 826 pH Mobile from Metrohm Ltd.

5.2.3. Analytical Methods

HPLC Method for Peptide Synthesis on PyPEG

| | | | | | |
|---|---|--|----|----|----|
| HPLC Column | Sunfire, C18, 150 X 4.6 mm, 3.5 μm particle size | | | | |
| Column Temperature ($^{\circ}\text{C}$) | 40 | | | | |
| Detection Wavelength (nm) | 220 | | | | |
| Gradient | Time (min) | Flow ($\text{mL} \cdot \text{min}^{-1}$) | %A | %B | %C |
| | 0.0 | 1.00 | 0 | 40 | 60 |
| | 15.0 | 1.00 | 0 | 90 | 10 |
| | 17.0 | 1.00 | 0 | 90 | 10 |
| | 17.5 | 1.00 | 0 | 40 | 60 |
| | 20.0 | 1.00 | 0 | 40 | 60 |
| Eluent A | Isopropanol | | | | |
| Eluent B | 0.1 vol% TFA/Acetonitrile (i.e. 2 mL TFA in 2 L Acetonitrile) | | | | |
| Eluent C | 0.1 vol% TFA/Water (i.e. 2 mL TFA in 2 L Water) | | | | |
| *Note | Old name (as on HPLC results): AA_2Aug2013 | | | | |

5.2.4. General Procedures

5.2.4.1. Quantification of Free Amine Groups on Silica Nanoparticles

0.1 M sodium hydroxide solution was prepared by dissolving sodium hydroxide (4.00 g) in de-ionised water (1 L). 0.1 M hydrochloric acid solution ($V_{HCl_standard}$) was then titrated against the 0.1 M sodium hydroxide solution and the volume of sodium hydroxide solution for neutralisation was determined. The titration was repeated twice to obtain the average volume of sodium hydroxide for neutralisation ($V_{NaOH_standard}$).

Silica nanoparticles ($Mass_{nanoparticles}$) were added into hydrochloric acid solution (20 mL). The mixture was stirred at room temperature for 30 minutes and then centrifuged (4500 rpm, 10 minutes). Supernatant (8 mL) was sampled and titrated against sodium hydroxide solution. The titration was repeated to obtain the average volume of sodium hydroxide for neutralisation (V_{NaOH_test}).

The quantity of free amine groups on silica nanoparticles was calculated based on the following equation:

$$\frac{\left(20 \text{ mL (HCl)} - V_{NaOH_test} \times \frac{V_{HCl_standard}}{V_{NaOH_standard}} \times \frac{20 \text{ mL (NaOH)}}{8 \text{ mL (NaOH)}}\right) \times 0.1 \text{ mmol} \cdot \text{mL}^{-1}}{Mass_{nanoparticles}}$$

5.2.4.2. Loading of Fmoc-Rink Linker and Amino Acid on Silica Nanoparticles

The loading of Fmoc-Rink linker and amino acid on silica nanoparticles was attempted with HBTU/DIEA/HOBt as in the MEPS of model peptides (Section 3.3.8.2.4 and Section 4.3.3.5).

5.2.4.3. Diafiltration of PyPEG

PyPEG (33.82 g) was dissolved in DCM (500 mL) and diafiltration was performed (Inopor 750, 45 washes, 500 mL DCM each wash). The purity of PyPEG was monitored by NMR (target ratio of peak integration area (7.8 ppm : 2.9 ppm) = 1 : 4).

5.2.4.4. Loading of Fmoc-Rink Linker on PyPEG

PyPEG (37.09 g, 24.0 mmol $-NH_2$, 1.0 eq) was dissolved in DCM (100 mL). Fmoc-Rink linker (46.30 g, 85.8 mmol, 3.6 eq) was dissolved separately in DCM (300 mL), followed by DIEA (23.47 g, 181.6 mmol, 7.6 eq). HBTU (14.05 g, 37.0 mmol, 1.5 eq) was dissolved separately in DMF (120 g). The HBTU solution was added into the Fmoc-Rink linker solution, followed by the PyPEG solution. The reaction was monitored by the ninhydrin test (200 μ L sample precipitated in 1.2 mL diisopropylether and precipitate put through ninhydrin test). If loading was incomplete, more reagents (0.2 eq Fmoc-Rink linker/HBTU) were added. After the reaction was complete, diafiltration was performed (Inopor 750, acetonitrile) and the purity of Fmoc-Rink-PyPEG was monitored by HPLC (major impurity = excess Fmoc-Rink linker).

5.2.4.5. MEPS of Fully Deprotected Fmoc-RADA- NH_2 on Fmoc-Rink-PyPEG

Step 1. De-Fmoc of Fmoc-Rink-PyPEG Fmoc-Rink-PyPEG (11.03 g, 5.3 mmol $-NH_2$, 1.0 eq) was dissolved in acetonitrile (500 mL), followed by HOBT (6.67 g) and piperidine (78.64 g). The mixture was stirred at room temperature for 15 minutes. The reaction solution was added into the OSN system and diafiltration was performed (Inopor 750, 8 washes, 1 L acetonitrile each wash). The permeates were monitored by the chloranil test.

Step 2, 4, 6, 8, 10 and 12. Coupling of Amino Acid Amino acid (8.0 mmol, 1.5 eq) and HOBT (1.09 g, 8.1 mmol, 1.5 eq) were added into the reaction solution, followed by DIEA (3.48 g, 26.9 mmol, 5.1 eq)

(pH: 9 - 10). HBTU (3.01 g, 7.9 mmol, 1.5 eq) was dissolved separately in DMF (31.11 g) and the HBTU solution was added into the reaction solution. The reaction solution was circulated in the OSN system at 20 °C and the reaction was followed by the ninhydrin test. If the coupling was not complete, more reagents were added (0.2 eq amino acid/HOBt/DIEA/HBTU). After the reaction was complete, diafiltration was performed (5 washes, 1 L acetonitrile each wash).

Step 3, 5, 7, 9 and 11. De-Fmoc of Fmoc-peptide-Rink-PyPEG HOBt (6.78 g) was added into the reaction solution, followed by piperidine (79.12 g). The reaction solution was circulated in the OSN system at 20 °C for 15 minutes. Diafiltration was performed (8 washes, 1 L acetonitrile each wash).

5.2.4.6. Modelling of MEPS in a Two-stage Membrane Cascade

The software used for the modelling was Aspen Customer Modeller from Aspen Tech Inc., which allows users to build equation-based models for unit operation and specify the operation procedure for MEPS.

The modelling of MEPS aims to:

1. produce a mathematical model that can describe accurately the mass balance of each component in each part of the membrane system (e.g. pipes, feed tank and membrane unit) throughout the entire MEPS process;
2. explore alternatives in system design (e.g. single-stage vs two-stage membrane cascade) and operation procedure (e.g. diafiltration time and reaction time) in order to improve the process performance (product yield, purity and process time).

The modelling work in this chapter includes:

1. Summary of the experimental data;
2. Proposed model for the single-stage membrane system;
3. Validation of proposed model;
4. Analysis of two-stage model.

5.2.4.6.1. Summary of Experimental Data

The information below is based on the third attempt at MEPS of Pyr-SAFDL-NH₂ (Section 4.3.3.5).

Table 5.1. Summary of OSN system parameters.

| Parameter | Value | Note |
|---|---|---|
| Feed tank volume | 2 L | |
| Pipe volume (feed tank to pump) | 50 mL | Approximation. |
| Pipe volume (pump to membrane) | 100 mL | |
| Membrane retentate volume | 50 mL | |
| Pipe volume (membrane to pump through heat exchanger) | 200 mL | |
| Total system volume | 400 mL | |
| Membrane | Inopor 450 | |
| Membrane area | 0.0512 m ² | 19 channels; total length = 0.25 m, length outside O-ring= 0.005m, channel diameter=0.0035 m. |
| Membrane permeance | 0.977 L · m ⁻² · h ⁻¹ · bar ⁻¹ | 1 L permeated under 20 bar. |
| Rejection of anchored peptided (both deprotected and protected) | 99.6 %* | |
| Rejection of amino acids | 33 % | Based on the rejection of Fmoc-Ala-OH in the anchor screening stage (Section 3.2.4.2) |
| Rejection of piperidine | 33 %** | |
| Feed flow into membrane | 3 m ³ · h ⁻¹ | |

***Table 5.2. Rejection of anchored peptide.**

| Compound | MW (g · mol ⁻¹) | Rejection (%) |
|--|-----------------------------|---------------|
| Fmoc-Leu-Rink-DDBA | 1392 | 100.0 ± 0.0 |
| H ₂ N-Leu-Rink-DDBA | 1170 | 99.7 ± 0.1 |
| Fmoc-Asp(OtBu)-Leu-Rink-DDBA | 1563 | 100.0 ± 0.0 |
| H ₂ N-Asp(OtBu)-Leu-Rink-DDBA | 1341 | 98.7 ± 0.5 |

*The rejections of H₂N-Asp(OtBu)-Leu-Rink-DDBA, Fmoc-Asp(OtBu)-Leu-Rink-DDBA, H₂N-Leu-Rink-DDBA, Fmoc-Leu-Rink-DDBA were measured during the diafiltrations in the MEPS of Pyr-SAFDL-NH₂ (Table 5.2). In general, Fmoc-protected anchored peptide fragments (Fmoc-Asp(OtBu)-Leu-Rink-DDBA and Fmoc-Leu-Rink-DDBA) had complete retentions by the ceramic membrane (Inopor 450), while their deprotected counterparts (H₂N-Asp(OtBu)-Leu-Rink-DDBA and H₂N-Leu-Rink-DDBA) had slightly lower rejections (98.7 ± 0.5 - 99.7 ± 0.1 %). These data were useful for the modelling of MEPS as discussed in the following section.

** Concentration of piperidine not directly measured. Rather, it was estimated based on the assumption that it took 14 wash volumes to remove piperidine (initial concentration=418 mmol) down to 0.1% of anchored peptide (0.001*33.65 mmol = 0.0337 mmol) in order for coupling to proceed to 99.9% completion. Equation used for estimation: $C_{\text{final}}/C_{\text{initial}} = \exp(-W \times (1-R_i))$ (Section 2.2.11).

Table 5.3. Summary of reaction conditions and results.

| Parameter | Value | Note |
|----------------------------|---|---|
| Scale | 33.65 mmol | Initial quantity of H ₂ N-Rink- DDBA |
| Number of amino acids | 6 | |
| Quantity of amino acid | 35.33 mmol | 1.05 eq with respect to starting linker-anchor |
| Coupling time | 1 hour | |
| Coupling conditions | At atmospheric pressure and 20 °C | |
| Average yield of coupling | 96.8 % in 30 minutes | 93.2 – 99.3 % relative to deprotected predecessor. |
| Rate constant for coupling | 0.26 kmol ⁻¹ · m ³ · s ⁻¹ * | |
| Quantity of piperidine | 418.32 mmol | |
| De-Fmoc time | 2 hours | |
| De-Fmoc conditions | At atmospheric pressure and 20 °C | |
| Average yield of de-Fmoc | 98.9 % in 1 hour | 98.3 – 99.5 % relative to protected predecessor. |
| Rate constant for de-Fmoc | 0.0018 kmol ⁻¹ · m ³ · s ⁻¹ ** | |

* Experimental data on the kinetics of coupling were not available. The reaction was assumed to be second-order with rate of reaction proportional to the concentrations of the deprotected anchored peptide and activated amino acid:

$$\frac{d[P_{deprotected}]}{dt} = -\frac{1}{V} \times (k_{coupling} \times [AA] \times [P_{deprotected}])$$

where [AA] (kmol · m⁻³) is the concentration of amino acid, [P_{deprotected}] (kmol · m⁻³) is the concentration of deprotected anchored peptide and V (m³) is the volume of the reactor.

Assuming 99.9 % yield in one hour and the concentration of amino acid is equal to that of the activated one, the rate constant can be calculated using the equation:

$$k_{coupling} = \frac{1}{t} \times \frac{1}{[AA]_{t=0} - [P_{deprotected}]_{t=0}} \times \ln\left(\frac{[P_{deprotected}]_{t=0} \times [AA]_t}{[AA]_{t=0} \times [P_{deprotected}]_t}\right)$$

** Experimental data on the kinetics of deFmoc were not available. The reaction was assumed to be second-order with rate of reaction proportional to the concentrations of the protected anchored peptide and piperidine:

$$\frac{d[P_{protected}]}{dt} = -\frac{1}{V} \times (k_{deFmoc} \times [piperidine] \times [P_{protected}])$$

where [piperidine] (kmol · m⁻³) is the concentration of piperidine, [P_{protected}] (kmol · m⁻³) is the concentration of protected anchored peptide and V is the volume of the reactor.

Assuming 99.9 % yield in two hours, the rate constant can be calculated using the equation:

$$k_{deFmoc} = \frac{1}{t} \times \frac{1}{[Piperidine]} \times \ln\left(\frac{[P_{protected}]_{t=0}}{[P_{protected}]_t}\right)$$

Summary of the operation procedure of MEPS:

Step 1. Loading of Fmoc-Leu-OH unto H₂N-Rink-DDBA

Step 2. Diafiltration (with 4 wash volumes of pure THF (400 mL each) at 20 bar)

Step 3. De-Fmoc of Fmoc-Leu-Rink-DDBA

Step 4. Diafiltration (with 14 wash volumes of pure THF (400 mL each) at 20 bar)

.....

Step 19. De-Fmoc of Fmoc-Ser(Bzl)-Ala-Phe-Asp(OtBu)-Leu-Rink-DDBA

Step 20. Diafiltration (with 14 wash volumes of pure THF (400 mL each) at 20 bar)

Step 21. Coupling of H-Pyr-OH with H₂N-Ser(Bzl)-Ala-Phe-Asp(OtBu)-Leu-Rink-DDBA

Step 22. Diafiltration (with 4 wash volumes of pure THF (400 mL each) at 20 bar)

The overall yield and purity of MEPS:

The overall yield of Pyr-SAFDL-Rink-DDBA was 71.2% ($33.65 \text{ mmol} \times 0.712 = 23.96 \text{ mmol}$) with a purity of 88.1 % according to the HPLC result.

5.2.4.6.2. Proposed Model for the Single-Stage Membrane System

The proposed model consists of a solvent tank, a circulation pump, a membrane unit, a back-pressure valve and five streams (Figure 5.3). The membrane unit was modelled as a Continuous Stirred Tank Reactor (CSTR) and the pipes were modelled as Plug Flow Reactor (PFR) with the rates of generation and consumption included for amino acids and anchored peptides. The circulation pump serves to set the feed flow rate into the membrane unit and the back-pressure valve serves to regulate the pressure at the retentate side of membrane unit.

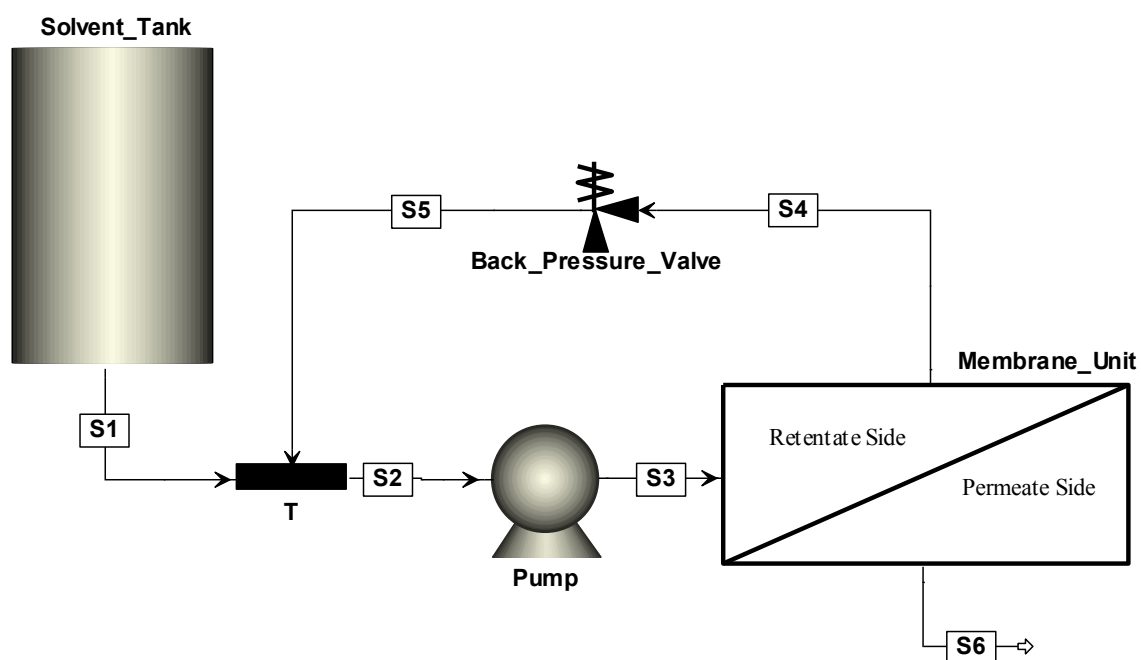


Figure 5.3. Schematic of the model for the single-stage membrane system.

5.2.4.6.3. General Equations for Mass Balance

The mass balance of piperidine, amino acids and anchored peptides in the membrane unit was modelled by the general equation, assuming perfect mixing:

$$\frac{d[Compound]}{dt} = \frac{1}{V} \times (F_{in} \times [Compound]_{in} - F_{out} \times [Compound] + V \times R_{generation} - V \times R_{consumption})$$

where F_{in} and F_{out} ($m^3 \cdot s^{-1}$) are the volumetric flow rate into and out of the reactor and V (m^3) is the volume of the reactor.

The mass balance of compounds in pipe was modelled by the general equation, assuming plug-flow through across the tubes:

$$\frac{\partial[\text{Compound}]}{\partial t} = u \times \frac{\partial[\text{Compound}]}{\partial x} + R_{\text{generation}} - R_{\text{consumption}}$$

where x (m) is the displacement from the pipe inlet and u ($\text{m} \cdot \text{s}^{-1}$) is the axial flow rate in the direction of x .

5.2.4.6.4. Rates of Generation and Consumption

Piperidine was only involved in the de-Fmoc reaction and was not consumed by the reaction. As a result, the rates of generation and consumption were zero.

In addition to coupling and de-Fmoc, side reactions between residual amino acid after a post-coupling diafiltration and the deprotected anchored peptide during de-Fmoc were considered in order to show the effect of the number of wash volumes in diafiltration on the purity of the coupled product. For example, after the loading of Fmoc-Leu-OH on $\text{H}_2\text{N-Rink-DDBA}$, 0.05 eq of activated Fmoc-Leu-OH was still present in the system. After diafiltration, residual activated amino acid was still present and could react with $\text{H}_2\text{N-Leu-Rink-DDBA}$ during the deFmoc of Fmoc-Leu-Rink-DDBA to form $\text{H}_2\text{N-(Leu)}_2\text{-Rink-DDBA}$ and more side products ($\text{H}_2\text{N-(Leu)}_3\text{-Rink-DDBA}$ $\text{H}_2\text{N-(Leu)}_N\text{-Rink-DDBA}$, where N can be infinite in theory). To reduce the complexity of the model, only the side reaction between the residual amino acid and the deprotected anchored peptide (the formation of $\text{H}_2\text{N-(Leu)}_2\text{-Rink-DDBA}$ in the above example) was considered for the mass balance of amino acids and deprotected anchored peptide, assuming the rate constant was the same as that of the coupling step.

Amino acids were consumed in the coupling reactions where they were first activated and then reacted with the deprotected anchored peptide ($\text{H}_2\text{N-Peptide-Anchor}$) during coupling and with the

deprotected form of the post-coupling anchored peptide during de-Fmoc. Assuming that the activation step was much quicker than the coupling step, the rate of consumption can be modelled as:

$$R_{consumption}(AA(i)) = k_{coupling} \times [AA(i)] \times [P(2 \times (i - 1))] + i \times k_{coupling} \times [AA(i)] \times [P(2 \times i)]$$

where i is the amino acid number in the peptide (AA(i)-AA($i-1$)-.....-AA(2)-AA(1)-Anchor) and $P(2 \times (i-1))$ refers to the deprotected anchored peptide that reacts with the specific amino acid. (Note: $P(0)$ refers to the H_2N - Anchor.)

The anchored peptides consist of two groups: the deprotected ones (H_2N -Peptide-Anchor) and the protected ones (Fmoc-Peptide-Anchor). The former were generated by the de-Fmoc step (assuming 99.9 % completion in two hours) and then consumed by the next coupling (assuming 99.9% completion in one hour) and the side reaction with residual amino acid (assuming to have same kinetics as coupling). The protected anchored peptides, on the other hand, were generated during coupling and then consumed in the subsequent de-Fmoc. The rates of generation and consumption are hence modelled by:

$$R_{generation}(P(2 \times i)) = k_{deFmoc} \times [piperidine] \times [P(2 \times i - 1)]$$

$$R_{consumption}(P(2 \times i)) = k_{coupling} \times [AA(i)] \times [P(2 \times i)] + k_{coupling} \times [AA(i + 1)] \times [P(2 \times i)]$$

$$R_{generation}(P(2 \times i - 1)) = k_{coupling} \times [AA(i)] \times [P(2 \times (i - 1))]$$

$$R_{consumption}(P(2 \times i - 1)) = k_{deFmoc} \times [piperidine] \times [P(2 \times i - 1)]$$

where $P(2 \times i)$ is the deprotected anchored peptide and $P(2 \times i-1)$ is the protected anchored peptide.

Lastly, the rates of generation for the side products formed during de-Fmoc are modelled by:

$$R_{generation}(I(i)) = k_{coupling} \times [AA(i)] \times [P(2 \times i)]$$

where $I(i)$ is the side product formed by residual amino acid AA(i) during deFmoc.

5.2.4.6.5. Scheduling

The MEPS process was modelled dynamically by calculating the mass balance of each chemical component in the OSN system. At the beginning of each reaction (coupling or de-Fmoc), the concentrations of reagents (amino acid for coupling and piperidine for de-Fmoc) were increased to set values in the membrane retentate side to simulate the addition of reagents directly into the system. The solution was then circulated in the system by the pump at atmospheric pressure to run the reaction for a fixed time. To start the diafiltration in the constant volume mode, the pressure in the system was increased to a set value by the back pressure valve and fresh solvent started to flow into the system from the solvent tank in order to maintain a constant liquid volume in the system. After a fixed time, the pressure of the system was set to the atmospheric pressure in order to stop the diafiltration. The details of operation schedule are presented in the following table.

Table 5.4. Operation schedule of MEPS in the model.

| Step | Cumulative time (min) | Action | Note |
|--------|-----------------------|---|---------------------------------------|
| 1 | 0 | [AA(1)] in membrane retentate set to $0.707 \text{ kmol} \cdot \text{m}^{-3}$ | AA(1) is Fmoc-Leu-OH |
| | | [P(0)] in membrane retentate set to $0.673 \text{ kmol} \cdot \text{m}^{-3}$ | P(0) is $\text{H}_2\text{N-Rink-DBA}$ |
| 2 | 60 (i.e. 0 + 60) | System pressure set to 20 bar | Diafiltration started |
| 3 | 156 (i.e. 60 + 96) | System pressure set to 0 bar | Diafiltration stopped. |
| | | [Piperidine] set to $8.36 \text{ kmol} \cdot \text{m}^{-3}$ | |
| 4 | 276 (i.e. 156 + 120) | System pressure set to 20 bar | Diafiltration started |
| 5 | 612 (i.e. 276 + 336) | System pressure set to 0 bar | Diafiltration stopped |
| | | [AA(2)] set to $0.707 \text{ kmol} \cdot \text{m}^{-3}$ | AA(2) is Fmoc-Asp(OtBu)-OH |
| 6 | 672 (i.e. 612 + 60) | System pressure set to 20 bar | Diafiltration started |
| | | | Repeat the steps for all amino acids |
| 21 | 3060 | System pressure set to 0 bar | Diafiltration stopped |
| | | [AA(6)] set to $0.707 \text{ kmol} \cdot \text{m}^{-3}$ | AA(6) is H-Pyr-OH |
| 22 | 3120 | System pressure set to 20 bar | Diafiltration started |
| 23 | 3216 | System pressure set to 0 bar | Diafiltration stopped. |

5.3. Results and Discussion

5.3.1.1. Silica Nanoparticles

According to the supplier, the nanoparticles were made of silica dioxide and had diameters between 10 nm and 20 nm. The surface of the nanoparticles was functionalised with amine. As the nanoparticles were much larger than the pores of the ceramic membranes (0.9 nm for Inopor 450 and 1.0 nm for Inopor 750), complete retention of nanoparticles by membrane was expected.

As peptide synthesis on nanoparticles was a relatively new concept, its chemistry was first investigated at small scale before moving to MEPS. Two pieces of information, namely the loading of free amine groups per gram of nanoparticle and the porosity of nanoparticle, were important for the design of experiment, but were unknown. The former was measured experimentally, so that the stoichiometry of reagents could be determined accurately. The latter could not be determined during the course of research due to equipment constraints, but was important for deciding the extent of loading of linker for peptide synthesis.

5.3.1.2. Loading of Free Amine Group on Silica Nanoparticles

Titration tests showed that silica nanoparticles had high loading of free amine group ($1.75 \text{ mmol} \cdot \text{g}^{-1}$ nanoparticles as compared to $0.72 \text{ mmol} \cdot \text{g}^{-1}$ for the PL-Rink resin in the SPPS of Pyr-SAFDL-NH₂). As the nanoparticles had diameters between 10 nm and 20 nm, the material could be either microporous (pore size < 2 nm) or mesoporous (2 nm < pore size < 50 nm) or both.

The porosity of nanoparticles has a significant influence on the distribution of free amine groups over the surface of the nanomaterial, but was unknown. If the nanoparticles are only porous to a small extent, most of the free amine groups are likely to be present over the surface of the particle, and hence the loading of linker can be significantly higher than those that are highly porous, in which

most of the free amine groups are present within the pores and therefore are difficult for the linker and amino acids to access.

5.3.1.3. Loading of Fmoc-Rink Linker on Silica Nanoparticles

The loading of Fmoc-Rink linker on nanoparticles was tested with 0.1, 0.5, 0.9, 1.8 and 2.7 eq Fmoc-Rink linker/HBTU in the presence of excess DIEA (4.1 - 11.5 eq) and the presence of unreacted linker (UV-active) in the solution was monitored by HPLC. Except for the case of 0.1 eq Fmoc-Rink linker/HBTU, whose HPLC result showed the disappearance of linker after two days of reaction, significant amounts of linker remained unreacted for all the other cases even after two days of reaction and additional HBTU (0.5 - 2.8 eq).

The loading results showed that most of the free amine groups were not present on the surface and hence were inaccessible to the linker even at high concentration (as for the case of 2.7 eq Fmoc-Rink linker). In other words, the nanoparticles were most likely to be porous and most of the free amine groups were hidden inside the pores. As 0.1 eq of linker was completely consumed during loading, but most of the 0.5 eq of linker remained unreacted, the effective loading of free amine groups on nanoparticles was definitely higher than $0.18 \text{ mmol} \cdot \text{g}^{-1}$ (corresponding to 0.1 eq of loading), but significantly lower than $0.88 \text{ mmol} \cdot \text{g}^{-1}$ (corresponding to 0.5 eq of loading).

5.3.1.4. Capping of Free Amine Groups

Although most of the free amine groups were inaccessible to the loading of linker, it was still important to cap them in order to prevent the synthesis of erroneous peptide on these sites. Capping tests were carried out with excess acetic anhydride (1045 eq) and DIEA (208 eq). Unexpectedly, the capping had to be repeated three times in order to proceed to completion based on the result of the ninhydrin test. This observation confirmed the inaccessibility of most of the free amine groups, since even small molecules such as acetic anhydride had difficulty reaching these sites.

One implication of such inaccessibility was the limited extent of linker loading and subsequent peptide synthesis on the nanoparticles.

5.3.1.5. Chemical Modification of Silica Nanoparticles

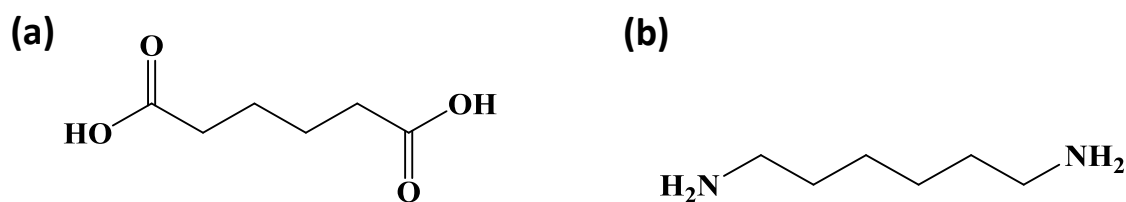


Figure 5.4. (a) adipic acid and (b) hexamethylenediamine.

To overcome the problem mentioned above, the free amine groups were first coupled with adipic acid, followed by another coupling with hexamethylenediamine (Figure 5.4). Such chemical modifications were aimed to extend the free amine groups away from the surfaces and pores of the nanoparticles, rendering them more accessible to the reagents for peptide synthesis.

The coupling of adipic acid with the free amine groups of nanoparticles was repeated three times with excess adipic acid (9.2 - 9.3 eq), HBTU (9.0 - 9.2 eq) and DIEA (26.5 - 27.4 eq) in order to completely consume the free amine groups (the ninhydrin test gave a negative result). The next coupling was carried out with excess hexamethylenediamine (8.8 eq), HBTU (9.6 eq) and DIEA (32.6 eq). As the ninhydrin test gave a positive result, the modified nanoparticles were subject to the coupling with Fmoc-Rink linker (0.5 eq) in the presence of excess HBTU (0.6 eq) and DIEA (52.1 eq). The coupling with linker was complete overnight and the loaded nanoparticles were added into piperidine solution (20 weight%) for de-Fmoc, which was repeated four times in order to drive the reaction to completion. The nanoparticles were then coupled with Fmoc-Ala-OH (0.5 eq) in the presence of HBTU (0.5 eq) and DIEA (0.6 eq). After one day, the amount of Fmoc-Ala-OH in the reaction mixture decreased by 50% based on HPLC results, suggesting that approximately 0.25 eq Fmoc-Ala-OH was coupled to the nanoparticles.

Unfortunately, due to the lack of quantitative and qualitative analysis techniques available for peptide synthesis on nanoparticles, the research work was not pursued further.

5.3.2. MEPS of Fully Deprotected Fmoc-RADA-NH₂ on Rink-PyPEG

5.3.2.1. Synthesis and Purification of PyPEG

PyPEG is a bulky anchor with a pyromellitic core and four PEG arms (Figure 5.1). Due to the polydispersity of PEG, the anchor has a range of molecular weight and hence it has a broad peak (RT = 7 - 12 min) in the HPLC result (Figure 5.5). The average molecular weight is estimated to be 6182 g · mol⁻¹.

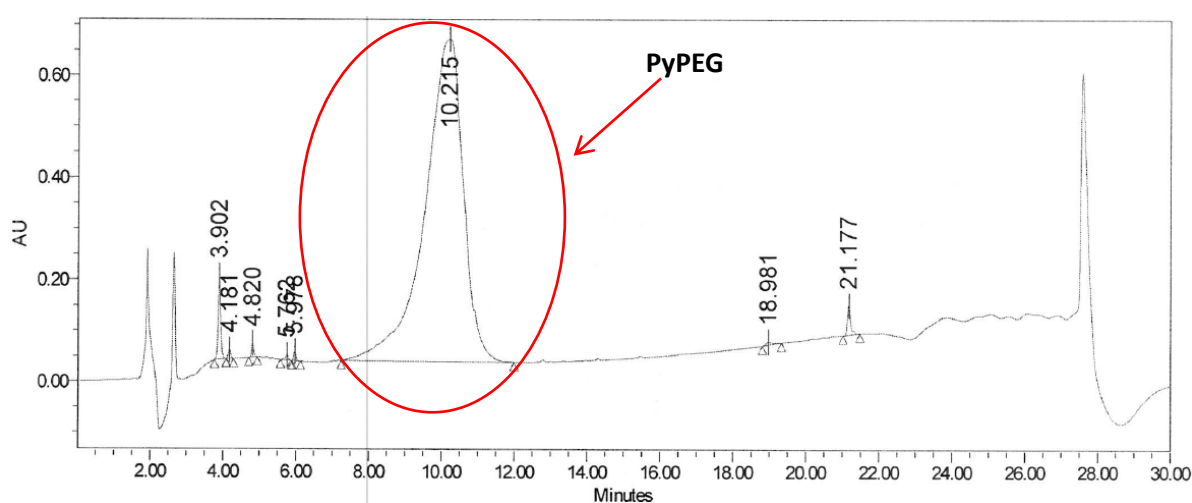


Figure 5.5. HPLC result of crude PyPEG.

The synthesis of PyPEG was performed by the research partner in the MemTide consortium, Miss Vida de la Paz Castro from IRB, in excess bis(3-aminopropyl)polyethylene glycol (8 eq; Mn = 1500 g · mol⁻¹) (Figure 5.6). As a result, diafiltration was performed on the crude product in order to remove the excess PEG.

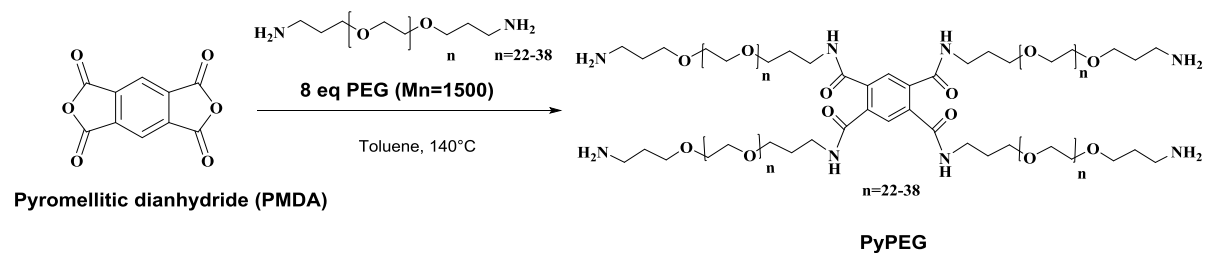


Figure 5.6. Synthesis of PyPEG.

Crude PyPEG was dissolved in DCM and diafiltration was first carried out with Inopor 450 before switching to Inopor 750 due to low permeance ($0.4 \text{ L} \cdot \text{m}^{-2} \cdot \text{h}^{-1} \cdot \text{bar}^{-1}$ as compared to $5.9 \text{ L} \cdot \text{m}^{-2} \cdot \text{h}^{-1} \cdot \text{bar}^{-1}$). HPLC analysis of the retentate and permeate samples showed that the rejection of PyPEG was 100% for both Inopor 450 and Inopor 750, meaning that Inopor 750 was a better choice for the diafiltration of PyPEG and its related compounds during MEPS. As the excess PEG was not UV-active, NMR was performed on the retentate samples to check its presence. As shown in Figure 5.7, the singlet at 7.8 ppm corresponds to proton A at the pyromellitic core, while the quadret at 2.9 ppm corresponds to proton B that is adjacent to the free amine group at the end of each PEG arm. In the absence of excess PEG, the ratio of integration areas for these two peaks should be 1 : 4. As 8 eq PEG was used to synthesise PyPEG, the starting ratio was expected to be 1 : 32. NMR of the crude PyPEG gave a ratio of 1 : 28.3, which was close to the expected value. Figure 5.8 shows that the ratio decreased from 1 : 28.3 to 1 : 13.0 after 26 wash volumes, after which it was only reduced marginally to 1 : 10.2 after another 20 wash volumes, and finally to 1 : 9.1 after another 20 wash volumes. The NMR results suggest that the removal of PEG became inefficient after approximately 30 wash volumes and about 1.3 eq of excess PEG remained in the system, probably due to interactions between the excess PEG and the PEG arms of the anchor.

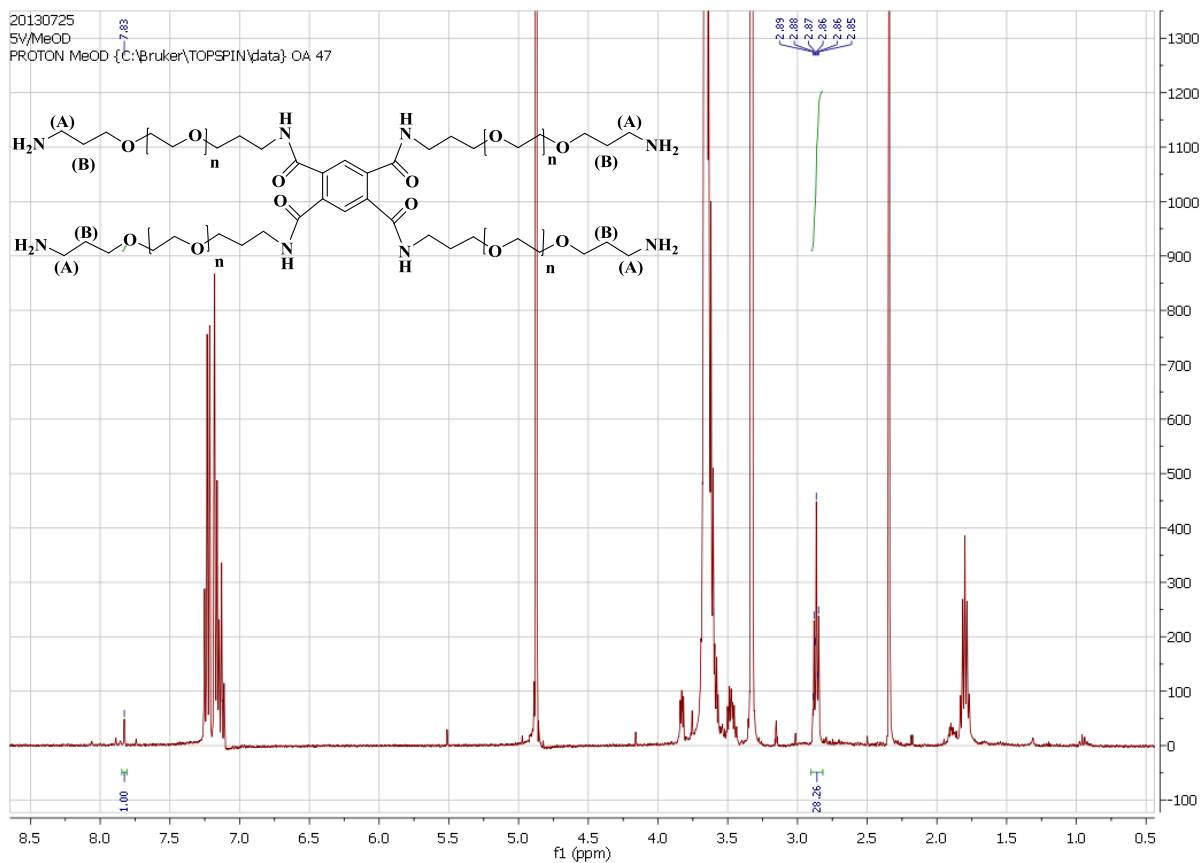


Figure 5.7. NMR result of of PyPEG.

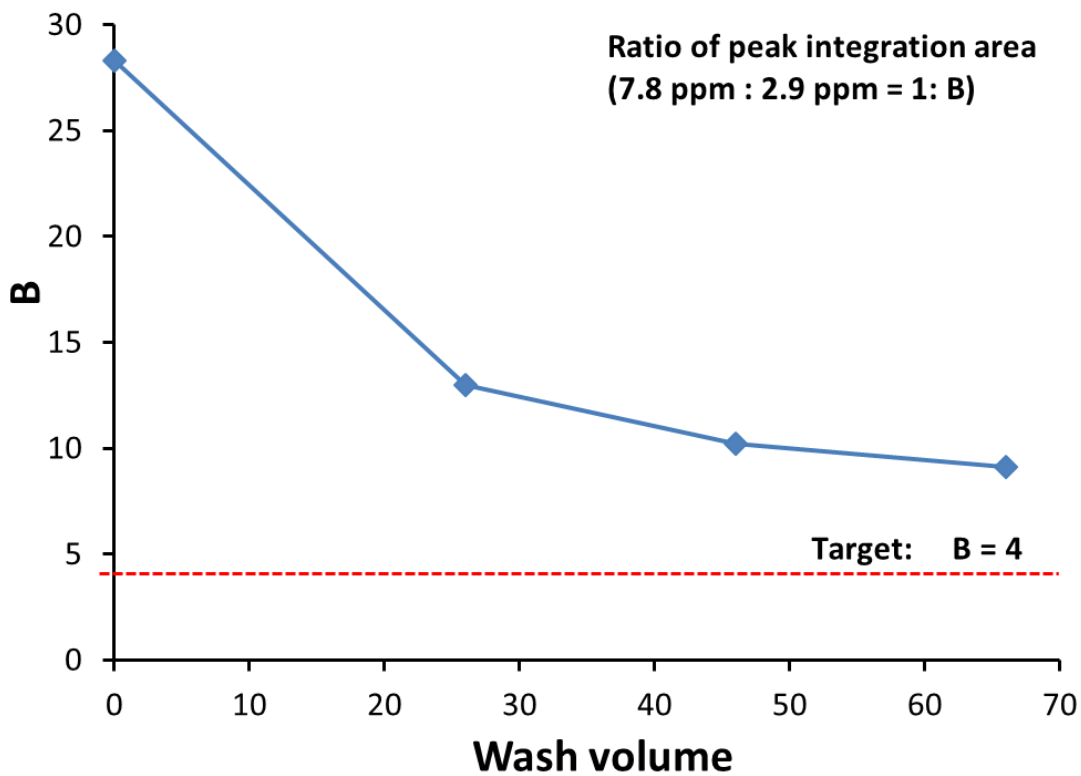


Figure 5.8. Ratio of peak integration area in NMR for retentate samples during diafiltration.

5.3.2.2. Loading of Fmoc-Rink Linker on PyPEG

The loading of linker on PyPEG was conducted with excess Fmoc-Rink (3.6 eq) and HBTU/DIEA due to the presence of excess PEG. HPLC results showed the disappearance of PyPEG and the appearance of a broader peak at a later retention time (RT = 14.5 - 21.0 min) over one night of reaction (Figure 5.9).

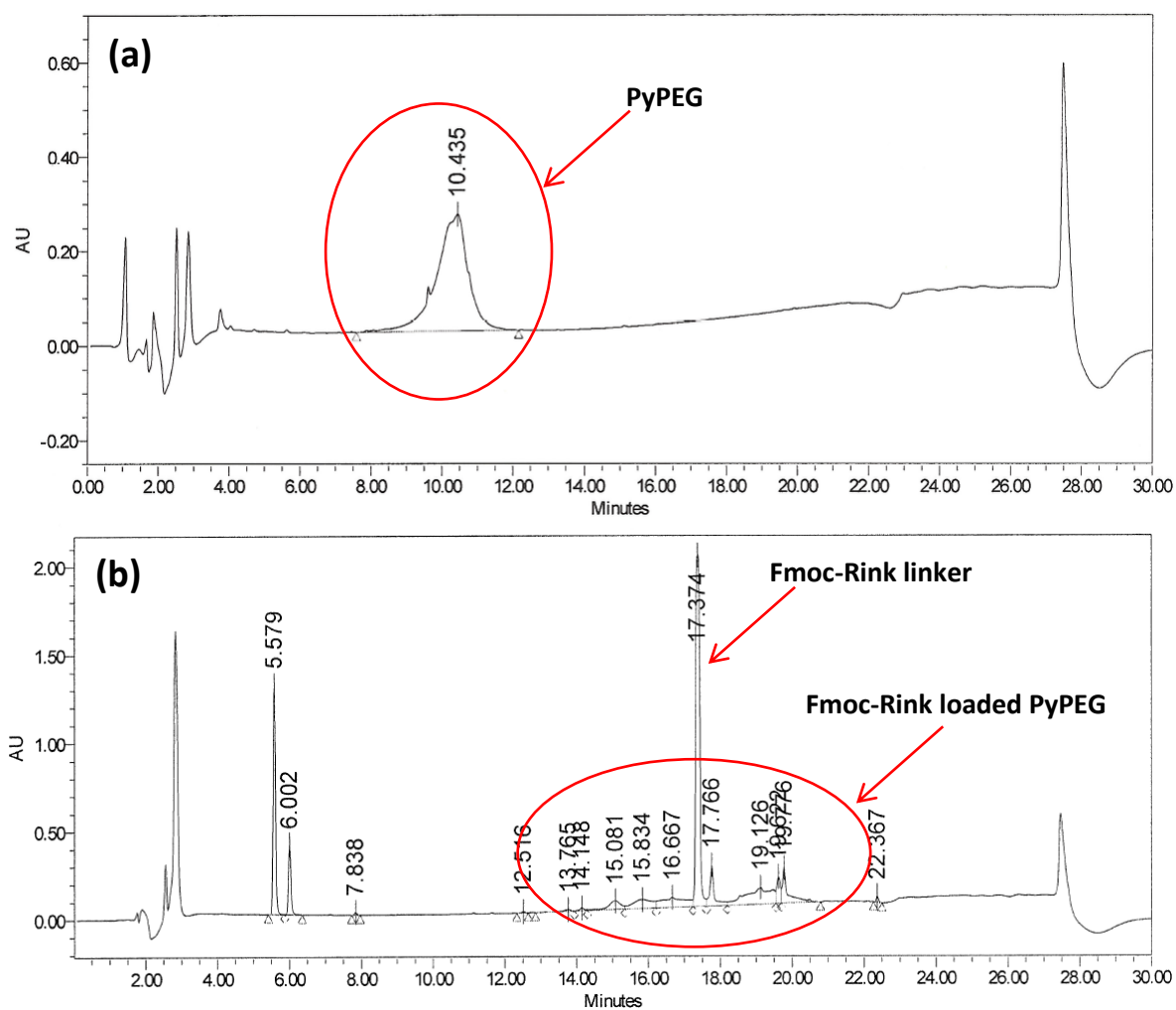


Figure 5.9. HPLC results of: (a) PyPEG and (b) loading of Fmoc-Rink linker overnight.

However, the ninhydrin test of the precipitated Fmoc-Rink-loaded compound gave a positive result (blue), indicating the presence of free amine groups. As each PyPEG molecule has four reactive sites for the loading of Fmoc-Rink linker, HPLC and ninhydrin test results suggested that partial loading on PyPEG was achieved overnight, but some of the free amine groups remained unreacted. Therefore, additional Fmoc-Rink linker was added into the reaction solution and the remaining free amine groups were finally consumed (Table 5.5).

Table 5.5. Addition of reagents for the loading of Fmoc-Rink linker over seven days.

| Step | Addition of reagents | Cumulative quantity | Reaction time (h) | Cumulative reaction time (h) | Ninhydrin test |
|------|---|--|-------------------|------------------------------|---------------------------------|
| 1 | Fmoc-Rink linker (3.6 eq) DIEA (7.6 eq) HBTU (1.5 eq) | Fmoc-Rink linker (3.6 eq) DIEA (7.6 eq) HBTU (1.5 eq) | 48 | 48 | + (i.e. blue) |
| 2 | Fmoc-Rink linker (0.3 eq) DIEA (0.2 eq) HBTU (0.2 eq) | Fmoc-Rink linker (3.9 eq) DIEA (7.8 eq) HBTU (1.7 eq) | 96 | 144 | + - (i.e. bluish yellow) |
| 3 | Fmoc-Rink linker (0.4 eq) DIEA (7.7 eq) HBTU (0.2 eq) | Fmoc-Rink linker (4.3 eq) DIEA (15.5 eq) HBTU (1.9 eq) | 3 | 147 | + - (i.e. bluish yellow) |
| 4 | Fmoc-Rink linker (0.6 eq) DIEA (0.3 eq) HBTU (0.2 eq) | Fmoc-Rink linker (4.9 eq) DIEA (15.8 eq) HBTU (2.1 eq) | 1 | 148 | - (i.e. yellow) |

Diafiltration was performed on the reaction solution with Inopor 750 in order to remove excess Fmoc-Rink linker and other excess reagents. The presence of Fmoc-Rink linker (UV active) in the retentate stream was monitored by HPLC (Figure 5.10).

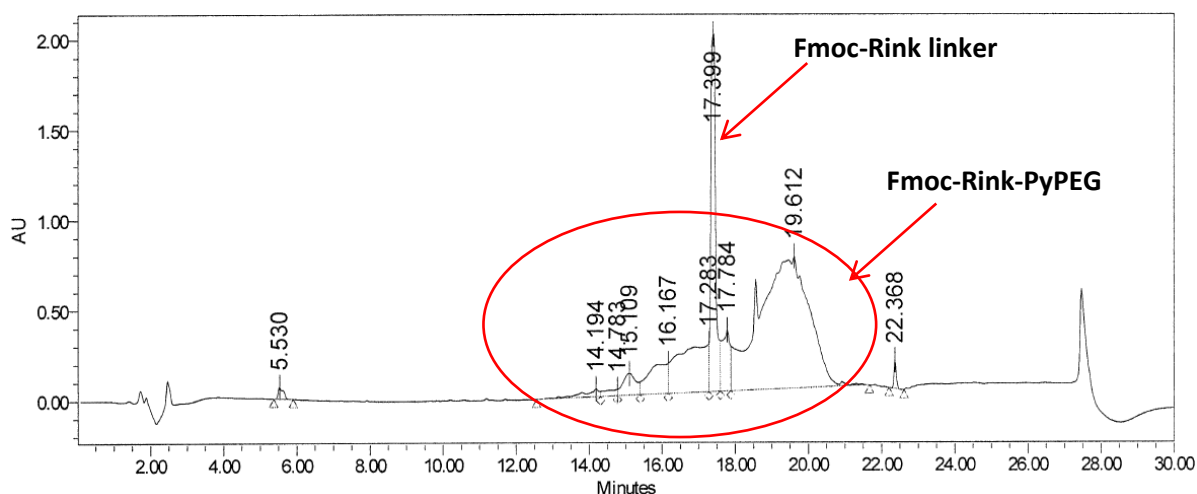


Figure 5.10. HPLC result of Fmoc-Rink-PyPEG before diafiltration.

The removal of excess linker by diafiltration was found to be inefficient in DCM and DCM/THF mixtures as the relative peak integration area of the linker with respect to Fmoc-Rink-PyPEG remained relatively constant after extensive washing with these solvents (Table 5.6). By switching the solvent to a DCM/acetonitrile mixture, significant progress was made as the relative peak integration area of the Fmoc-Rink linker decreased from 15.1 % to 7.2 % after 15 washes (500 mL each wash). Further washing with acetonitrile and acetonitrile/THF mixture was inefficient as the relative peak integration area of Fmoc-Rink linker only decreased marginally from 7.2 % to 4.8 % after excessive washing (Table 5.6).

Table 5.6. Solvent swap during diafiltration and its effect on the removal of Fmoc-Rink linker.

| Description | Relative peak integration area of Fmoc-Rink linker |
|---|--|
| Original sample | 15.1 |
| 10 washes with pure DCM (1 L each) | 18.0 |
| 5 washes with DCM/THF (50/50, v/v, 500 mL each) | 15.1 |
| 15 washes with DCM/acetonitrile (50/50, v/v, 500 mL each) | 7.2 |
| 5 washes with pure acetonitrile (500 mL each) | 6.8 |
| 5 washes with acetonitrile/THF (50/50, v/v, 500 mL each) | 5.0 |
| 10 washes with pure acetonitrile (500 mL each) | 4.8 |

As Fmoc-Rink linker could be removed by switching solvent for diafiltration, its rejection by Inopor 750 was definitely lower than 100 %. Its inefficient removal (first in DCM and DCM/THF mixtures, and then in acetonitrile and acetonitrile/THF mixtures) suggests that the Fmoc-Rink linker was probably trapped by the PEG arms of the anchor and hence could not permeate through the membrane. This trapping is likely the result of strong dipole-dipole interaction between the PEG arms of the anchor and the linker, similar to the case of excess PEG which still remained with the product even after excessive washing (Figure 5.8). The extent of trapping, however, could be manipulated by changing the solvent, which could interact with the PEG in competition against the linker (or vice versa). With a dielectric constant of 38 as compared to 9 for DCM, acetonitrile is significantly more polar than DCM. Therefore, it could interact more strongly with the PEG than DCM and free more linker from the PEG arms, which could then permeate through the membrane during diafiltration. As a result of this finding, acetonitrile was used as the solvent for the MEPS on Fmoc-Rink-PyPEG, which is discussed in the following section.

5.3.2.3. MEPS of Fully Deprotected Fmoc-RADA-NH₂ on Rink-PyPEG

The couplings of Fmoc-Ala-OH were more straightforward than those of Fmoc-Asp(OtBu)-OH and Fmoc-Arg(Pbf)-OH. Starting from 1.5 eq amino acid and coupling reagents, the first coupling of Fmoc-Ala-OH was nearly complete in 30 minutes according to the result of the ninhydrin test and required an additional 0.2 eq of amino acid and coupling reagents to proceed to completion, while the next coupling went to completion smoothly in 30 minutes. In contrast, the coupling of Fmoc-Asp(OtBu)-OH could not proceed to completion even after the addition of 0.2 eq amino acid and coupling reagents on top of the starting materials. Diafiltration had to be performed before the addition of another 0.2 eq materials in order to drive the coupling to completion. To a greater extent, the coupling of Fmoc-Arg(Pbf)-OH also turned out to be problematic, as the reaction could not finish even after diafiltration (6 wash volumes) and the addition of a further 1.5 eq amino acid and coupling reagents.

The HPLC result of retentate sample for each post-coupling diafiltration provides some hint about the cause of problematic couplings for Fmoc-Asp(OtBu)-OH and Fmoc-Arg(Pbf)-OH. Based on the peak heights of amino acid in Figure 5.11, the amount of Fmoc-Ala-OH left in the system after diafiltration was much less than Fmoc-Asp(OtBu)-OH and Fmoc-Arg(Pbf)-OH. Although this observation could be attributed to the higher rejections of Fmoc-Asp(OtBu)-OH and Fmoc-Arg(Pbf)-OH as compared to Fmoc-Ala-OH, it was more likely that the polar side-chains of these two amino acids interacted with the PEG arms of the anchor as in the purification of Fmoc-Rink-PyPEG and PyPEG, and hence had difficulty in accessing the active site for coupling. As a result, additional materials were needed to drive the couplings to completion. In contrast, Fmoc-Ala has a non-polar side-chain and hence had far less interaction with the PEG arms of the anchor. It could then reach the active site more readily, leading to fast and complete couplings.

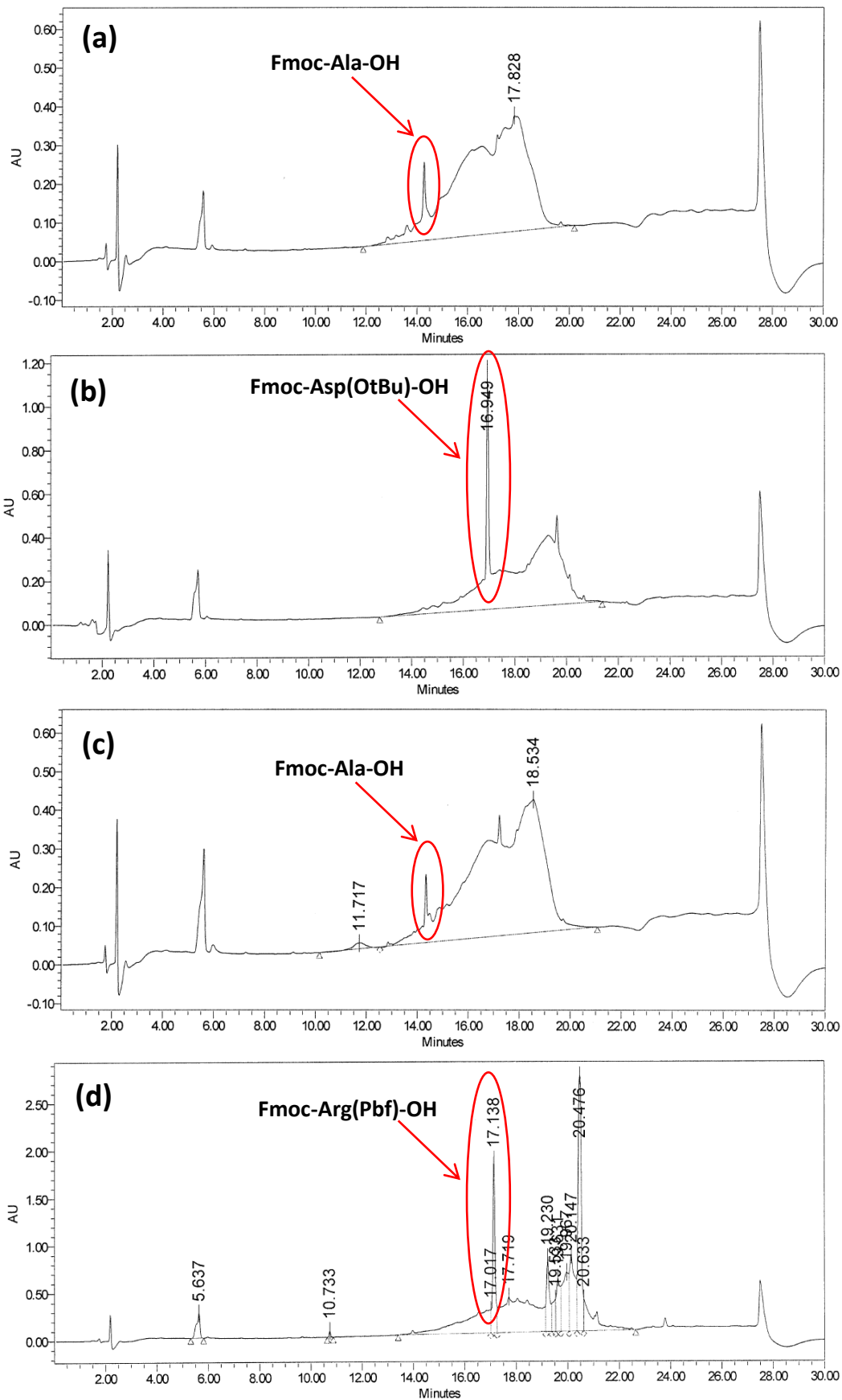


Figure 5.11. HPLC results for: (a) Fmoc-A-Rink-PyPEG, (b) Fmoc-DA-Rink-PyPEG, (c) Fmoc-ADA-Rink-PyPEG and (d) Fmoc-RADA-Rink-PyPEG after post-coupling diafiltration (10 wash volumes for (a)-(c); 6 wash volumes for (d)).

The synthesis of Fmoc-RADA-NH₂ was stopped after the coupling of Fmoc-Arg(Pbf)-OH failed to proceed to completion after repeated diafiltrations and additions of reagents. Diafiltration was performed with different polar solvents in order to search for a candidate that could interact with the PEG arms of the anchor even more strongly than acetonitrile and hence undo the trapping of Fmoc-Arg(Pbf)-OH. To test the effect of polar solvent on the removal of Fmoc-Arg(Pbf)-OH, diafiltration was performed in cycles, first with pure acetonitrile and then with a mixture of polar solvent (DMF, DMSO, isopropanol and ethanol) with acetonitrile (Table 5.7). Experimental data showed that the removal of the hydrophilic amino acid was inefficient with all tested solvents, as the relative peak integration area of the amino acid remained approximately constant with respect to the anchored product.

Table 5.7. Solvent swap during diafiltration and its effect on the removal of Fmoc-Arg(Pbf)-OH.

| Description | Relative peak integration area of Fmoc-Arg(Pbf) |
|---|---|
| 3 washes with pure acetonitrile (1 L each) | 8.49 |
| 2 washes with acetonitrile/DMF (50/50, v/v, 1 L each) | 8.66 |
| 2 washes with pure acetonitrile (1 L each) | 7.55 |
| 2 washes with acetonitrile/DMSO (50/50, v/v, 1 L each) | 7.42 |
| 2 washes with pure acetonitrile (1 L each) | 8.18 |
| 2 washes with acetonitrile/isopropanol (50/50, v/v, 1 L each) | 6.90 |
| 2 washes with acetonitrile/ethanol (50/50, v/v, 1 L each) | 7.05 |

In summary, although PyPEG could be retained completely by the membrane and hence avoid the loss of anchored peptide during diafiltration, its polar PEG arms tended to interact strongly with polar compounds (PEG, Fmoc-Rink linker, Fmoc-Asp(OtBu)-OH and Fmoc-Arg(Pbf)-OH) and create a trapping effect, which prevented these compounds from accessing the active site for reaction. Polar solvents such as acetonitrile could be used in order to free the polar compounds from the PEG arms, as the solvents compete against the polar compound for the interaction with the PEG arms. A better solvent than acetonitrile had to be identified for the research work to continue, as Fmoc-Asp(OtBu)-OH and Fmoc-Arg(Pbf)-OH were trapped to a great extent by the PEG arms of the anchor in acetonitrile, and several polar solvents that were tested failed to mitigate the situation.

5.3.3. Modelling of Membrane Cascade for MEPS

5.3.3.1. Validation of MEPS in Single-stage System

The MEPS of fully protected Pyr-SAFDL-Rink-DDBA comprised repetitive cycles of coupling, post-coupling diafiltration, de-Fmoc and post-de-Fmoc diafiltration as shown in Figure 5.12. For example, the first cycle consisted of the coupling of Fmoc-Leu-OH with H₂N-Rink-DDBA, post-coupling diafiltration for the removal of excess activated Fmoc-Leu-OH and by-products of coupling, de-Fmoc of Fmoc-Leu-Rink-DDBA and post-de-Fmoc diafiltration for the removal of piperidine and by-products of de-Fmoc.

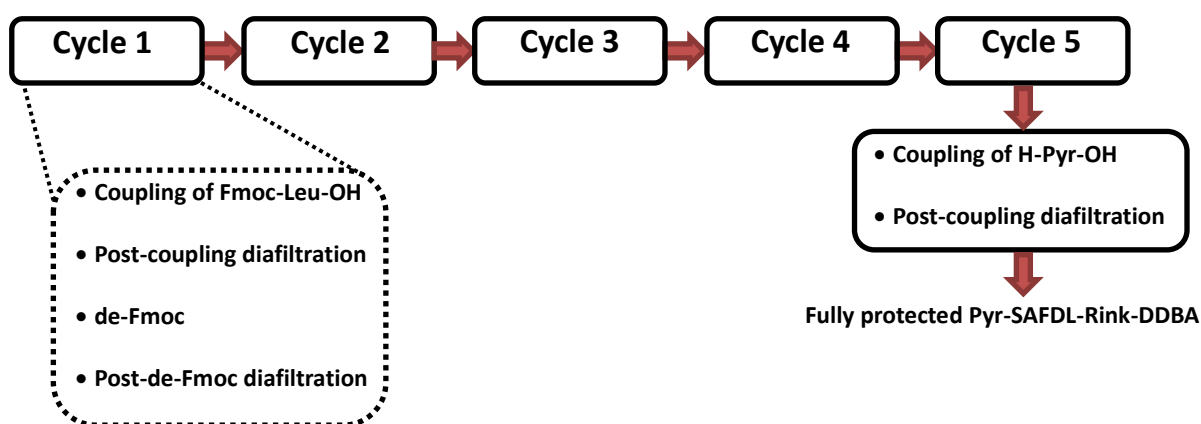
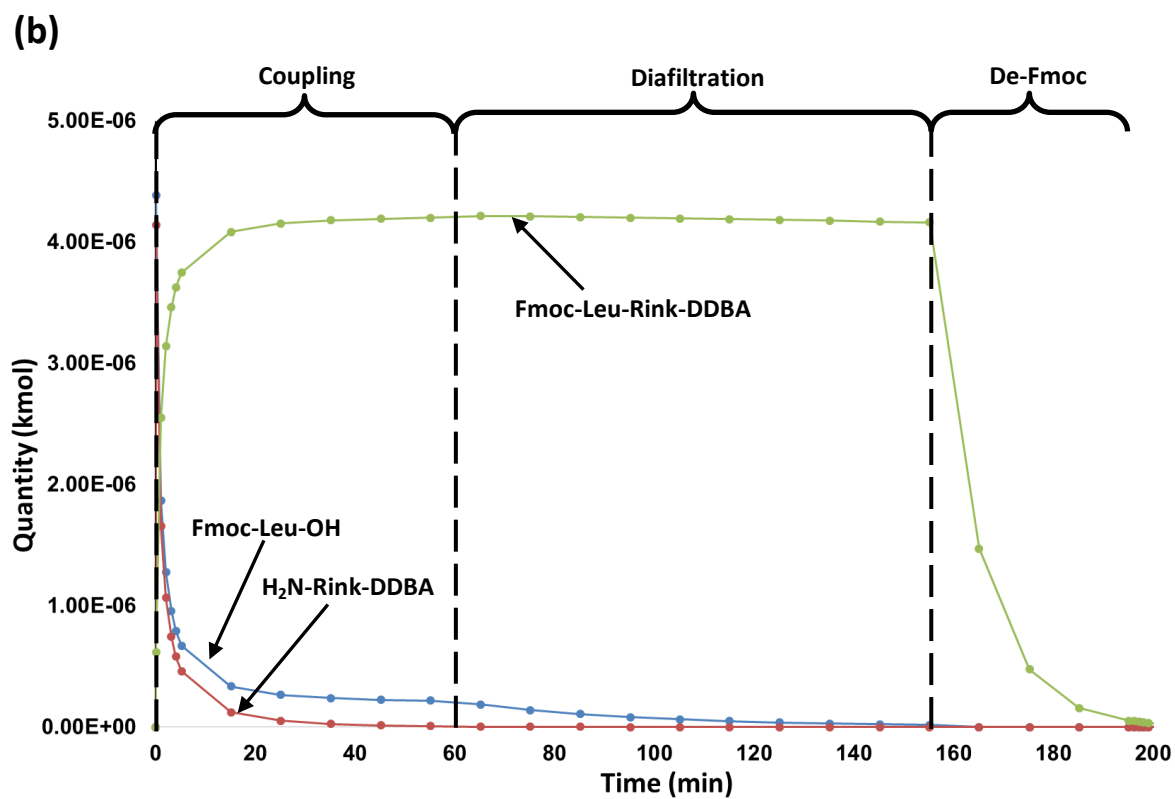
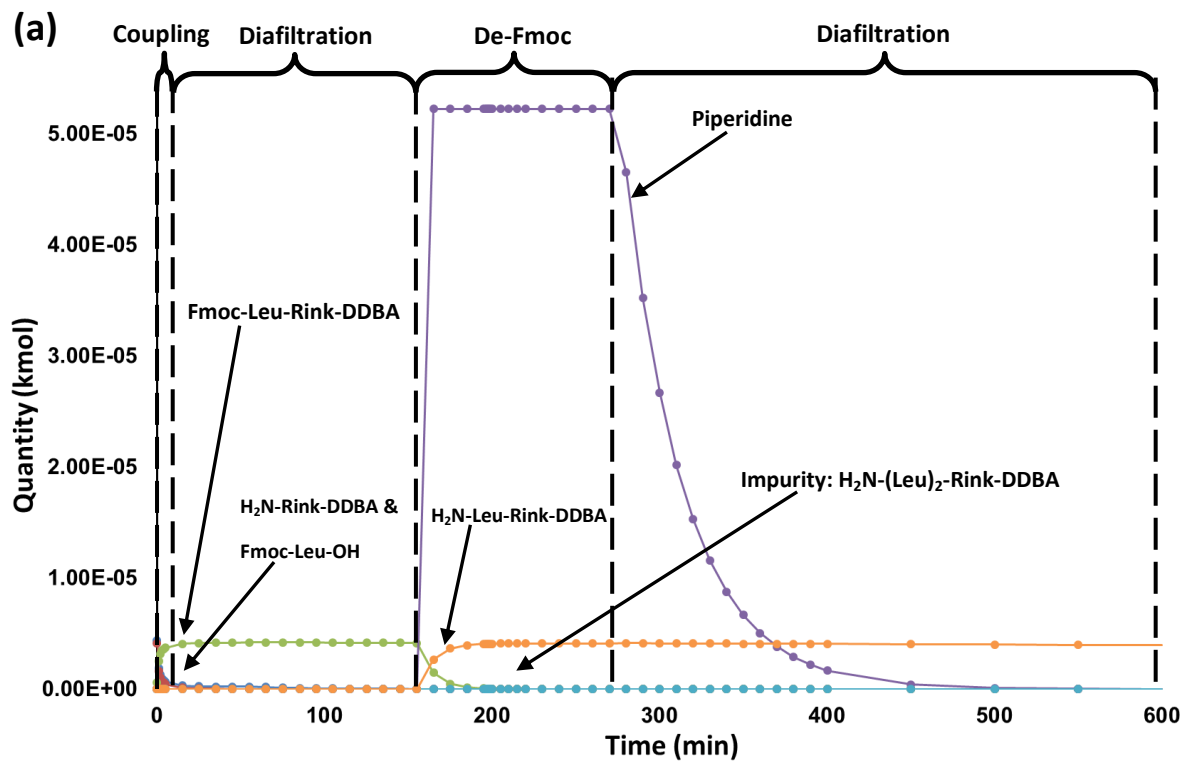


Figure 5.12. MEPS of fully protected Pyr-SAFDL-Rink-DDBA.

In the present model, the concentration of each component in each part of the system was modelled dynamically for the entire MEPS process. For demonstration purposes, the concentrations of relevant components in the first cycle of coupling, post-coupling diafiltration, de-Fmoc and post-de-Fmoc diafiltration are shown in Figure 5.13, where the concentrations of Fmoc-Leu-OH, H₂N-Rink-DDBA, Fmoc-Leu-Rink-DDBA, H₂N-Leu-Rink-DDBA, piperidine and H₂N-(Leu)₂-Rink-DDBA in the retentate side of the membrane (Membrane_Unit in Figure 5.3) versus time are shown. Due to the mixing provided by the feed pump, the concentrations of components in the retentate side of the membrane are good representations of the overall concentrations in the system.



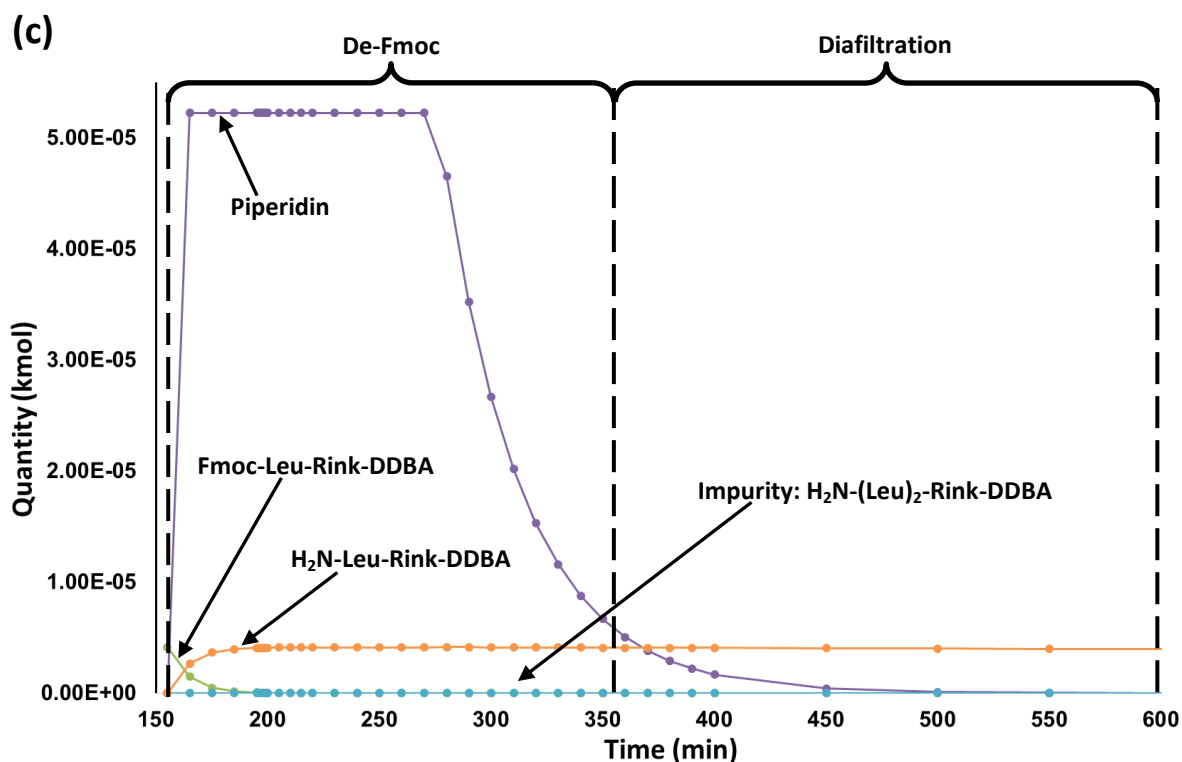


Figure 5.13. The concentrations of the relevant components in: (a) the entire first cycle of operation; (b) in the coupling and diafiltration; (c) in the de-Fmoc and diafiltration.

As shown in Figure 5.13, the concentrations of all the relevant components were modelled according to the actual experiment. In the coupling of Fmoc-Leu-OH (Figure 5.13 (b)), the concentrations of Fmoc-Leu-OH and H₂N-Rink-DDBA decreased exponentially, while the concentration of the target product, Fmoc-Leu-Rink-DDBA, increased. During the post-coupling diafiltration (Figure 5.13 (b)), the concentration of excess Fmoc-Leu-OH (rejection = 33.0 %) decreased, while that of Fmoc-Leu-Rink-DDBA remained relatively constant due to its high rejection (99.6 %). In the de-Fmoc of Fmoc-Leu-Rink-DDBA (Figure 5.13 (c)), the concentration of piperidine increased substantially in the retente side of the membrane and then remained constant, as piperidine was not consumed by the reaction. At the same time, the concentration of Fmoc-Leu-Rink-DDBA decreased exponentially, whereas that of the deprotected product, H₂N-Leu-Rink-DDBA, increased. Due to the presence of minute amounts of Fmoc-Leu-OH in the system during de-Fmoc, the formation of impurity (H₂N-(Leu)₂-Rink-DDBA) occurred, albeit at a negligible extent. In the post-de-Fmoc diafiltration (Figure 5.13 (c)), the

concentration of piperidine (rejection = 33.0 %) decreased exponentially, while that of H₂N-Leu-Rink-DDBA remained relatively constant due to its high rejection (99.6 %).

The validation of this model is done by comparing the simulated overall yield and purity of the final product with the experimental values. As the modelled overall yield and purity (72.5 % and 93.5 % respectively) were close to experimental values (71.2 % and 88.1 % respectively), the present model successfully simulated the MEPS process in a single-stage system.

5.3.3.2. Two-stage Membrane Cascade System

To simulate the two-stage system (Figure 5.15), the single-stage system was modified with the addition of a feed tank (Figure 5.14) in order to check if the model was still valid with the new element. The total volume of the system was kept the same (400 mL) and the corresponding modelled yield and purity of the final anchored peptide (72.0 % and 93.5 % respectively) were close to the original model.

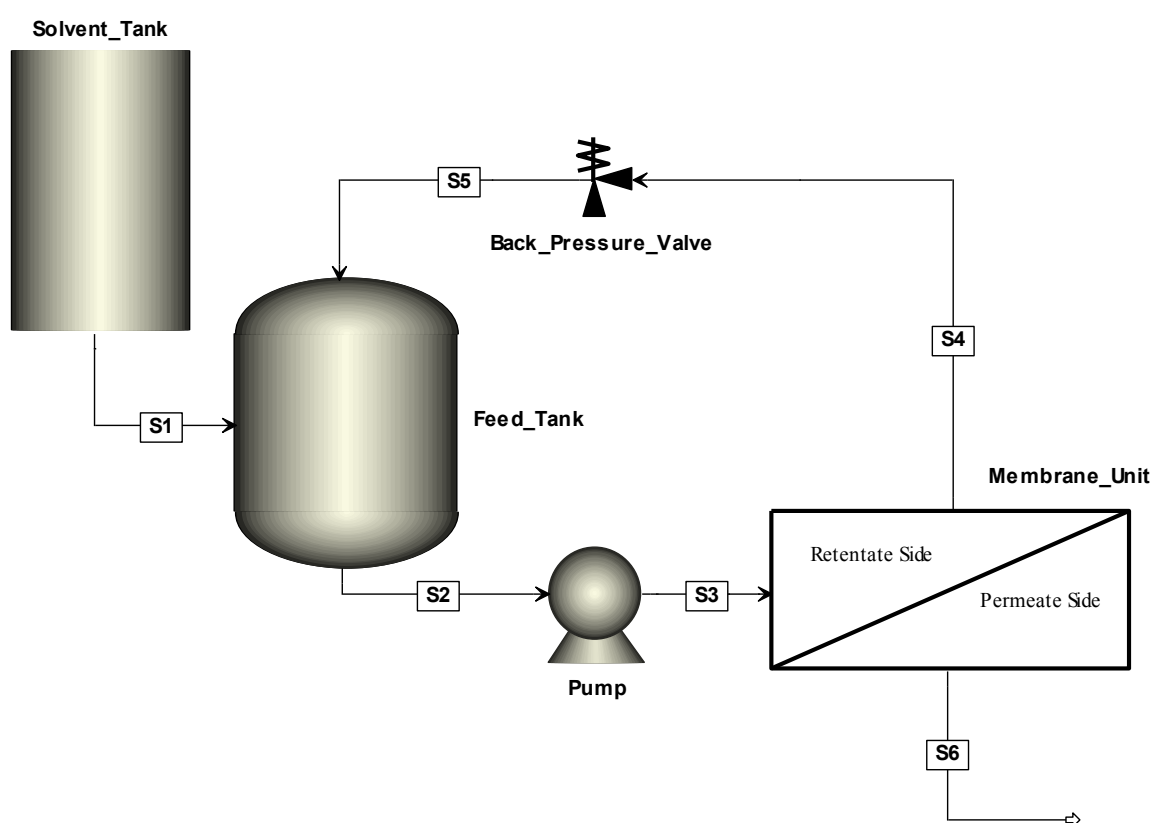


Figure 5.14. Schematic of the modified single-stage membrane system.

The two-stage system (Figure 5.15) was modelled based on the modified single-stage system (Figure 5.14). The permeate stream from the stage-one membrane was fed into the stage-two membrane. Part of the feed permeated through the stage-two membrane, and the remaining part was recycled back to the feed tank. The stage-two membrane served to recover the anchored peptide that permeated through the stage-one membrane, reducing the overall yield loss significantly.

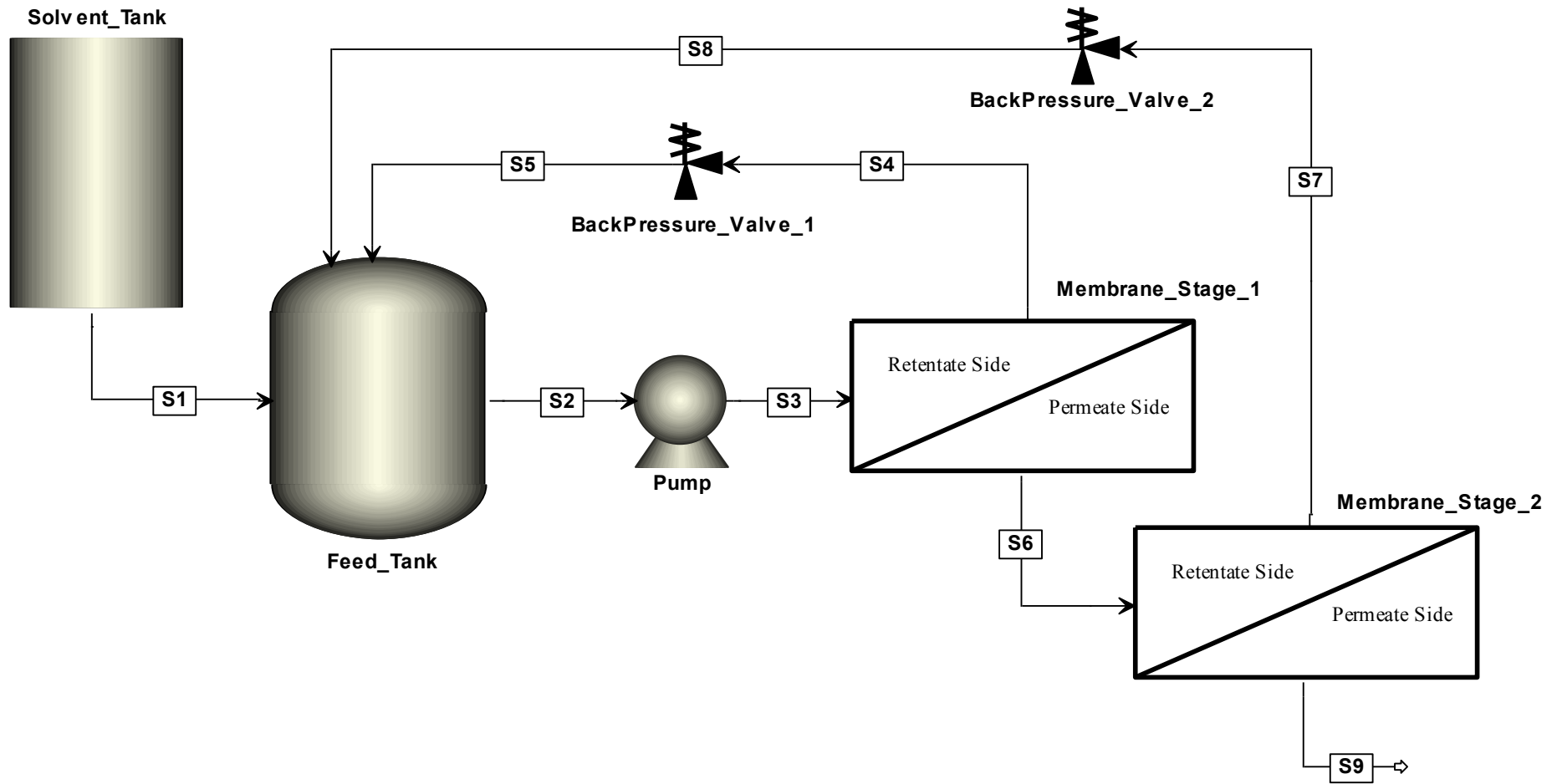


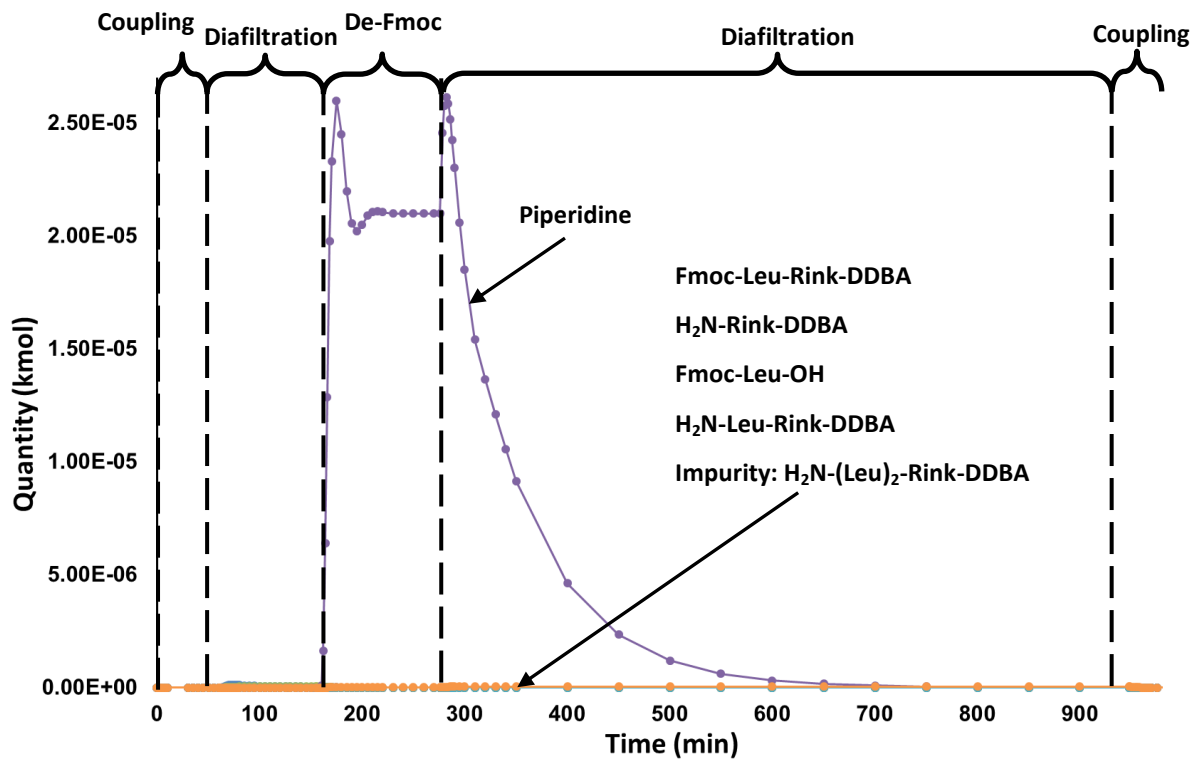
Figure 5.15. Schematic of the two-stage membrane cascade system.

The operation procedure in the two-stage system was a slightly modified version of that in the single-stage system: the operation time of post-de-Fmoc diafiltration was doubled in order to remove the piperidine in the system.

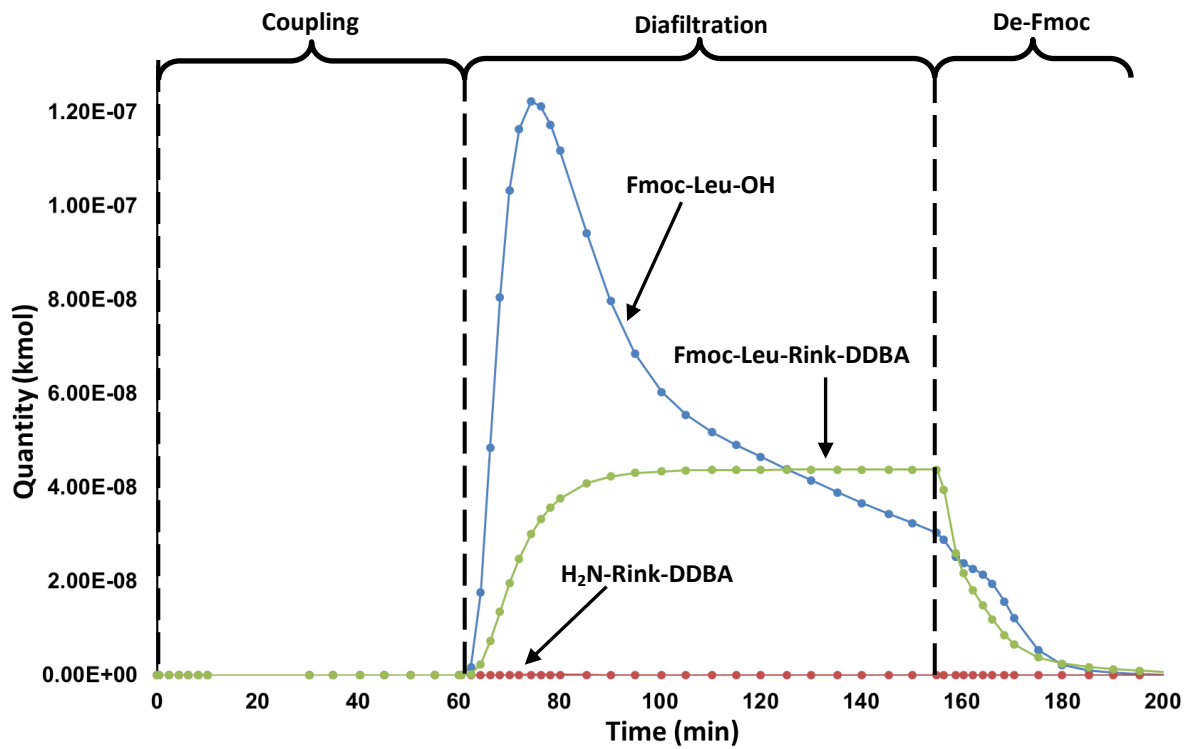
For demonstration purposes, the concentrations of components (Fmoc-Leu-OH, H₂N-Rink-DDBA, Fmoc-Leu-Rink-DDBA, H₂N-Leu-Rink-DDBA, piperidine and H₂N-(Leu)₂-Rink-DDBA) in the retentate side of stage-two membrane (Membrane_Stage_2 in Figure 5.15) in first cycle and the coupling of Fmoc-Asp(OtBu)-OH (i.e. the first step in the second cycle) are shown below (Figure 5.16). The concentrations of these components in the feed tank (Feed_Tank in Figure 5.15) are not shown again as they shared the similar trends as in the retentate side of the membrane unit in the single-stage system (Figure 5.13).

During the post-coupling diafiltration (Figure 5.16 (b)), the concentration of excess Fmoc-Leu-OH increased in the retentate side of the stage-two membrane and then decreased to a negligible level, whereas the concentration of Fmoc-Leu-Rink-DDBA increased and then remained constant. The initial accumulation of materials (Fmoc-Leu-OH and Fmoc-Leu-Rink-DDBA) was due to the difference between the rates of material entering the retentate side of the stage-two membrane and the rates of them permeating through the stage-two membrane. The accumulation of materials levelled off, as shown by the concentration of Fmoc-Leu-Rink-DDBA, as the retentate stream of the stage-two membrane was recycled back to the feed tank. As the rejection of Fmoc-Leu-Rink-DDBA was significantly higher than that of Fmoc-Leu-OH (99.6 % as compared to 33.0 %), the concentration of the former stayed relatively constant, whereas the concentration of the latter decreased to a negligible level by the end of the diafiltration. The trends shown in Figure 5.16 (b) were identical to those of PEG 400 and PEG 2000 in the study of Kim et al. (2013) (note: Figure 8 in this article).

(a)



(b)



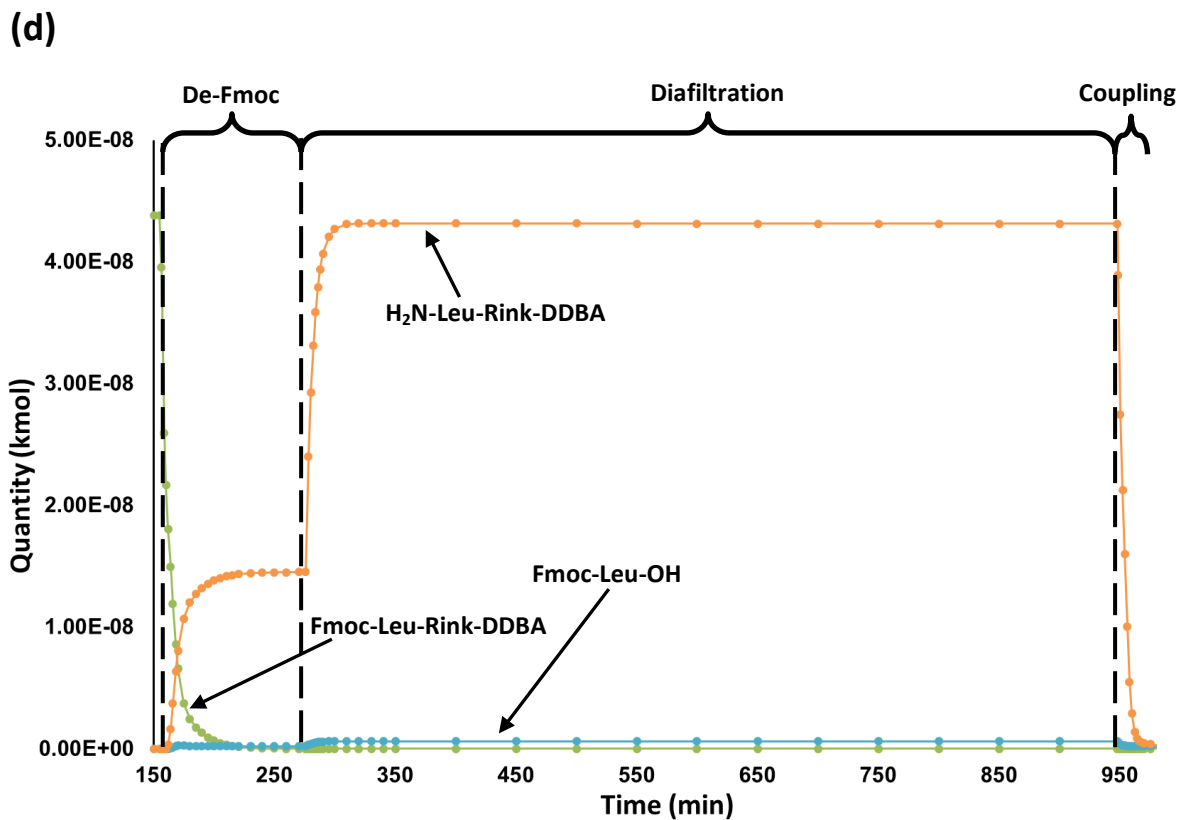
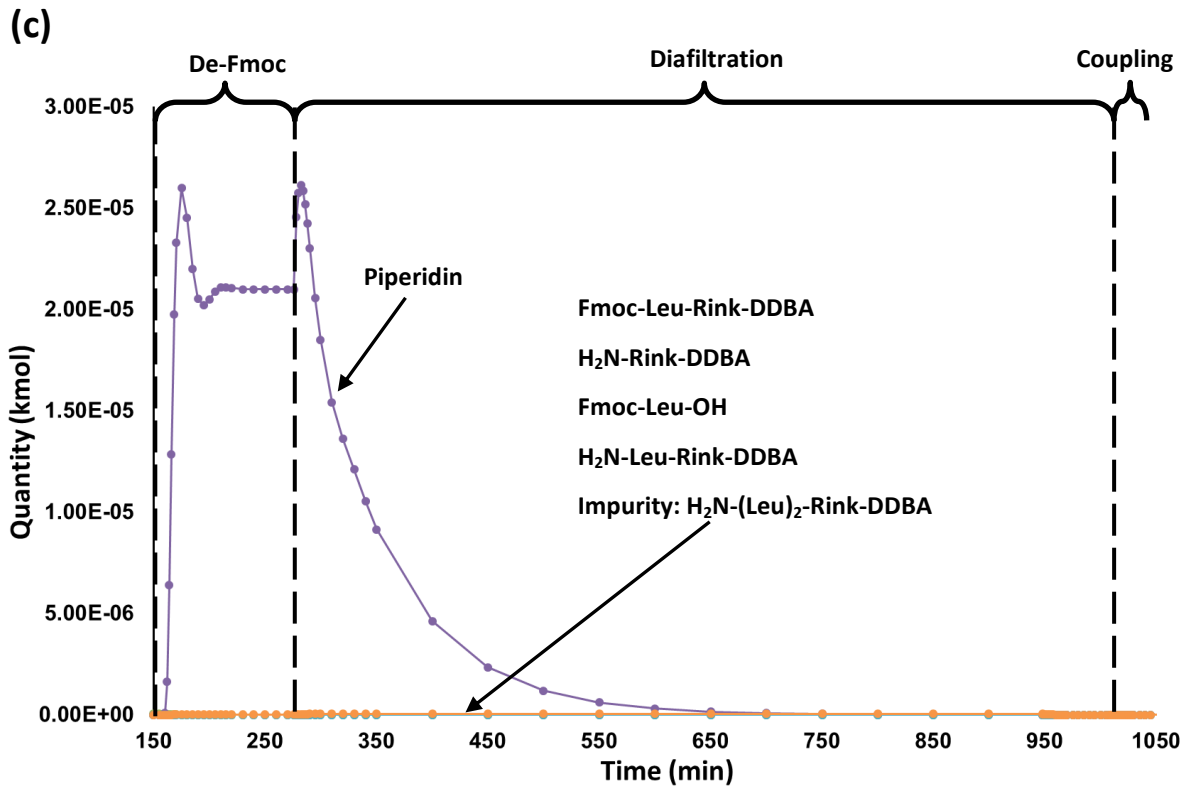


Figure 5.16. The concentrations of the relevant components in: (a) the entire first cycle of operation and coupling of Fmoc-Asp(OtBu)-OH; (b) in the coupling, diafiltration and de-Fmoc; (c) & (d) in the de-Fmoc, diafiltration and coupling.

During the de-Fmoc (Figure 5.16 (c) & (d)), the stage-one membrane was operated at 20 bar, while the stage-two membrane was operated at 0 bar. This set-up allowed the piperidine solution to permeate through the stage-one membrane into the stage-two membrane and then was completely recycled back to the feed tank as the retentate stream coming out of the stage-two membrane. As a result, the concentration of piperidine increased and then levelled off as shown in Figure 5.16 (c). At the same time, the Fmoc-Leu-Rink-DDBA was deprotected, forming H₂N-Leu-Rink-DDBA, whose concentration increased and levelled off like the concentration of piperidine. Figure 5.16 (d) shows that this approach served to deprotect all the Fmoc-Leu-Rink-DDBA in the retentate side of the stage-two membrane, as the concentration of Fmoc-Leu-Rink-DDBA decreased to negligible level.

Another diafiltration was performed after the de-Fmoc, during which the same initial accumulation of both piperidine and H₂N-Leu-Rink-DDBA occurred as in the post-coupling diafiltration (Figure 5.13 (b)). Figure 5.16 (b) shows that the present extent of diafiltration was sufficient for the removal of piperidine, as the concentration of piperidine decreased exponentially to a negligible level, while the concentration of H₂N-Leu-Rink-DDBA remained relatively constant.

In terms of performance metrics (Table 5.8), the MEPS in two-stage membrane cascade system had a significantly higher overall yield (98.3 %) and a similar purity (92.9 %) as compared to the experimental values of the single-stage MEPS (71.2 % and 88.1 % respectively) at the expense of a slightly longer process time (2.5 h · mmol⁻¹ as compared to 2.2 h · mmol⁻¹). As a result of the high yield, the two-stage MEPS would have 84.6 % higher building block utility, 33.5% lower material cost, 24.2 % shorter process time and 11.3 % lower E-factor than SPPS (Figure 5.17). The volumetric efficiency was slightly lower (13.5 %) due to the increase in system volume in the two-stage system, but could be improved by increasing the scale of peptide synthesis. Nevertheless, the modelling data showed that the two-stage MEPS process would be an attractive alternative to the existing SPPS.

Table 5.8. Performance of SPPS, MEPS (single-stage) and MEPS (Two-stage).

| Synthesis method* | SPPS | MEPS (Single-Stage) | MEPS (Two-stage) |
|--|-------|---------------------|------------------|
| Scale (mmol) | 5.00 | 33.65 | 33.65 |
| System volume (mL) | 70 | 400 | 750 |
| Before cleavage and global deprotection | | | |
| Overall yield (%) | 72.6 | 71.2 | 93.8 |
| Building Block Utility (%) | 48.4 | 67.8 | 89.3 |
| Material cost (Euro · mmol ⁻¹) | 70.84 | 61.65 | 47.12 |
| Material cost excluding resin/anchor cost (Euro · mmol ⁻¹) | 45.57 | 22.21 | 18.56 |
| Process time (h · mmol ⁻¹) | 3.3 | 2.2 | 2.5 |
| Volumetric efficiency (mmol · L ⁻¹) | 51.9 | 59.9 | 44.9 |
| E-factor | 1294 | 915 | 1148 |

*Details of SPPS and MEPS (Single-Stage) are discussed in Section 4.3.4.

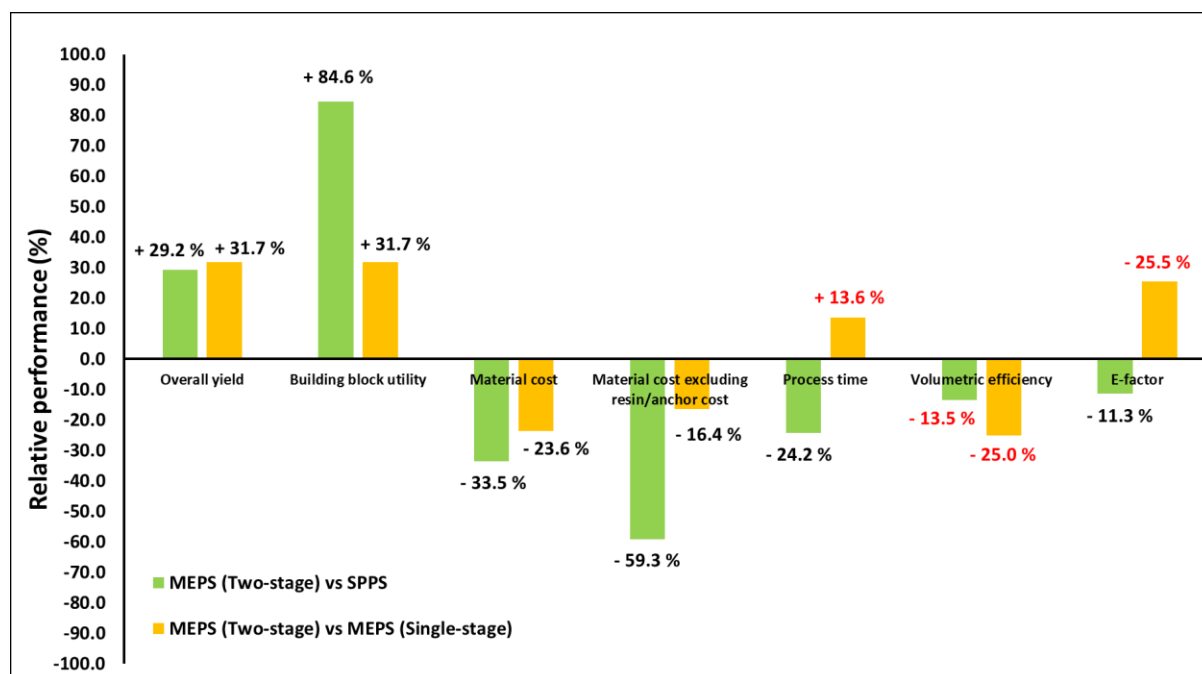


Figure. 5.17. Performance of MEPS (Two-stage) in comparison to SPPS and MEPS (Single-stage).

On the other hand, the two-stage MEPS would have a 31.7 % higher building block utility and 23.6 % lower material cost than the single-stage MEPS, but with 13.6 % longer process time, 25.0 % lower volumetric efficiency and 25.5 % higher E-factor (Figure 5.17). The longer process time and higher E-factor were the direct consequence of the extended post-de-Fmoc diafiltration, whereas the lower volumetric efficiency was a result of the increase in the system volume. However, these underperforming figures were outweighed by the significantly lower material cost of the two-stage process.

5.4. Conclusions

Based on titration tests, every gram of silica nanoparticle (diameter: 10 - 20 nm) had 1.75 mmol free amine groups. This loading was significantly higher than that of PL-Rink resin ($0.72 \text{ mmol} \cdot \text{g}^{-1}$), which was used for the SPPS of partially deprotected Pyr-SAFDL-NH₂. The loading test of nanoparticles with 0.1, 0.5, 0.9, 1.8 and 2.7 eq Fmoc-Rink linker/HBTU in the presence of excess DIEA (4.1 - 11.5 eq) showed that, except for the case of 0.1 eq linker, most of the linker remained unreacted after two days of reaction and the addition of more HBTU (0.5 - 2.8 eq). This suggested that most of the free amine groups were not present on the surface and hence were inaccessible to the Fmoc-Rink linker even at high concentration (as for the case of 2.7 eq Fmoc-Rink linker). The capping of unreacted amine was carried out with excess acetic anhydride (1045 eq) and DIEA (208 eq), but had to be repeated three times in order to proceed to completion based on the result of the ninhydrin test, confirming the inaccessibility of most of the free amine groups (i.e. not on the surface of the nanoparticles). By coupling the free amine group with adipic acid, and then another coupling with hexamethylenediamine, more free amine groups could be accessed as the coupling with 0.5 eq Fmoc-Rink linker was complete overnight. After the de-Fmoc with piperidine, the next coupling with 0.5 eq Fmoc-Ala-OH only reached 50 % completion after one day of reaction and the cause was unknown. The peptide synthesis on nanoparticles was terminated due to the lack of quantitative and qualitative analysis techniques.

The removal of excess PEG from crude PyPEG (average molecular weight is approximately $6182 \text{ g} \cdot \text{mol}^{-1}$) by diafiltration with Inopor 750 showed that the anchor had complete rejection and 1.3 eq of excess PEG remained in the system after extensive washing (66 wash volumes), probably due to the interaction between the excess PEG and the PEG arms of the anchor. PyPEG was then loaded with excess Fmoc-Rink linker and purified by diafiltration again. The removal of excess linker by diafiltration was found to be efficient only in a DCM/acetonitrile mixture, suggesting that the Fmoc-

Rink linker was probably trapped by the PEG arms of the anchor and hence could not flow freely in the solvent and permeate through the membrane. This trapping is likely the result of strong dipole-dipole interaction between the PEG arms of the anchor and the Fmoc-Rink linker, similar to the purification of crude PyPEG where excess PEG still remained with the product even after excessive washing. MEPS of fully deprotected Fmoc-RADA-NH₂ was then performed on Fmoc-Rink-PyPEG, but all couplings had various degrees of difficulty to proceed to completion with 1.5 eq amino acid and coupling reagents. The couplings of Fmoc-Ala-OH were more straightforward than those of Fmoc-Asp(OtBu)-OH and Fmoc-Arg(Pbf)-OH. The first coupling of Fmoc-Ala-OH required an additional 0.2 eq of materials to proceed to completion, while the coupling of the next Fmoc-Ala-OH (after Fmoc-Asp(OtBu)-OH) went to completion smoothly in 30 minutes. In contrast, the coupling of Fmoc-Asp(OtBu)-OH could not proceed to completion even after the addition of 0.2 eq amino acid and coupling reagents on top of the starting materials. Diafiltration had to be performed before the addition of another 0.2 eq materials in order to drive the coupling to completion. To a greater extent, the coupling of Fmoc-Arg(Pbf)-OH also turned out to be problematic, as the reaction could not finish even after diafiltration (6 wash volumes) and the addition of 1.5 eq amino acid and coupling reagents, whose quantities were the same as the starting materials. The HPLC results of retentate samples for each post-coupling diafiltration suggested that Fmoc-Asp(OtBu)-OH and Fmoc-Arg(Pbf)-OH, with polar side-chains, had stronger interaction with the PEG arms of the anchor as in the case of Fmoc-Rink-PyPEG and PyPEG, and hence had difficulty in accessing the active site for coupling. In contrast, Fmoc-Ala-OH has a non-polar side-chain and hence had far less interaction with the PEG arms of the anchor. It could then reach the active site more readily, leading to fast and complete couplings. The synthesis of full deprotected Fmoc-RADA-NH₂ was stopped after the coupling of Fmoc-Arg(Pbf)-OH failed to proceed to completion after repeated diafiltrations and additions of reagents.

The modelling of single-stage MEPS of fully protected Pyr-SAFDL-Rink-DDBA was validated with experimental values. The modelled yield and purity of the final anchored peptide (72.5 % and 93.5 % respectively) were close to the experimental values (71.2 % and 88.1 % respectively). Based on the validated single-stage model, the two-stage membrane cascade system was constructed. With a slightly modified operation procedure based on that of the single-stage MEPS (i.e. the operation time of post-de-Fmoc diafiltration was doubled in order to remove the piperidine that was retained by the stage-two membrane), the two-stage MEPS had a significantly higher yield (98.3 %) and a similar purity (92.9 %) as compared to the experimental values of the single-stage MEPS (71.2 % and 88.1 % respectively) at the expense of a slightly longer process time ($2.5 \text{ h} \cdot \text{mmol}^{-1}$ as compared to $2.2 \text{ h} \cdot \text{mmol}^{-1}$). Although the two-stage MEPS had 13.6 % longer process time, 25.0 % lower volumetric efficiency and 25.5 % higher E-factor compared to the single-stage process, these underperforming metrics were outweighed by the significantly lower material cost (23.6 %) of the two-stage process. As compared to SPPS, the two-stage MEPS had 84.6 % higher building block utility, 33.5 % lower material cost, 24.2 % shorter process time and 11.3 % lower E-factor. The volumetric efficiency was slightly lower (13.5 %) due to the increase in system volume in the two-stage system, but could be improved by increasing the scale of peptide synthesis. Therefore, the modelling data showed that the two-stage MEPS process would be an attractive alternative to the existing SPPS.

Chapter Six – Conclusions and Suggestions for Future Work

6.1. Overall Conclusions

The two case studies of MEPS (the syntheses of fully deprotected Fmoc-RADA-NH₂ and partially deprotected Pyr-SAFDL-NH₂) achieved the aim and objectives of this research project.

They proved that the novel process is scalable (10.01 mmol and 33.65 mmol respectively as compared to 0.9 mmol and 1.8 mmol in Dr. So's work (Section 2.2.13.5)) and technically viable for obtaining a high purity and a decent yield that were comparable to those of conventional methods (SPPS and LPPS (by precipitation)). An in-depth understanding of the various aspects of MEPS was obtained and was used to improve the performance of this novel process. As a results, the second case study of MEPS (i.e. the synthesis of partially deprotected Pyr-SAFDL-NH₂) had noticeably better performance than the first one (i.e. the synthesis of fully deprotected Fmoc-RADA-NH₂). The investigation of alternative anchors and nanofiltration system shows that significant improvement of the process can be made, rendering the new process even more attractive compared to the existing peptide synthesis technologies (i.e. SPPS and LPPS). All the findings are summarised below.

6.2. Summary of Findings

In the first case study, MEPS before cleavage and global deprotection achieved an overall yield of 78.6 % and a purity of 98.5 %, which were similar to those of SPPS (78.3 % and 85.3 % respectively). In the second case study, the overall yield and purity of product before cleavage and global deprotection were 71.2% and 88.1 %, which were comparable to those of SPPS (72.6 % and 98.6 %) and LPPS (by precipitation) (72.4 % and 100.0 %). However, significant yield loss occurred during the cleavage and global deprotection in both case studies, undermining the performance of MEPS with respect to SPPS, whose overall yield loss was marginal (only 5 % according to industrial experience).

As shown in the second case study, it is beneficial to perform MEPS at the highest concentration of anchor in the starting solution in order to minimise the material cost and process time (both normalised by the synthesis scale). At a concentration of 10.4 weight % of H₂N-Rink-DDBA in THF at the beginning of synthesis, MEPS outperformed SPPS and LPPS (by precipitation) in general (8.7 - 49.1 % lower material cost, 33.3 - 91.7 % shorter process time, 15.4 - 55.6 % higher volumetric efficiency and 29.3 - 68.8 % lower E-factor) except for purity, overall yield and building block utility before cleavage and global deprotection.

In terms of chemistry, all the couplings could proceed to completion with close-to-equivalent (1.05 eq) amino acid, HBTU and HOBT under basic conditions in 30 minutes, and all de-Fmoc could be finished in 5.0 - 10.0 weight % piperidine solution in 1 hour. Due to the low equivalent of amino acids used, no formation of side product was observed due to the presence of residual amino acid after the post-coupling diafiltration. The challenge in performing the synthesis was the removal of piperidine, as residual piperidine after post-deFmoc diafiltration was found to be detrimental to the next coupling, as it not only consumed the activated amino acid, but also hindered the coupling in the presence of excess activated amino acids. The only solution to this problem was the addition of DIEA during diafiltration, which seemed to assist the removal of residual piperidine at a dilute concentration (below 0.08 M).

Although the anchored peptide had rejection higher than 99 % (in the second case study, Fmoc-L-Rink-DDBA, H₂N-L-Rink-DDBA, Fmoc-DL-Rink-DDBA and H₂N-DL-Rink-DDBA had rejections between 98.7 % and 100.0 %), significant yield loss occurred during diafiltration in both case studies as extensive diafiltration was necessary for the removal of piperidine. The ideal anchor, which should have complete rejection by the membrane and offer ease of peptide synthesis, has not yet been found. In the initial anchor screening (Chapter Three, Section 3.2.4.2), all five anchors (molecular weight between 757 g · mol⁻¹ and 8209 g · mol⁻¹) shared similar rejection values by the ceramic

membranes (90.0 - 96.9 % for Inopor 450), despite their huge differences in molecular weight, which is a commonly used indicator for the corresponding molecular size. In other words, even though the largest compound (DPEG) has almost ten-fold the molecular weight of the smallest one (DDBA), it would still suffer significant yield loss during diafiltrations in MEPS. In the later part of this study (Chapter Five), the two alternative anchors (amine-functionalised silica nanoparticles and PyPEG) were tested for their promising rejection values (PyPEG had 100 % rejection by both Inopor 450 and Inopor 750; the rejection of silica nanoparticles was not available, but, with the a diameter significantly larger than the pore size of the ceramic membranes (10 - 20 nm as compared to 0.9 - 1.0 nm), they were expected to have complete rejection by the membrane.). However, they were found to have difficulties with the peptide chemistry for reasons that would require more resources for investigation in the future.

Despite the setback in finding the ideal anchor, the modelling of two-stage MEPS had promising results as the yield loss through the membrane could be overcome by the addition of the second-stage membrane, which served to retain the anchored peptide that permeated through the first membrane, and to recycle it back to the feed tank. With a slightly modified operation procedure based on that of the single-stage MEPS (i.e. the operation time of post-de-Fmoc diafiltration was doubled in order to remove the piperidine that was retained by the second-stage membrane), the two-stage MEPS had a significantly higher yield (98.3 %) and a similar purity (92.9 %) as compared to the experimental values of the single-stage MEPS (71.2 % and 88.1 % respectively) at the expense of a slightly longer process time ($2.5 \text{ h} \cdot \text{mmol}^{-1}$ as compared to $2.2 \text{ h} \cdot \text{mmol}^{-1}$). Although the two-stage MEPS had 13.6 % longer process time, 25.0% lower volumetric efficiency and 25.5 % higher E-factor as compared to the single-stage process, these underperforming metrics were outweighed by the significantly lower material cost (23.6 %) of the two-stage process. As compared to SPPS, the two-stage MEPS had 84.6% higher bluiding block utility, 33.5 % lower material cost, 24.2 % shorter process time and 11.3 % lower E-factor. The volumetric efficiency was slightly lower (13.5 %) due to

the increase in system volume in the two-stage system, but could be improved by increasing the scale of peptide synthesis. Therefore, the modelling data showed that the two-stage MEPS process would be an attractive alternative to the existing SPPS.

6.3. Updates on the Major Aspects of MEPS

By scaling up MEPS from 0.9 mmol and 1.8 mmol in the original work of Dr. So to 10.01 mmol and 33.65 mmol in this research project, the various components of MEPS (anchor, chemistry and OSN system) were investigated more closely. Much effort was invested in screening anchor/membrane, understanding and mitigating side-reactions, assessing the performance of MEPS relative to SPPS and LPPS (by precipitation), as well as finding alternative anchors and OSN system that could improve the performance of the present MEPS process (note: the third attempt at the MEPS of partially deprotected Pyr-SAFDL-NH₂ as reference). As a result, a better understanding of the novel process is obtained for the further development in the future. The major aspects of MEPS are updated as shown below (* indicates an update or a new statement is made with respect to the original list that is based on the hypothesis/observations in Dr So.'s work (Section 2.2.13.8)).

1. With regard to the choice of membrane:

- Ceramic multi-tube membrane has better stability and higher membrane area: volume ratio than polymeric OSN flat sheet membrane (note: spiral module of polymeric membrane is difficult to obtain).

2. For soluble anchor:

- A branched structure is expected to have higher rejection than a linear structure with the same molecular weight.
- * Over the range of molecular weight between 757 g · mol⁻¹ and 8209 g · mol⁻¹, the rejection curve is a plateau (Figure 3.15 in Section 3.3.3), in contrast to the original hypothesis that the rejection of anchor increases proportionally with its molecular size, which is reflected by the molecular weight.

3. In terms of peptide synthesis:

- * 1.05 eq amino acid and coupling reagents are sufficient for each coupling in liquid phase (Table 3.9 and Table 3.11 in Section 3.3.5, and Table 3.15 in Section 3.3.7), in contrast to the original case studies where 2 eq amino acid and coupling reagents were required for each coupling.
- * 5.0 weight % piperidine is sufficient for each de-Fmoc (Table 3.10 and Table 3.12 in Section 3.3.5), in contrast to the original case studies where 20 % piperidine solution was required for each de-Fmoc. 10.0 weight % piperidine can be used to shorten the time of de-Fmoc and hence reduce the extent of side reactions (e.g. racemisation).
- * The piperidine that remains in the system after post-de-Fmoc diafiltrations not only consumes the activated amino acid by forming a side-product irreversibly (Figure 4.14 and Table 4.4 in Section 4.3.3.2), but also hinders the coupling even additional activated amino acid is added for unknown reasons (as shown by the results in the second attempt at MEPS in the second case study (Section 4.3.3.4)).
- * Replacing piperidine with diethylamine results in slower reaction rate and the formation of solid (dibenzofulvene), but cannot resolve the problem of incomplete coupling due to the presence of residual base, even though diethylamine is a milder base compared to piperidine (Table 4.6 in Section 4.3.3.3).
- Cleavage and global deprotection result in a significant yield loss of peptide product.

4. Concerning the OSN system and operation procedure:

- * Single-stage system is insufficient for retaining the anchored peptide (as significant yield loss occurred (28.8 % in the third attempt at MEPS in the second case study (Table 4.3 in Section 4.3.3), even though the anchored peptide had an average rejection of 99.6 % (Table 5.2 in Section 5.2.4.6.1)).

- * The removal of piperidine after each de-Fmoc is critical for the next coupling to proceed to completion, but this requires a large number of wash volumes and the addition of a base into the system during diafiltration. The large number of wash volumes result in substantial mass loss of anchored peptide. (14 wash volumes per post-de-Fmoc diafiltration with the addition of DIEA in the third attempt at MEPS in the second case study (Section 5.2.4.6.1). The cumulative mass loss due to diafiltration was 28.8 %.)

- * The removal of excess amino acid after each coupling is less critical than expected as only a small excess of amino acid (0.05 eq) is present after each coupling, in contrast to the original hypothesis that the removal of excess amino acid after each coupling is critical for preventing the formation of error sequence during the subsequent de-Fmocs and couplings.

5. About the performance of MEPS:

- * The overall yield and concentration of anchor are the two most important parameters that determine the performance of MEPS.
- * Operating MEPS at the highest concentration of anchor is favourable in terms of solvent cost, process time, volumetric efficiency and E-factor, which are all normalised by the quantity of final product that is proportional to the concentration of anchor (as shown by the third attempt at MEPS in the second case study (Table 4.9 and Figure 4.24 in Section 4.3.4)).
- * MEPS is advantageous over SPPS in terms of building block utility (for amino acid) as couplings can proceed to completion with close-to-equivalent amount of amino acid in MEPS whereas a larger excess (≥ 0.5 eq) is required in SPPS.
- * In descending order, anchor, amino acids and coupling reagents are the three major components of the material cost of MEPS which is operated at the highest concentration of anchor (Figure 4.25 in Section 4.3.4). If the costs of amino acids and coupling reagents predominate in the material cost (i.e. ≥ 50 %), MEPS would be considerably advantageous over SPPS in terms of material cost due to its higher building block utility.

6.4. Recommendations for Future Work

The search for the ideal anchor should continue in order to identify a compound that has complete rejection and can be cleaved easily from the peptide at the end of the synthesis. One promising direction is the synthesis of peptide on nanoparticles, which have larger diameters (in the range of 70 nm as used in the study of Stutz et al. (2012)) than the ones tested in this study (10 - 20 nm), as the larger nanoparticles would probably offer the amino acids an easier access to the active sites on their surfaces.

It would be useful to optimise the cleavage and global deprotection procedure in order to reduce the yield loss during this stage. As this depends on the selected anchor, it is advisable to perform this optimisation after finalising the choice of anchor in the future.

It would also be useful to explore different configurations of membrane cascade and operation procedure for MEPS with the model developed with Aspen Customer Modeller. By combining the material cost and the cost related to the process time (for labour and use of equipment etc), and using this as the objective function for the optimisation of the two-stage MEPS, the most cost-efficient combination of system configure and operation procedure can be obtained. The optimised model should then be validated with experiments for the synthesis of longer peptides (i.e. 10 - 20 amino acid residues).

Reference

Abdelmoty, I., Albericio, F., Carpino, L.A., Foxman, B.M., & Kates, S.A. (1994) Structural studies of reagents for peptide bond formation: crystal and molecular structures of HBTU and HATU. *Letters in Peptide Science*, 1(2), 57-67.

Abe, H., Suzuki, H., Fujita, S., Nagano, K., Yamada, T., Ebata, N., & Chiba, K. (2012, March). New liquid phase peptide synthesis "Molecular HivingTM Technology". In *Peptide Science: Proceedings of the Japanese Peptide Symposium* (Vol. 2011, pp. 131-132).

Albericio, F. (ed.) (2000) *Solid-phase Synthesis: a Practical Guide*. Boca Raton, FL: CRC Press. ISBN 0824703596.

Albericio, F., Bofill, J. M., El-Faham, A., & Kates, S. A. (1998). Use of onium salt-based coupling reagents in peptide synthesis. *The Journal of Organic Chemistry*, 63(26), 9678-9683.

Albericio, F., Kneib-Cordonier, N., Biancalana, S., Gera, L., Masada, R. I., Hudson, D., & Barany, G. (1990). Preparation and application of the 5-(4-(9-fluorenylmethyloxycarbonyl) aminomethyl-3, 5-dimethoxyphenoxy)-valeric acid (PAL) handle for the solid-phase synthesis of C-terminal peptide amides under mild conditions. *The Journal of Organic Chemistry*, 55(12), 3730-3743.

Amblard, M., Fehrentz, J.A., Martinez, J., & Subra, G. (2006) Methods and protocols of modern solid phase peptide synthesis. *Molecular Biotechnology*, 33(3), 239-254.

Angell, Y.M., Alsina, J., Barany, G., & Albericio, F. (2002) Practical protocols for stepwise solid-phase synthesis of cysteine-containing peptides. *The Journal of Peptide Research*, 60(5), 292-299.

Anim-Mensah, A.R. (2012) *Nanofiltration Membranes Assessment for Organic Systems Separations: Solute Purification and Organic Solvent Recovery for Reuse*. Saarbrücken: LAP Lambert Academic Publishing. ISBN: 3659143782

Baker, R.W. (2012) *Membrane Technology and Applications (3rd ed.)*. Hoboken: Wiley-Blackwell. ISBN: 0470743727

Barany, G., & Merrifield, RB. (1979) Solid-phase Peptide Synthesis. *The Peptides*, Vol. 2. New York, NY: Academic Press.

Bayer, E., & Mutter, M. (1972) Liquid phase synthesis of peptides. *Nature*, 237, 512-513.

Benoiton, L.N. (2005) *Chemistry of Peptide Synthesis*. Boca Raton, FL: CRC Press. ISBN 1574444549.

Benoiton, N.L., & Chen, F.M. (1981) 2-Alkoxy-5 (4 H)-oxazolones from N-alkoxycarbonylamino acids and their implication in carbodiimide-mediated reactions in peptide synthesis. *Canadian Journal of Chemistry*, 59(2), 384-389.

Bergbreiter, D.E. (2002). Using soluble polymers to recover catalysts and ligands. *Chemical Reviews*, 102(10), 3345-3384.

Bhanushali, D., & Bhattacharyya, D. (2003) Advances in solvent-resistant nanofiltration membranes. *Annals of the New York Academy of Sciences*, 984(1), 159-177.

Bhanushali, D., Kloos, S., & Bhattacharyya, D. (2002). Solute transport in solvent-resistant nanofiltration membranes for non-aqueous systems: experimental results and the role of solute-solvent coupling. *Journal of Membrane Science*, 208(1), 343-359.

Bodanszky, M. (1985). In search of new methods in peptide synthesis. A review of the last three decades. *International Journal of Peptide and Protein Research*, 25(5), 449-474.

Bonner, A.G., Udell, L.M., Creasey, W.A., Duly, S.R., & Laursen, R.A. (2001) Solid-phase precipitation and extraction, a new separation process applied to the isolation of synthetic peptides. *The Journal of Peptide Research*, 57(3), 257.

Bourgin, D. (2005) Challenges in Industrial Production of Peptides. Presentation at Conference on Pharmaceutical Ingredients (CPI). Retrieved from http://bio.lonza.com/uploads/tx_mwaxmarketingmaterial/Lonza_PowerpointSlidesCollections_Challenges_in_Industrial_Production_of_Peptides.pdf

Boussu, K., De Baerdemaeker, J., Dauwe, C., Weber, M., Lynn, K. G., Depla, D., ... & Van der Bruggen, B. (2007). Physico-chemical characterization of nanofiltration membranes. *ChemPhysChem*, 8(3), 370-379.

Cano-Odena, A., Vandezande, P., Fournier, D., Van Camp, W., Du Prez, F.E., & Vankelecom, I.F. (2010). Solvent-resistant nanofiltration for product purification and catalyst recovery in click chemistry reactions. *Chemistry-A European Journal*, 16(3), 1061-1067.

Carpino, L. A., Ghassemi, S., Ionescu, D., Ismail, M., Sadat-Aalaei, D., Truran, G. A., ... & Morgan, B. (2003) Rapid, continuous solution-phase peptide synthesis: application to peptides of pharmaceutical interest. *Organic Process Research & Development*, 7(1), 28-37.

Carpino, L.A., & Han, G.Y. (1970) 9-Fluorenylmethoxycarbonyl function, a new base-sensitive amino-protecting group. *Journal of the American Chemical Society*, 92(19), 5748-5749.

Carpino, L.A., & Han, G.Y. (1972) 9-Fluorenylmethoxycarbonyl amino-protecting group. *The Journal of Organic Chemistry*, 37(22), 3404-3409.

Chapman, P., Loh, X.X., Livingston, A.G., Li, K., & Oliveira, T.A.C. (2008). Polyaniline membranes for the dehydration of tetrahydrofuran by pervaporation. *Journal of Membrane Science*, 309(1), 102-111.

Chapman, P.D., Oliveira, T., Livingston, A.G., & Li, K. (2008). Membranes for the dehydration of solvents by pervaporation. *Journal of Membrane Science*, 318(1), 5-37.

Chavan, S.A., Maes, W., Gevers, L.E., Wahlen, J., Vankelecom, I.F., Jacobs, P.A., ... & De Vos, D.E. (2005). Porphyrin-functionalized dendrimers: synthesis and application as recyclable photocatalysts in a nanofiltration membrane reactor. *Chemistry-A European Journal*, 11(22), 6754-6762.

Chen, J., Yang, G., Zhang, H., & Chen, Z. (2006). A review: Non-cross-linked polystyrene bound reagents, catalysts and syntheses. *Reactive and Functional Polymers*, 66(12), 1434-1451.

Chiba, K., Sugihara, M., Yoshida, K., Mikami, Y., & Kim, S. (2009). Synthesis of hydrophobic phase-tagged prolyl peptides featuring rapid reaction/separation. *Tetrahedron*, 65(38), 8014-8020.

Coin, I., Beyermann, M., & Bienert, M. (2007) Solid-phase peptide synthesis: from standard procedures to the synthesis of difficult sequences. *Nature Protocols*, 2(12), 3247-3256.

Cormier, A.R., Pang, X., Zimmerman, M.I., Zhou, H.X., & Paravastu, A.K. (2013). Molecular structure of RADA16-I designer self-assembling peptide nanofibers. *ACS Nano*, 7(9), 7562-7572.

Craik, D. J., Fairlie, D. P., Liras, S., & Price, D. (2013). The future of peptide-based drugs. *Chemical Biology & Drug Design*, 81(1), 136-147.

Czarnik, A.W. (1998) Solid-phase synthesis supports are like solvents. *Biotechnology and Bioengineering*, 61(1), 77-79.

Danquah, M.K., & Agyei, D. (2012) Pharmaceutical applications of bioactive peptides. *OA Biotechnology*, 1(2):5.

Darnoko, D., & Cheryan, M. (2006). Carotenoids from red palm methyl esters by nanofiltration. *Journal of the American Oil Chemists' Society*, 83(4), 365-370.

de Jesús, E., & Flores, J.C. (2008). Dendrimers: solutions for catalyst separation and recycling - a review. *Industrial & Engineering Chemistry Research*, 47(21), 7968-7981.

de Morais Coutinho, C., Chiu, M.C., Basso, R.C., Ribeiro, A.P.B., Gonçalves, L.A.G., & Viotto, L.A. (2009). State of art of the application of membrane technology to vegetable oils: a review. *Food Research International*, 42(5), 536-550.

DeTar, D. F., & Silverstein, R. (1966). Reactions of carbodiimides. I. The mechanisms of the reactions of acetic acid with dicyclohexylcarbodiimide. *Journal of the American Chemical Society*, 88(5), 1013-1019.

Dickerson, T.J., Reed, N.N., & Janda, K.D. (2002). Soluble polymers as scaffolds for recoverable catalysts and reagents. *Chemical Reviews*, 102(10), 3325-3344.

Dobrak-Van Berlo, A., Vankelecom, I.F., & Van der Bruggen, B. (2011). Parameters determining transport mechanisms through unfilled and silicalite filled PDMS-based membranes and dense PI membranes in solvent resistant nanofiltration: comparison with pervaporation. *Journal of Membrane Science*, 374(1), 138-149.

Vigneaud, V. D., Ressler, C., Swan, C. J. M., Roberts, C. W., Katsoyannis, P. G., & Gordon, S. (1953). The synthesis of an octapeptide amide with the hormonal activity of oxytocin. *Journal of the American Chemical Society*, 75(19), 4879-4880.

Espitia, P.J.P., Soares, N.F.F., Coimbra, J.S.R., Andrade, N.J., Cruz, R.S., & Medeiros, E.A.A. (2012) Bioactive peptides: synthesis, properties, and applications in the packaging and preservation of food. *Comprehensive Reviews in Food Science and Food Safety*, 11, 187-204

Fan, J., & Gao, Y. (2006). Nanoparticle-supported catalysts and catalytic reactions - a mini-review. *Journal of Experimental Nanoscience*, 1(4), 457-475.

Fields, G. B., & NOBLE, R. L. (1990). Solid phase peptide synthesis utilizing 9-fluorenylmethoxycarbonyl amino acids. *International Journal of Peptide and Protein Research*, 35(3), 161-214.

Fischer, P.M. (2003) Diketopiperazines in peptide and combinatorial chemistry. *Journal of Peptide Science*, 9(1), 9-35.

Fischer, P.M., & Zheleva, D.I. (2002). Liquid-phase peptide synthesis on polyethylene glycol (PEG) supports using strategies based on the 9-fluorenylmethoxycarbonyl amino protecting group: application of PEGylated peptides in biochemical assays. *Journal of Peptide Science*, 8(9), 529-542.

Gaines, S.M., & Bada, J.L. (1988) Aspartame decomposition and epimerization in the diketopiperazine and dipeptide products as a function of pH and temperature. *The Journal of Organic Chemistry*, 53(12), 2757-2764.

Garcia Martin, F., & Albericio, F. (2008) Solid supports for the synthesis of peptides. From the first resin used to the most sophisticated in the market. *Chimica oggi*, 26(4).

Geens, J., De Witte, B., & Van der Bruggen, B. (2007). Removal of API's (active pharmaceutical ingredients) from organic solvents by nanofiltration. *Separation Science and Technology*, 42(11), 2435-2449.

Geens, J., Hillen, A., Bettens, B., Van der Bruggen, B., & Vandecasteele, C. (2005). Solute transport in non-aqueous nanofiltration: effect of membrane material. *Journal of Chemical Technology and Biotechnology*, 80(12), 1371-1377.

Gevers, L.E.M., Vandezande, P., Vermant, J., Martens, J.A., Vankelecom, I.F.J., & Jacobs, P.A. (2006). A novel method to prepare porous membranes/polymers with easy control over porosity and increased compaction resistance. *Desalination*, 199(1), 34-36.

Gibbins, E., D'Antonio, M., Nair, D., White, L.S., Freitas dos Santos, L.M., Vankelecom, I.F., & Livingston, A.G. (2002). Observations on solvent flux and solute rejection across solvent resistant nanofiltration membranes. *Desalination*, 147(1), 307-313.

Gisin, B. F., & Merrifield, R. B. (1972). Carboxyl-catalyzed intramolecular aminolysis. Side reaction in solid-phase peptide synthesis. *Journal of the American Chemical Society*, 94(9), 3102-3106.

Goodman, M., & Levine, L. (1964) Peptide synthesis via active esters. IV. Racemization and ring-opening reactions of optically active oxazolones. *Journal of the American Chemical Society*, 86(14), 2918-2922.

Goodman, M., & McGahren, W.J. (1965) Optically active peptide oxazolones. Preliminary racemization studies under peptide-coupling conditions. *Journal of the American Chemical Society*, 87(13), 3028-3029.

Grandas, A., Pedroso, E., Giralt, E., Granier, C., & Van Rietschoten, J. (1986) Convergent solid phase peptide synthesis IV. : Synthesis of the 35–43 and 32–34 protected segments of the toxin II of androctonus australis hector. *Tetrahedron*, 42(24), 6703-6711.

Gude, M., Ryf, J., & White, P.D. (2002) An accurate method for the quantitation of Fmoc-derivatized solid phase supports. *Letters in Peptide Science*, 9(4), 203-206.

Huang, H., & Rabenstein, D.L. (1999) A cleavage cocktail for methionine-containing peptides. *The Journal of Peptide Research*, 53(5), 548-553.

Isidro-Llobet, A., Alvarez, M., & Albericio, F. (2009). Amino acid-protecting groups. *Chemical Reviews*, 109(6), 2455-2504.

Jablonski, J. A., Shpritzer, R., & Powers, S. (2002). Racemization induced by excess base during activation with uronium salts. *Peptides: Frontiers of Peptide Science*, 323-324.

Jiang, Y. (2007). *New Generation Polyimide Membranes for Separations in Organic Solvents Nanofiltration* (MSc thesis). Imperial College London, London.

Jung, N., Wiehn, M., & Bräse, S. (2007). Multifunctional linkers for combinatorial solid phase synthesis. In *Combinatorial Chemistry on Solid Supports* (pp. 1-88). Berlin/Heidelberg: Springer.

Kelley, W.S. (1996) Therapeutic peptides: the devil is in the details. *Nature Biotechnology*, 14(1), 28-31.

Kemp, D.S., Wang, S.W., Busby III, G., & Hugel, G. (1970) Microanalysis by successive isotopic dilution. New assay for racemic content. *Journal of the American Chemical Society*, 92(4), 1043-1055.

Kent, S.B. (1988) Chemical synthesis of peptides and proteins. *Annual Review of Biochemistry*, 57(1), 957-989.

Keymanesh, K., Soltani, S., & Sardari, S. (2009). Application of antimicrobial peptides in agriculture and food industry. *World Journal of Microbiology and Biotechnology*, 25(6), 933-944.

Kim, J.F., Freitas da Silva, A.M., Valtcheva, I.B., & Livingston, A.G. (2013). When the membrane is not enough: a simplified membrane cascade using Organic Solvent Nanofiltration (OSN). *Separation and Purification Technology*, 116, 277-286.

King, D. S., FIELDS, C. G., & FIELDS, G. B. (1990). A cleavage method which minimizes side reactions following Fmoc solid phase peptide synthesis. *International Journal of Peptide and Protein Research*, 36(3), 255-266.

Knorr, R., Trzeciak, A., Bannwarth, W., & Gillessen, D. (1989) New coupling reagents in peptide chemistry. *Tetrahedron Letters*, 30(15), 1927-1930.

Korhonen, H., & Pihlanto, A. (2006) Bioactive peptides: production and functionality. *International Dairy Journal*, 16, 945-960.

Koros, W.J., Ma, Y.H., & Shimidzu, T. (1996) Terminology for membranes and membrane processes. *Journal of Membrane Science*, 120, 149-159.

Kuroda, N., Hattori, T., Kitada, C., & Sugawara, T. (2001) Solution-phase automated synthesis of tripeptide derivatives. *Chemical and Pharmaceutical Bulletin*, 49(9), 1138-1146.

Kwiatkowski, J., & Cheryan, M. (2005). Performance of nanofiltration membranes in ethanol. *Separation Science and Technology*, 40(13), 2651-2662.

Lax, R. (2010) The Future of Peptide Development in the Pharmaceutical Industry. 2010 PharManufacturing: The International Peptide Review. Retrieved from <http://www.polypeptide.com/assets/002/5188.pdf>

Leader, B., Baca, Q.J., & Golan, D.E. (2008) Protein therapeutics: a summary and pharmacological classification. *Nature Reviews Drug Discovery*, 7, 21-39.

Li, K. (2007) *Ceramic Membranes for Separation and Reaction*. Hoboken, NJ: Wiley-Blackwell. ISBN: 0470014407

Lloyd-Williams, P., Albericio, F., & Giralt, E. (1997) *Chemical Approaches to the Synthesis of Peptides and Proteins (New Directions in Organic & Biological Chemistry Series)*. Boca Raton, FL: CRC Press. ISBN 0849391423

Loh, X.X., Sairam, M., Bismarck, A., Steinke, J.H.G., Livingston, A.G., & Li, K. (2009). Crosslinked integrally skinned asymmetric polyaniline membranes for use in organic solvents. *Journal of Membrane Science*, 326(2), 635-642.

Lu, J., & Toy, P.H. (2009). Organic polymer supports for synthesis and for reagent and catalyst immobilization. *Chemical Reviews*, 109(2), 815-838.

Lundt, B.F., Johansen, N.L., Volund, A., & Markussen, J. (1978) Removal of t-butyl and t-butoxycarbonyl protecting groups with trifluoroacetic acid. *International Journal of Peptide and Protein Research*, 12(5), 25-268.

Maes, N., Zhu, H.Y., & Vansant, E. F. (1995). The use of the logarithmic adsorption isotherm for the determination of the micropore-size distribution. *Journal of Porous Materials*, 2(1), 97-105.

Malins, L. R., Mitchell, N. J., & Payne, R. J. (2014). Peptide ligation chemistry at selenol amino acids. *Journal of Peptide Science*, 20(2), 64-77.

Marchetti, P. (2013). *Organic Solvent Nanofiltration in the Peptide Industry* (PhD thesis). Imperial College London, London.

Marchetti, P., Jimenez Solomon, M. F., Szekely, G., & Livingston, A. G. (2014). Molecular separation with organic solvent nanofiltration: a critical review. *Chemical Reviews*, 114(21), 10735-10806.

Martin, F.G., & Albericio, F. (2008) Solid supports for the synthesis of peptides. From the first resin used to the most sophisticated in the market. *Chemistry Today*, 26(4), 29-34.

McLay, R.N., Pan, W., & Kastin, A.J. (2001) Effects of peptides on animal and human behavior: a review of studies published in the first twenty years of the journal *Peptides*. *Peptides*, 22, 2181-2255.

Meneses, C., Nicoll, S.L., & Trembleau, L. (2009) Multigram-scale synthesis of short peptides via a simplified repetitive solution-phase procedure. *The Journal of Organic Chemistry*, 75(3), 564-569.

Mergler, M., & Dick, F. (2005) The aspartimide problem in Fmoc-based SPPS. Part III. *Journal of Peptide Science*, 11(10), 650-657.

Mergler, M., Dick, F., Sax, B., Stähelin, C. & Vorherr, T. (2003b) The aspartimide problem in Fmoc-based SPPS. Part II. *Journal of Peptide Science*, 9(8), 518-526.

Mergler, M., Dick, F., Sax, B., Weiler, P. & Vorherr, T. (2003a) The aspartimide problem in Fmoc-based SPPS. Part I. *Journal of Peptide Science*, 9(1), 36-46.

Merrifield, R. B. (1963). Solid phase peptide synthesis. I. The synthesis of a tetrapeptide. *Journal of the American Chemical Society*, 85(14), 2149-2154.

Merrifield, R. B., Gisin, B. F., & Bach, A. N. (1977). The limits of reaction of radioactive dicyclohexylcarbodiimide with amino groups during solid-phase peptide synthesis. *The Journal of Organic Chemistry*, 42(8), 1291-1295.

Mertens, P.G.N., Vankelecom, I.F.J., Jacobs, P.A., & De Vos, D.E. (2005). Gold nanoclusters as colloidal catalysts for oxidation of long chain aliphatic 1, 2-diols in alcohol solvents. *Gold Bulletin*, 38(4), 157-162.

Michels, T., Dölling, R., Haberkorn, U., & Mier, W. (2012) Acid-mediated prevention of aspartimide formation in solid phase peptide synthesis. *Organic Letters*, 14(20), 5218-5221.

Montalbetti, C.A.G.N., & Falque, V. (2005) Amide bond formation and peptide coupling. *Tetrahedron*, 61, 10827-10852.

Morikawa, O., Iyama, E., Oikawa, T., Kobayashi, K., & Konishi, H. (2006). Conformational properties of C_{2v}-symmetrical resorcin [4] arene tetraethers. *Journal of Physical Organic Chemistry*, 19(3), 214-218.

Mutter, M., Hagenmaier, H., & Bayer, E. (1971) New method of polypeptide synthesis. *Angewandte Chemie International*, 10(11), 811-812.

Nissen, F., Kraft, T.E., Ruppert, T., Eisenhut, M., Haberkorn, U., & Mier, W. (2010) Hot or not - the influence of elevated temperature and microwave irradiation on the solid phase synthesis of an affibody. *Tetrahedron Letters*, 51(48), 6216-6219.

Nunes, S.P., & Peinemann, K. (Eds.) (2006) *Membrane Technology in the Chemical Industry (2nd ed.)*. Weinheim: Wiley-VCH. ISBN: 3527313168

Nutt, R.F., Brady, S.F., Darke, P.L., Ciccarone, T.M., Colton, C.D., Nutt, E.M., Rodkey, J.A., Bennett, C.D., Waxman, L.H., & Sigal, I.S. (1988) Chemical synthesis and enzymatic activity of a 99-residue peptide with a sequence proposed for the human immunodeficiency virus protease. *Proceedings of the National Academy of Sciences of United States of America*, 85, 7129-7133.

Offer, J., Quibell, M., & Johnson, T. (1996) On-resin solid-phase synthesis of asparagine N-linked glycopeptides: Use of N-(2-acetoxy-4-methoxybenzyl) (AcHmb) aspartyl amide-bond protection to prevent unwanted aspartimide formation. *Journal of the Chemical Society, Perkin Transactions 1*, (2), 175-182.

- Okada, Y. (2001) Synthesis of peptides by solution methods. *Current Organic Chemistry*, 5(1), 1-43.
- Okada, Y., Suzuki, H., Nakae, T., Fujita, S., Abe, H., Nagano, K., ... & Chiba, K. (2012). Tag-assisted liquid-phase peptide synthesis using hydrophobic benzyl alcohols as supports. *The Journal of Organic Chemistry*, 78(2), 320-327.
- Patel, A. (2007) *New Generation Polyaniline Membranes for Separation in Organic Solvent Nanofiltration* (MSc thesis). Imperial College London, London.
- Pathare, R., & Agrawal, R. (2010). Design of membrane cascades for gas separation. *Journal of Membrane Science*, 364(1), 263-277.
- Patterson, D.A., Yen Lau, L., Roengpithya, C., Gibbins, E.J., & Livingston, A. G. (2008). Membrane selectivity in the organic solvent nanofiltration of trialkylamine bases. *Desalination*, 218(1), 248-256.
- Pearson, D.A., Blanchette, M., Baker, M.L., & Guindon, C.A. (1989) Trialkylsilanes as scavengers for the trifluoroacetic acid deblocking of protecting groups in peptide synthesis. *Tetrahedron Letters*, 30 (21), 2739-2742.
- Peptide Therapeutics Foundation (2010). Development trends for peptide therapeutics. Retrieved from http://www.peptidetherapeutics.org/PTF_report_summary_2010.pdf
- Peptide Therapeutics Foundation (2010). Peptide Therapeutics Database. Retrieved from <http://www.peptidetherapeutics.org/annual-report.html>
- Perez Espitia, P.J., de Fátima Ferreira Soares, N., dos Reis Coimbra, J. S., de Andrade, N. J., Souza Cruz, R., Medeiros, A., & Antonio, E. (2012) Bioactive peptides: synthesis, properties, and applications in the packaging and preservation of food. *Comprehensive Reviews in Food Science and Food Safety*, 11(2), 187-204.
- Peterson, Q.P., Goode, D.R., West, D.C., Botham, R.C., & Hergenrother, P.J. (2010) Preparation of the caspase-3/7 substrate Ac-DEVD-pNA by solution-phase peptide synthesis. *Nature Protocols*, 5(2), 294-302.
- PhRMA. (2007) Drug Discovery and Development. Retrieved from http://www.innovation.org/drug_discovery/objects/pdf/RD_Brochure.pdf
- Phylogica (2012). 2012 Phylogica Update Report. Retrieved from <http://www.phylogica.com/media/articles/Investors---Analyst-Coverage/20120713-Van-Leeuwenhoeck-1006/VanLeeuwenhoeck13July2012.pdf>
- Pillai, V. R., Mutter, M., Bayer, E., & Gatfield, I. (1980). New, easily removable poly (ethylene glycol) supports for the liquid-phase method of peptide synthesis. *The Journal of Organic Chemistry*, 45(26), 5364-5370.
- Pink, C.J., Wong, H.T., Ferreira, F.C., & Livingston, A.G. (2008). Organic solvent nanofiltration and adsorbents; a hybrid approach to achieve ultra low palladium contamination of post coupling reaction products. *Organic Process Research & Development*, 12(4), 589-595.

Quibell, M., Owen, D., Packman, L. C., & Johnson, T. (1994). Suppression of piperidine-mediated side product formation for Asp (OBu t)-containing peptides by the use of N-(2-hydroxy-4-methoxybenzyl)(Hmb) backbone amide protection. *Journal of the Chemical Society, Chemical Communications*, (20), 2343-2344.

Ramage, R., Swenson, H.R., & Shaw, K.T. (1998). A novel purification protocol for soluble combinatorial peptide libraries. *Tetrahedron Letters*, 39(47), 8715-8718.

Raman, L.P., Cheryan, M., & Rajagopalan, N. (1996). Deacidification of soybean oil by membrane technology. *Journal of the American Oil Chemists' Society*, 73(2), 219-224.

Reddy, P.A., Jones, S.T., Lewin, A.H., & Carroll, F. (2012) Synthesis of hemopressin peptides by classical solution phase fragment condensation. *International Journal of Peptides*, 2012.

Rothe, M., & Mazánek, J. (1974) Nebenreaktionen bei der Festphasensynthese von Peptiden, IV1) Intrachenare und interchenare Aminolyse der Benzylesterbindung zum polymeren Träger und ihre Auswirkungen. *Justus Liebigs Annalen der Chemie*, 3, 439–459.

Sairam, M., Loh, X.X., Bhole, Y., Sereewatthanawut, I., Li, K., Bismarck, A., ... & Livingston, A. G. (2010). Spiral-wound polyaniline membrane modules for organic solvent nanofiltration (OSN). *Journal of Membrane Science*, 349(1), 123-129.

Sairam, M., Loh, X.X., Li, K., Bismarck, A., Steinke, J.H.G., & Livingston, A.G. (2009). Nanoporous asymmetric polyaniline films for filtration of organic solvents. *Journal of Membrane Science*, 330(1), 166-174.

Sakakibara, S. (1999) Chemical synthesis of proteins in solution. *Peptide Science*, 51(4), 279-296.

Sarin, V.K., Kent, S.B., & Merrifield, R.B. (1980) Properties of swollen polymer networks. Solvation and swelling of peptide-containing resins in solid-phase peptide synthesis. *Journal of the American Chemical Society*, 102(17), 5463-5470.

Scarpello, J.T., Nair, D., Freitas dos Santos, L.M., White, L.S., & Livingston, A.G. (2002). The separation of homogeneous organometallic catalysts using solvent resistant nanofiltration. *Journal of Membrane Science*, 203(1), 71-85.

Schäfer, A.I., Fane, A.G., & Waite, T.D. (2005) *Nanofiltration: Principles and Applications*. Amsterdams: Elsevier Advanced Technology. ISBN: 1856174050

Schätz, A., Reiser, O., & Stark, W. J. (2010). Nanoparticles as semi-heterogeneous catalyst supports. *Chemistry-A European Journal*, 16(30), 8950-8967.

See Toh, Y.H., Lim, F.W., & Livingston, A.G. (2007). Polymeric membranes for nanofiltration in polar aprotic solvents. *Journal of Membrane Science*, 301(1), 3-10.

See Toh, Y.H., Loh, X.X., Li, K., Bismarck, A., & Livingston, A.G. (2007). In search of a standard method for the characterisation of organic solvent nanofiltration membranes. *Journal of Membrane Science*, 291(1), 120-125.

See-Toh, Y.H., Ferreira, F.C., & Livingston, A.G. (2007). The influence of membrane formation parameters on the functional performance of organic solvent nanofiltration membranes. *Journal of Membrane Science*, 299(1), 236-250.

Sereewatthanawut, I., Baptista, I.I.R., Boam, A.T., Hodgson, A., & Livingston, A.G. (2011). Nanofiltration process for the nutritional enrichment and refining of rice bran oil. *Journal of Food Engineering*, 102(1), 16-24.

Sereewatthanawut, I., Lim, F.W., Bhole, Y.S., Ormerod, D., Horvath, A., Boam, A.T., & Livingston, A.G. (2010). Demonstration of molecular purification in polar aprotic solvents by organic solvent nanofiltration. *Organic Process Research & Development*, 14(3), 600-611.

Sheehan, J. C., & Hess, G. P. (1955). A new method of forming peptide bonds. *Journal of the American Chemical Society*, 77(4), 1067-1068.

Sheppeck, J.E., Kar, H., & Hong, H. (2000) A convenient and scaleable procedure for removing the Fmoc group in solution. *Tetrahedron Letters*, 41(28), 5329-5333.

Sherrington, D.C. (1998) Preparation, structure and morphology of polymer supports. *Chemical Communications*, (21), 2275-2286.

Siew, W.E., Livingston, A.G., Ates, C., & Merschaert, A. (2013). Continuous solute fractionation with membrane cascades - a high productivity alternative to diafiltration. *Separation and Purification Technology*, 102, 1-14.

Silva, F.P., & Machado, M.C.C. (2012) Antimicrobial peptides: clinical relevance and therapeutic implications. *Peptides*, 36, 308-314

Silva, P., Han, S., & Livingston, A.G. (2005). Solvent transport in organic solvent nanofiltration membranes. *Journal of Membrane Science*, 262(1), 49-59.

Silva, P., Peeva, L.G., & Livingston, A.G. (2010). Organic solvent nanofiltration (OSN) with spiral-wound membrane elements - highly rejected solute system. *Journal of Membrane Science*, 349(1), 167-174.

Smith, M., Moffatt, J. G., & Khorana, H. G. (1958). Carbodiimides. VIII. 1 Observations on the reactions of carbodiimides with acids and some new applications in the synthesis of phosphoric acid esters. *Journal of the American Chemical Society*, 80(23), 6204-6212.

Sneider, W. (2001) History of Insulin. *eLs*.

So, S. (2009). *The Novel Membrane Enhanced Peptide Synthesis Process* (PhD thesis). Imperial College London, London.

So, S., Peeva, L.G., Tate, E.W., Leatherbarrow, R.J., & Livingston, A.G. (2010a). Membrane enhanced peptide synthesis. *Chemical Communications*, 46(16), 2808-2810.

So, S., Peeva, L.G., Tate, E.W., Leatherbarrow, R.J., & Livingston, A.G. (2010b). Organic solvent nanofiltration: a new paradigm in peptide synthesis. *Organic Process Research & Development*, 14(6), 1313-1325.

Solé, N. A., & Barany, G. (1992). Optimization of solid-phase synthesis of [Ala⁸]-dynorphin A. *The Journal of Organic Chemistry*, 57(20), 5399-5403.

Soroko, I., Bhole, Y., & Livingston, A.G. (2011). Environmentally friendly route for the preparation of solvent resistant polyimide nanofiltration membranes. *Green Chemistry*, 13(1), 162-168.

Sotto, A., Boromand, A., Balta, S., Kim, J., & Van der Bruggen, B. (2011). Doping of polyethersulfone nanofiltration membranes: antifouling effect observed at ultralow concentrations of TiO₂ nanoparticles. *Journal of Materials Chemistry*, 21(28), 10311-10320.

Speicher, A., Klaus, T., & Eicher, T. (1998) O-(1-Benzotriazolyl)-N,N,N',N'-tetramethyluronium-hexafluorophosphat (HBTU) und O-(7-Aza-1-benzotriazolyl)-N,N,N',N'-tetramethyluronium-hexafluorophosphat (HATU) - zwei moderne Kupplungsreagenzien zur Peptidsynthese. *Journal für Praktische Chemie/Chemiker-Zeitung*, 340(6), 581-583.

Stafie, N., Stamatialis, D.F., & Wessling, M. (2004). Insight into the transport of hexane-solute systems through tailor-made composite membranes. *Journal of Membrane Science*, 228(1), 103-116.

Stathopoulos, P., Papas, S., & Tsikaris, V. (2006) C-terminal N-alkylated peptide amides resulting from the linker decomposition of the Rink amide resin. A new cleavage mixture prevents their formation. *Journal of Peptide Science*, 12(3), 227-232.

Stawikowska, J., & Livingston, A.G. (2012). Nanoprobe imaging molecular scale pores in polymeric membranes. *Journal of Membrane Science*, 413, 1-16.

Stawikowska, J., & Livingston, A.G. (2013). Assessment of atomic force microscopy for characterisation of nanofiltration membranes. *Journal of Membrane Science*, 425, 58-70.

Steinberg, S.M., & Bada, J.L. (1983) Peptide decomposition in the neutral pH region via the formation of diketopiperazines. *The Journal of Organic Chemistry*, 48(13), 2295-2298.

Stutz, C., Bilecka, I., Thünemann, A. F., Niederberger, M., & Börner, H. G. (2012). Superparamagnetic core-shell nanoparticles as solid supports for peptide synthesis. *Chemical Communications*, 48(57), 7176-7178.

Stutz, C., Meszynska, A., Lutz, J. F., & Börner, H. G. (2013). Convenient routes to efficiently N-PEGylated peptides. *ACS Macro Letters*, 2(8), 641-644.

Szekely, G., Jimenez-Solomon, M. F., Marchetti, P., Kim, J. F., & Livingston, A. G. (2014). Sustainability assessment of organic solvent nanofiltration: from fabrication to application. *Green Chemistry*, 16(10), 4440-4473.

Tam, J. P., Yu, Q., & Miao, Z. (1999). Orthogonal ligation strategies for peptide and protein. *Peptide Science*, 51(5), 311-332.

Tam, J. P., Xu, J., & Eom, K. D. (2001). Methods and strategies of peptide ligation. *Peptide Science*, 60(3), 194-205.

Tana, G., Kitada, S., Fujita, S., Okada, Y., Kim, S., & Chiba, K. (2010). A practical solution-phase synthesis of an antagonistic peptide of TNF- α based on hydrophobic tag strategy. *Chemical Communications*, 46(43), 8219-8221.

Tansel, B., Sager, J., Rector, T., Garland, J., Strayer, R. F., Levine, L., ... & Bauer, J. (2006). Significance of hydrated radius and hydration shells on ionic permeability during nanofiltration in dead end and cross flow modes. *Separation and Purification Technology*, 51(1), 40-47.

Tarleton, E.S., Robinson, J.P., Millington, C.R., & Nijmeijer, A. (2005). Non-aqueous nanofiltration: solute rejection in low-polarity binary systems. *Journal of Membrane Science*, 252(1), 123-131.

Tauzin, B. (2008) Biotechnology Research Continues to Bolster Arsenal Against Disease with 633 Medicines in Development. 2008 PhRMA Report. Retrieved from <http://www.amcp.org/WorkArea/DownloadAsset.aspx?id=13198>

Thayer, A.M. (2011) Small firms develop better peptide drug candidates to expand this pharmaceutical class and attract big pharma partners. *Chemical & Engineering News*, 89, 22, 13-20.

Trusheim, M. R., Aitken, M. L., & Berndt, E. R. (2010, May). Characterizing Markets for Biopharmaceutical Innovations: Do Biologics Differ from Small Molecules?. In *Forum for Health Economics & Policy* (Vol. 13, No. 1).

Tsuru, T., Sudoh, T., Yoshioka, T., & Asaeda, M. (2001). Nanofiltration in non-aqueous solutions by porous silica-zirconia membranes. *Journal of Membrane Science*, 185(2), 253-261.

Tsuru, T. (2008). Nano/subnano-tuning of porous ceramic membranes for molecular separation. *Journal of Sol-Gel Science and Technology*, 46(3), 349-361.

Van der Bruggen, B., Mänttari, M., & Nyström, M. (2008) Drawbacks of applying nanofiltration and how to avoid them: a review. *Separation and Purification Technology*, 63(2), 251-263.

Vandezande, P., Gevers, L.E., & Vankelecom, I.F. (2008) Solvent resistant nanofiltration: separating on a molecular level. *Chemical Society Reviews*, 37(2), 365-405.

Vandezande, P., Gevers, L.E., Jacobs, P.A., & Vankelecom, I.F. (2009). Preparation parameters influencing the performance of SRNF membranes cast from polyimide solutions via SEPI. *Separation and Purification Technology*, 66(1), 104-110.

Vandezande, P., Gevers, L.E., Paul, J.S., Vankelecom, I.F., & Jacobs, P.A. (2005). High throughput screening for rapid development of membranes and membrane processes. *Journal of Membrane Science*, 250(1), 305-310.

Vandezande, P., Gevers, L.E.M., Vankelecom, I.F.J., & Jacobs, P.A. (2006). High throughput membrane testing and combinatorial techniques: powerful new instruments for membrane optimisation. *Desalination*, 199(1), 395-397.

Vanherck, K., Vandezande, P., Aldea, S.O., & Vankelecom, I.F. (2008). Cross-linked polyimide membranes for solvent resistant nanofiltration in aprotic solvents. *Journal of Membrane Science*, 320(1), 468-476.

Vankelecom, I.F., Merckx, E., Luts, M., & Uytterhoeven, J.B. (1995). Incorporation of zeolites in polyimide membranes. *The Journal of Physical Chemistry*, 99(35), 13187-13192.

Vanneste, J., De Ron, S., Vandecruys, S., Soare, S. A., Darvishmanesh, S., & Van der Bruggen, B. (2011). Techno-economic evaluation of membrane cascades relative to simulated moving bed chromatography for the purification of mono-and oligosaccharides. *Separation and Purification Technology*, 80(3), 600-609.

Vanneste, J., Ormerod, D., Theys, G., Van Gool, D., Van Camp, B., Darvishmanesh, S., & Van der Bruggen, B. (2013). Towards high resolution membrane-based pharmaceutical separations. *Journal of Chemical Technology and Biotechnology*, 88(1), 98-108.

Vercauteren, S., Keizer, K., Vansant, E.F., Luyten, J., & Leysen, R. (1998). Porous ceramic membranes: preparation, transport properties and applications. *Journal of Porous Materials*, 5(3-4), 241-258.

Wade, J.D., Mathieu, M.N., Macris, M., & Tregear, G.W. (2000) Base-induced side reactions in Fmoc-solid phase peptide synthesis: Minimization by use of piperazine as α -deprotection reagent. *Letters in Peptide Science*, 7(2), 107-112.

Werbitzky, O. (2004) Specific Challenges in Large-Scale Manufacturing of Peptide as API's. Presentation at TIDES Conference. Retrieved from http://bio.lonza.com/uploads/tx_mwaxmarketingmaterial/Lonza_PowerpointSlidesCollections_Specific_Challenges_in_Large-Scale_Manufacturing_of_Peptide_as_APis.pdf

White, L.S. (2002). Transport properties of a polyimide solvent resistant nanofiltration membrane. *Journal of Membrane Science*, 205(1), 191-202.

White, L.S. (2006). Development of large-scale applications in organic solvent nanofiltration and pervaporation for chemical and refining processes. *Journal of Membrane Science*, 286(1), 26-35.

Windridge, G., & Jorgensen, E. C. (1971). 1-Hydroxybenzotriazole as a racemization-suppressing reagent for the incorporation of im-benzyl-L-histidine into peptides. *Journal of the American Chemical Society*, 93(23), 6318-6319.

Wong, H.T., See-Toh, Y.H., Ferreira, F.C., Crook, R., & Livingston, A.G. (2006). Organic solvent nanofiltration in asymmetric hydrogenation: enhancement of enantioselectivity and catalyst stability by ionic liquids. *Chemical Communications*, (19), 2063-2065.

Wong, P.Y. (2008) *Organic Solvent Nanofiltration - Applications* (MSc thesis). Imperial College London, London.

Xu, J., Feng, X., Chen, P., & Gao, C. (2012). Development of an antibacterial copper (II)-chelated polyacrylonitrile ultrafiltration membrane. *Journal of Membrane Science*, 413, 62-69.

Yang, X.J., Livingston, A.G., & Freitas dos Santos, L. (2001) Experimental observations of nanofiltration with organic solvents. *Journal of Membrane Science*, 190(1), 45-55.

Yang, Y., Sweeney, W.V., Schneider, K., Thörnqvist, S., Chait, B.T., & Tam, J.P. (1994) Aspartimide formation in base-driven 9-fluorenylmethoxycarbonyl chemistry. *Tetrahedron letters*, 35(52), 9689-9692.

Ye, Z., Zhang, H., Luo, H., Wang, S., Zhou, Q., Du, X., ... & Zhao, X. (2008). Temperature and pH effects on biophysical and morphological properties of self-assembling peptide RADA16-I. *Journal of Peptide Science*, 14(2), 152-162.

Yokoi, H., Kinoshita, T., & Zhang, S. (2005). Dynamic reassembly of peptide RADA16 nanofiber scaffold. *Proceedings of the National Academy of Sciences of the United States of America*, 102(24), 8414-8419.

Yoshida, J. I., & Itami, K. (2002). Tag strategy for separation and recovery. *Chemical Reviews*, 102(10), 3693-3716.

Yu, Y., Jawa, A., Pan, W., & Kastin, A.J. (2004) Effects of peptides, with emphasis on feeding, pain, and behaviour A 5-year (1999-2003) review of publications in Peptides. *Peptides*, 25, 2257-2289.

Zheng, F., Li, C., Yuan, Q., & Vriesekoop, F. (2008). Influence of molecular shape on the retention of small molecules by solvent resistant nanofiltration (SRNF) membranes: a suitable molecular size parameter. *Journal of Membrane Science*, 318(1), 114-122.

Zhu, H.Y., & Vansant, E.F. (1995). Determination of porosity in pillared clays by N₂ adsorption isotherms. *Journal of Porous Materials*, 2(1), 107-113.

Appendix

A1. Mass Balance of Constant Volume Diafiltration in a Single-stage System

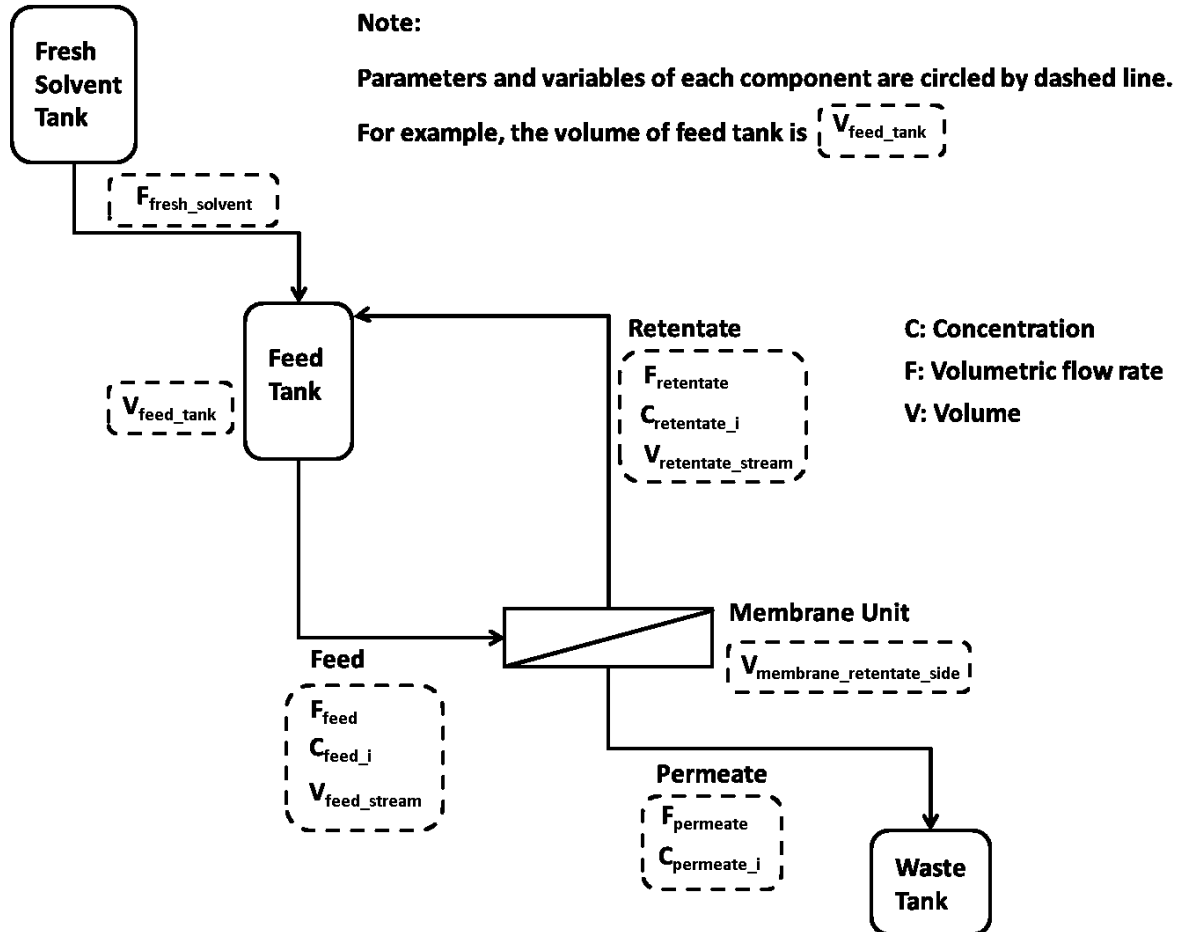


Figure A1. A single-stage system for constant volume diafiltration.

Assumptions:

- 1) The feed tank liquid volume ($V_{\text{feed_tank}}$) remains constant over time, hence $F_{\text{fresh_solvent}}$ is equal to F_{permeate} .
- 2) The rejection of component i (R_i) remains constant over time.
- 3) The retentate stream, feed stream and feed tank are a well-mixed system, hence $C_{\text{retentate}_i}$ is equal to C_{feed_i} .

- Mass balance of the system:

$$V_{feed_tank} \times \frac{dC_{feed_i}}{dt} = -F_{permeate} \times C_{permeate_i} \quad \text{Equation A1}$$

- Based on the definition of rejection:

$$R_i = \left(1 - \frac{C_{permeate_i}}{C_{retentate_i}} \right)$$

$$C_{permeate_i} = (1 - R_i) \times C_{retentate_i} \quad \text{Equation A2}$$

- Based on assumption 3:

$$C_{retentate_i} = C_{feed_i} \quad \text{Equation A3}$$

- Substitute Equation A2 into Equation A3:

$$C_{permeate_i} = (1 - R_i) \times C_{feed_i} \quad \text{Equation A4}$$

- Substitute Equation A4 into Equation A1 and then integrate:

$$\text{Step 1.} \quad V_{feed_tank} \times \frac{dC_{feed_i}}{dt} = -F_{permeate} \times (1 - R_i) \times C_{feed_i}$$

$$\text{Step 2.} \quad \int_{C_{feed_i}(initial)}^{C_{feed_i}(t)} \frac{1}{C_{feed_i}} dC_{feed_i} = \int_0^t -\frac{F_{permeate}}{V_{feed}} \times (1 - R_i) dt$$

$$\text{Step 3.} \quad \frac{C_{feed_i}(t)}{C_{feed_i}(initial)} = \exp\left(-\frac{F_{permeate}}{V_{feed}} \times (1 - R_i) \times t\right)$$

$$\text{Step 4.} \quad \frac{C_{feed}(t)}{C_{feed}(initial)} = \exp\left(-\frac{V_{permeate}}{V_{feed}} \times (1 - R_i)\right)$$

$$\text{Step 5.} \quad \frac{C_{feed}(t)}{C_{feed}(initial)} = \exp(-W \times (1 - R_i)) \quad \text{Equation A5}$$

Using Equation A5, $C_{feed_i}(t) / C_{feed_i}(initial)$ can be plotted against wash volume (W) as shown below.

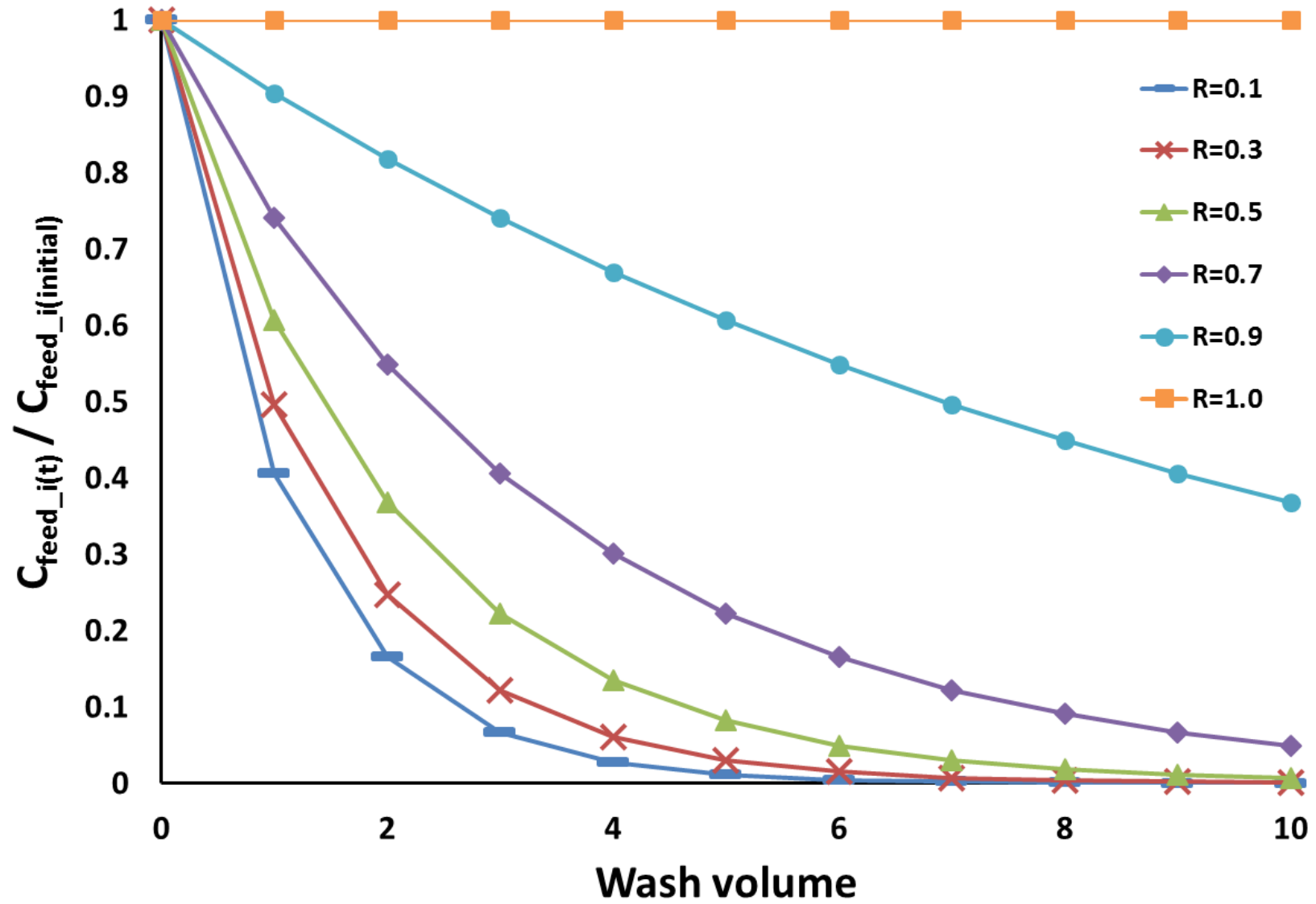


Figure A2. Concentration of component i at time (t) over initial concentration during constant volume diafiltration.